THE STUDY AND MEASUREMENTS OF THE BEHAVIOUR AND CHARACTERISTICS OF ELECTROMAGNETIC RELAYS

A thesis submitted to

THE UNIVERSITY OF ASTON IN BIRMINGHAM

FOR

THE DEGREE OF DOCTOR OF PHILOSOPHY

BY

PRANTOSH DHAR, M.Sc.(Tech.)

November, 1968

SUMMARY

The thesis presents a theoretical and practical study of the dynamic behaviour of electromagnetic relays.

After discussing the problem of solving the dynamic equations analytically and presenting a historical survey of the earlier works in the relay and its dynamics, the simulation of a relay on the analogue computer is discussed.

It is shown that the simulation may be used to obtain specific solutions to the dynamic equations. The computer analysis provides the dynamic characteristics for design purposes and may be used in the study of bouncing, rebound oscillations and stability of the armature motion.

An approximate analytical solution to the two dynamic equations is given based on the assumption that the dynamic variation of the pull with the position of the armature is linear. The assumption is supported by the Computer-aided analysis and experimental results. The solution is intended to provide a basis for a rational design.

A rigorous method of analysing the dynamic performance by using Ahlberg's theory is also presented. This method may be justified to be the extension of Ahlberg's theory by taking the mass and frictional damping forces into account. While calculating the armature motion mathematically, Ahlberg considers the equilibrium of two kinds of forces, namely pull and load, and disregards the mass and friction forces; whereas the present method deals with the equilibrium of all four kinds of forces. It is shown how this can

be utilised to calculate the dynamic characteristics for a specific design. The utility of this method also extends to the study of stability, contact bounce and armature rebound.

The magnetic circuit and other related topics which are essential to the study of relay dynamics are discussed and some necessary experimental results are given.

ACKNOWLEDGEMENTS

I wish to express my gratitude to the University of Aston for granting me a research assistantship during this work and to the Department of Electrical Engineering for providing the research facilities.

My grateful thanks are due to Dr. D. Karo, formerly Reader of the Department of Electrical Engineering, for initiating this work and for his help and encouragement. I extend my special thanks to Professor W.K. Roots for supporting this work and for his stimulating interest as the work progressed. My thanks are also due to Mr. J. Hamilton of the Department of Electrical Engineering for the helpful discussions regarding the analogue computer simulation on the HYBRID-48 computer.

I wish to thank Messrs. E.Roberts, F.Hunt, H.Roberts and C.Penn for their assistance and co-operation.

CONTENTS

LIST OF SYMBOLS

A	=	pole face area of the magnet
a	=	area
C	=	spring constant
E	=	e.m.f. of a d.c. source
F	=	force
f_o	=	acceleration of the armature in operation
G	=	total conductance
G_c	=	coil conductance
G_e	=	the equivalent conductance of the eddy current paths
i	=	instantaneous current in the relay coil
i_s	=	steady state current
l	=	length
m	=	effective mass of the armature
M	=	magnetomotive force
N	=	number of turns in the relay coil
p	=	leakage permeance
R	=	total resistance of the relay coil circuit
S	=	total reluctance of the magnetic circuit
S_L	=	leakage reluctance
S_o	=	closed gap reluctance for the flux ϕ_g
t	=	time
U	=	field energy
V_o	=	velocity in operation

x	=	displacement of the armature
x_g	=	length of the working air gap
ϕ	=	mean flux per turn of the coil
ϕ_g	=	working air gap flux
τ	=	frictional damping coefficient
$\mathcal{P}_a$	=	permeance with respect to a given length of air gap
ρ	=	resistivity
μ_o	=	permeability of free space
μ_r	=	relative permeability
μ	=	absolute permeability

Chapter 1

INTRODUCTION

1.1 General

Electromagnetic relays have been in use in various fields as low power switching devices, and are particularly well known for their continued and reliable service in telegraph and telephone systems. These switching devices are used in industrial electronic and instrumentation systems, computing devices, control apparatus, safety devices and in highly sophisticated spacecrafts; in all of which their operation is intended to control a larger power in another circuit, or to give switching actions according to some pre-arranged time or process schedule.

The motor element in the electromagnetic switching relay is the electromagnet. A simple relay structure is shown in fig. 1.1. When a current is passed through the relay coil a magnetic field is developed giving rise to a pull which acts on the armature. The contacts are then actuated by the moving armature.

Relay engineering covers many topics such as the statics of electromagnets, dynamics of the electromechanical system, spring statics and vibration, science of the contact, coil heating and heat dissipation. For calculating the time of operation and of release, velocity, acceleration and kinetic energy the study of relay dynamics is essential. The formula for the time of flux development in operation with the armature at rest can be easily set up to calculate the time with desirable accuracy, but it is difficult to set up such a

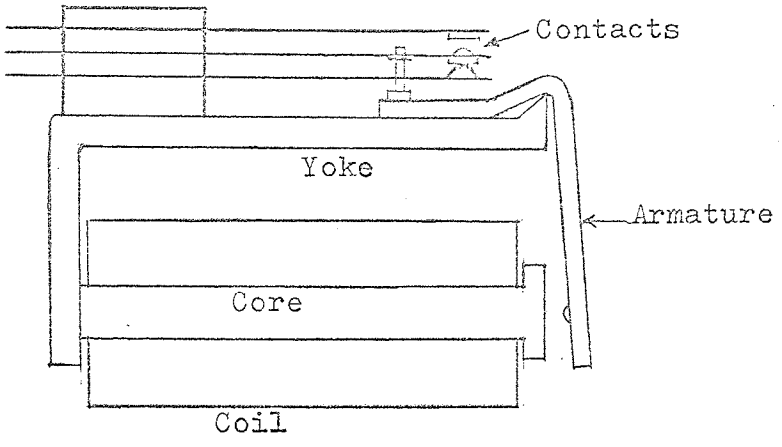

Fig.1.1 Relay

formula for the motion time. It seems such a formula does not exist. To calculate the time of operation, velocity and acceleration what is essentially needed is a theory for the dynamic behaviour.

Velocity is of importance when the contact bounce as well as the armature impact and rebound are considered. It is essential to know precisely how velocity can be regulated changing different parameters.

The research reported in this thesis was devoted to the study of the dynamic behaviour of electromagnetic relays. For this study different measurements are involved and a clear understanding of the static performance of the electromagnet is required. Therefore, the magnetic circuit and other relevant topics are also studied in brief.

1.2 The dynamic equations

The electrical and mechanical equations which govern jointly the dynamic performance of electromagnetic relays may be derived from Lagrange's equations of generalised mechanics. As there is only one electrical and one mechanical co-ordinate, these equations may be derived directly as shown in sec. 4.2 of Peek and Wagar[3]. The electrical equation may be given by:

$$S\phi + G\frac{d\phi}{dt} = Ni_s \qquad (1.1)$$

Where S is the total reluctance of the magnetic circuit, ϕ is the mean flux linked by the coil at any instant, G is the total conductance, N is the total number of turns in the coil and i_s is the steady state current. S is given by:

$$S = \frac{Ni}{\phi}$$

where i is the instantaneous current. G is the sum of the coil conductance or coil constant G_c and the equivalent conductance G_e of the eddy current paths.

$$\therefore \quad G = G_c + G_e = \frac{N^2}{R} + G_e$$

where R is the total resistance of the coil circuit.

The mechanical equation is given by:

$$m \frac{d^2x}{dt^2} + \gamma \frac{dx}{dt} + c\,x = F - F_o \qquad (1.2)$$

where m is the effective mass of the armature, x is the co-ordinate defining the armature position, t is time, γ is the frictional damping co-efficient and c is the spring constant which is the reciprocal of the spring compliance. F and F_o are the instantaneous magnetic pull and initial load respectively. Equation (1.2) is for a relay with a linear spring load, because the expression, Force = $F_o + c\,x$ represents a linear load relation. For any load the mechanical equation may be written as

$$m \frac{d^2x}{dt^2} + \gamma \frac{dx}{dt} + F_r(x) = F - F_o$$

where $F_r(x)$ is the spring load at any position, x.

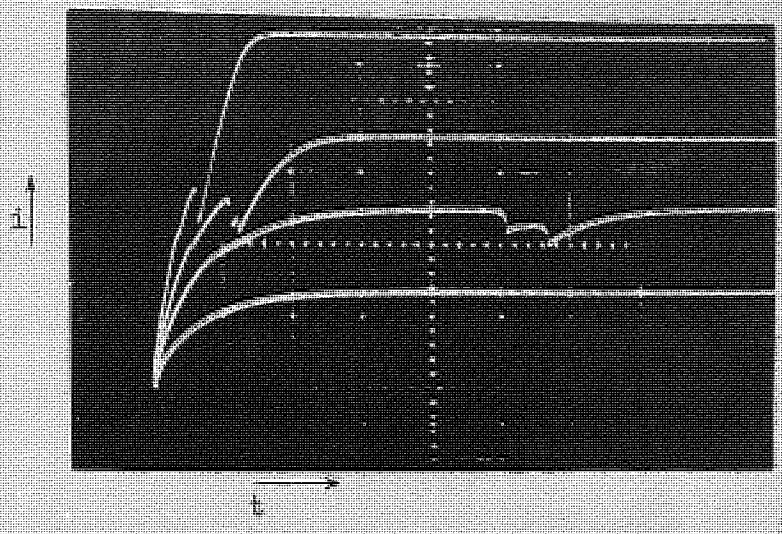

Fig. 1.2 Current oscillograms for a telephone type relay at four different voltages.

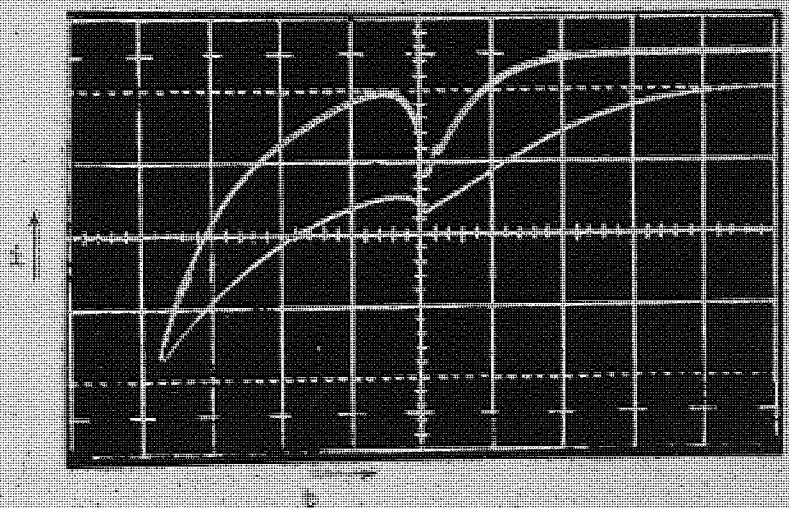

Fig. 1.3 Current oscillograms for a general purpose industrial relay (upper trace) and a reed relay (lower trace).

Equations (1.1) and (1.2) govern the concurrent change of x and ϕ. With the armature at rest, x is constant and the relay may be considered as an inductor with constant inductance when the permeability is assumed to be constant. Eq.(1.1) may be solved to give initial flux development in operation and decay in release, both of which are exponential like the current growth in a circuit with constant inductance.

The current oscillograms of an electromagnetic relay for four different feeding voltages are shown in fig.1.2 for interest. The oscillograms are for a telephone type relay. Fig. 1.3 shows two more current oscillograms, one for a general purpose industrial relay (upper trace) and the other for a reed relay (lower trace). These are shown for comparison. The lowest curve in fig. 1.2 was obtained when the armature was locked. The oscillograms in both the figures show that the variation of the current is very complicated when the armature moves. The times at which the motion ends is marked by the downward points in the curves.

Before discussing the solution to the dynamic equations an introduction of the equivalent magnetic circuit may be given.

1.3 The equivalent magnetic circuit

The magnetic circuit approach is used to develop the performance relations of the electromagnet. Field relations may be simply derived from the magnetic circuit with lumped parameters. The detail treatment is given in chapter 10. The equivalent magnetic circuit which

represents the low density field relations satisfactorily is shown in fig. 1.4.

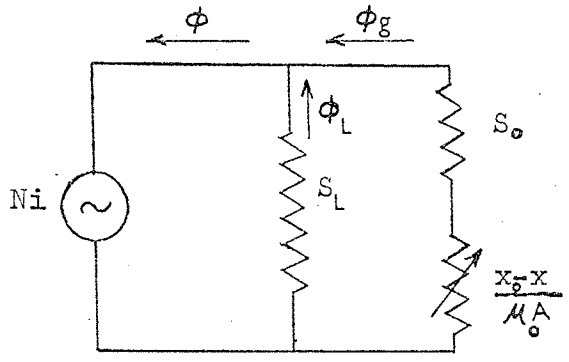

Fig. 1.4 Equivalent magnetic circuit

In this figure S_L is the leakage reluctance, S_o is the closed gap reluctance for the air gap flux ϕ_g and ϕ_L is the leakage flux. Whereas x_o is the total travel of the armature, A is the pole face area of the magnet and μ_o is the permeability of free space. The total flux ϕ linked by the coil is given by

$$\phi = \phi_g + \phi_L$$

1.4 Solution to the dynamic equations

The static and dynamic field patterns may be assumed to be the same. In that case, the pull F in eq.(1.2) may be evaluated from the static magnetisation relations. Eqns.(1.1) and (1.2) are two non-linear simultaneous differential equations. The analytical solution to these equations are not possible at present. In eq.(1.1) S is a function of x and ϕ. If a linear magnetisation is assumed,

then S is a function of x only, and the equation still remains a non-linear one. In eq.(1.2) F is a function of x, ϕ and t. Even for the linear magnetisation when F becomes a function of x and t only, (1.2) is a non-linear equation, analytical solution of which is not possible. The same applies to (1.1) as well.

An expression for S may be written from the equivalent magnetic circuit:

$$S = \frac{S_L \left(S_o + \frac{x_o - x}{\mu_o A}\right)}{S_o + S_L + \frac{x_o - x}{\mu_o A}} \qquad (1.3)$$

$$= f(x)$$

The pull formula which may be used to calculate the pull acting on the armature may be written as:

$$F = \left(\frac{S_L}{S_L + S_o + \frac{x_o - x}{\mu_o A}}\right)^2 \times \frac{\phi^2}{2 \mu_o A} \qquad (1.4)$$

$$= f(x, t)$$

Eq.(1.4) is a general pull expression which is derived in sec.10.8 This may be written in the form:

$$F = K \phi^2 \qquad (1.5)$$

where $$K = \left(\frac{S_L}{S_L + S_o + \frac{x_o - x}{\mu_o A}}\right)^2 \times \frac{1}{2 \mu_o A}$$

Combining eqs. (1.2) and (1.5) there is obtained an expression for ϕ. This expression for ϕ may be substituted in eq. (1.1); eliminating ϕ, it gives a third-order non-linear differential equation in x and t, which is given in the following.

$$\frac{Gm}{2}\left(1-\frac{1}{K}\frac{dK}{dx}\right)\frac{d^3x}{dt^3}+\left\{m\left(S-N\,i_s\sqrt{K}\right)+\frac{\tau G}{2}\left(1-\frac{1}{K}\frac{dK}{dx}\right)\right\}\frac{d^2x}{dt^2}+\left\{\tau\left(S-N\,i_s\sqrt{K}\right)+\frac{Gc}{2}-\frac{G}{2K}\cdot\frac{dK}{dx}(cx+F_o)\right\}\frac{dx}{dt}+\left\{c\left(S-N\,i_s\sqrt{K}\right)\right\}x+F_o\left(S-N\,i_s\sqrt{K}\right)=0 \qquad (1.6)$$

The analytical solution to this equation which could give the dynamic relations is not known. As the solution to eqs. (1.1), (1.2) and (1.6) is not possible, the analysis of the dynamic behaviour of electromagnetic relays becomes a difficult problem.

1.5 Text outline

As discussed in sec. 1.4 an analytical treatment of the dynamic problem in a relay is difficult, because the solution to the dynamic equations is not possible. However, specific solutions by computing devices may be obtained. This work involved an analogue computer simulation performed for these solutions. In addition an approximate analytical solution is also presented.

After giving a historical survey on the earlier works in the relay and its dynamics in chapter 2, the analogue computer simulation is presented in chapter 3. The results of the computations are given in chapter 4. The approximate analytical solution mentioned above is presented in chapter 5 and an experimental design using this solution is given in chapter 6.

Ahlberg[9,10,11] contributes a novel theory for the dynamic behaviour and deals with the electrical equation only. The mechanical equation is not needed. A rigorous analysis of the dynamic behaviour by using Ahlberg's theory is also a part of this work.

After discussing in detail the extension of Ahlberg's theory in chapter 7, the experimental verification of the analysis is presented in chapter 8 which is followed by chapter 9 giving some discussions on various topics, such as contact bounce, stability, reed relays etc. Chapter 10 presents a discussion on the magnetic circuit and pull relations, and chapter 11 presents the results of magnetisation measurements and pull measurements. The results in chapter 11 are used in different chapters for various analyses.

1.6 Time of operation

The time of operation of a relay is defined by many authors as the time to operate the last contact. Becoming fully aware of this, the time of operation is used in the text generally to indicate the time for full operation, i.e. the time at which the armature finishes its travel. Of course, the instants at which the contacts

open or close can easily be found when the x vs. t relation is known.

1.7 Motion of the armature

The position of the armature is indicated by the co-ordinate x. The position in which the armature is released corresponds to x = 0. The direction of motion is positive when the armature moves towards the pole face of the electromagnet and it is negative when the same moves away from the pole face.

Chapter 2

HISTORICAL SURVEY

The development of an electromagnetic relay is closely associated with that of an electromagnet. The first electromagnet was built by Sturgeon in 1825, following the discovery of electromagnetism by Örsted in 1820. Morse invented the relay and used it to repeat or renew the weakend signals of telegraphy. Wheatstone is also named as the inventor. Although the first relay came in existence around 1839, the first use of an electromagnet to actuate an armature was made before that by Professor Joseph Henry in 1831, when he exhibited in his class in Albany Academy a telegraph which contained that electromagnet (ref.2 , Page). Later Henry included a relay in his telegraph equipment and it seems he did it independently.

The study of electromagnets plays an important role in relay engineering. Many other branches of electrical engineering are also concerned with this study. S.P. Thompson[1] says in the preface to the first edition of his book

" Electrical engineering embraces many branches, but most of these are concerned with electromagnets. The dynamo for generating electric currents, the motor for transforming their energy back into work, the arc lamp, the electric bell, the telephone, the recent electromagnetic machinery for coal mining and for separation of ore, and many other electromechanical contrivances, come within the purview of the electrical engineer. In every one of these, and many more of the

useful applications of electricity, the central organ is an electromagnet. "

The study of electromagnets requires the knowledge of electricity and magnetism both of which are quite developed at present, but in those days the behaviour of the electromagnet was unknown; because the magnetic part of the problem was buried in obscurity, although the electric part was clear due to the effort of ohm, Helmholtz, Maxwell and others. Gradually the magnetic part became clear and the idea of the magnetic circuit and reluctance came in. The idea of a magnetic circuit was more or less familiar to many early researchers. The role of magnetomotive force in a magnetic circuit and the change of the magnetic circuit property due to the permeability of the material comprising the circuit are all gradually analysed. In a famous paper Kennelly[24] establishes the magnetic reluctance doing a similar function in a magnetic circuit as resistance does in an electric one.

Among the early authors who developed the science of electromagnet S.P. Thompson's name may be mentioned. The use of this science was made by many people to study the design principles of relays. Among them who dealt with the design principles, the people of telegraph and telephone industries are well known.

Bähler[20,21] studied relays critically and his work is mainly theoretical, but may be called first of its kind; and it seems no one before him paid much attention on this subject.

D.D. Miller[42] published a paper regarding the design characteristics of electromagnets, in 1924; and then many people did design work in their respective firms. Some related texts were also published and among the authors of the texts, Roters[16] may be mentioned.

It may be mentioned here that, in the design of electromagnets there are two different approaches, one is to map the field accurately for a structure and the other one gives the field relations in terms of the lumped parameters of a magnetic circuit. In this work the latter approach is followed.

The theory of the magnetic circuit of a relay was given by Bähler, and Ekelöf[12] extends Bähler's effort in a paper published in 1953. Subsequently Ekelöf[13,14,15] published three more papers on the study of electromagnetic relays. Eddy current effect was also studied by him. In the meantime Peek[18,64,66] Wagar[63,64] and Logan[19] published a few valuable papers in the Bell system technical journal. The materials of these papers and other works of many engineers in Bell Telephone Laboratories may be found in the text by Peek and Wagar[3] Many useful papers are available in NARM relay symposium proceedings particularly related to design(25-30). Still Carr[37] says in the 8th annual NARM relay symposium, "The electromagnetic relay is probably the least understood, least standardised and the most abused of all components used in electronic equipment."

On the whole, the primary interest in the study of relay performances was concentrated more in static characteristics rather than in

dynamic characteristics, because in those days the relay was used as an 'off - on' device and the specification was set in its capability to operate contact loads. The other requirement was that it should de-energise when the current is switched off. The dynamic phenomena are very difficult to analyse and for a long time nobody paid much attention on these. According to Ahlberg[9] the first work dealing with the motion of the relay armature was published by Flad in 1920 (page 8). Now, relays are used in modern telephone systems, control apparatus, instrumentation systems and various other equipments, and the speed is one of the most important aspects. In general, for switching applications the calculation of action times is necessary.

The investigations of the present work were devoted to the study of the dynamic performance which is essential for calculating the time of operation, velocity and acceleration. Therefore, a survey of the earlier theories for the dynamic behaviour will be of great interest.

As mentioned earlier, Bähler studied the relay performance critically, and the study was concerned with the dynamics of electromagnetic relays as well. To analyse the dynamic behaviour Bähler sets up three simultaneous equations, one electrical, one mechanical and another equation describing the relation between the flux, current and travel. Bähler solves the simultaneous equations after making an assumption that mass can be disregarded. The analyses and

formulae are very complicated to be conveniently dealt with by a practical relay designer.

Jasse[36] deals mainly with the power electromagnets. He sets up two simultaneous differential equations, one for the constant voltage, current and variable inductance and one for the acceleration and pull, whereas friction and spring load are neglected. After solving the equations, fairly simple formulae are obtained for current and velocity. In ordinary electromagnetic relay spring load cannot be neglected, obviously these formulae are not very useful in this case.

Roters gives a step by step solution which can give useful pictures of the characteristics for specific cases but does not give much of an analytic picture (page 378). Okada, Kubokoya, Shinohera published a paper on the dynamical analysis of nonpolarised relay in 1948 (ref.32). The authors derive the dynamic equations from Lagrange's equations and solve them after making the assumptions that the total reluctance of the magnetic circuit is constant and load stays at the initial value. The treatment is approximate and is not suitable for the calculation of time of a speed relay. The same assumptions are made by the present author for the first section of the travel in the rational design theory, but the section is limited to a very small distance for which these may be quite justified.

Peek[18] gives three theories for estimating the time of operation, the "single-stage approximation", "two-stage approximation" and "three-stage approximation". The first one, the "single stage approximation" may be applicable in the case of slow operation and

the other two theories are applicable in all cases including the case of fast operation. In his theories Peek makes a number of approximations, yet the theories may be quite suitable for calculating the time fairly accurately in many cases, but the two theories, i.e. the "two stage approximation" and "three stage approximation" are quite complicated and they do not give much useful information regarding the velocity and acceleration. In the second stage of the two stage approximation, the acceleration is assumed constant. In the three stage approximation a new stage is introduced in between the first and second stages of the two-stage approximation and it is assumed that S and Ni do not change with x. In the final stage ϕ is taken as constant, as in the second stage of the two-stage approximation.

Logan[22] extends Norton's[23] effort by publishing his results of the dynamic measurements on electromagnetic devices and this gives some useful pictures of the dynamic behaviour.

In a different paper, Logan[19] presents a time formula after making an assumption that the pull varies linearly with time. The assumption is just arbitrary though Logan supports it by the oscillogram. The time formula is very complicated.

Shinohara[34] presents an analysis of the dynamic performance considering mass, spring and other design parameters. The analysis is approximate but with all experimental results gives quite useful information. Masuzawa and Tomita[33] treats relays like electro-accoustic transducers and solve the electrical and mechanical dynamic

equations for a relay. The time formula is fairly simple (Page 248) but a doubt arises regarding the validity of the theory, because the armature in a relay moves from one equilibrium position to another equilibrium one and it is a large amplitude motion; whereas, in a transducer it is a case of small amplitude sustained oscillations. Tomita[35] extends the previous treatment given by him and Masuzawa, and derives the time formula considering the force factor and eddy current; the analysis is similar as in the case of a transducer but it is very complicated.

Ahlberg[9,10,11] published three papers which describe a new theory for the dynamic behaviour. After presenting a survey on the earlier theories he presents an analysis which calculates the motion mathematically. Ahlberg neglects the mass and friction,and considers an equilibrium between two forces, namely, the pull and load during the motion. The theory seems very useful in dynamical analysis, particularly it gives some analytical expressionsfor velocity and acceleration which were not treated so precisely by any author before. The effect of mass and friction are not taken into consideration quantitatively, but mass cannot be neglected in relays, particularly in high speed relays.

Because of considering an equilibrium between two kinds of forces, which permits the calculation of time and velocity from the static load and pull characteristics, Ahlberg gets negative times and velocities for some sections of the travel. For these sections he suggests some stabilising measures. As time cannot be negative there are definite

times to travel those sections; according to Ahlberg these times are very short and may be neglected while calculating the total time of operation.

The present author takes the mass and friction forces into account and extends Ahlberg's theory to analyse the dynamic behaviour using the basic approach due to Ahlberg. The present treatment does not give any negative time, and gives positive velocity where it should be so. The analytical expressions derived by Ahlberg are extended in the case of the equilibrium between the four kinds of forces and the equivalent magnetic circuit is used to derive the expressions when the magnetisation is linear. Because of using this magnetic circuit, the formulae result in a little simplified form.

As previously mentioned, there are two approaches of describing the field relations of an electromagnet. Taking the magnetic circuit approach the present treatment which makes use of the equivalent magnetic circuit with lumped parameters in deriving the formulae has the virtues of simplicity and generality.

Chapter 3

ANALOGUE COMPUTER SIMULATION OF AN ELECTROMAGNETIC RELAY

3.1 Introduction.

It was discussed in chapter 1 that the analytical solution of the two dynamic equations which govern jointly the dynamic performance of electromagnetic relays is not possible at present. However, specific solutions may be achieved on the analogue or digital computer.

Simulation of electromechanical systems on the analogue computer is quite well known. A relay is an electromechanical device and may be simulated on the computer. The analogue simulation in this case, is programming the computer for getting a numerical solution to the dynamic equations. Once it is done, specific solutions can be achieved for the purpose of studying the dynamic behaviour.

This chapter presents the simulation in detail with the necessary computer circuits. A brief description of the HYBRID-48 computer which was used for the simulation , and its computing components is also given. The specific solutions are given in chapter 4.

3.2 The simulation of a relay.

A relay was simulated for the study of the armature motion during operation. For the simulation of a physical system, a mathematical model representing the system is required. If a set of equations can be formulated to describe the system then these equations represent the mathematical model. For an electromagnetic relay the mathematical model

for the 'operate case' consists of the two nonlinear simultaneous differential equations (1.1) and (1.2) which may be rewritten:

$$S\phi + G\frac{d\phi}{dt} = N i_s \qquad (3.1)$$

$$m\frac{d^2x}{dt^2} + r\frac{dx}{dt} + C X = F - F_o \qquad (3.2)$$

A flow diagram for the solution of these equations may be produced and the actual circuit connections may be done on the computer.

To simulate the system logic facilities were utilised. When the growing magnetic pull does not exceed the initial load there cannot be any motion, i.e. 'x' is zero. Now, if 'x' is represented by the voltage output from an integrator, then this integrator should not compute until the above condition is satisfied and this can be 'set up' by using logic circuits. Similarly the condition that the armature should remain in fully operated position while the core flux 'ϕ' would go on increasing can be simulated holding 'x' and computing 'ϕ'.

The computer circuit diagrams for the solution of equations (3.1) and (3.2) may now be given. Eq. (3.1) may be rewritten in the form:

$$\frac{1}{G}(S\phi - N i_s) = -\frac{d\phi}{dt} \qquad (3.3)$$

By the help of eq.(3.3) the flow diagram in fig.(3.1) can be produced and this would represent the computer circuit necessary to solve eq. (3.1).

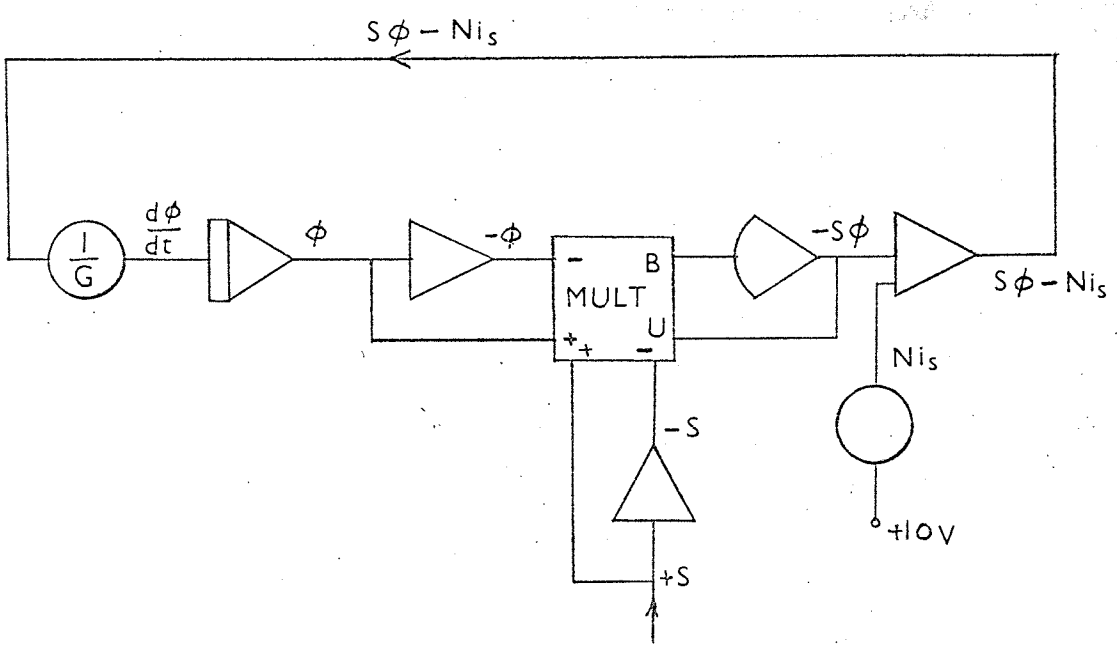

Fig. 3.1 Computer circuit necessary to solve eq. 3.1.

Equation (3.2) may be rewritten in the form:

$$\frac{d^2x}{dt^2} = \frac{1}{m}\left(F - F_o - cx - \gamma\frac{dx}{dt}\right) \qquad (3.4)$$

Following eq. (3.4) the computer circuit needed to solve eq.(3.2) may be produced. Fig.(3.2) shows the circuit.

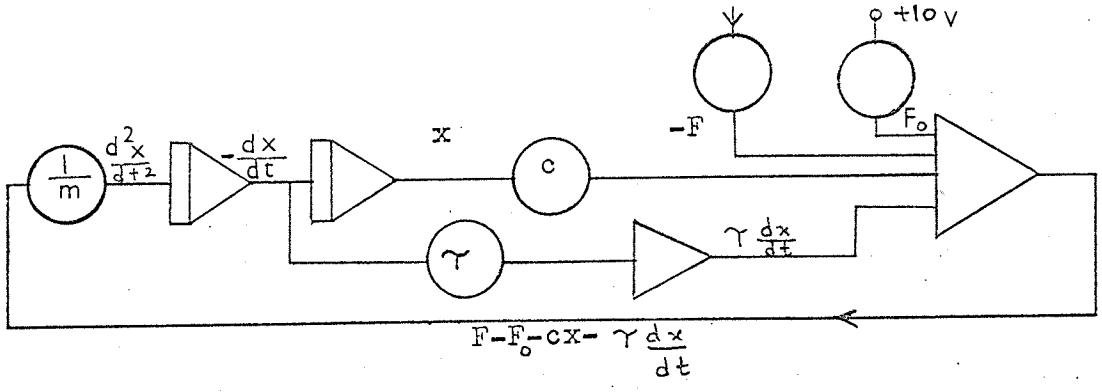

Fig.3.2 Computer circuit necessary to solve eq. 3.2

The programming symbols for the computer components are given in appendix. 1.

The circuits in figs. (3.1) and (3.2) should be connected through necessary computing components to get the required solution of the two simultaneous equations (3.1) and (3.2). The complete analogue computer programme diagram is given in sec. 3.8.

Before presenting the numerical values of the parameters and the complete programme diagram, it may be interesting to give a brief introduction of the HYBRID-48 computer. The description of some of the computing components may also be given. These are presented in the following two sections.

3.3 The HYBRID-48 computer:

This computer consisting of solid-state computing components may be operated as an analogue or a hybrid computer. It has got a large analogue section with extremely wide bandwidth and offers very flexible mode control, parallel logic facilities and high speed switching, all of which are due to the presence of the Logic and Mode Control (LMC) and Electronic Mode Control (EMC) features, making it suitable for high speed repetitive and iterative operation.

The digital facilities in the computer can be utilised to simulate a physical system. The logic elements can control individual amplifiers in the analogue section and the access to the amplifiers for electrical connection is provided in the logic module.

It is well known that the various mathematical operations in an analogue computer are done on voltages and the analogue section of the HYBRID-48 computer operates on $\pm$ 10 volts.

3.4 Description of some units in the computer:

In the analogue computer there are electronic circuits to perform on voltages the various operations of summation, multiplication, division, integration and function generation. Besides these operations, sometimes squaring and square root extraction are also needed.

Linear computations such as summation, integration, inversion and multiplication by a constant are performed by using the operational amplifiers which are high gain d.c. amplifiers. These amplifiers are the basic building brick of the analogue computer and the use of them for doing these computations is quite well known. The symbol for an operational amplifier is almost internationally recognised as the one given in appendix 1.

It is interesting to mention that a simple multiplication by a constant may be done by the potentiometer which is the simplest part of the computer. When the product of two variables is required, a sophisticated multiplier like quarter square multiplier or bipolar multiplier is employed. Function generating devices are required to generate functions during computation.

Bipolar multipliers:

These multipliers which can be used to get the product of two variables are also used for other functions such as, squaring, division and extraction of the square root of á variable input.

The bipolar multipliers have a good frequency response. These are generally used in conjunction with a d.c. amplifier. For multiplication, the bipolar multipliers are connected to the other components for obtaining a four quadrant operation according to the quarter square law

$$x\,y = \frac{1}{4}\,(x + y)^2 - (x - y)^2$$

Here x and y are two arbitrary variables.

The circuit arrangement for four quadrant multiplication can be seen in the part of the circuit in fig.(3.1); where the product of s and ϕ is performed.

Diodes:

These are used in a modern analogue computer for doing various functions. There are some built-in silicon diodes in the computer. These diodes being solid state devices have none of the disadvantages of the thermionic diodes. They have very small leakage current for reverse voltages. The forward resistance is also very small and produces a nearly constant forward voltage drop. The solid state diodes were used in conjunction with other components for simulating the non-linear spring load.

Diode function generators:

Non-linear function generation, by fitting a number of linear segments, is well known and this can be achieved by means of diodes. In the HYBRID-48 computer the Variable Slope, Variable Breakpoint Diode Function Generators (VDFG's) are available. The VDFG consists of 10 segment variable slope, variable breakpoint diode function generators; each VDFG may be used separately or combined to form a 20 segment VDFG.

Comparator:

The electronic comparator is used to compare two input voltages. If the algebraic sum of the inputs is positive, the output is a logic '1' and it is a logic '0' when the sum is negative. In the HYBRID-48, the logic '1' and logic '0' appear at the logic panel and can be used to control individual amplifiers.

3.5 Generation of spring load characteristics.

The linear load characteristic may be generated by using a potentiometer. Fig. 3.3 shows the arrangement in which potentiometer 32 does the multiplication by a constant giving a voltage output which

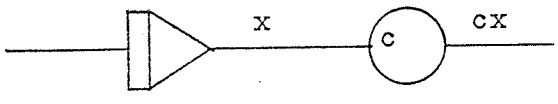

Fig. 3.3.

is equivalent to the product 'cx'. The linear load relation thus produced, is shown in fig. 3.4. The designations of the computing components are arbitrary everywhere in this chapter.

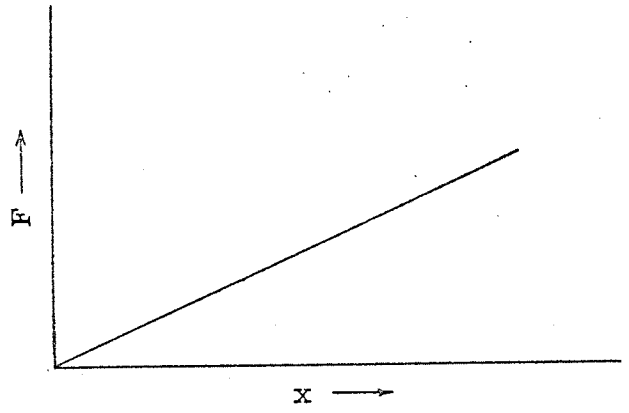

Fig. 3.4 Linear spring load relation

The non-linear spring load characteristic may be generated by using some additional circuitry in combination with the circuit in fig. 3.3. A non-linear load characteristic is shown in fig. 3.5.

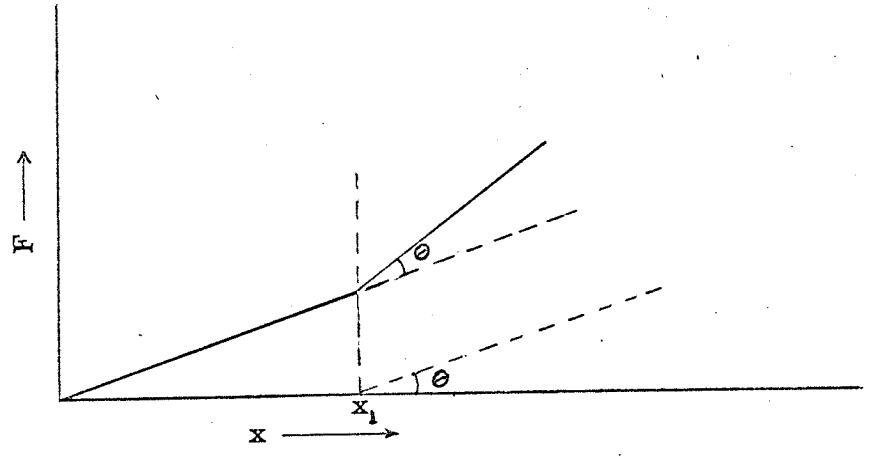

Fig. 3.5 Non-linear spring load relation

To produce this, a circuit consisting of a computing amplifier and a pair of diodes, as shown in fig. 3.6, is required with other components. The forward voltage drop of diode D_2 is blocked and cannot appear at the output of amplifier 10, when the summing junction is at negative potential. The computer circuit diagram for generating the load relation in fig. 3.5 is shown in fig. 3.7. A reference negative voltage is applied to R_1 by means of potentiometer 05. When 'x' exceeds this value, a negative signal appears at the output of amplifier 10 and diode D_1 conducts.

The first section in fig. 3.5 is generated by potentiometer 32. The equation of this section is:

$$F = c\,x, \quad x < x_1$$

The load relation shown by the dashed line in fig. 3.5 is generated by potentiometer 06 and amplifier 30, and the equation for this relation is:

$$F = c^1\,x, \quad x > x_1$$

where c^1 is a spring constant.

The reference point 'x_1' at which amplifier 10 would give an output is set up by potentiometer 05 as mentioned before, and the product '$c^1\,x$' is accomplished by potentiometer 06. In fig. 3.7 the summing amplifier 31 gives the required non-linear load characteristic as its output. If the slope of the characteristic decreases at x_1, then c^1x should be subtracted from cx and amplifier 30 will not be required. The output of potentiometer 06 may be connected directly to summing amplifier 31 in this case.

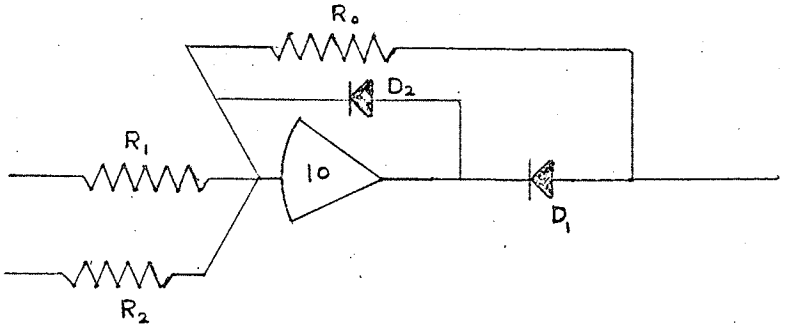

Fig. 3.6

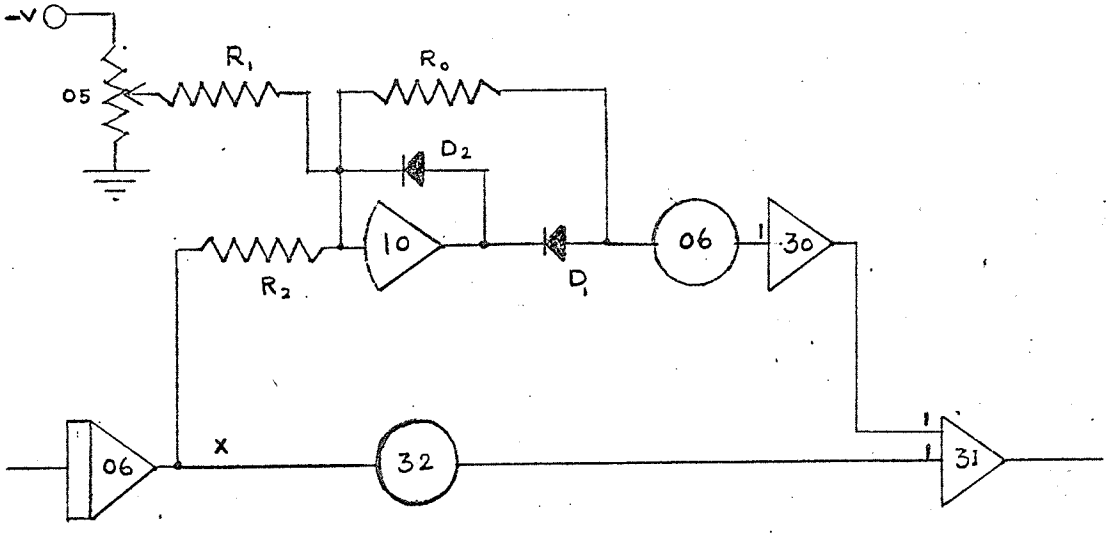

Fig. 3.7

3.6 Generation of functions S and K.

Expressions for S and F in equations (3.3) and (3.4) respectively, are given in section 1.4. The expressions may be written as:

$$S = \frac{S_L \left(S_o + \frac{x_o - x}{\mu_o A} \right)}{S_o + S_L + \frac{x_o - x}{\mu_o A}} = f(x)$$

and

$$F = K \phi^2$$

K is given by:

$$K = \left(\frac{S_L}{S_o + S_L + \frac{x_o - x}{\mu_o A}} \right)^2 \cdot \frac{1}{2 \mu_o A}$$

$$\sqrt{K} = \frac{S_L}{S_o + S_L + \frac{x_o - x}{\mu_o A}} \cdot \frac{1}{\sqrt{2 \mu_o A}} = f(x)$$

The magnetic circuit constants S_o, S_L and A can be estimated or measured for a specific case. Knowing x_o and μ_o, S and $\sqrt{K}$ can be calculated. The variation of S and $\sqrt{K}$ with x is shown in figs. 3.8 and 3.9 respectively by full lines.

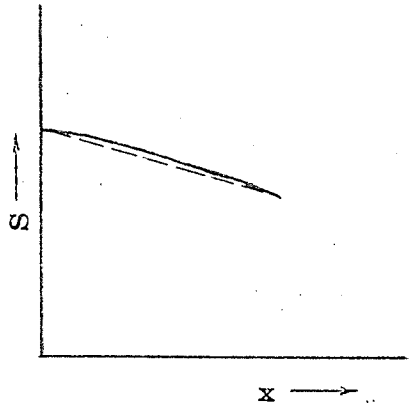

Fig. 3.8 S vs. x relation

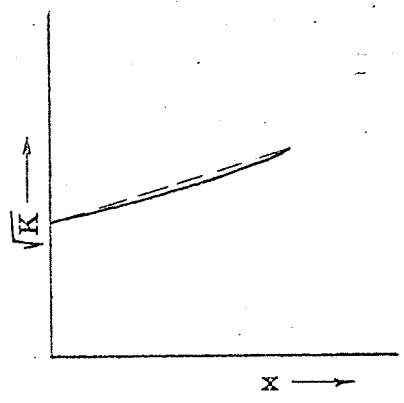

Fig.3.9 $\sqrt{K}$ vs. x relation

The functions may be generated by diode function generators. The diode function generator circuit for 10 segment operation is given in fig. 3.10. The functions were accurately generated by using the 'breakpoint' controls and 'slope' controls in the working units of the V.D.F.G's.

Computation for engineering purposes, may be done making a straight line approximation of the two curves in figs. 3.8 and 3.10. Because the curvature in the two characteristics is small. The dashed lines give the approximate functions. The functions can now be generated by using two potentiometers and an amplifier for each one. Figs. 3.11 and 3.12 show the computer diagrams for generating 'S' and '$\sqrt{K}$' respectively by this method. K can be obtained by squaring $\sqrt{K}$.

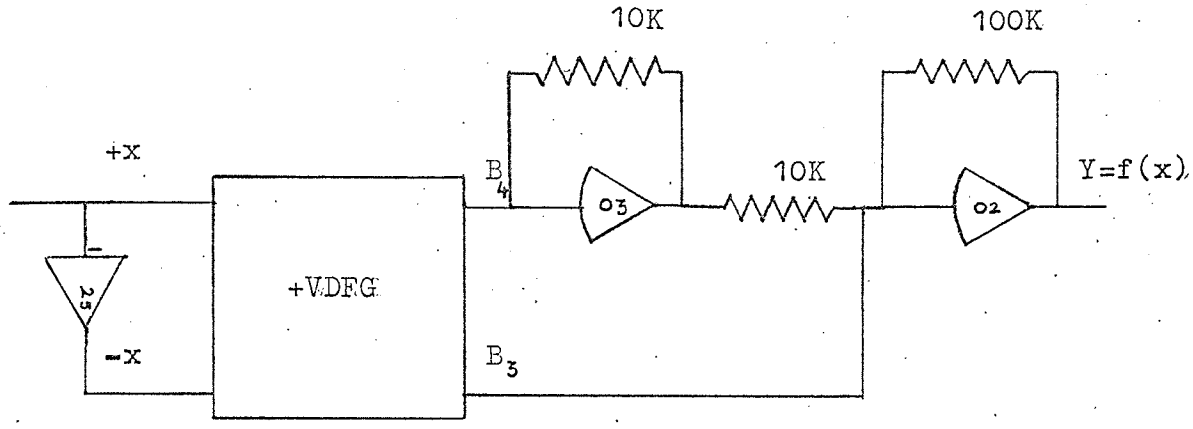

Fig. 3.10 Diode function generator circuit for 10 segment operation

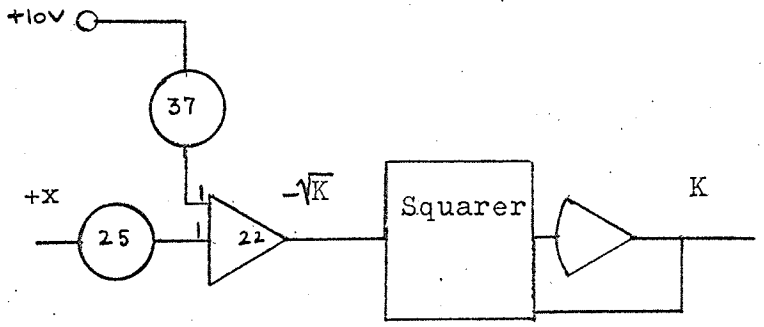

Fig.3.12 Computer diagram for generating K

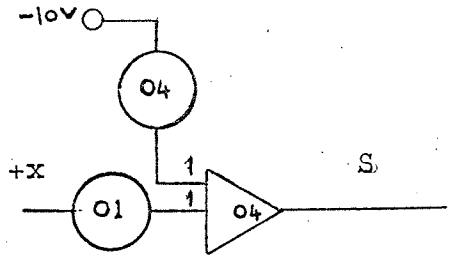

Fig.3.11 Computer diagram for generating S

3.7 Numerical values of the parameters.

It is required to know the numerical values of the parameters of equations (3.3) and (3.4) for obtaining a solution to these equations on the analogue computer.

Measurement of different parameters of a telephone type relay was made and some representative values of these parameters were used for the numerical values.

The following is a list of the parameters and their initial values used in the sumulation.

$m = 8 \times 10^{-3}$ Kg

$\gamma = 10^{-3}$ newton metre second

$c = 7766$ newton/metre

$G = 273.9 \times 10^{3}$ mhos

$Ni_s = 275$ ampere turns

$G_e = 24.6 \times 10^{3}$ mhos

$G_c = 249.30 \times 10^{3}$ mhos

$N = 25000$ turns

$R = 2507$ ohms

$i_s = 11$ milli amperes

$i_s R = 27.58$ volts

$S_o = 299 \times 10^4$ At/Wb

$S_L = 715 \times 10^4$ At/Wb

$A = 1.54 \times 10^{-4}$ metre^2

$\mu_o = 4\pi \times 10^{-7}$ Henry/metre

$x_o = .827 \times 10^{-3}$ metre

$F_o =$ 50 gram force = .4905 newton

Substituting the above values of the parameters into equations (3.3) and (3.4), there is obtained a mathematical model which corresponds to the same of an electromagnetic relay.

Substitution of the above values into the equations gives:

$$\frac{1}{273.90 \times 10^3} (S\phi - 275) = -\frac{d\phi}{dt}$$

$$\frac{d^2x}{dt^2} = \frac{1}{8 \times 10^{-3}} (F - .4905 - 7766 \times -10^{-3} \frac{dx}{dt}) =$$

$$= 125 K\phi^2 - 61.3125 - .125 \frac{dx}{dt} - 970.8 \times 10^3 x$$

Substituting the values of the constants in the expressions for S and K, there is obtained:

$$S = \frac{715 \times 10^4 \left(299/+ \frac{\cdot 827 \times 10^{-3} - x}{.1935 \times 10^{-9}}\right)}{299 \times 10^4 + 715 \times 10^4 + \frac{.827 \times 10^{-3} - x}{.1935 \times 10^{-9}}}$$

$$K = \left(\frac{715 \times 10^4}{299 \times 10^4 + 715 \times 10^4 + \frac{.827 \times 10^{-3} - x}{.1935 \times 10^{-9}}}\right)^2 \times \frac{1}{2 \times .1935 \times 10^{-9}}$$

and

$$\sqrt{K} = \frac{715 \times 10^{4}}{299 \times 10^{4} + 715 \times 10^{4} + \frac{.827 \times 10^{-3} - x}{.1935 \times 10^{-9}}} \times \frac{1}{2 \times .1935 \times 10^{-9}}$$

The values of S and $\sqrt{K}$ available from the above expressions for these respectively, corresponding to different values of x, are given in table 3.1. These are plotted against the corresponding

Table 3.1 Values of 'S' and '$\sqrt{K}$' corresponding to different armature positions.

x m m	S At/Wb x 10^{4}	K x 10^{4}
0	360.32	2.5116
.1	346.94	2.6064
.2	332.92	2.7057
.3	317.57	2.8152
.4	300.94	2.9322
.5	282.85	3.0602
.6	263.11	3.2001
.7	241.48	3.3532
.827	210.83	3.5703

values of x, and the curves obtained thereby are shown in figs. 3.13 and 3.14 In these figures one unit of S and $\sqrt{K}$ is represented by 500 x 10^{4} and 5 x 10^{4} respectively, for the sake of scaling which is given in later section in detail. For the similar reason 1 mm

represents one unit of x.

The initial level and slopes for the two curves are given in table 3.2.

Table 3.2

Curve in figure	Initial level	Slope
3.13	.72	.3644
3.14	.5017	.2581

The potentiometer settings for the programme diagrams in figures 3.11 and 3.12 are given in the following table.

Table 3.3

Pots	Setting
00	.72
01	.3644
25	.5017
37	.2581

The simulation was done using both the methods of function generation for generating 'S' and ' $\sqrt{K}$' and these methods are mentioned in sec.3.6. The computed results did not differ practically. The results in Chapter 4 are given for the simulation by the potentiometer and amplifier method of function generation. Only the computation for a verification of the linearity of the dynamic pull vs. position characteristic, by generating the functions by the diode function generators, is presented in sec.4.8.

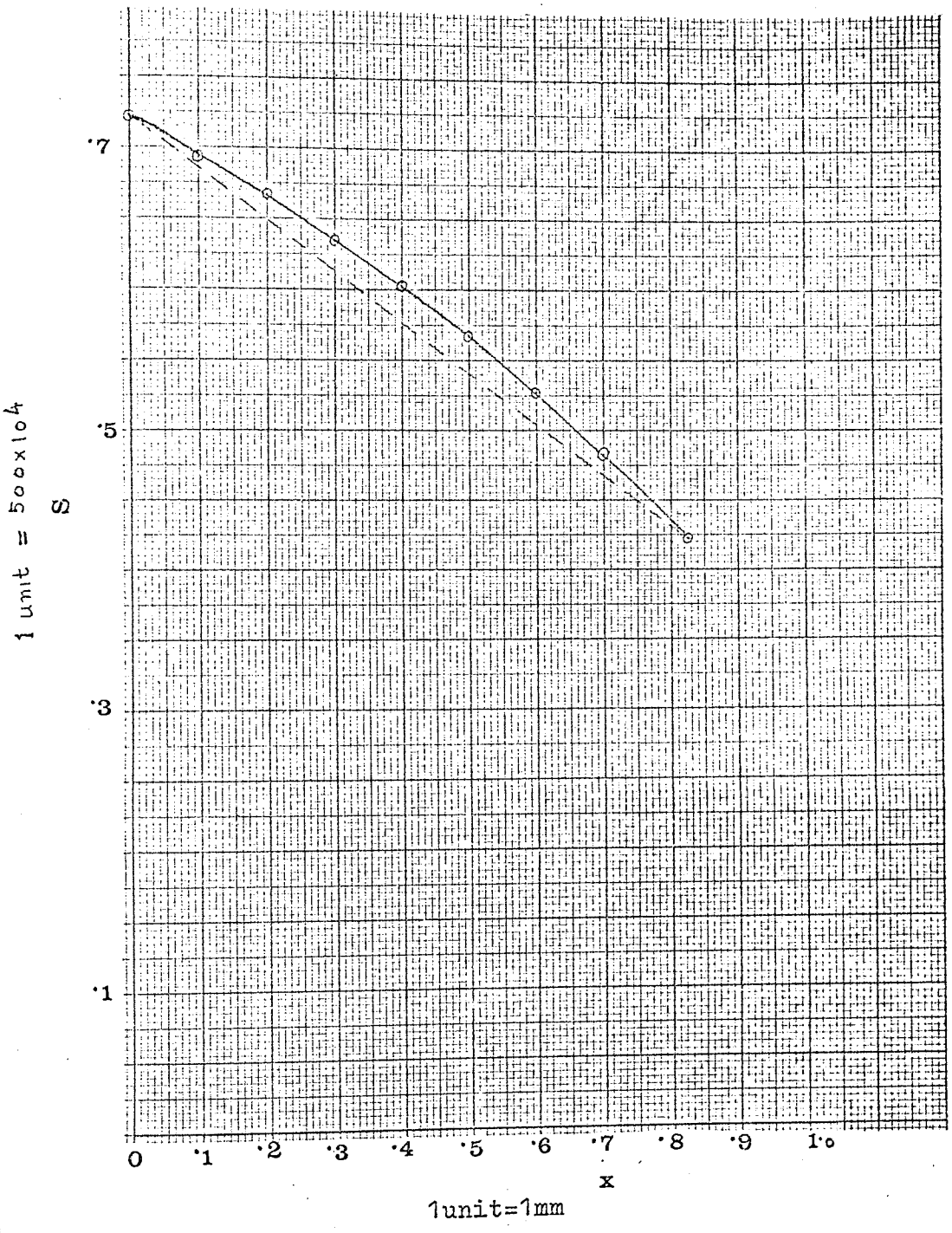

Fig. 3.13

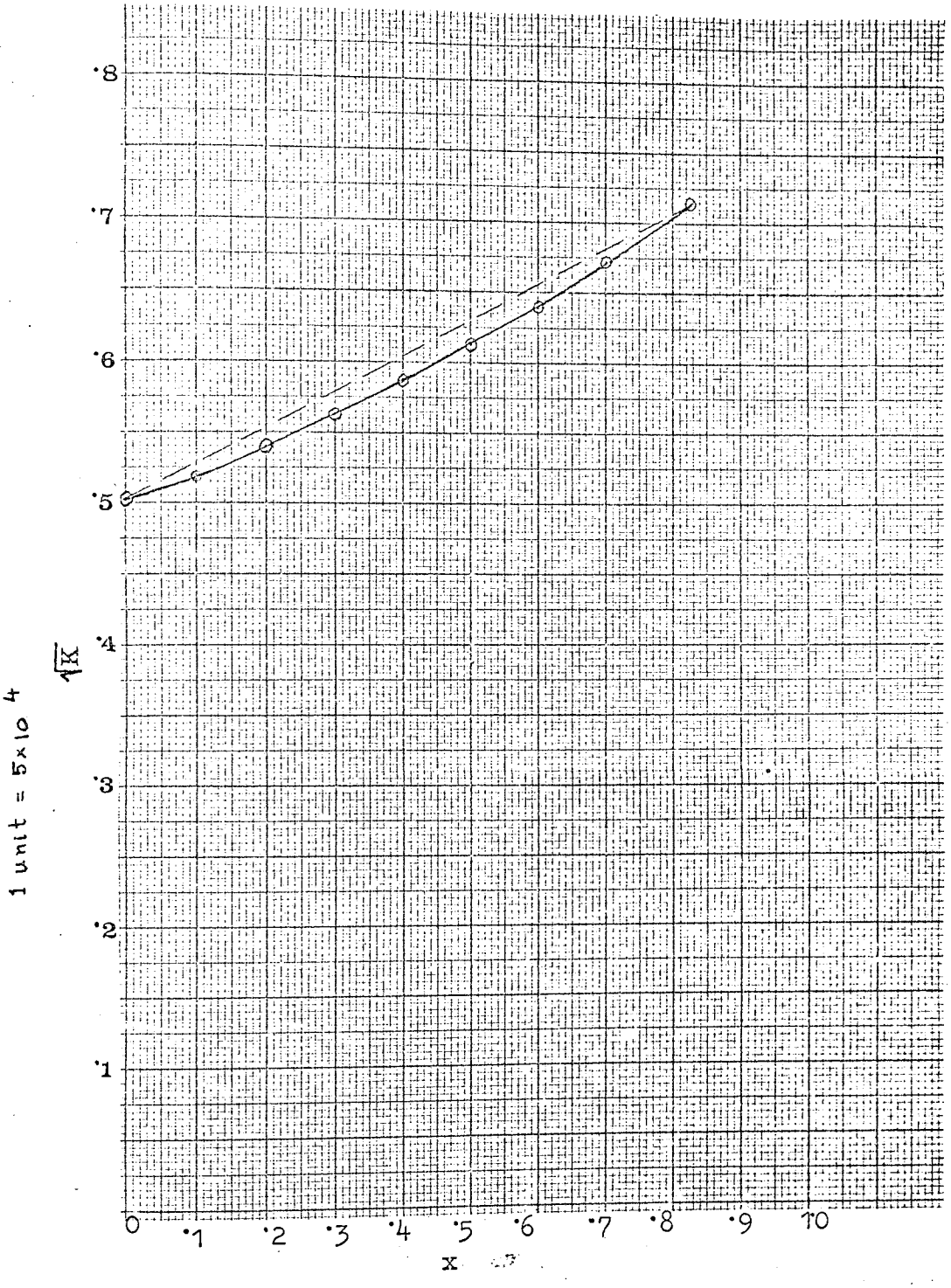

1 unit = 1 m m

Fig. 3.14

3.8 Scaling

For solving differential equations on the analogue computer it is required to do magnitude scaling of the equations. Magnitude scaling will save from the overloading of the amplifiers. The output from the amplifiers in voltage form which represents different variables must be less than the base voltage all the time during computation.

To magnitude scale the equations it is advantageous to adopt the "unit scaling" technique which offers a number of advantages one of which is, the programme may be used in any machine irrespective of its reference voltage. In unit scaling, the reference or base voltage of the computer is taken as a unit for measuring amplifier outputs. So in the HYBRID-48, one unit represents 10 volts. The relation between a physical variable and the corresponding computer variable becomes somewhat simpler in terms of unit scaling. This may be made clear by giving an example. Suppose, in a physical system, the maximum value of a variable x which represents displacement, is 1×10^{-3} metre, then the corresponding computer variable is simply $\frac{x}{1 \times 10^{-3}}$, which has a maximum value of one. Every computer variable is the ratio of the corresponding problem variable to its maximum value. Obviously, the output of the computer components become normalized or per-unit quantities.

It is clear that an estimation of the maximum values of the variable parameters is required for magnitude scaling. Table 3.4

gives the estimated maximum of the variables and the scaled ones. Scaled variables are given in per unit values.

Table 3.4

Item	Estimated maximum	Scaled variables.
ϕ	1000×10^{-7} Weber	$\phi/10^{-4}$
x	$.827 \times 10^{-3}$ m	$x/10^{-3}$
$\dot{x}$	1 m/sec	$\dot{x}/1$
$\ddot{x}$	600 m/sec^2	$\ddot{x}/1000$
F	2 5 N	F/25
S	500×10^4 At/Wb	$S/500 \times 10^4$
K	25×10^8	$K/25 \times 10^8$
$G\frac{d\phi}{dt}$	500	$G\frac{d\phi}{dt}/500$
$S\phi$	500	$S\phi/500$

Magnitude scaling of equations (3.5) and (3.6) gives the following scaled equations:

$$\frac{1}{273.90 \times 10^3} \times \frac{S\phi - 275}{500}(1) = -\frac{d\phi}{dt} / 500$$

or $$\frac{S\phi - 275}{500}(1) = -273.90 \times 10^3 \frac{d\phi}{dt} / 500$$

This may be rewitten in the form :

$$\frac{S\phi}{500}(1) - \frac{275}{500}(1) = -273.90 \times 10^3 \frac{d\phi}{dt} / 500 \qquad (3.7)$$

$$\frac{d^2x}{dt^2} / 1000 = 125 \times 25 \times 10^{-3} \frac{K\phi^2}{25} - 61.3125 \times 10^{-3} (1)$$

$$- .125 \times 10^{-3} \frac{dx}{dt} - 970.8 \times 10^{3} \times 10^{-6} \times \frac{x}{10^{-3}} \quad (3.8)$$

The computer flow diagram of the scaled equations (3.7) and (3.8) is shown in fig. 3.15. The potentiometer settings for the relay are listed in table 3.5. The settings of Pots 00, 01, 25 and 27 are given again in this table for showing them together with other potentiometer settings.

Table 3.5 Potentiometer settings.

Potentiometer No.	Setting	Constants involved in equations (3.1) and (3.2)
02	.5498	Ni_s
16	.1824	$\frac{1}{G}$
00	.72	
01	.3644	
25	.5017	
37	.2581	
35	.313	
36	.0613	F_o
32	.9708	c
33	.1	
38	.0125	
28	.827	
26	.2682	

The initial conditions for the integrators in this case are all zero. The integrators' time constants are listed in the following table. The designations of the integrators are arbitrary as mentioned earlier.

Table 3.5a

Integrator No.	Time Constant Second
13	.01
07	.001
06	.001

For displaying on the oscilloscope the present problem does not need time scaling. But for the x-y recorder which is a slow device, the time scaling is essential. It was required to slow down the problem by a factor of 100, which could be done by dividing each integrator gain by the same factor. In the computer, there is already an arrangement which permits slowing down a problem by a factor of 100, by operating a push button. When the push button is pressed in, the problem speeds up by a factor of 100. The integrator time constants were chosen in the 'pushed-in' configuration of the button. It is, therefore, obvious that when the push button is out the problem slows down by a factor of 100.

The complete programme diagram in fig. 3.15 consists of the logic

circuits and a circuit for simulating non-linear spring load in addition to the computer circuit needed for solving equations (3.1) and (3.2). In this, the upper part is for the electrical equation and the lower part is for the mechanical equation. The two parts are connected through different computing components as indicated before in sec.3.2.

In the programme diagram generated 'S' is fed into multiplier 03 to get 'Sϕ'. The designation of multiplier 03 is done so, because it works in conjunction with amplifier 03. To generate the magnetic pull, the product of 'K' and 'ϕ^2' is accomplished in multiplier 23. Potentiometers 32, 35, 38 and 36 are used to simulate the spring retractile force, magnetic pull, frictional damping force and initial load / and the output of these potentiometers respectively, are fed into summer 27. The output of the summer would obviously give the acceleration when properly scaled. Comparator 23 is used to provide logic facility to simulate the condition that the velocity is zero when the armature reaches the pole face of the electromagnet. Comparator 22 is also used to provide digital facility to simulate the condition that the armature cannot move till the attractive force overcomes the initial load.

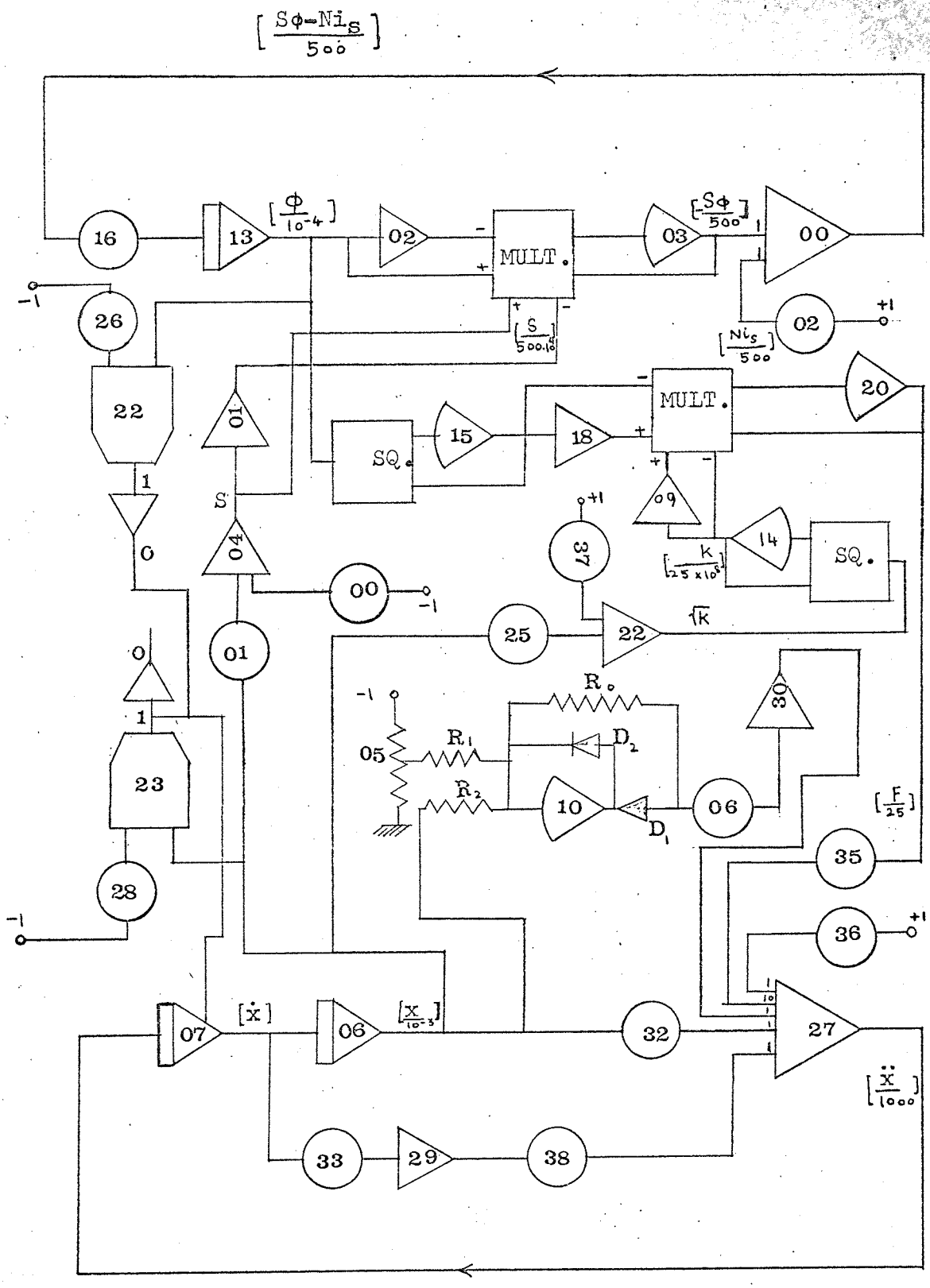

Fig.3.15 Analogue-computing flow diagram

3.9 Operation

The computer can be controlled by various push buttons in the control panel.

For displaying the results on the oscilloscope the computer was operated in the repetitive computation mode under the control of the master or slave timer. If the reset time is short then the behaviour of the system in varying conditions can be observed on the scope by changing the problem parameters. For recording the characteristics on the x-y recorder, the computer was operated in the ordinary computation mode after slowing down the problem by a factor of 100 in this case.

Chapter 4

ANALYSIS ON THE COMPUTER

4.1 Introduction

The dynamic characteristics available from the analogue computation for specific cases are presented and discussed. The linear and non-linear load cases are treated in detail and the computed characteristics are shown. A test of stability is presented and this is very important in selecting the spring load.

The computed results indicate clearly that the performance analysis and synthesis may be made on the computer. Moreover, they reveal some interesting phenomena one of which is, the magnetic pull is influenced by the spring load in a load controlled relay. The analysis on the computer also justifies the assumption that the pull varies linearly with the position of the armature during operation and this assumption may be used to develop a theory for calculating the time of operation for a specific design.

4.2 Analysis on the computer

After simulating an electromagnetic relay on the computer, a study of the dynamic behaviour for a wide range of variation of the input steady state power, mass, spring load, magnetic circuit constants and other parameters, may be possible. As the change of potentiometer settings can change the value of the constant parameters of the simulated system, it is quite easy to see the variation of the characteristics on the oscilloscope or plot them on the x-y recorder.

As indicated in the preceding paragraph, the analysis may be made for changing parameters such as, different spring loads, final magnetomotive forces and magnetic circuit designs easily and quickly. The characteristics which may be of interest are flux vs. position, $\frac{d\phi}{dt}$ vs. time, velocity vs. time, M vs. time, ϕ vs t, ϕ_g vs. position etc. A test of stability of the aramature motion for various spring combinations, different leakage permeances and other varying conditions is possible. The motion of the armature is stable, if there is an absence of negative velocity which can be seen clearly in the computed velocity relations.

4.3 A linear load case

A relay having a linear load characteristic was studied. Numerical values of the parameters are given in sec. 3.7. The potentiometer settings are the same as given in table 3.5.

The constant voltage applied to the coil circuit is such that it gives rise to a steady-state current of 11 mA. The computed results are discussed in the following.

Core flux (ϕ) vs time characteristic

Oscillogram 1 in fig. 4.1 shows the characteristic. The total time of flux growth is 245 milliseconds. Of course, the armature finished its journey before this time. The flux rise is not exponential and there is a marked dip in the curve due to the motion causing a great change of inductance.

The final value of the flux after 245 ms. is 1080×10^{-7} weber.

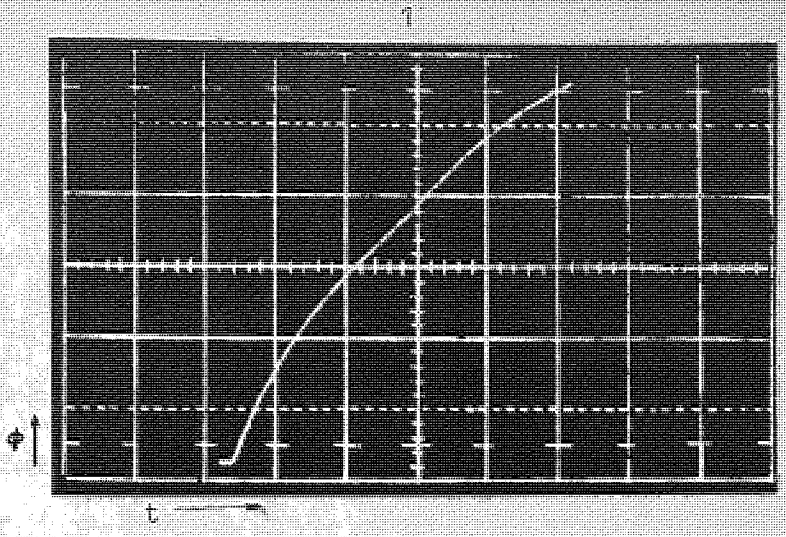

Time scale: 10ms/scale division

Flux scale : 40×10^{-7} Weber/scale division

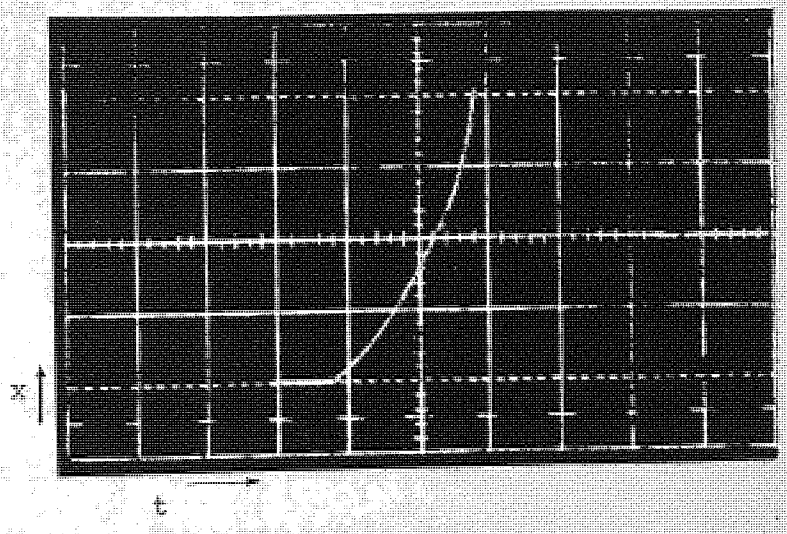

Time scale: 10ms/scale division

Position scale: 04mm/scale division

Fig.4.1 Core flux(Φ)vs.time(oscillogram1) and armature position vs. time(oscillogram2) at M_s=275 At. A linear load case.

In the oscillogram the time was measured from left to right and the horizontal portion represents the reset time of the computer, which is 10 ms. The computed flux at the end of the armature motion is 705 x 10^{-7} weber, and this occurs at 131 ms. The measurement on an actual relay having the almost same parameters but with a different spring load characteristic which is comparable, is shown in oscillogram 1 of fig.7.2 which gives the measured flux at the end of the motion to be 674 x 10^{-7} weber. The computed and measured values lie within a reasonable limit.

Position vs. time characteristic

Oscillogram 2 in fig. 4.1 shows the characteristic. The curve is steep in the later part. The length of the horizontal portion of the trace is 44 ms. in the time scale and consists of the reset time of the computer and the "waiting time" of the armature, the latter one of which is 34 ms. Therefore, it takes 34 ms. to overcome 50 gf initial load. Oscillogram 1 in fig. 4.2 shows the ϕ vs. t (upper trace) and position vs. time (lower trace) relation in the same picture for comparison. The flux grows to a value determined by the back tension before the motion commences. The displacement of the armature in 97 ms. which is the "motion time", is .827 mm and the total time of operation is 131 ms. The movement is very fast in the end. The nature of the computed characteristic is similar to the measured one for a linear load, given in fig. 5.2 (oscillogram 2)

1

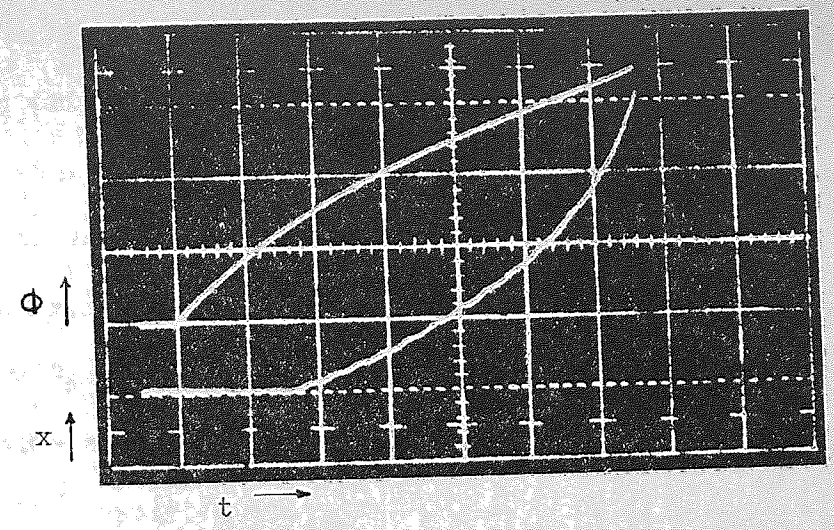

Time scale:4ms/scale division, position scale: .04mm/scale division, flux scale: 40×10^{-7} Wb/scale division

2

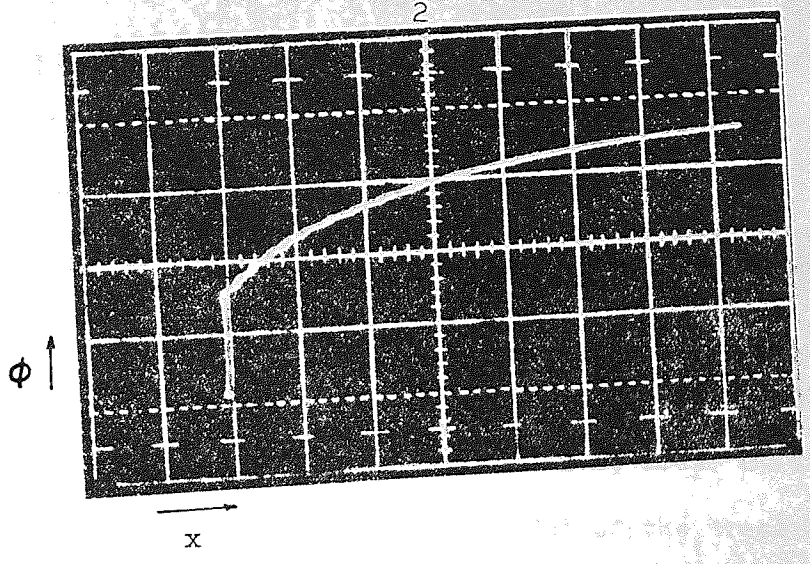

Position scale: .022mm/scale division, flux scale: 40×10^{-7} Wb/scale division.

Fig. 4.2 Oscillogram 1: Flux vs. time (upper trace) and position vs. time(lower trace). Oscillogram 2: Flux vs. position.

Flux vs. position characteristic,

Oscillogram 2 in fig. 4.2 shows the flux vs. position characteristic for a linear load. The flux attains a particular value at x = 0, give rise to a pull to overcome the back tension and then varies with the position in a very complicated manner. This characteristic is very significant in the theory explained in section 7.3 to consider the extension of Ahlberg's method. At x = 0, the value of flux is 280×10^{-7} weber and at x = .827 mm it is 705×10^{-7} weber.

Magnetomotive force (M) vs. time characteristic:

The upper trace of oscillogram in fig. 4.3 shows how instantaneous magnetomotive force changes with time. The m.m.f. and current relations are similar in nature. In fact, current can be computed from the m.m.f. relation just by dividing m.m.f. values by N, the number of turns in the relay coil. Magnetomotive force or current varies in a very complicated manner and finally decreases at the end of the armature motion due to the rapid change of inductance. In the beginning when armature does not move, i.e., up to 34 ms. the variation appears to be exponential. End of the trace here marks the end of the motion. The maximum value of the m.m.f is 175 At and this occurs at 109 ms. from the switching on of the current. Therefore, the maximum current at that moment is 7 mA.

Pull vs. time characteristic:

The lower trace of oscillogram 2 in fig. 4.3 shows the dynamic pull characteristic. The pull, unlike the current or magnetomotive

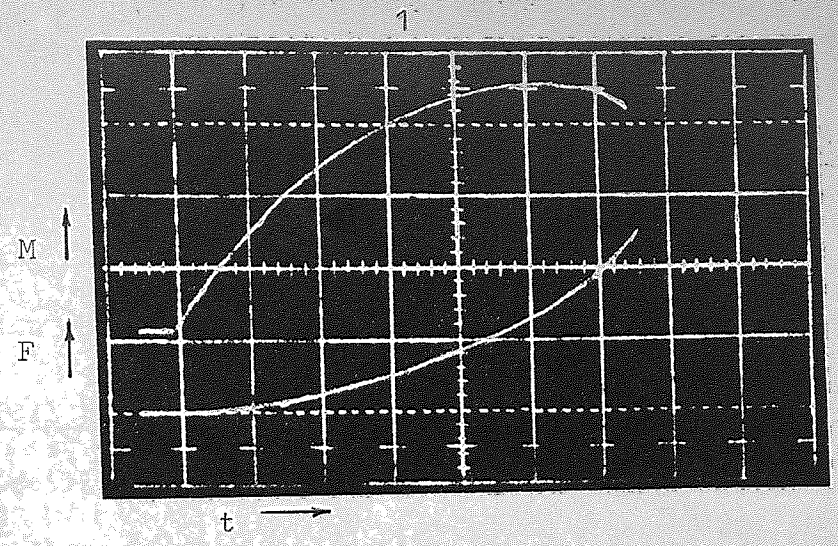

t:4ms/div,F:.5N/div.,M: 10At/div.

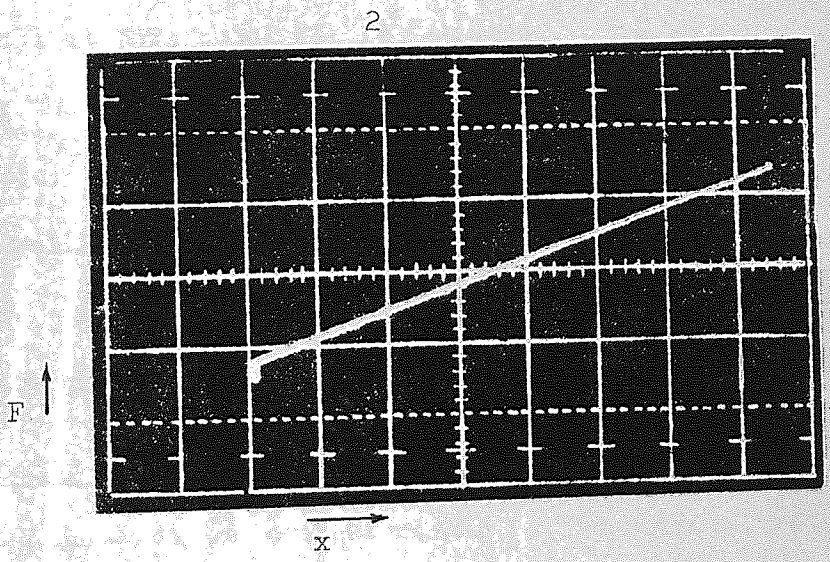

x:.022mm/div.,F: .5N/div.

Fig. 4.3 Osc.1: Instanteneous mmf vs. time(upper trace) and pull vs. time(lower trace). Osc.2: Pull vs. position

force, increases continuously with time and attains the maximum value at the end of the operation in this case. Whereas the maximum value of current occurs sometime before the end of the motion. The maximum pull is 7 Newton. The spring load at the position when the armature is operated is 6.42 N.

Pull vs. position characteristic:

Oscillogram 2 in fig. 4.3 shows the characteristic. The pull varies linearly with the position of the armature in this case. The vertical portion of the curve shows that at x = 0, the pull attains a value to overcome the back tension and the computed value of the pull at this point is .4975 Newton. The final value of the pull from the curve is 7 Newton. The spring load at this point is 6.42 Newton.

The pull vs. position characteristic suggest that the variation is linear. An analysis was made to test this linearity and the results are presented in sec. 4.

Velocity vs. time characteristic:

Fig. 4.4 shows the characteristic. The computed velocity was recorded in the x - y recorder. The variplotter was used for recording. The values of the velocity obtained there by, are plotted fresh against the corresponding values of the time as shown in the figure.

Acceleration vs. time characteristic:

Fig. 4.5 shows the characteristic. The computed acceleration like the velocity was recorded in the x-y recorder.

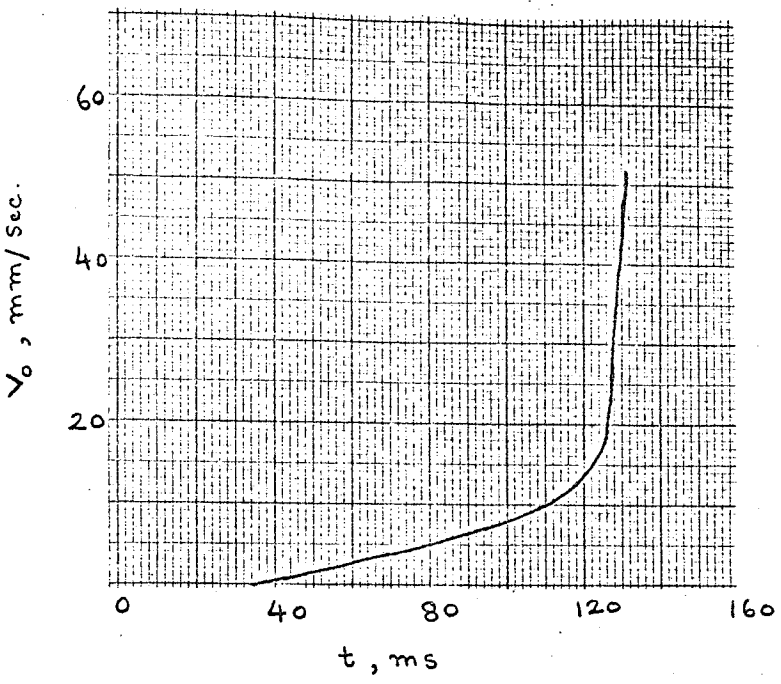
60
40
20
V_o, mm/sec.
0
40
80
120
160
t, ms

Fig. 4.4

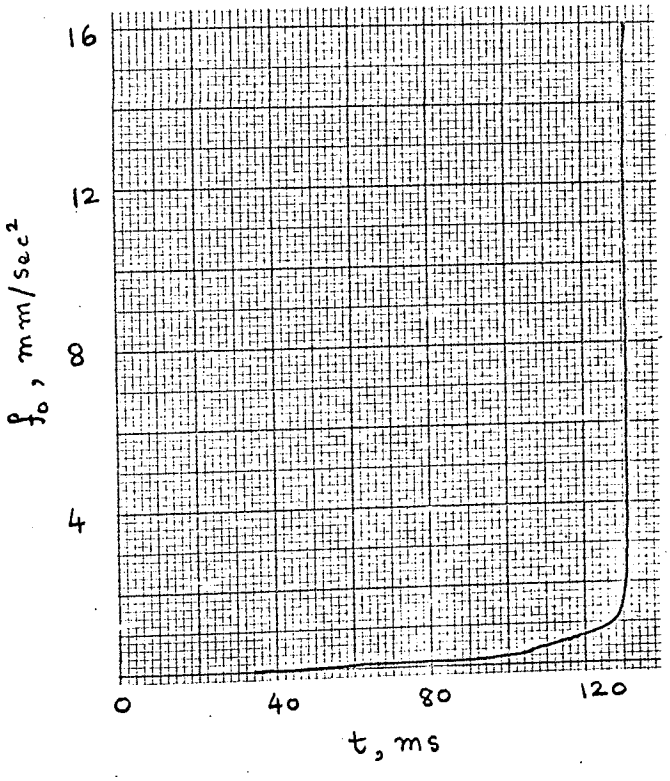
16
12
8
4
f_o, mm/sec^2
0
40
80
120
t, ms

Fig. 4.5

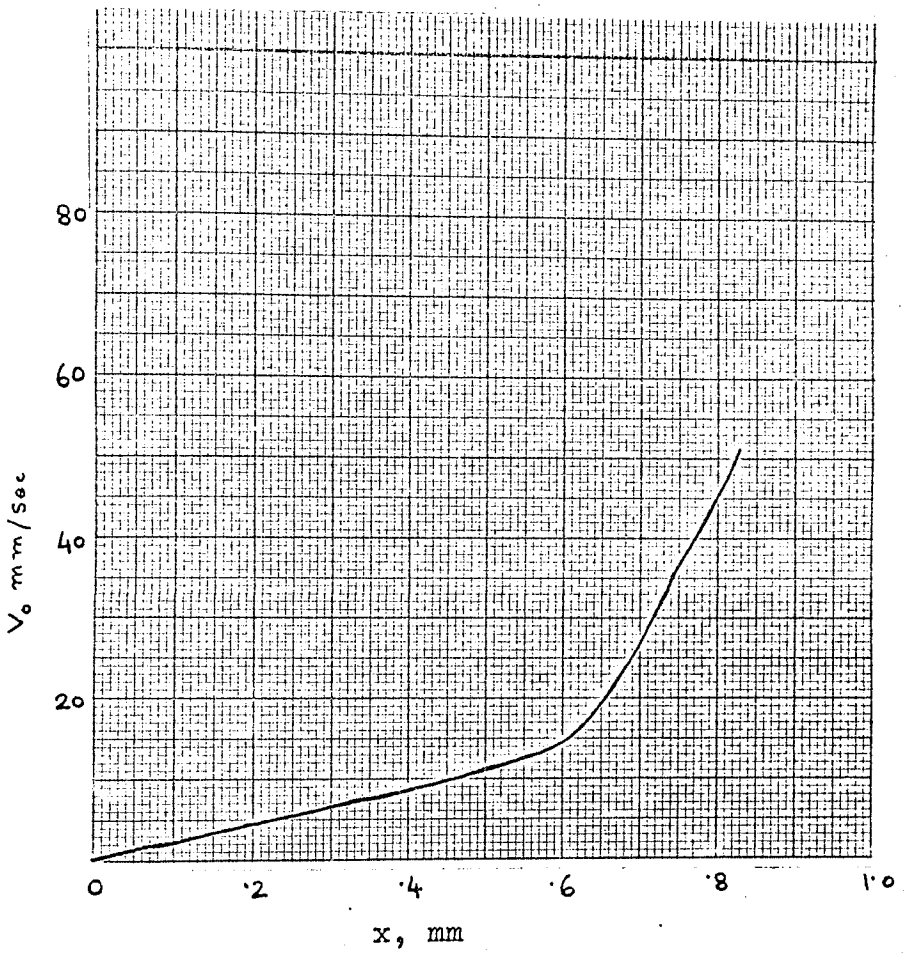

Fig. 4.6

Velocity vs. position characteristic:

This was recorded in the x-y recorder. Fig. 4.6 shows the characteristic. Coming to the cases of velocity and acceleration it is clear that both are great at the end. It can be seen in the velocity vs. position characteristic that velocity in the early portion of the travel is small and gradually increases and quite high in the later section of the travel.

4.4 The same linear load case described in sec. 4.3, but with different feeding voltage.

The study was made on the same relay mentioned in sec. 4.3. The constant voltage across the coil circuit is different in this case, obviously the steady state current is also different. The current is 9 mA and the final magnetomotive force is 225 At. The computed characteristics are shown in figs. 4.7, 4.8, 4.9, 4.10 and 4.11. The characteristics in figs. 4.7 and 4.8 were displayed on the oscilloscope and photographed. Whereas, the characteristics in figs. 4.9, 4.10 and 4.11 were recorded in the x-y recorder after slowing down the problem 100 times by changing the integrator's gain. The setting of Pot 02 in fig. 3.15 was .45. Other potentiometer settings are given in table 3.5

The characteristics are discussed in the following

Core flux vs. time: Oscillogram 1 in fig. 4.7 shows the characteristic. The maximum flux is 900×10^{-7} weber and the time of the growth is 300 ms. When the final current is 11 mA,

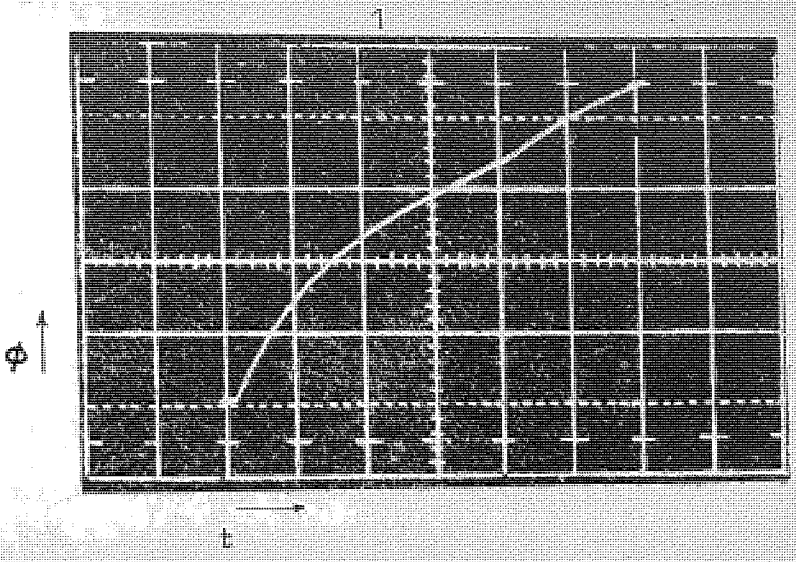

t: 10ms/div., Φ = 40x10^{-7}Wb/div.

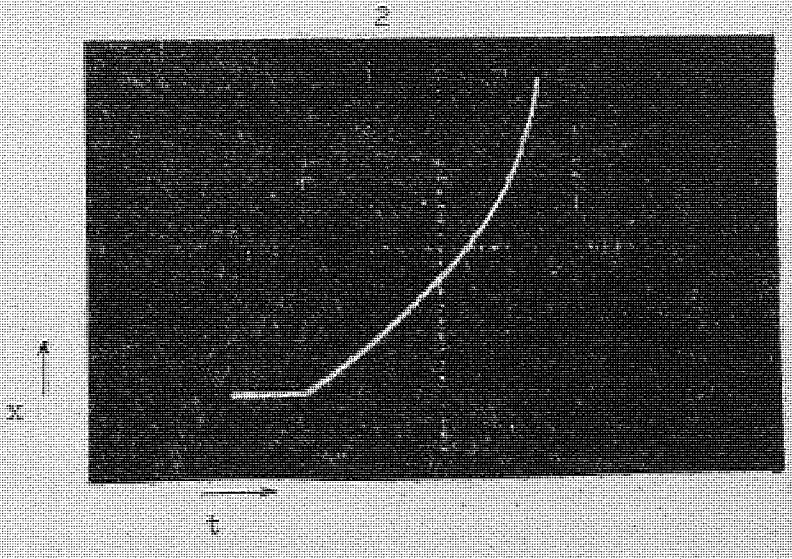

t:10ms/div., x: .04mm/div.

Fig. 4.7 Core flux(Φ)vs. time(Osc.1) and x vs. t(Osc.2) at M=225At. A linear load case.

the value of flux is 1080 x 10^{-7} Wb and the time is 245 ms. The value of flux at the position where the armature finishes its journey in the present case is 684 x 10^{-7} Wb. In the '11 mA' case it is 705 x 10^{-7} Wb. The difference is small. From this it is clear that the motion of the armature regulates the flux generating a back e.m.f. in the coil so that the flux value at the end of the motion is not high because of high feeding voltage which might accelerate the motion on the other hand. Of course, the flux increases afterwards to a high value rapidly. The patterns of the two oscillograms for '9 mA' and '11 mA' are similar.

Position vs. time: Oscillogram 2 in fig. 4.7 shows the characteristic. The horizontal portion of the trace represents in time scale the combination of the reset time of the computer and the 'waiting time' of the relay. The latter one is 45 milliseconds. The final value of x is .827 mm and the time to cover this distance is 212 milliseconds.

Magnetomotive force (M) vs.time: Oscillogram 1 in fig. 4.8 shows the relation (upper trace). The magnetomotive force and so the current varies in a very complicated manner and there is a marked depression at the end of the travel due to the rapid change of inductance. The maximum value of mmf. is 175 At. which occurs at 170 ms. In the '11 mA' case the maximum value is 175 At which occurs at 109 ms. It is significant that the mmf. values in the two cases are equal. Of course, the times are different. In both cases the same current is required to overcome the back tension, but the 'waiting times' are

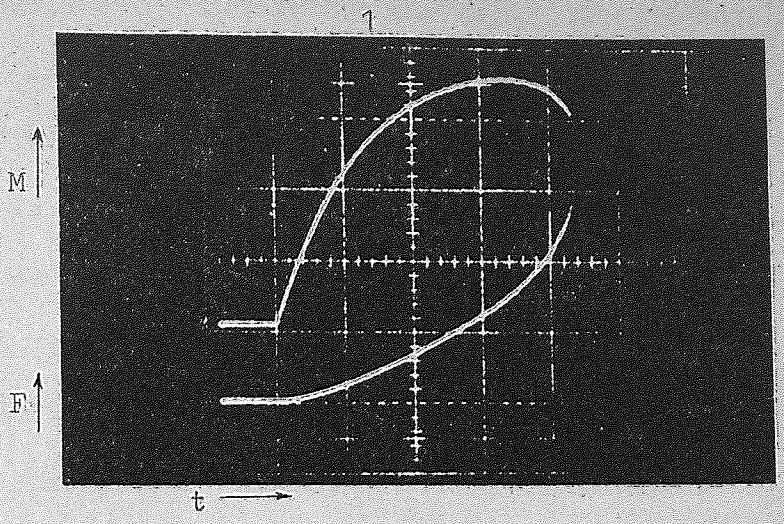

t: 10 ms/div., M: 10 At/div., F: .5 N/div.

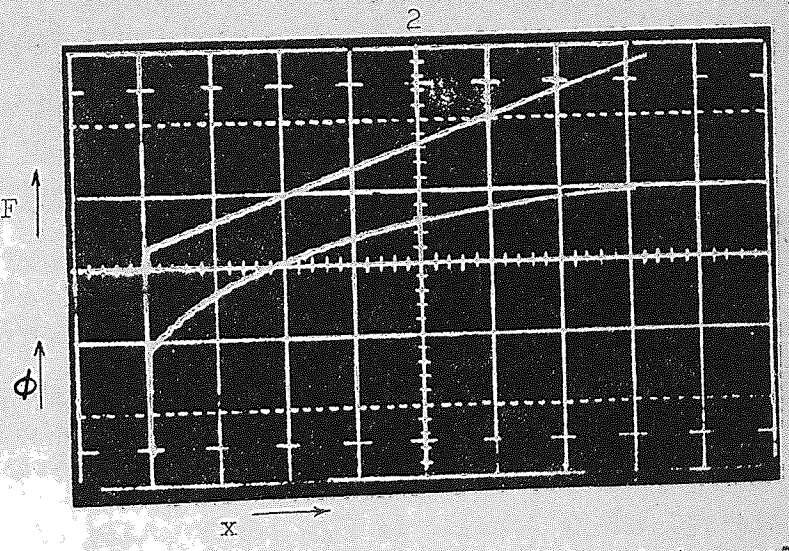

x: .022 mm/div., F: .5N/div., ϕ :40x 10^{-7} Wb/div.

Fig. 4.8 Showing M (upper trace) and F(lower trace) ϕ vs. time in osc.1; F (upper trace) and (lower trace) vs. position in osc.2.

different. The time is 45 milliseconds in the present case and the mmf. curve is exponential up to this time and approximately so up to a little further. From the equal values of the mmf's in the two cases, it signifies that there is an electrodynamic regulation of current in the relay coil due to the motion of the armature or in other words the armature regulates the current to keep an equilibrium between the four kinds of forces which influence its motion. Therefore if the current tries to be high enough as in the case of '11 mA', the armature moves faster, causing a greater $\frac{d\phi}{dt}$ which gives rise to a higher back emf keeping the current level down. The whole phenomenon is very complicated, yet it seems that the current cannot grow above a certain limit even if a greater feeding voltage is applied, which only accelerates the motion.

Pull vs. time: Oscillogram 1 in fig. 4.8 shows the variation of the pull with time. The nature of the curve is similar as in the case of '11 mA'. The pull increases continuously and attains a maximum value at the end of the operation. Of course, the pull goes on increasing as the coil current increases when the armature is operated. The value of the pull at the end of the operation is 6.75 Newton.

Pull vs. position: Oscillogram 2 of fig. 4.8 shows the characteristic (upper trace). The pull varies linearly with the position of the armature. At x = 0, pull is .498 Newton and at x = .827 mm. i.e. final position of the armature, pull is 6.75 Newton.

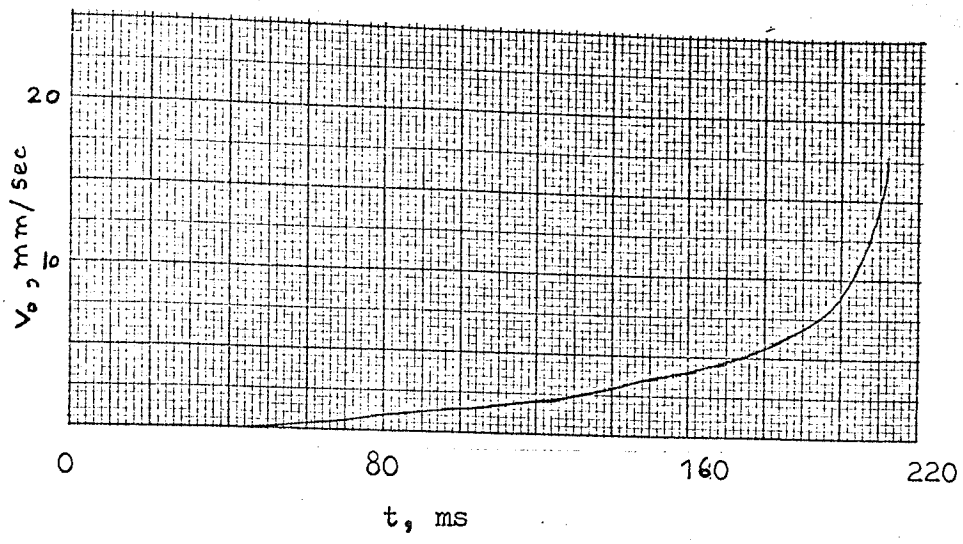

Fig. 4.9

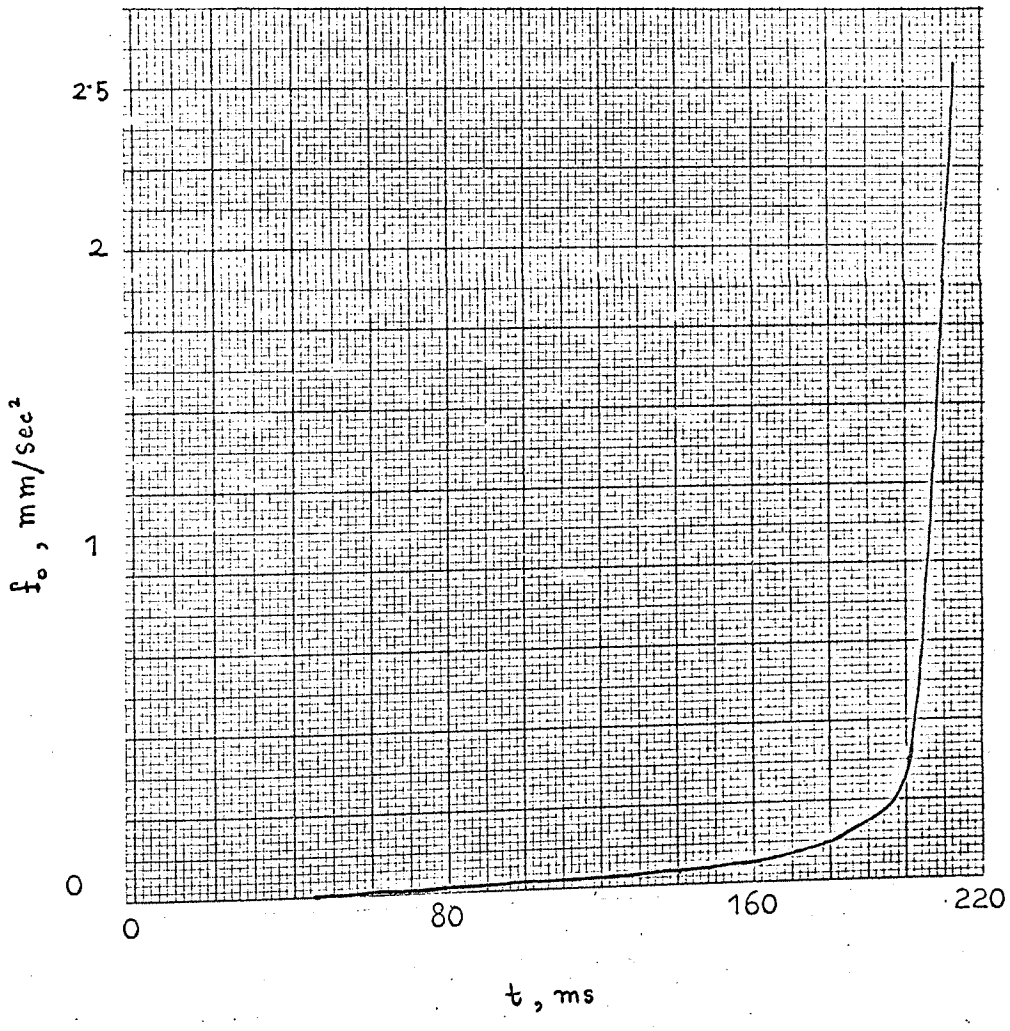

Fig. 4.10

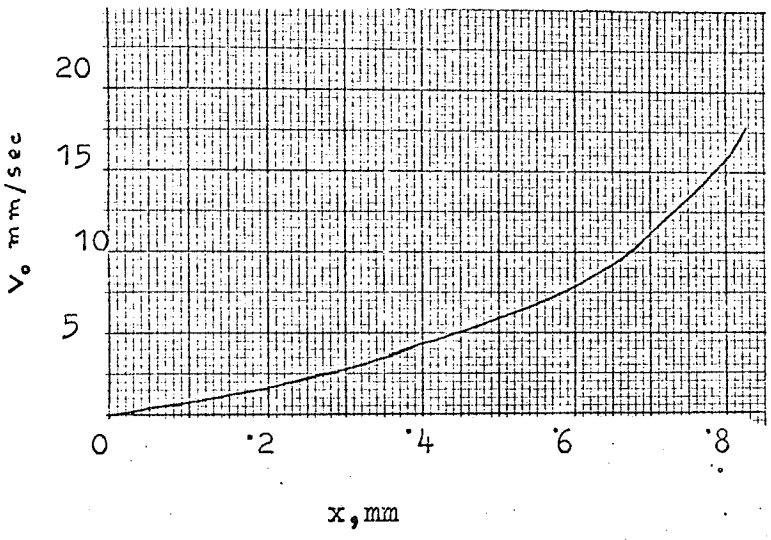

Fig. 4.11

Flux vs. position: Oscillogram 2 of fig. 4.8 shows the characteristic (lower trace) which is similar as in the '11 mA' case. The flux grows rapidly during the early period and the growth is comparatively slow during the later period. The characteristic appears like a parabola.

The velocity vs. time, acceleration vs. time and velocity vs. position characteristics are shown in figs. 4.9, 4.10 and 4.11 respectively.

4.5 A non-linear load case

A relay whose load characteristic is non-linear was studied. The following is a list of the values of the constant parameters.

$m = 8 \times 10^{-3}$ kg

$\gamma = 10^{-3}$ Newton. metre^{-1} second.

$C = 4620$ N/m

$C' = 2620$ N/M

$G = 273.9 \times 10^{3}$ mhos

$G_e = 24.6 \times 10^{3}$ mhos

$G_c = 249.30 \times 10^{3}$ mhos

$N = 25000$ turns

$NI_s = 250$ ampere turns

$R = 2507$ ohms

$I_s = 10$ milliamperes

$S_o = 299 \times 10^{4}$ At/Wb

$S_L = 715 \times 10^{4}$ At/Wb

It was mentioned in sec. 3.5 that C' is a spring constant and the significance of that constant was explained in there.

$A = 1.54 \times 10^{-4}$ metre^2

$x_o = .827 \times 10^{-3}$ metre

$F_o = .4905$ Newton.

The potentiometer settings are given in the following table.

Table 4.1 Potentiometer settings for the non-linear load case

Potentiometer	Setting	Constants involved
16	.1824	$\frac{1}{G}$
02	.5000	Ni_s
00	.7200	
01	.3640	
25	.5017	
37	.2581	
36	.0613	F_o
32	.5778	C
33	.1000	
38	.0125	
28	.8270	
26	.2708	
05	.41	x_1
06	.3278	C'

The characteristics from the computation are discussed in the following.

Flux vs. time:

Oscillogram 1 in fig. 4.12 shows the characteristic which is similar as in the other two previous cases in secs. 4.3 and 4.4. The variation is not exponential. The motion causes slight dip in the characteristic. The flux was computed for 291 milliseconds. Of course, the time of operation found from the timer controlling the computing time, is 121 milliseconds. The value of the flux attained after 291 ms is 1050×10^{-7} Weber. ϕ becomes 640×10^{-7} Weber at the end of the operation

M vs. t

Oscillogram 2 in fig. 4.12 shows the characteristic (upper trace). The change of the slope of the load curve affects the motion which influence the current in the coil. There is a little depression at a point in the curve. In this case the maximum current occurs almost at the end of the operation. This current is 5.9 mA and the current at the end of the travel is 5.2 mA.

Pull vs. time

Oscillogram 2 in fig. 4.12 shows the characteristic (lower trace). The mode of variation or the nature of the curve is apparently similar to the curves of the other two cases. The pull attained after 121 milliseconds is 5.5 Newton.

Spring load vs. position

Oscillogram 1 in fig. 4.13 shows the simulated non-linear spring

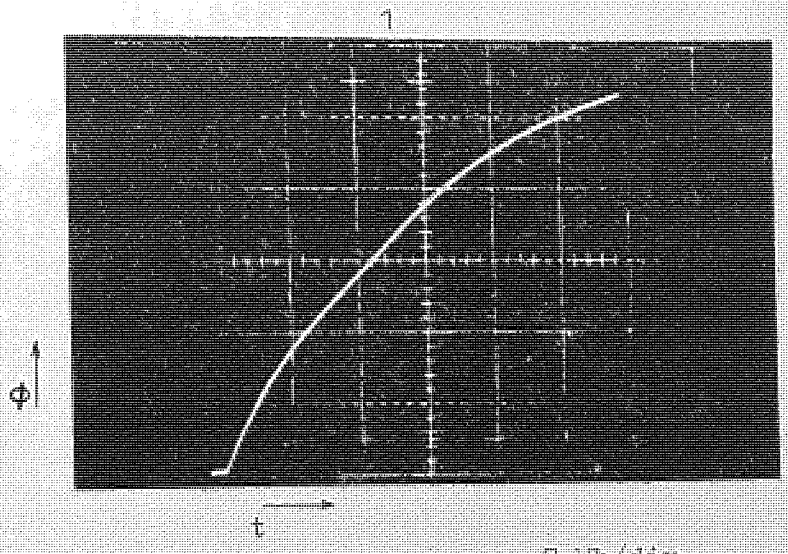

t: 10 ms/div., Φ:40x10^{-7} Wb/div.

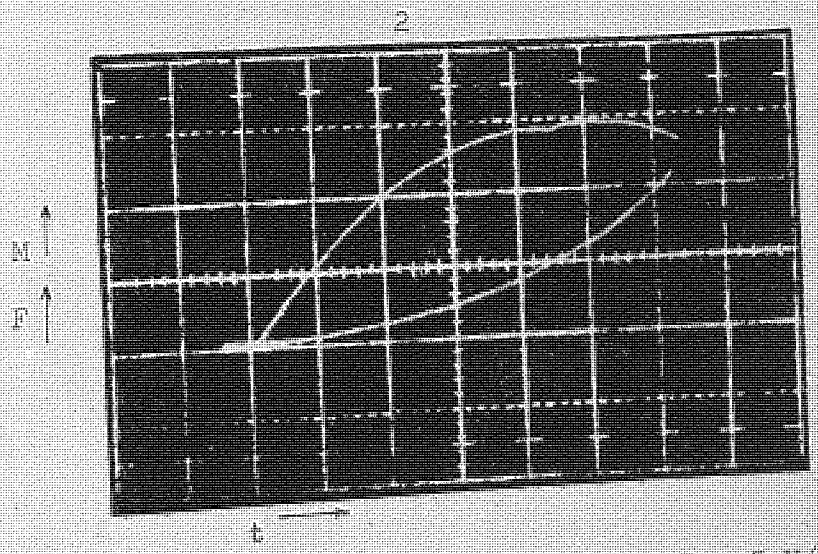

t: 4 ms/div., M: 10 At/div., F: .5 N/div.

Fig. 4.12 Osc.1: Φ vs. t; osc.2: M vs. t(upper trace), F vs. t (lower trace).

1

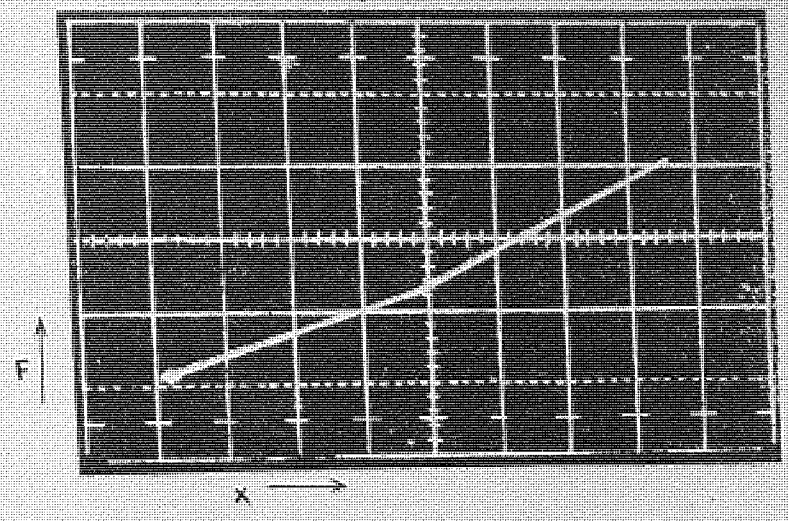

x : ·022 mm/div. ; F : ·32 N/div.

2.

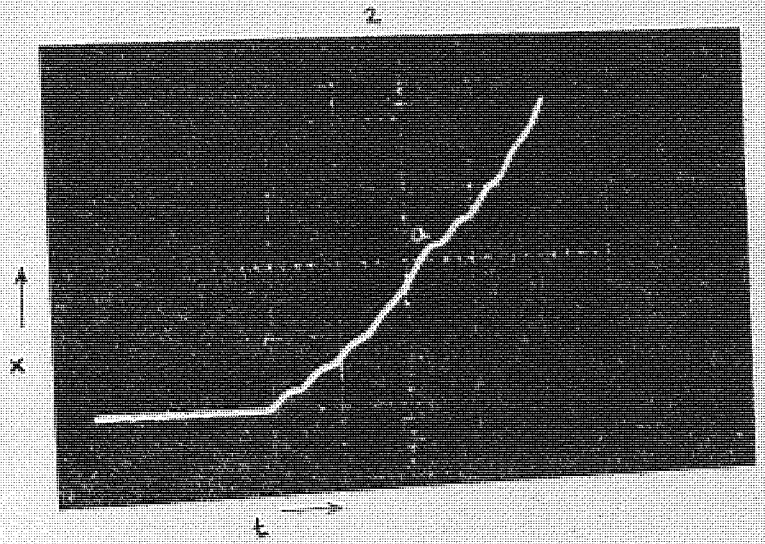

t : 4 ms/div. ; x : ·04 mm/div.

Fig. 4·13

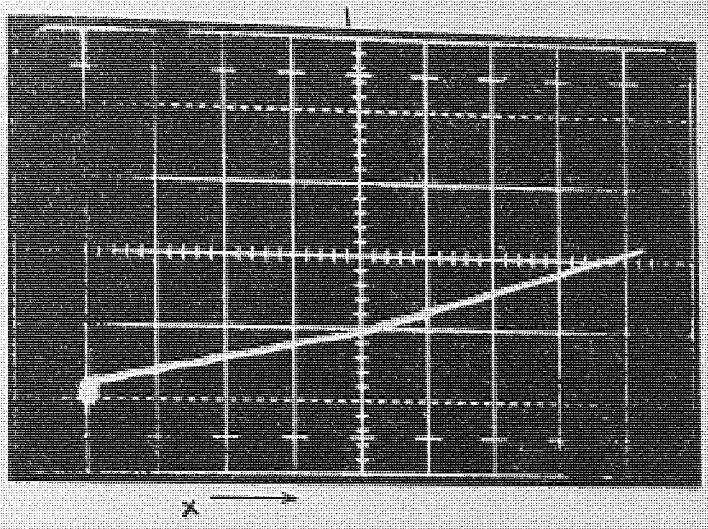

X : ·022 m m/ div. , F : ·5 N/ div

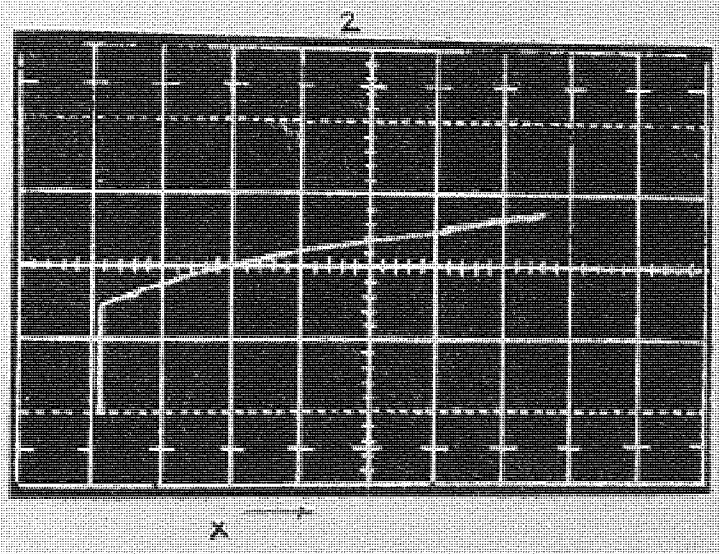

X : ·022 m m/ div. , Φ : 40 x 10⁻⁷ / div.
Wb

Fig. 4·14

load relation. The initial value is 50 gf.

x vs. time:

Oscillogram 2 in fig. 4.13 shows the computed relation. The pattern of the curve is almost similar to the x vs. t characteristics in secs. 4.3 and 4.4. The position where the slope of the load characteristic changes is clear in the trace and the point is marked by the letter 'a'. The waiting time t_w is 42 milliseconds. The time of operation is 121 ms and the motion time is 79 ms. The distance travelled by the armature in 79 ms. is .827 mm. The distance at which the slope of the load curve changes is .41 mm.

Pull vs. position:

Oscillogram 1 in fig. 4.14 shows the characteristic. The pull varies linearly at first then changes its slope at a point and varies linearly again. The pull varies linearly in each of the two sections of the curve and follows the spring load characteristic. i.e. the pull curve changes its slope when the load curve does. The position at which both the curves change their slope is .41 mm. It appears that the pull is greatly influenced by the load in this particular case.

Flux vs. position:

Oscillogram 2 in fig. 4.14 shows the relation. The variation is quite complicated.

4.6 Stability of the armature motion.

This can be tested on the computer for various conditions. A test was performed for a non-linear load case. The simulated load is shown in fig. 4.15 (oscillogram 1). The potentiometer settings are given in the following table.

1

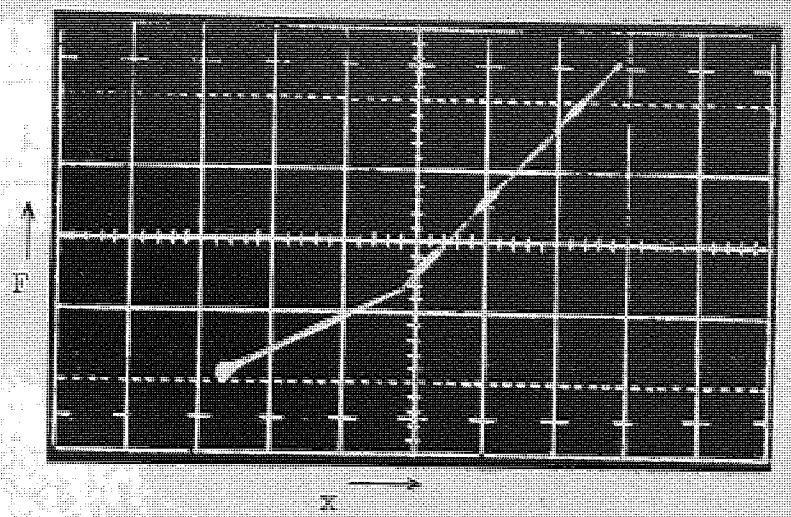

x: .0290 mm/scale div.

F: .162 N/scale div.

2

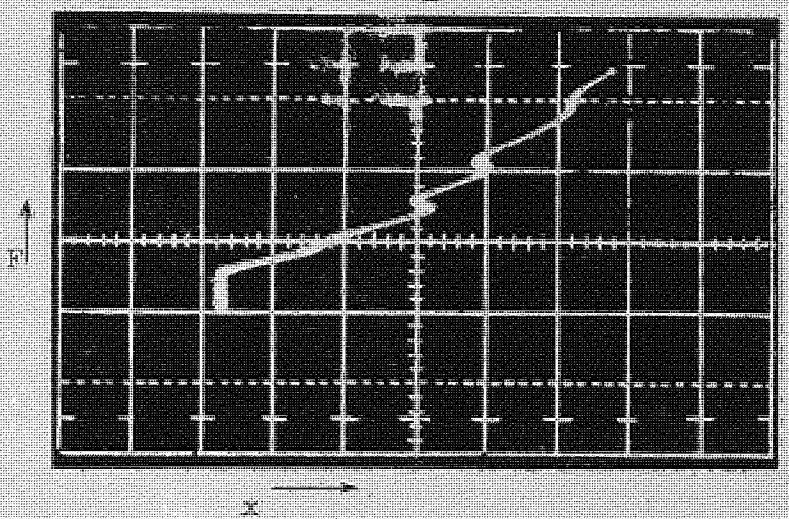

x: .0290 mm/scale div.

F: .25 N/scale div.

Fig. 4.15 Oscillograms showing the simulated spring load characteristic and the computed dynamic pull characteristic (osc.2)

Table 4.2 Potentiometer settings

Potentiometer	Setting
02	.5414
16	.1824
00	.72
01	.364
25	.5017
37	.2581
36	.0613
32	.3160
33	.1
38	.0125
28	.827
26	.2782
05	.3680
06	.3996

The computed dynamic pull vs. position characteristic is shown in fig. 4.15 (oscillogram 2). This may be called the dynamic load characteristic. Oscillogram in fig. 4.16 shows the variation of x with time. These two characteristics show clearly that the motion becomes unstable at two positions, i.e. the negative velocities occur. Therefore in this specific case the motion is unstable.

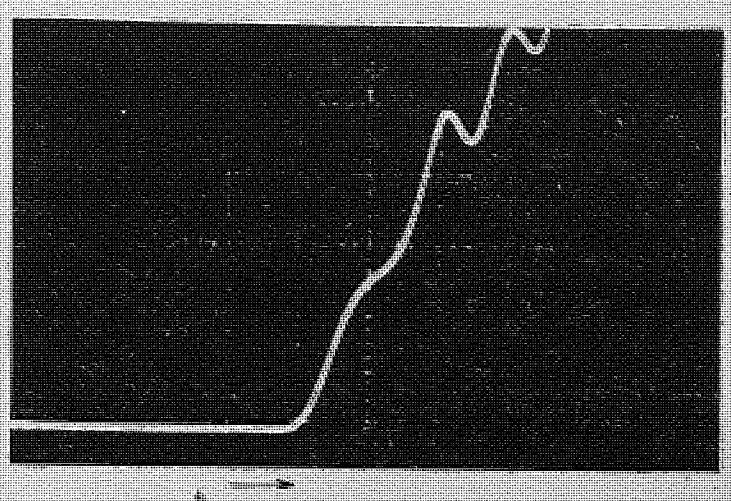

t: 10 ms/div.

x: .02 mm/div.

Fig. 4.16 x vs. t

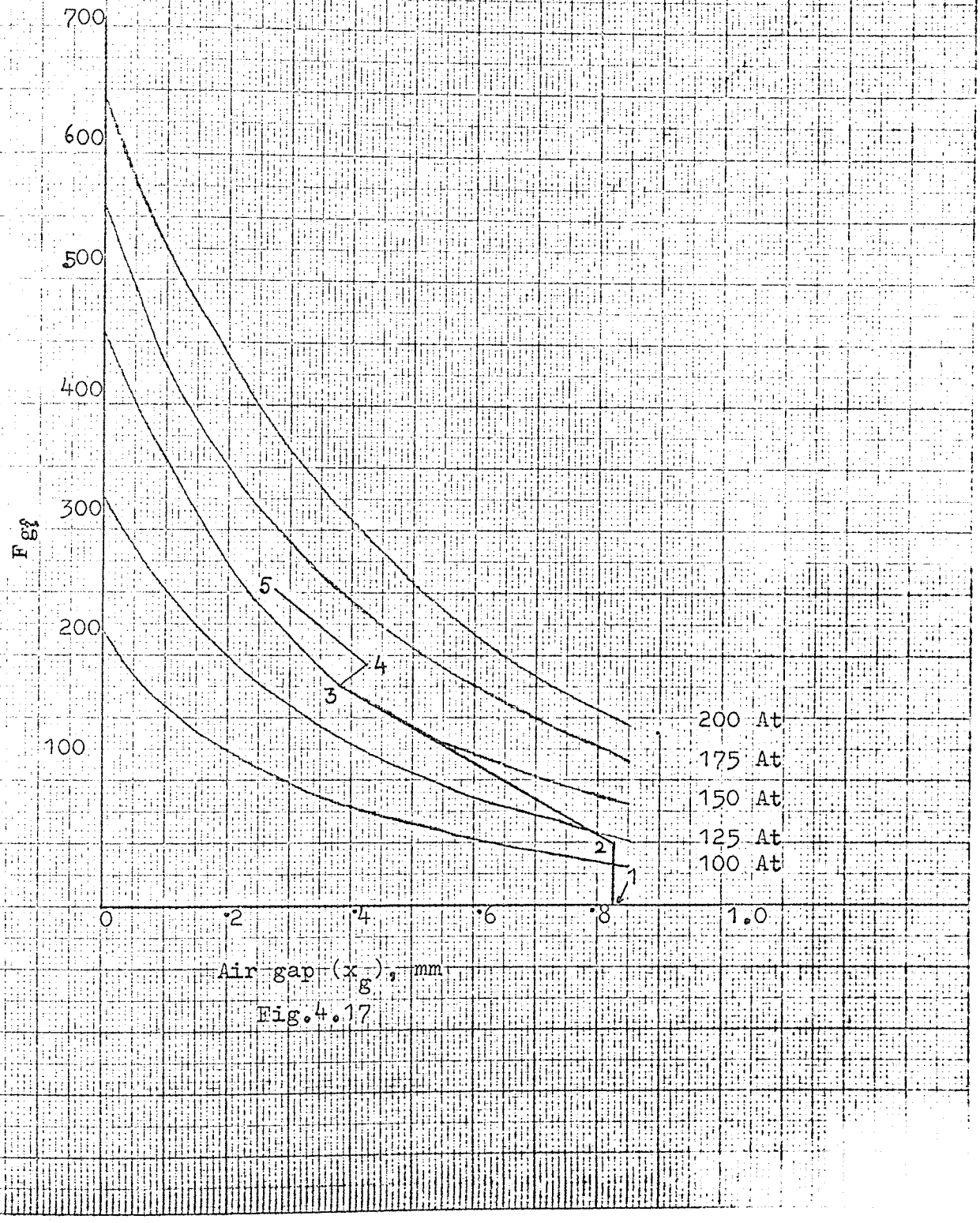
700
600
500
400
300
200
100
F_{gf}
5
4
3
2
1
200 At
175 At
150 At
125 At
100 At
0
·2
·4
·6
·8
1.0
Air gap (x_g), mm

Fig.4.17

The velocity formula (7.33) deduced in sec. 7.6 indicates that $\frac{1}{2\delta_p} + s - a$ must be a positive quantity when the direction of motion is positive. This may be verified from the computed results.

The steady state pull characteristics of the simulated relay are the same as for the test relay mentioned in sec. 7.3. The pull characteristics were measured on the latter relay and are given in sec. 11.7. Fig.4.17 shows these characteristics and the part of the computed dynamic load characteristic, combined in the same diagram. $\bar{s}$ and a may be obtained from this diagram. The need of this diagram and s and a are all discussed in sec. 7.6 Point 3 in the dynamic load curve may be investigated.

At point 3 on line 2 - 3

$$a = .612 \text{ mm}$$

$$s = .478 \text{ mm}$$

$$\frac{1}{2\delta_p} = 6.92 \times 10^{-4} \text{ m} = .692 \text{ mm}$$

$$\therefore \quad \frac{1}{2\delta_p} + s - a = .692 + .478 - .612 = .558 \text{ mm}$$

$$\therefore \quad \frac{1}{2\delta_p} + s - a > 0.$$

It was observed on the computer that the unstable motion occured in this case could be easily avoided by changing the slope of the load curve or other parameters.

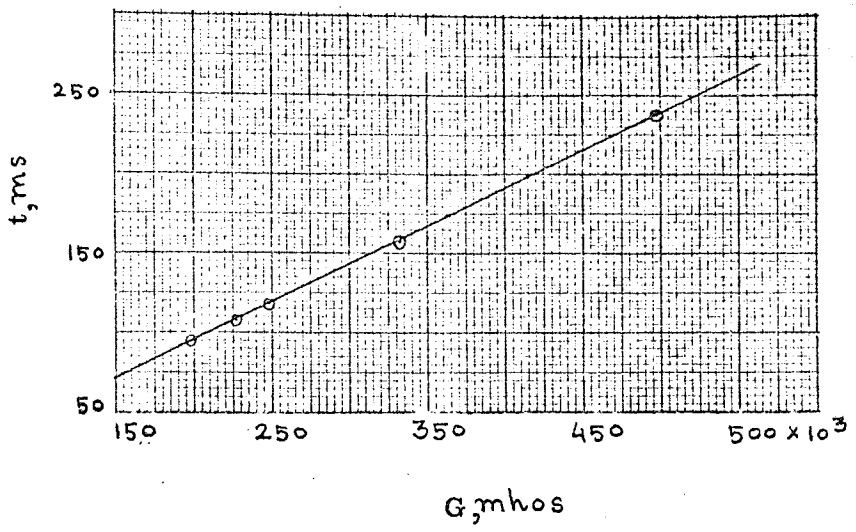

Fig. 4.18

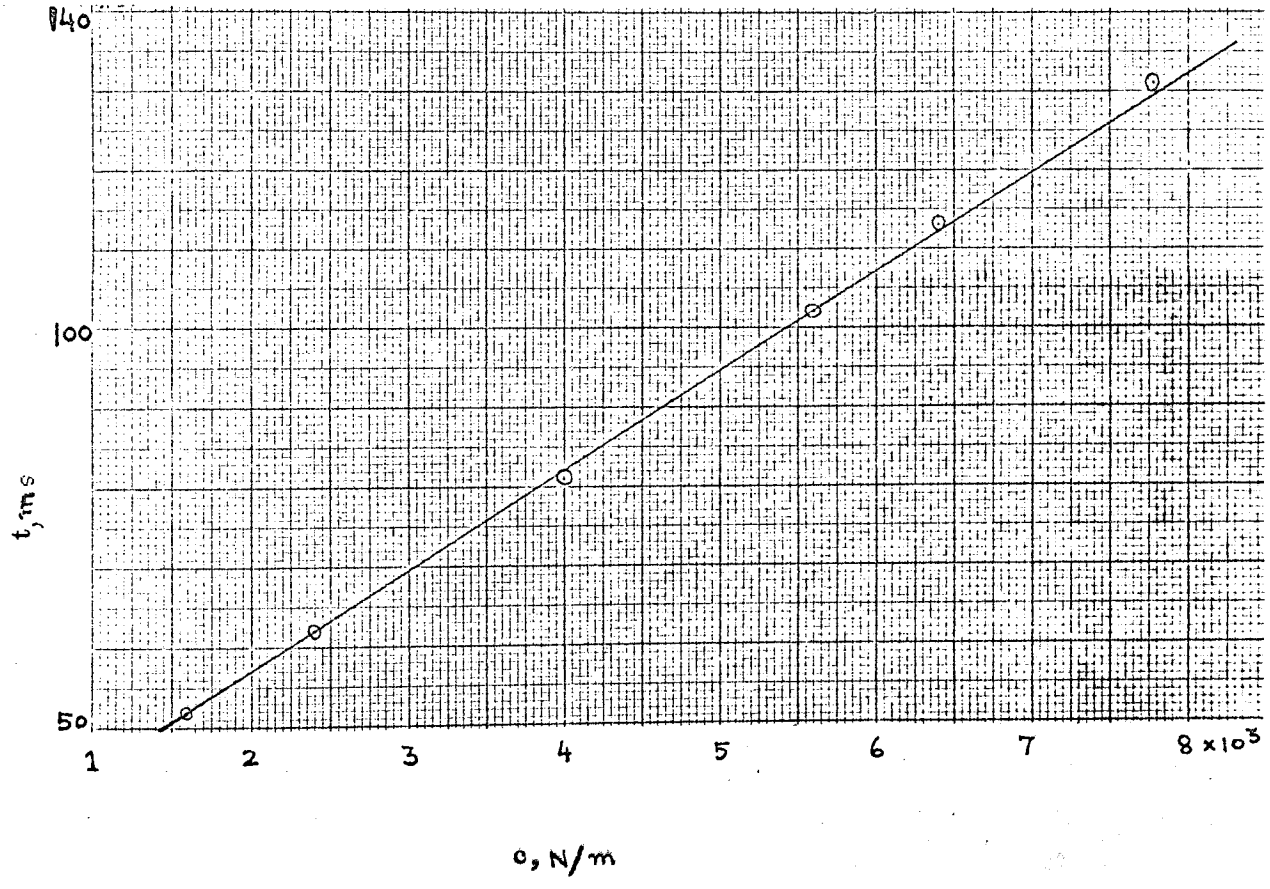

Fig. 4.19

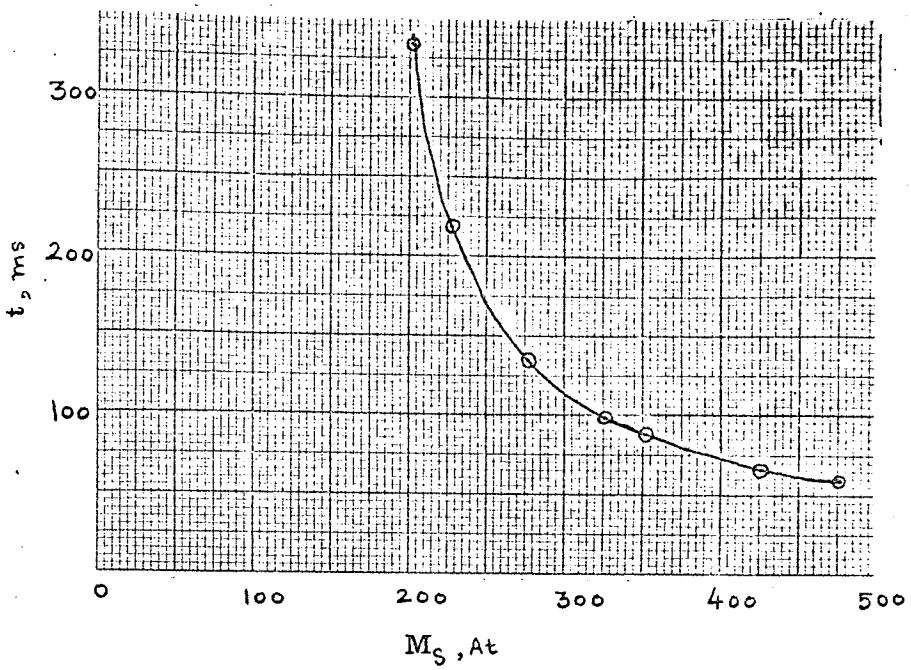

Fig. 4.10

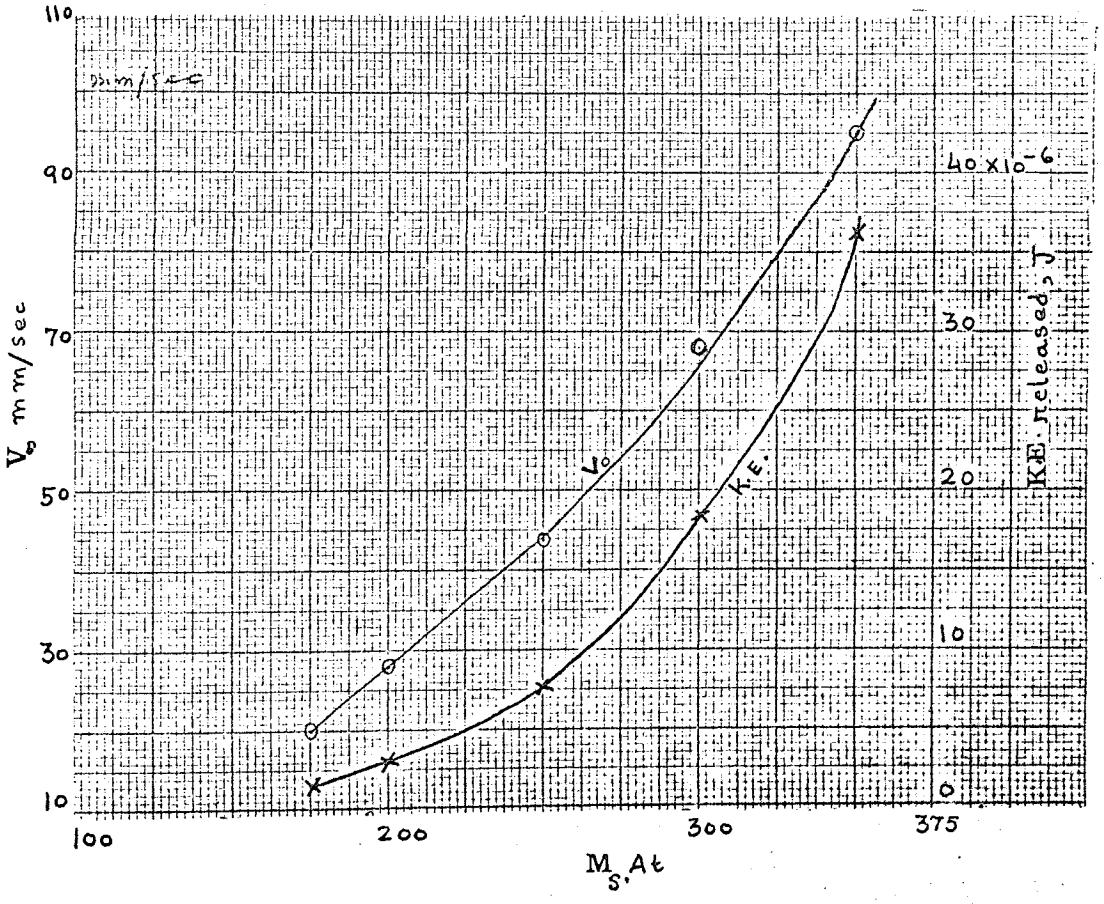

Fig. 4.21

4.7 Computations of velocity, time and kinetic energy.

How the time of operation is influenced by G, C and M_s are shown in figs. 4.18, 4.19 and 4.20 respectively. In each case other parameters were kept constant.

The variation of the final velocity (V_H) and of the extra kinetic energy released in the relay structure, with M_s are shown in fig. 4.21.

4.8 Computed dynamic pull relations

It has been shown in secs. 4.3 and 4.4 that the pull varies linearly with the position of the moving armature. This was analysed more critically by varying different parameters.

All the three traces of oscillogram 1 in fig. 4.22 show the variation of the pull for three different spring loads. All the curves are linear. Oscillogram 2 in the same figure shows the three pull relations for three different masses. All the three relations are linear.

Fig. 4.23 shows the pull relation for the case described in sec. 4.3. The functions K and S were generated exactly by the diode function generators to see whether the characteristic deviates from linearity. The curve is still linear.

From the specific cases studied in this chapter, it is seen that the pull varies linearly with the position of the moving armature. The conclusions from the specific cases do not necessarily generalise a phenomenon, but it may be interesting to develop some design principles based on this property.

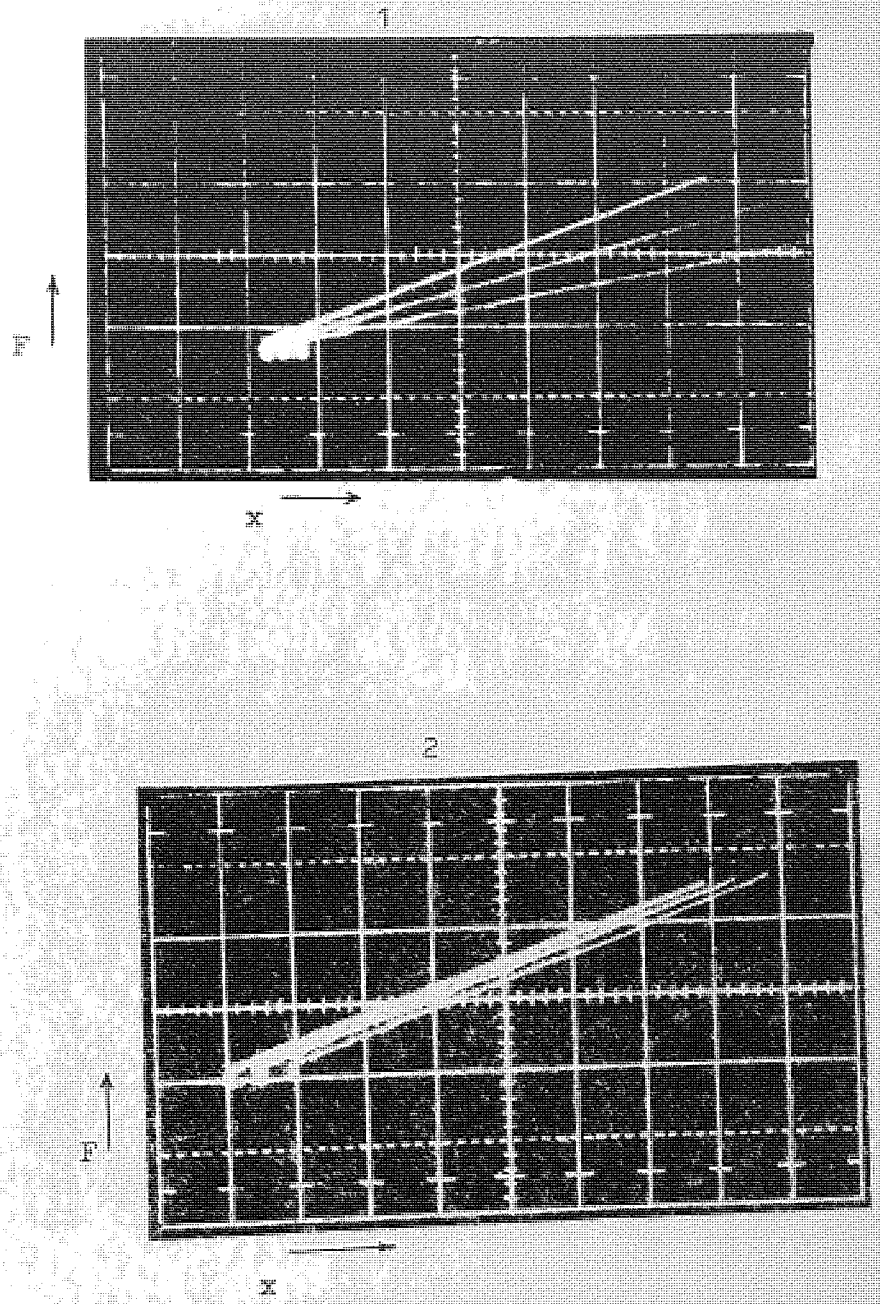

Fig. 4.22 Computed dynamic pull relations for three different spring loads(Osc.1) and three different masses(Osc.2).

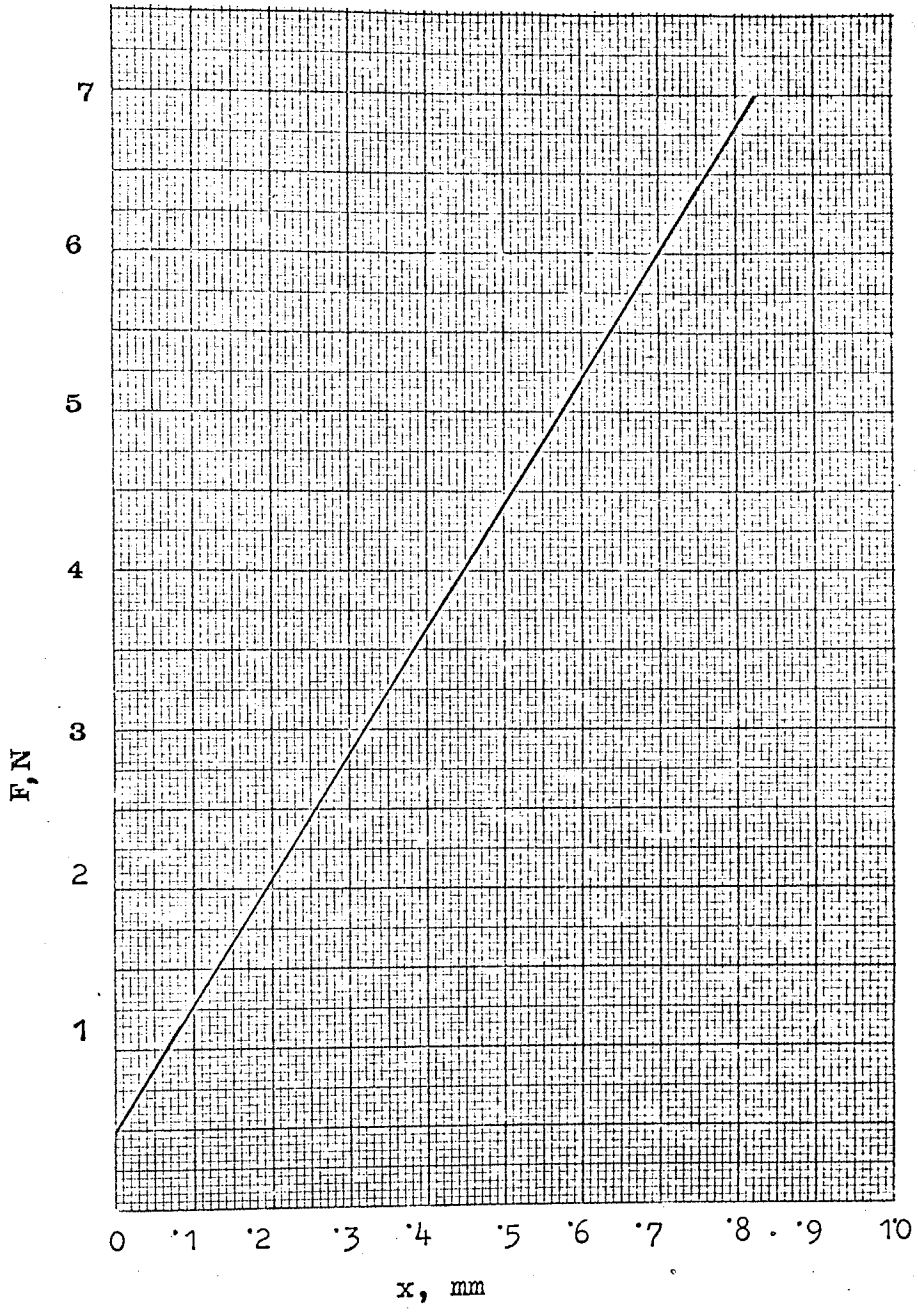

Fig. 4.23 Dynamic pull relation

4.9 Discussion

The simulation and programming have been proved very useful to study different cases. The same programming may be used for relays with similar magnetic structures but with different parameter values.

It is seen that the dynamic pull vs. position relation is linear. This property is used to develop a theory to calculate the time of operation, as presented in chapter 5.

Chapter 5

A RATIONAL DESIGN THEORY

5.1 Introduction.

The time of operation of relays is of great interest in almost all switching applications, and it is therefore essential to estimate the time for development purposes. If the design principles are known, it may be possible to design relays for different switching speeds to meet specific requirements and the analytical solution to the dynamic equations (1.1) and (1.2) are needed for this purpose. As discussed earlier, the analytical solution is impossible at this moment; however, approximate solutions may be possible to achieve. A solution of this kind is always useful to give an idea in which way the designer should change the parameters to get the required performance.

An approximate solution for the 'operate' case is presented in this chapter and for obtaining the solution, a theory for the dynamic behaviour is developed. The theory suggests a procedure of linearizing the two non-linear simultaneous differential equations (1.1) and (1.2) and makes use of the analysis made on the analogue computer. The formulae available from the solution, may be employed to design a relay having specified dynamic characteristics, in a rational manner.

In addition, the discussions of eddy currents, magnetic circuit, and ampere turn sensitivity which are of interest in relay design,

are also presented. A practical design using the theory is presented in the following chapter.

The theory presented in this chapter may be applicable to other electromagnets to estimate their time characteristics.

5.2 An experimental investigation of the dynamic pull-position relation.

In sec.4.8 it was discussed about the linear variation of the pull with the position of the armature during operation. An experiment was performed to see how the variation occurs. A telephone type relay with a linear spring load was chosen. The load characteristic is shown in fig.5.1. The dynamic flux and position recordings were done on the cathode ray oscillograph. The two oscillograms are shown in fig.5.2. The equivalent magnetic circuit constants are the same as in the case of the relay mentioned in sec. (7.3).Measurement of the circuit constants are given in sec. (11.3).Using these values, the pull is determined for every position from the general pull expression (1.4). The necessary data of the test relay and the results of the experiment are given below.

Magnetic circuit constants

$$S_o = 299 \times 10^4 \text{ At/Wb}$$

$$S_L = 715 \times 10^4 \text{ At/Wb}$$

$$A = 1.54 \times 10^{-4} \text{ m}^2$$

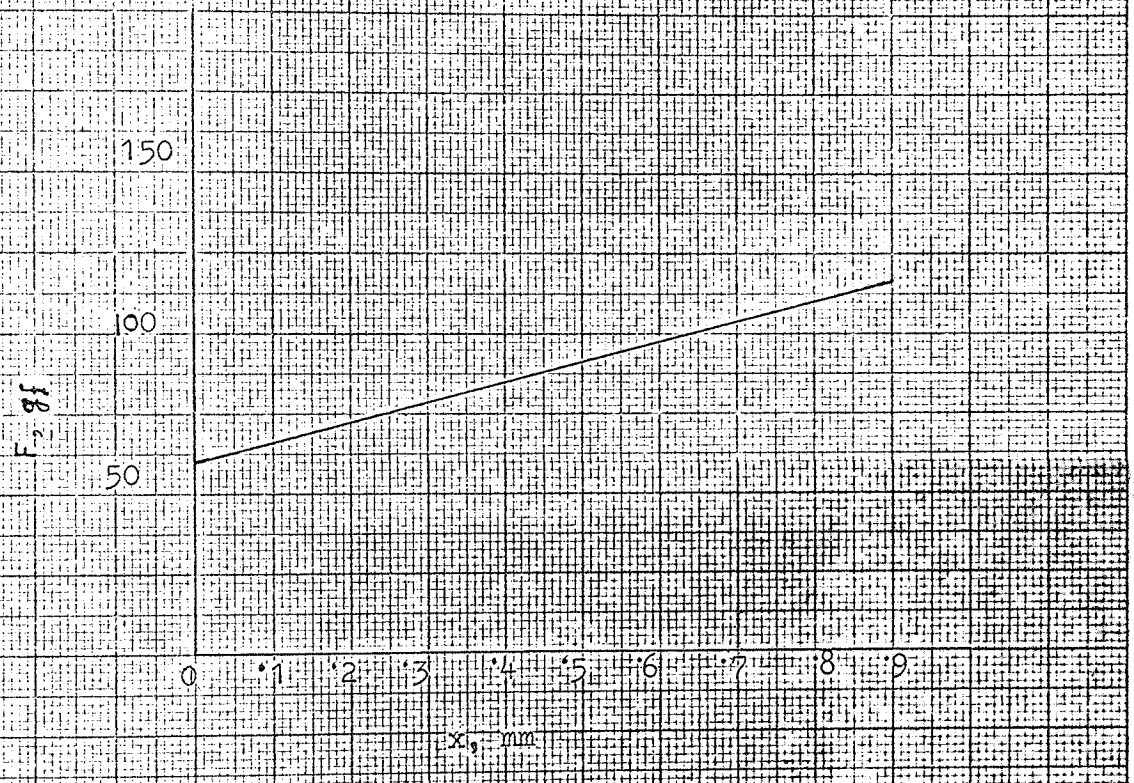

Fig.5.1 Load characteristic

1

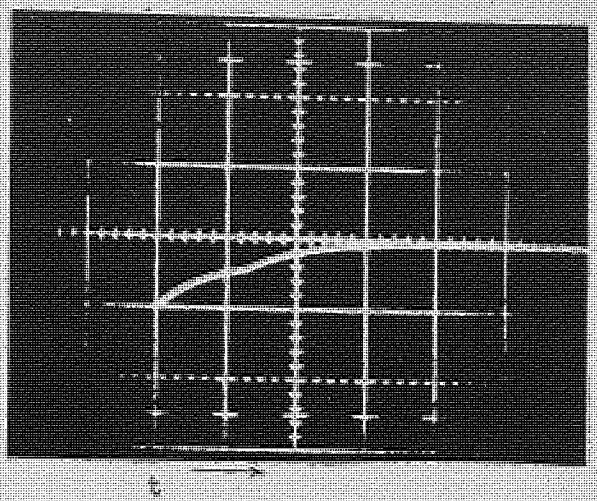

Time: 20 ms/div.

Flux : 125x10^{-7} Wb/div.

2

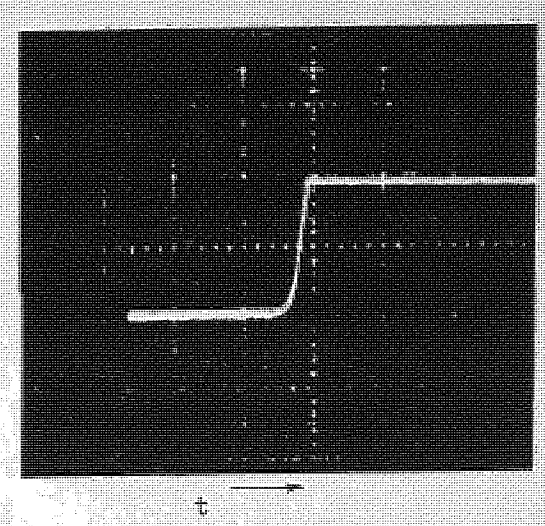

Time: 10 ms/div.

Position: .1 mm/div.

Fig. 5.2 Oscillograms showing flux and position vs. time. Scale factors are given above.

Other data

Final current in the relay coil is i_s = 6 m A

The coil has N = 25000 turns

Resistance of the coil R_c = 2500 Ω

External resistance in series with R_c is zero.

Residual air gap is .3 mm.

Total movement of the armature x_o = .9 mm.

Results

ϕ and x can be obtained from the oscillograms in fig.5.2.

Table 5.1 Measured core flux and position of the armature

$m^x m$	ϕ x 10^{-7} Weber
0	315
.1	331.25
.2	333
.4	335
.7	337
.9	338

Calculation of pulls:

The pull formula:

$$F = \left(\frac{S_L}{S_o + S_L + \frac{x_o - x}{\mu_o A}} \right)^2 \frac{\phi^2}{2 \mu_o A}$$

$$\mu_o A = 4\pi \times 10^{-7} \times 1.54 \times 10^{-4} = \cdot 1935 \times 10^{-9} \text{ H.m.}$$

At x = o,

$$F = \left(\frac{715 \times 10^4}{299 \times 10^4 + 715 \times 10^4 + \frac{.9}{.1935 \times 10^{-9}}} \right)^2 \frac{(315 \times 10^{-7})^2}{2 \times .1935 \times 10^{-9}}$$

$$= 0.599 \text{ Newton}$$

Similarly, other values of F corresponding to the values of x can be calculated. The values of F and x are given in the following table.

Table 5.2 Pull and position.

x m m	F Newton
0	0,599
.2	0.781
.4	0.918
.6	1.093
.8	1.325
.9	1.467

The curve in fig. 5.3 shows the variation of ϕ with x. Taking the values of the pull and position given in table 5.2, a curve is plotted, and this curve in fig. 5.4 shows the variation of the pull with the position of the armature. The dashed line represents a linear pull characteristic and may be taken as a mean curve of the plotted points except the top one at the end. The deviation from the linearity is more in the

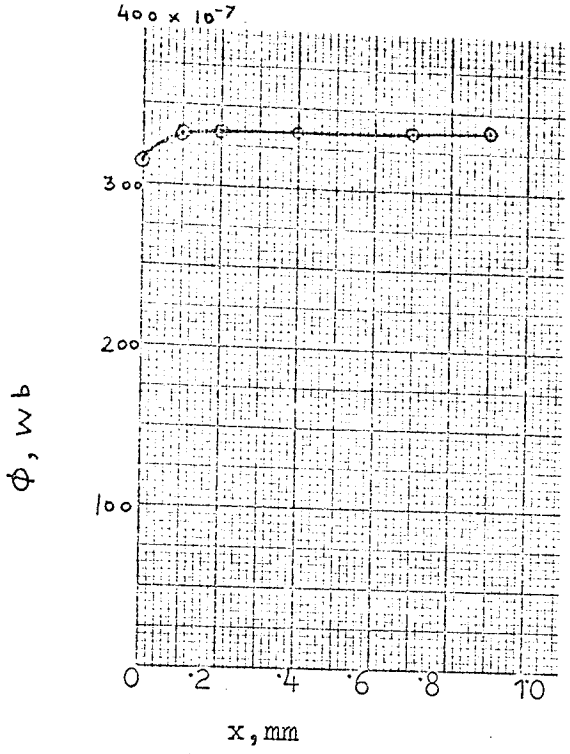

Fig.5.3 ϕ-x curve

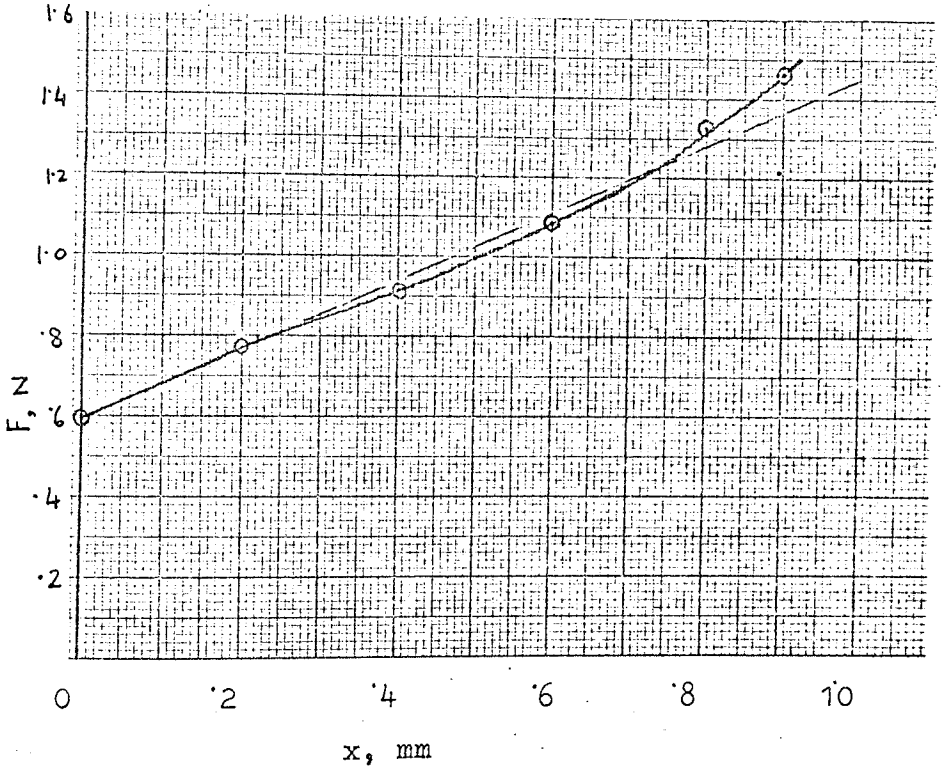

Fig.54 Dynamic pull vs. position characteristic

end and one of the causes for this, may be the saturation in the core at the end of the motion. Looking at the actual characteristic and the linear one, it may be concluded that for practical design purposes it will be sufficiently accurate to make an assumption that in a linear load case, the pull varies linearly with the position of the armature during operation.

5.3 Discussion on the assumption that the pull varies linearly with the position of the armature during operation.

The assumption has already been supported by an experiment and the analogue computer analysis. It may be interesting to mention a similar assumption made by Logan[19] who assumes that the pull varies linearly with time during the motion, but the computer does not indicate this phenomenon.

Peek[18] assumes a constant difference between the load and pull during the period of motion in the theory of the two-stage approximation; obviously, the pull varies linearly with the position, when the load characteristic is linear. Ahlberg[9] calculates the motion mathematically considering an equilibrium between the load and pull. In this case also, the pull varies linearly in a linear load case. The linear variations mentioned here in this paragraph are not of the same kind as in the present assumption, but these merely indicate that the assumption may be justified for getting an approximate solution.

From the preceding discussion it may be concluded that the pull varies linearly with the position in a linear load case, and no other special condition is put on the variation. In a non-linear load case the pull varies linearly but follows every linear section of the non-linear load, i.e. the slope of the pull curve changes when the slope of the load curve changes.

5.4 An approximate solution to the dynamic equation for the 'operate' case - a rational approach to the analysis of the dynamic behaviour.

When the armature does not move the variation of flux is governed by the electrical equation (1.1). The reluctance S may be calculated from the reluctance expression by putting zero for x, i.e. the armature is in open or 'unoperated' position. The total time of operation may be divided mainly into two parts. The first part is the waiting time which may be denoted by t_w and the second part is the motion time or the time required by the armature to reach the pole face of the electromagnet from the moment it started its movement.

The total travel of the armature may be divided into two sections and the first section may be limited to a very small distance.

Let t_1 and t_2 be the times taken to cover the first and second sections respectively, then the 'total operate' time t_o may be written as:

$$t_o = t_w + t_1 + t_2$$

Knowing the back tension, t_w can easily be calculated from the following formula.

$$t_w = \frac{G}{S_1} \ln \frac{1}{1 - \frac{\phi_1}{\phi_s}} \qquad (5.1)$$

where, S_1 is the total reluctance of the magnetic circuit when the armature is in open position, ϕ_1 is the flux in the core when the generated pull equals the back tension or the initial load and ϕ_s is the steady-state flux given by $\frac{Ni_s}{S_1}$. The above expression for t_w results from the solution of eq.(1.1) which may be re-written in the form:

$$t = \frac{G}{S_1} \int_0^{\phi_1} \frac{d\phi}{\phi_s - \phi} \qquad (5.1a)$$

In eq.(1.1) Ni_s and S have been replaced ϕ_s S_1 and S_1 respectively, because the equation is describing here the flux development during the period the armature is at rest. Now, integration of the right hand side of eq.(5.1a) gives the formula for t_w in eq. (5.1).

First section

Two assumptions would be made for the first section of the travel. The assumptions are, a) the total reluctance S remains constant at the value S_1, during the motion and b) the load remains constant at its initial value. It is described in sec.(0.5) that the magnetic circuit of an electromagnetic relay may be represented by an equivalent circuit containing two parallel branches when the magnetisation is linear. It can be shown by calculation and actual measurements that for a small movement of the armature, the total reluctance varies negligibly.

In the equivalent circuit which is given in fig. 10.9 the variable reluctance in one of the branches represents the reluctance of the air-gap which changes due to the movement of the armature. Slight variation of the reluctance of one branch does not cause an appreciable variation of the total reluctance of the parallel network. So, it will be sufficiently accurate to assume S as constant in the first section. The dynamic equations for the first section of the travel may be written from eqn.(1.1) and (1.2) and these are given by:

$$S_1 \phi + G \frac{d\phi}{dt} = N i_s \qquad (5.2)$$

and

$$m \frac{d^2x}{dt^2} + \gamma \frac{dx}{dt} = F - F_o \qquad (5.3)$$

It has already been assumed that the load is constant and stays at F_o, the initial value. Obviously, the term cx in eq. (1.2) equals to zero. As the frictional damping force is negligible in relays, the term $\gamma \frac{dx}{dt}$ may, therefore, be neglected for the sake of simplification and eq.(5.3) may be written as follows:-

$$m \frac{d^2x}{dt^2} + F_o = F \qquad (5.4)$$

Eqs.(5.2) and (5.4) are linear homogoneous equations because, S_1 is constant and F is a function of time in this particular case.

The solution to eq.(5.2) is the same as given in eq.(5.1)

where t_w should be replaced by t and may be written in the form:

$$\phi = \phi_s \left[1 - e^{\frac{-s_1 t}{G}}\right] \qquad (5.5)$$

The flux relation (5.5) indicates that the field grows according to the exponential law of the electric circuit set up by Hemholtz, when the reluctance of the magnetic circuit remains constant.

The solution to eq.(5.4) may be done by using Laplace's transformation method and the various steps may be shown in the following:

$$m \frac{d^2x}{dt^2} + F_o = F$$

$$\text{or} \quad m \frac{d^2x}{dt^2} + K\phi_s^2 \left(1-e^{\frac{-s_1 t_w}{G}}\right)^2 = K\phi^2 = K\phi_s^2 \left(1-e^{\frac{-s_1 t}{G}}\right)^2 \qquad (5.6)$$

$$\text{as} \quad F_o = K\phi_1^2 = K\phi_s^2 \left(1 - e^{\frac{-s_1 t_w}{G}}\right)^2.$$

The preceding expression for F_o follows from eq.(5.1) which may be written in the form similar to (5.5).

In eq. (5.6) t consists of t_w and t_{m1}, where t_{m1} is the motion time which will be denoted by t in the following steps. Now, eq.(5.6) may be written as:

$$m \frac{d^2x}{dt^2} = K\phi_s^2 \left[\left(1-e^{\frac{-s_1 t}{G}} e^{\frac{-s_1 t_w}{G}}\right)^2 - \left(1-e^{\frac{-s_1 t_w}{G}}\right)^2\right]$$

$$= K\phi_s^2 \left[e^{\frac{-2s\,t_w}{G}} \cdot e^{\frac{-2\,st}{G}} - 2\,e^{\frac{-st_w}{G}} \cdot e^{\frac{-s\,t}{G}} + 2\,e^{-\frac{st_w}{G}} - e^{-\frac{2st_w}{G}}\right]$$

$$\text{or,}\quad m\frac{d^2x}{dt^2} = K\phi_s^2\left[M_1 e^{\frac{-2st}{G}} - M_2 e^{\frac{-st}{G}} + M_2 - M_1\right]$$

where, $M_1 = e^{\frac{-2st_w}{G}}$ and $M_2 = 2\,e^{\frac{-st_w}{G}}$

The preceding equation may be written as:

$$m\frac{d^2x}{dt^2} = K\phi_s^2\left[M_1\left(e^{\frac{-2s_1t}{G}} - 1\right) + M_2\left(1 - e^{\frac{-s_1t}{G}}\right)\right]$$

$$\text{or}\quad \frac{d^2x}{dt^2} = \frac{K\phi_s^2}{m}\left[M_1\left(e^{\frac{-2s_1t}{G}} - 1\right) + M_2\left(1 - e^{\frac{-s_1t}{G}}\right)\right]$$

$$\text{or,}\quad \frac{d^2x}{dt^2} = \alpha\left[M_1\left(e^{-2\gamma t} - 1\right) + M_2\left(1 - e^{-\gamma t}\right)\right] \qquad (5.7)$$

where $\alpha = \frac{K\phi_s^2}{m}$ and $\gamma = \frac{s_1}{G}$. Of course, α in this case is not the same as α in chapter 7.

Taking Laplace's transform of both sides of equation (5.7) there is obtained:

$$s^2\bar{x} - sx(o) - x'(o) = \frac{\alpha M_1}{s+2\gamma} - \frac{\alpha M_1}{s} + \frac{\alpha M_2}{s} - \frac{\alpha M_2}{s+\gamma}$$

At $t = o$, $x = o$, $x' = o$.

$$\therefore\quad s^2\bar{x} = \frac{\alpha M_1}{s+2\gamma} - \frac{\alpha M_1}{s} + \frac{\alpha M_2}{s} - \frac{\alpha M_2}{s+\gamma}$$

$$\text{or,}\quad \bar{x} = \frac{\alpha M_1}{s^2(s+2\gamma)} - \frac{\alpha M_1}{s^3} + \frac{\alpha M_2}{s^3} - \frac{\alpha M_2}{s^2(s+\gamma)} \qquad (5.8)$$

The first and fourth terms in the right hand side of the above expressions are decomposed into partial fraction which are given below.

$$\frac{\alpha M_1}{s^2(s+2\gamma)} = \frac{\alpha M_1}{2\gamma s^2} + \frac{\alpha M_1}{4\gamma^2(s+2\gamma)} - \frac{\alpha M_1}{4\gamma^2 s}$$

$$\text{and } \frac{\alpha M_2}{s^2(s+\gamma)} = \frac{\alpha M_2}{s\gamma^2} - \frac{\alpha M_2}{s^2\gamma} - \frac{\alpha M_2}{\gamma^2(s+\gamma)}$$

After rearranging the terms expression (5.8) can thus be written as:

$$\bar{x} = \frac{\alpha(M_2 - M_1)}{s^3} + \frac{\alpha M_2}{s\gamma^2} - \frac{\alpha M_2}{s^2\gamma} - \frac{\alpha M_2}{\gamma^2(s+\gamma)}$$

$$- \frac{\alpha M_1}{4\gamma^2 s} + \frac{\alpha M_1}{2\gamma s^2} + \frac{\alpha M_1}{2\gamma s^2} + \frac{\alpha M_1}{4\gamma^2(s+2\gamma)}$$

Taking inverse Laplace's transform, the solution thus obtained, is given by:

$$x = \frac{\alpha(M_2 - M_1)}{2} t^2 + \frac{\alpha M_2}{\gamma^2} - \frac{\alpha M_2}{\gamma} t - \frac{\alpha M_2}{\gamma^2} e^{-\gamma t}$$

$$- \frac{\alpha M_1}{4\gamma^2} + \frac{\alpha M_1}{2\gamma} t + \frac{\alpha M_1}{4\gamma^2} e^{-2\gamma t}$$

$$= \frac{\alpha(M_2 - M_1)}{2} t^2 + \left(\frac{\alpha M_2}{\gamma^2} - \frac{\alpha M_1}{4\gamma^2}\right) + \left(\frac{\alpha M_1}{2\gamma} - \frac{\alpha M_2}{\gamma}\right) t -$$

$$\left(\frac{\alpha M_2}{\gamma^2} - \frac{\alpha M_1}{4\gamma^2} e^{-\gamma t}\right) e^{-\gamma t}$$

$$= \frac{\alpha(M_2 - M_1)}{2} t^2 + (4M_2 - M_1) \frac{\alpha}{4\gamma^2} + (M_1 - 2M_2) \frac{\alpha t}{2\gamma}$$

$$- (4M_2 - M_1 e^{-\gamma t}) \frac{\alpha}{4\gamma^2} e^{-\gamma t}$$

$$\therefore x = (4M_2 - M_1) \frac{\alpha}{4\gamma^2} + (M_1 - 2M_2) \frac{\alpha t}{2\gamma} + \frac{\alpha(M_2 - M_1)}{2} t^2 -$$

$$(4M_2 - M_1 e^{-\gamma t}) \frac{\alpha}{4\gamma^2} e^{-\gamma t} \qquad (5.9)$$

The simplification of the above expression is given in appendix.2. It thus gives the following expression

$$x = \left(\frac{M_2}{6} - \frac{M_1}{3}\right) \gamma \alpha t^3$$

$$= \chi t^3, \quad \text{where} \quad \chi = \frac{\gamma\alpha}{3} \left(\frac{M_2}{2} - M_1\right).$$

Substituting the values of the constants M_1, M_2, α and γ there is obtained:

$$x = \chi t^3$$

$$= \frac{1}{3} \times \frac{S_1}{G} \times \frac{K\phi_s^2}{m} \left(e^{-\frac{s_1 t_w}{G}} - e^{-\frac{2st_w}{G}} \right)$$

$$= \frac{K M_s^2}{3mG s_1} \left(1 - e^{-\frac{s_1 t_w}{G}}\right) e^{-\frac{s_1 t_w}{G}} \cdot t^3 \qquad (5.10)$$

If the first section is limited to x_1, and the time to cover this distance is t_1, then t_1 is obtained from the above expression by substituting x_1 for x and t_1 for t.

$$\therefore \quad t_1 = \sqrt{3 \frac{x_1}{\frac{KM_s^2}{3mGs_1}\left(1 - e^{-\frac{s_1 t_w}{G}}\right) e^{-\frac{s_1 t_w}{G}}}} \qquad (5.11)$$

Second section

The assumption of the linear variation of pull with position of the armature would be utilized here. According to the assumption, the pull varies linearly with the position in the second section of the travel which is very much bigger than the first section. The pull may be given by :

$$F = A_o + c_1 x \qquad (5.12)$$

where x stands for the position of the armature measured from the origin of the second section and c_1 and A_o are the two constants. Inserting (5.12) in the mechanical equation (1.2), there is obtained:

$$m \frac{d^2x}{dt^2} + \tau \frac{dx}{dt} + c x = A_o + c_1 x - F_o \qquad (5.13)$$

This is the mechanical equation for the second section provided F_o is the sum of spring load, acceleration force and frictional damping force at the end of the first section, which is the beginning of the second section. The sum of these acceleration and frictional damping forces is equal to the difference between A_o and the initial spring load in this section and this can be realised from the characteristics shown in fig.5.5. Therefore,

A_o and F_o cancel each other and equation (5.13) may be

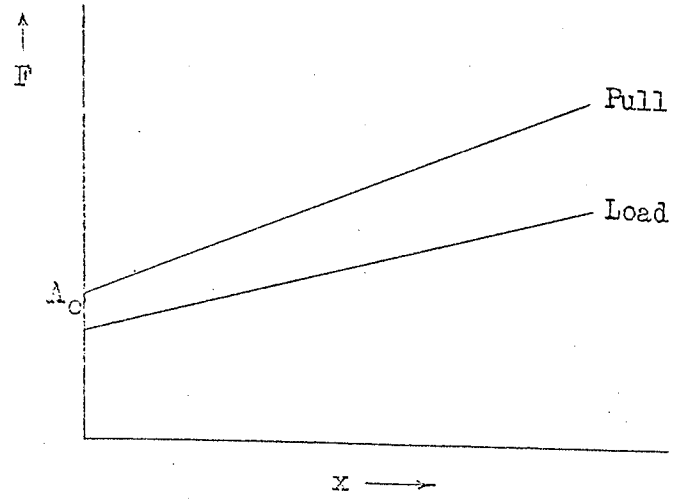

Fig.5.5 Pull and load relations in the second section of the travel.

written as:

$$m\frac{d^2x}{dt^2} + \gamma\frac{dx}{dt} + c\,x = c_1\,x$$

Neglecting the frictional force, the preceding equation becomes:

$$m\frac{d^2x}{dt^2} + c\,x = c_1\,x$$

or $$m\frac{d^2x}{dt^2} + (c - c_1)\,x = 0$$

or $$\frac{d^2x}{dt^2} + \left(\frac{c - c_1}{m}\right)x = 0$$

If n^2 is written for $\frac{c_1 - c}{m}$, there is obtained:

$$\frac{d^2x}{dt^2} - n^2 x = 0 \qquad (5.14)$$

The negative sign indicates that c_1 is greater than c, which should be the usual case. Equation (5.14) is a linear homogenous equation and may be solved quite easily.

At the end of the first section, the armature attains a velocity which may be obtained by differentiating x in equation (5.11), and obviously, it enters into the second section with this initial velocity. Solving (5.14) by Laplace's transformation method:

$$\mathcal{L}\left[m \frac{d^2x}{dt^2} - n^2 x \right] = 0$$

$$s^2 \bar{x} - s\,x(o) - x^1(o) - n^2 \bar{x} = o \qquad (5.15)$$

The initial conditions are : $x(o) = o$ and $x'(o) = u$. The individual sections are treated separately and for this reason $x(o) = o$ in the second section. Putting the initial conditions in (5.15), there is obtained:

$$s^2 \bar{x} - u - n^2 \bar{x} = o$$

$$\bar{x}\,(s^2 - n^2) = u$$

$$\bar{x} = \frac{u}{s^2 - n^2}$$

$$\therefore \quad x = \frac{u}{n} \sinh nt \quad (5.16), \qquad \because \mathcal{L}^{-1}[\bar{x}] = \mathcal{L}^{-1}\left[\frac{u}{s^2 - n^2}\right]$$

Now, a relation for ϕ is to be obtained. An expression for ϕ may be obtained considering the equilibrium between the four forces i.e. the spring load, mass force, frictional damping force and magnetic pull. Mass force means the acceleration force. A stabilised motion is considered here and for the same the direction of motion

is always positive and a momentary equilibrium exists between the four kinds of forces at every instant of time during the motion. Neglecting the frictional damping force, it may be written:

Magnetic pull = spring load + mass force.

$$\therefore \quad F = c\,x + m\,\ddot{x}$$

$$\text{or,} \quad K\phi^2 = c\left[\frac{u}{n}\ sh\ nt\right] + m\frac{d^2}{dt^2}\left[\frac{u}{n}\ sh\ nt\right]$$

$$= c\,\frac{u}{n}\ sh\ nt + mun\,(sh\ nt)$$

$$\text{So,} \quad K\phi^2 = sh\ nt\ \left(\frac{cu}{n} + mun\right)$$

$$= un\left(\frac{c}{n^2} + m\right) sh\ nt$$

$$\therefore \quad \phi^2 = \frac{un}{K}\left(m + \frac{c}{n^2}\right) sh\ nt$$

$$= \frac{u}{Kn}\left(m\,n^2 + c\right) sh\ nt \qquad (5.17)$$

$$\therefore \quad \phi = \sqrt{\frac{u}{Kn}\left(m\,n^2 + c\right) sh\ nt} \qquad (5.18)$$

Equation (5.18) may also be written in the form:

$$\phi = \frac{u}{Kn}\left(m \cdot \frac{c_1 - c}{m} + c\right) sh\left(\sqrt{\frac{c_1 - c}{m}}\right)t, \quad \because \frac{c_1 - c}{m} = n^2$$

After simplification there is obtained,

$$\phi = \sqrt{\frac{u}{Kn}\,(c_1)\ sh\left(\sqrt{\frac{c_1 - c}{m}}\right)t}$$

$$= \sqrt{\frac{u\,c_1}{K\sqrt{\frac{c_1 - c}{m}}}\ sh\left(\sqrt{\frac{c_1 - c}{m}}\right)t} \qquad (5.19)$$

If x_2 measures the length of the second section and t_2 is the time required to move this distance then x_2 may be obtained by substituting x_2 and t_2 for x and t respectively in eq. (5.16)

$$\therefore \quad x_2 = \frac{u}{n} \text{ sh } nt_2 \tag{5.20}$$

Similarly, ϕ_2, the increase of flux at the end of the section from the initial value at the beginning of the section, may be obtained from eq. (5.19) and written as:

$$\phi_2 = \sqrt{\frac{uc_1}{K\sqrt{\frac{c_1 - c}{m}}} \cdot \text{sh}\left[\sqrt{\frac{c_1 - c}{m}}\right] t_2} \tag{5.21}$$

The total time of operation may be calculated from eqns. (5.1), (5.11) and (5.20) and the calculation of the dynamic characteristics for a specific design may be done by using the same equations, and expressions (5.5) and (5.21). The static characteristics may be estimated knowing the statics of the electromagnet, while some other properties may be determined from the overall knowledge of the static and dynamic performance. A calculation of the time for full operation by the help of the equations already mentioned, may be presented and a practical measurement of the time when the relay is made will indicate how good they are for design and development.

The case of linear spring load has been considered here; the treatment may be extended to the case of non-linear spring load as well.

5.5 Conductance of the eddy current paths.

It is needed to estimate the effective conductance of the eddy current paths, G_e which comes in the expression for G in the electrical equation (1.1). The effective conductance may be determined experimentally when a model is available, otherwise it is to be estimated and an expression for G_e is required.

It is well known that eddy currents are induced in the conductive members of the magnetic structure due to the changing flux. A rigorous analytical treatment for this effect of the flux is difficult, but some relations may be developed, which may be used to obtain an expression for G_e to account the influence of eddy-currents on the relay performance.

Neglecting the other magnetic members, the eddy current is assumed to be confined to the core which may be cylindrical or rectangular and can be considered as made up of concentric hollow shells. Each shell can be thought of as a short-circuited turn linking a part of the core flux. The outermost shell, of course, encloses all the core flux. An analytical solution may be achieved by making two more assumptions which are : a) the magnetization is linear; b) the flux in the core is directed parallel to the axis and has radial symmetry. A solution of this kind is presented in section 11.2 of Peek and Wagar. The return path has been taken to be equivalent to an air gap of reluctance S_E. Considering the core like a torroid with no air gap, i.e. $S_E = o$, an expression for G_e is

derived, which is given by:

$$G_e = \frac{l}{8\pi\rho} , \qquad (5.22)$$

where l is the length of the core, and ρ is the resistivity of its material. ρ for magnetic iron may be taken to be 4.4×10^{-6} in.- ohms or 11.18×10^{-8} m-ohm. If the core cross-section is rectangular, ρ shall be replaced by ρ' in eq. (5.22), which is given by :

$$\rho' = \rho . \frac{1 + q}{(\pi q)^{1/2}} \qquad (5.23)$$

where q is the ratio of the sides of the rectangular section.

The value of G_e calculated from expression (5.22) agrees very well with the experimentally determined value. Therefore, the estimation for design purposes may be made by using this expression.

5.6 The magnetic circuit

The magnetic circuit constants are essential for the calculation of static and dynamic characteristics for the design, and/performance analysis for the during the development studies. These constants may be estimated from the design dimensions of the electromagnet when the field is represented by the design magnetic circuit which is discussed in sec.10.5. The magnetic circuit parameters determine both the coil and eddy current time constants,

and also the work capacity and ampere-turn sensitivity of the electromagnet.

When all the other conditions such as, contact pressure and separation, spring vibration, additional stroke distance to allow for contact wear etc., are considered and the final work requirement is fixed, the design of the motor should be such that the motor is capable of doing the work, which depends on the magnetic circuit and ampere-turns.

5.7 Ampere turn sensitivity

When the armature moves, mechanical work is done against the contact springs. If this work is expressed by v, then the ratio $v/(Ni)^2$ is called the ampere turn sensitivity. Here Ni denotes the just operate ampere turns which is the minimum value needed to generate a pull at every position of the armature to exceed the static load. While designing a relay a consideration should be given regarding the ampere turn sensitivity of the electromagnet, the limiting value of which gives the maximum output possible for a specific ampere turn.

Chapter 6

EXPERIMENTAL DESIGN VERIFICATION

6.1 Introduction

After estimating the magnetic circuit constants the estimation of the time of operation by using the theory described in sec.5.4 is presented. A relay was developed according to the dimensions and parameters specified in the calculations and the time of operation was measured. The agreement between the calculated and measured time is discussed.

6.2 The magnetic material

The magnetic material chosen was Swedish iron according to the specification DTD 5092 or 5102. The BvsH curve of the material is shown in fig.11.1 and the maximum relative permeability μ_r available from the curve is 5100. After making the magnet structures it is essential to anneal all the magnetic parts properly for removing the machining strains to get their best magnetic properties.

6.3 Estimation of magnetic circuit constants

The constants of the equivalent magnetic circuit are estimated from the design dimensions. At first the constants of the design magnetic circuit should be evaluated, then the constants of the "equivalent" circuit can be calculated from the "design" values by using eqns.(10.9). The two circuits are shown in figs. 10.7 and 10.9 The constants of the design magnetic circuit are

S_c, the minimum core reluctance,

S_o', the closed gap reluctance of the working air gap flux.

$\mu_o A'$, the constant in which A' is the effective pole face area,

S_L', the leakage reluctance.

The determination of the above constants are described in secs. 3.10 of Peek and Wagar[3] and a descriptive treatment regarding the estimation of the magnetic reluctance is given in section 9.4 of the same text.

The permeability of free space $\mu_o = 4\pi \times 10^{-7}$ H/m

The relative permeability μ_o of the iron of the magnetic structure = 5100

In fig. 6.1 the magnetic structure of the relay is shown. The design dimensions are given below:

Design dimensions

l_{1-2} = 56 mm; l_{1-8} = 2 mm; l_{3-4} = 15.5 mm;

l_{4-5} = 59.5 mm; l_{6-7} = 16.5. mm

The diameter of the core d = 8 mm.

The diameter of the pole face = 13.06 mm.

Residual air-gap when the armature is in cotact with the pole face = the width of the non magnetic. Separator = .29 mm.

Distance between the core and yoke = 9.5 mm.

Calculation of the cross sectional areas of the magnetic parts

$$a_{1-2} = \frac{\pi d^2}{4} = \frac{3.14 \times (8 \times 10^{-3})^2}{4} = .5024 \times 10^{-4} \text{ m}^2$$

$$a_{1-8} = \frac{\pi \times (13.06 \times 10^{-3})^2}{4} = 1.339 \times 10^{-4} \text{ m}^2$$

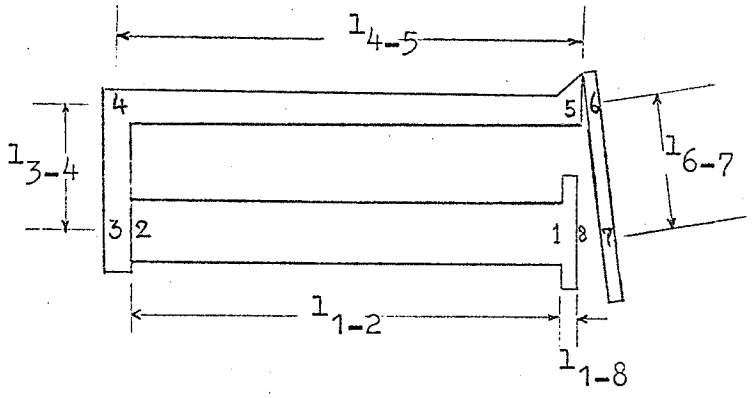

Fig.6.1 Magnetic structure

a_{4-5} = breadth x depth = 19 mm x 4 mm

= $.76 \times 10^{-4}$ m^2

$a_{3-4} = 3 \times 19 \times 10^{-6} = .57 \times 10^{-4}$ m^2

$a_{6-7} = 2 \times 10^{-3} \times 18 \times 10^{-3} = .36 \times 10^{-4}$ m^2

Core reluctance S_c.

The reluctance of an iron member is given by:

$$S = \frac{l}{\mu_o \mu_r a} \qquad (6.1)$$

where S is the reluctance, and l and a are the length and cross-sectional area of the iron part.

$$\therefore S_c = S_{1-8} + S_{1-2}$$

$$= \frac{l_{1-8}}{\mu_o \mu_r a_{1-8}} + \frac{l_{1-2}}{\mu_o \mu_r a_{1-2}}$$

$$= \frac{2 \times 10^{-3}}{4\pi \times 10^{-7} \times 5100 \times 1.339 \times 10^{-4}} + \frac{56 \times 10^{-3}}{4\pi \times 10^{-7} \times 5100 \times .5024 \times 10^{-4}}$$

$= .2331 \times 10^4 + 17.4 \times 10^4 = 17.63 \times 10^4$ At/wb

The closed gap reluctance S_o'

The closed gap reluctance S_o' for the gap flux ϕ_g is given by:

$$S_o' = S'_{3-4} + S'_{4-5} + S'_{6-7} + S'_{2-3} + \frac{x_h}{\mu_o a_h} + \frac{x_{go}}{\mu_o A'}$$

where x_h and x_{go} are the heel gap and main gap separations when the armature is operated, A' is the geometrical pole face area.

S'_{3-4}, S'_{4-5} etc. are the reluctances of the parts of the magnetic circuit indicated by the numbers.

$$S'_{3-4} = \frac{l_{3-4}}{\mu_o \mu_r a_{3-4}} = \frac{15.5 \times 10^{-3}}{6.406 \times 10^{-3} \times .57 \times 10^{-4}} = 4.24 \times 10^4 \text{ At/wb}$$

It may be mentioned here that $\mu_o \mu_r = 4\pi \times 10^{-7} \times 5100$

$= 6.406 \times 10^{-3}$

$$S'_{4-5} = \frac{l_{4-5}}{\mu_o \mu_r a_{4-5}} = \frac{59.5 \times 10^{-3}}{6.406 \times 10^{-3} \times .76 \times 10^{-4}} = 12.32 \times 10^4 \text{ At/wb}$$

$$S'_{6-7} = \frac{l_{6-7}}{\mu_o \mu_r a_{6-7}} = \frac{16.5 \times 10^{-3}}{6.406 \times 10^{-3} \times .36 \times 10^{-4}} = 7.15 \times 10^4 \text{ At/wb}$$

S'_{2-3} is the sum of the two reluctances; one for the joint where there is an iron to iron contact and an equivalent length of air gap .0005 mm may be taken for the contact, another component reluctance is for a small length of the iron path after the joint.

$$\therefore \quad S'_{2-3} = \frac{.0005 \times 10^{-3}}{\mu_o a_{2-3}} + \frac{1.5 \times 10^{-3}}{\mu_o \mu_r a_{2-3}}$$

$$= 79.24 \times 10^4 + .47 \times 10^4 = 79.71 \times 10^4 \quad \text{At/wb}$$

In the hinged armature relay there is an iron to iron contact at the heel gap and the reluctance of the gap may be taken constant. This reluctance is $\frac{x_h}{\mu_o a_h}$, where x_h is .005 mm and a_h is the mating area.

$$\therefore \quad \frac{x_h}{\mu_o a_h} = \frac{.0005 \times 10^{-3}}{4\pi \times 10^{-7} \times a_h} = \frac{.0005 \times 10^{-3}}{4\pi \times 10^{-7} \times 1.35 \times 10^{-4}}$$

$$= 29.49 \times 10^4 \text{ At/wb}$$

$$\frac{x_{go}}{\mu_o A'} = \frac{.29 \times 10^{-3}}{4\pi \times 10^{-7} \times 1.339 \times 10^{-4}} = 172.43 \times 10^4 \text{ At/wb}$$

$$\therefore \quad S_o' = 4.24 \times 10^4 + 12.32 \times 10^4 + 7.15 \times 10^4 + 79.71 \times 10^4$$
$$+ \quad 29.49 \times 10^4 + 172.43 \times 10^4 = 305.34 \times 10^4 \quad \text{At/wb.}$$

$\mu_o A'$

Here A' is the mating area of the armature and pole face at the main air gap. The heel gap is neglected. The effective pole face area A' may, therefore, be taken as the geometrical pole face area of the magnet.

$$A' = \frac{\pi \times (13.06 \times 10^{-3})^2}{4} = 1.339 \times 10^{-4} \text{ m}^2$$

$$\mu_o A' = (4\pi \times 10^{-7} \times 1.339 \times 10^{-4}) = .1683 \times 10^{-9} \text{ H.m}$$

The leakage reluctance S_L'

This takes into account the leakage from the core to the yoke, and the fringing at the air gaps. Fig. 6.2 shows a magnet structure with two legs as in the present case. The leakage reluctance between the core and yoke may be estimated by

$$\frac{P_1 + P_2}{2\pi}$$

$$D = D' + d$$

$$\frac{1}{S_L} = \left(\frac{c_1 l_1}{3} + c_1 l_2 + c_2 d\right) \mu_o$$

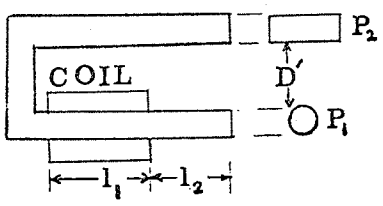

Fig.6.2 Leakage of the magnetic circuit

treating them as equivalent to two parallel cylinders. The

end surfaces of the core and yoke may be treated as equivalent to two hemispheres.

Expressions for the reluctances between two cylinders and two spheres are given in sec.9.4 of Peek and Wagar[3]. These expressions given by potential theory for the fields between the respective members are

$$S = \frac{ch^{-1}u}{2\pi b} \qquad (6.2)$$

and

$$S = \frac{1}{2\pi r\left[1 + \left(\frac{r}{D}\right) + \left(\frac{r}{D}\right)^2 + \left(\frac{r}{D}\right)^3 + 2\left(\frac{r}{D}\right)^4 + 3\left(\frac{r}{D}\right)^5 + \ldots\ldots\right]} \qquad (6.3)$$

for cylinders and spheres respectively. In expression (6.2) b is the length of each cylinder and D is the distance between the axes and r_1 and r_2 are the radii of the two cylinders as shown in fig. 6.3

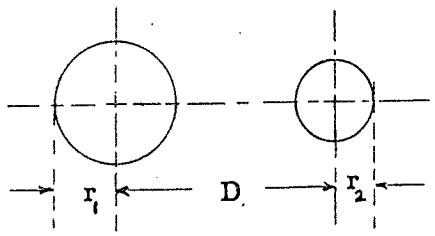

Fig. 6.3 Parallel cylinders.

In expression (6.3) r is the radius of each sphere and D is the distance between the centres of the spheres as shown in fig.6.4.

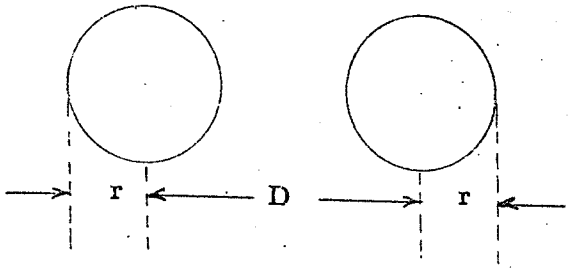

Fig. 6.4 Two spheres

Now the leakage permeance which is $\frac{1}{S_L}$ is the sum of the three permeance terms as shown in fig. 6.2. P_1 and P_2 are the perimeters and P_2 is equal to the perimeter of an equivalent cylinder whereas P_1 is the perimeter of the core which is already cylindrical. The factors c_1 and c_2 are obtained from the relations (6.2) and (6.3) respectively, and the numerical values of these factors plotted for different values of D/d are given in sec.9.4 of Peek and Wagar. The quantity $c_2 d$ in fig. 6.2 is one half the permeance between the corresponding spheres given by the inverse of the expression for S in (6.3). The leakage reluctance between the part of the core covered by the magnetising coil and the yoke has an effective value which is one third of the leakage reluctance between the two members due to the drop in potential along the core, whereas, for the end part of the core the field is uniform and the reluctance is the same as given by the expression in (6.2). In fig. 6.2, c_1 is the permeance per unit length. The total permeance is given by

$$= \mu_o \left(\frac{c_1 l_1}{3} + c_1 l_2 + c_2 d \right) = \frac{1}{S_L'} \qquad (6.4)$$

$$\therefore \quad S_L' = \frac{1}{\left(\frac{c_1 l_1}{3} + c_1 l_2 + c_2 d\right) \mu_o} \qquad (6.5)$$

In (6.4) one or both of the terms in l_2 and d correspond to fields shunted by the armature; thus in effect the leakage due to the fringing at the end of the two legs is considered.

The core and yoke assembly with the dimensions for the design is given in fig. 6.5.

The leakage reluctance may be calculated by using formula (6.5). After calculating D/d for the terms in l_1, l_2 and d by using the equation given in fig. 6.2, c_1 and c_2 are found from the corresponding curves in fig. 9.14 of Peek and Wagar.

For $\frac{c_1 l_1}{3}$

$$P_1 = 2\pi r = 2 \times 3.142 \times 8 = 25.12 \text{ mm}$$

$$P_2 = 2(b + d) = 2 (19 + 4) = 46 \text{ mm}$$

$$d = \frac{P_1 + P_2}{2\pi} = \frac{25.12 + 46}{2 \times 3.142} = \frac{71.12}{6.28} = 11.32 \text{ mm}$$

$$D = D' + d = 9.5 + 11.32 = 20.82 \text{ mm.}$$

$$D/d = \frac{20.82}{11.32} = 1.84$$

$$\therefore \quad c_1 = 2.55$$

$$\text{and} \quad \frac{c_1 l_1}{3} = \frac{2.55 \times 56 \times 10^{-3}}{3} = 47.6 \text{ mm.}$$

For $c_1 l_2$

$$P_1 = 2\pi r = 3.142 \times (2r) = 3.142 \times 13.06 = 41.01 \text{ mm}$$

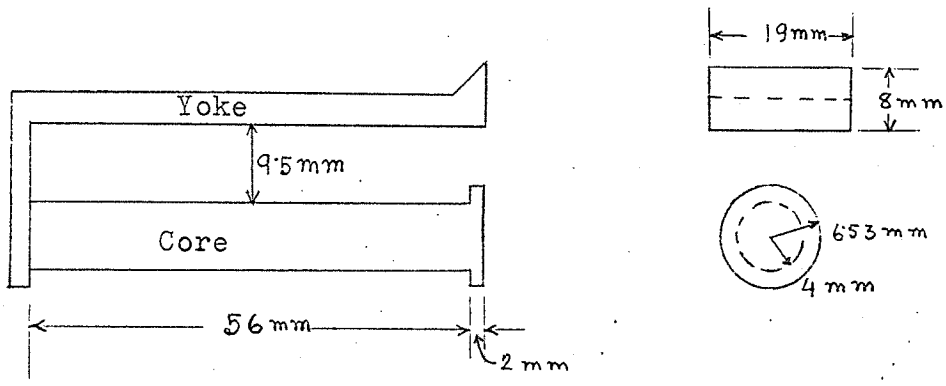

Fig.6.5

P_2 is the same as for the previous case.

$$d = \frac{P_1 + P_2}{2\pi} = \frac{41.01 + 46}{2\pi} = 13.86 \text{ mm}$$

$$D = D' + d = 6.97 + 13.86 = 20.83 \text{ mm.}$$

$$D/d = \frac{20.83}{13.86} = 1.50$$

$\therefore$ $c_1 = 3.25$

and $c_1 l_2 = 3.25 \times 2 = 6.5$ mm

For $c_2 d$

$P_2 = 2(b + d) = 2(19 + 8) = 54$ mm

P_1 is the same as for the previous case.

$$d = \frac{P_1 + P_2}{2\pi} = \frac{41.01 + 54}{6.284} = 15.13 \text{ mm.}$$

$$D = D' + d = 6.97 + 15.13 = 22.10 \text{ mm.}$$

$$D/d = \frac{22.10}{15.13} = 1.46 \quad \therefore \; c_2 = 2.5$$

and $c_2 d = 2.5 \times 15.13 \times 10^{-3} = 37.83$ mm.

The total permeance is :

$$= \left(\frac{c_1 l_1}{3} + c_1 l_2 + c_2 d \right) \mu_o$$

$$= (47.6 + 6.5 + 37.83) \times 10^{-3} \times 4\pi \times 10^{-7}$$

$$= 91.93 \times 10^{-3} \times 4\pi \times 10^{-7} \quad \text{wb/At}$$

$$\therefore S_L' = \frac{1}{91.93 \times 10^{-3} \times 4\pi \times 10^{-7}} = 866 \times 10^4 \quad \text{At/wb}$$

The values of the design magnetic circuit are listed in

the following:

$S_c = 17.63 \times 10^4$ At/wb

$S_o' = 305.34 \times 10^4$ At/wb

$S_L' = 866 \times 10^4$ At/wb

$\mu_o A' = (\mu_o \times 1.339 \times 10^{-4})$

$= .1683 \times 10^{-9}$ Hm

Calculation of the constants of the equivalent magnetic circuit

It is discussed in sec. 10.5 that the low density magnetisation relations may be expressed in terms of the equivalent magnetic circuit. The following relations exist between the constants of this circuit and the design magnetic circuit.

$$S_L = S_c + S_L'$$

$$\mu_o A = \frac{\mu_o A'}{\sigma^2}$$

$$S_o = \sigma^2 S_o' + \sigma . S_c$$

$$\sigma = 1 + \frac{S_c}{S_L'}$$

Therefore,

$$S_L = S_c + S_L' = (17.63 + 866) \times 10^4 = 883.63 \times 10^4 \text{ At/wb}$$

$$\sigma = 1 + \frac{S_c}{S_L'} = 1 + \frac{17.63 \times 10^4}{866 \times 10^4} = 1 + .0203$$

$$= 1.02$$

$$\mu_o A = \frac{\mu_o \times A'}{\sigma^2} = \frac{\mu_o \times 1.339 \times 10^{-4}}{(1.02)^2} = (\mu_o \times 1.29 \times 10^{-4}) \text{ Hm}$$

$$S_o = \sigma^2 S_o' + \delta S_c = 1.04 \times 305.34 \times 10^4 + 1.02 \times 17.63 \times 10^4$$

$$= 317.55 \times 10^4 + 17.98 \times 10^4$$

$$= 335.53 \times 10^4 \quad \text{At/wb}$$

The following is a list of the three constants of the equivalent magnetic circuit with their numerical values.

$S_o = 335.53 \times 10^4$ At/wb

$\mu_o A = (\mu_o \times 1.29 \times 10^{-4}) = .1621 \times 10^{-9}$ H.m

$S_L = 883.63 \times 10^4$ At/wb

6.4 Calculation of pull characteristics

When the constants of the magnetic circuit are known the pull can be calculated for an air gap x_g when the steady state mmf Ni is known. The pull in terms of the equivalent magnetic circuit is given by:

$$F = \frac{\phi_g^2}{2\mu_o A} \qquad (6.6)$$

or, $$F = \left(\frac{Ni}{S_o + \frac{x_o - x}{\mu_o A}} \right)^2 \times \frac{1}{2\mu_o A} \qquad (6.7)$$

Eq.(6.7) gives the low density pull relation. Eqns.(6.6) and (6.7) are derived in sec.10.8

Table 6.1 shows an illustrative computation of the steady state pull, and the pull characteristics thus computed are shown in fig. 6.6

Table 6.1 Computation of pull

$S_o = 335.53 \times 10^4$ At/wb, $\mu_o A = \mu_o \times 1.29 \times 10^{-4}$ Hm

$= .1621 \times 10^{-9}$ H.m, $x_o = .55$ mm.

Ni At	Air-gap $x_g = x_o - x$ mm.	ϕ_g $\times 10^{-7}$ Weber	F N	F gf
	0	298.0	2.74	279.31
100	.1	251.0	1.94	198.09
	.2	217.9	1.46	149.29
	.3	192.1	1.14	116.03
	.4	171.7	.909	92.69
	.5	155.2	.743	75.73
	.55	148.2	.677	69.06
	.0	447.0	6.16	628.26
150	.1	377.7	4.4	448.55
	.2	326.8	3.29	335.8
	.3	288.1	2.56	260.98
	.4	257.6	2.047	208.64
	.5	232.8	1.672	170.40
	.55	222.3	1.524	155.38

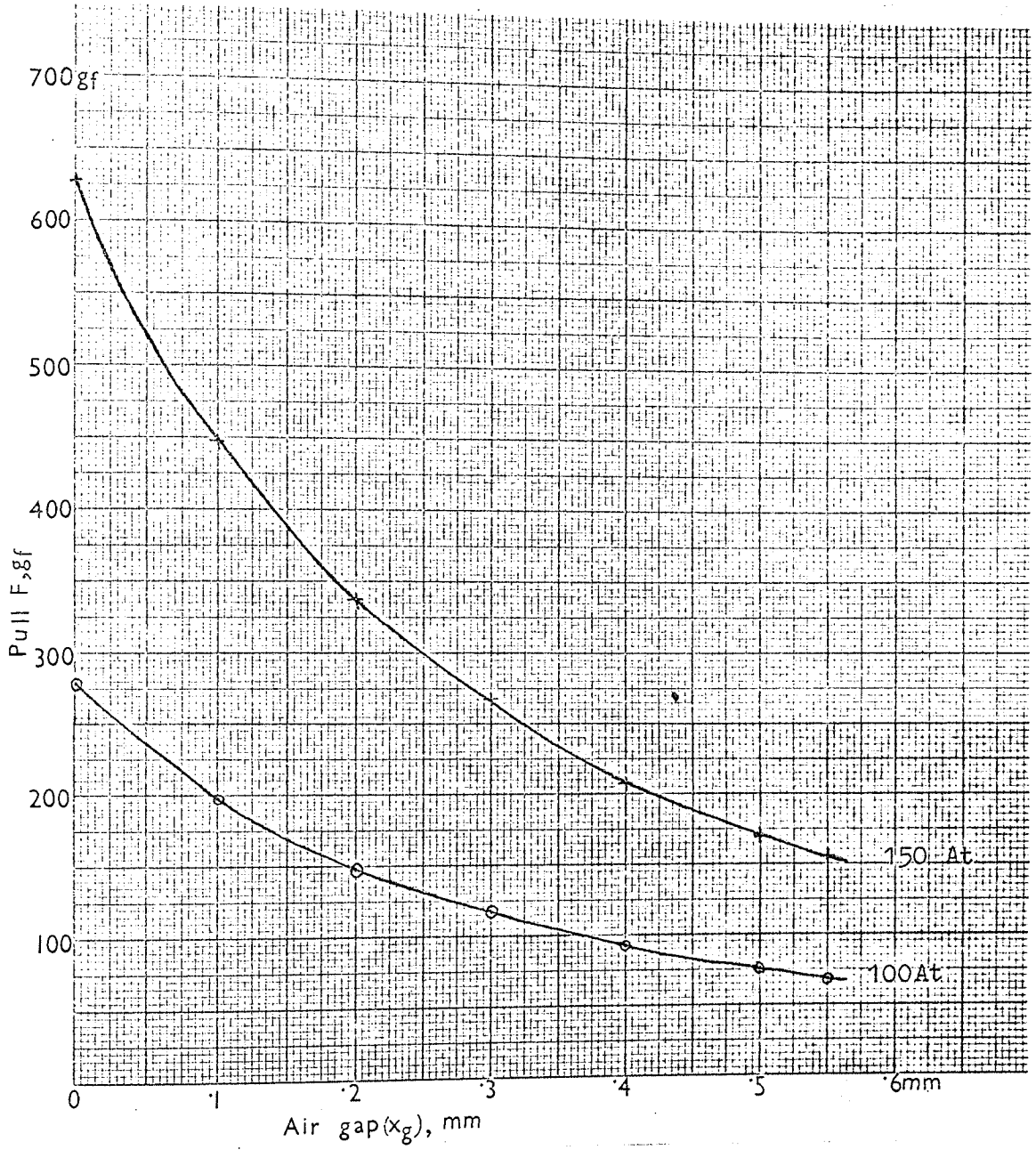

Fig.6.6 Pull characteristics

6.5 Calculation of total conductance, G

The total conductance is the sum of the coil and eddy current conductances. As G controls the time of operation, the coil conductance G_c should be chosen according to the speed requirement of the relay. The steady state power $i_s^2 R$ is jointly determined by E, the applied voltage across the coil circhit and its resistance R. Therefore, the choice of the coil conductance G_c $(= \frac{N^2}{R})$ determines the steady state ampereturns as well as the steady state power when E is already specified. G_c varies with the coil dimensions which depend upon the magnet size, or in other words G_c has influence on the choice of the overall magnet size.

Considering mainly the speed of the relay and analysing the other factors discussed above a coil was chosen, which has the following parameters:

Number of turns N = 7680 turns

Resistance of the coil = 932 ohms

$$\therefore \quad G_c = \frac{N^2}{R} = \frac{(7680)^2}{932} = 63.3 \times 10^3 \text{ mhos}$$

G_e the conductance of the eddy current paths can be estimated by using eq. 5.22.

$$G_e = \frac{1}{8\pi\rho} = \frac{58 \times 10^{-3}}{8\pi \times 11.18 \times 10^{-8}} = 20.6 \times 10^3 \text{ mhos.}$$

$$\therefore \quad G = G_c + G_e = 63.3 \times 10^3 + 20.6 \times 10^3 = 83.9 \times 10^3 \text{ mhos.}$$

6.6 Effective mass of the armature.

Knowing the moment of inertia I of the armature about the axis of the hinge, the effective mass m of the armature may be determined by adding to the armature term the effective masses of the other moving parts. I may be determined from the dimensions of the armature or may be determined by experimenting in a model. If x is measured at a distance l from the hinge then the part of the effective mass contributed by the armature is $I/(l)^2$. In the present case l is the distance between the axis through the hinge and a point on the armature opposite to the centre of the pole face. A discussion regarding the determination of the effective mass m is given in sec. 2.8 of Peek and Wagar.[3]

I was determined by measuring it in a model. The effective mass m is 7 gms.

6.7 Estimation of the time of operation from the time formulae presented in sec. 5.4.

The steady state current i_s can be calculated when the applied voltage E and the resistance of the coil are known.

$E = 23.3$ volts

$R = 932$ ohms

$i_s = \frac{23.3}{932} = 25$ mA.

steady-state power input $= i_s^2 R$

$= (25 \times 10^{-3})^2 \times 932$

$= .583$ watt.

$M_s = Ni_s = 7680 \times 25 \times 10^{-3} = 192$ At.

Spring load characteristic

Fig. 6.7 shows a linear load relation which is referred to the point on the armature opposite to the centre of the pole face. The load relation may be called the armature load relation. All other forces are also referred to the same point.

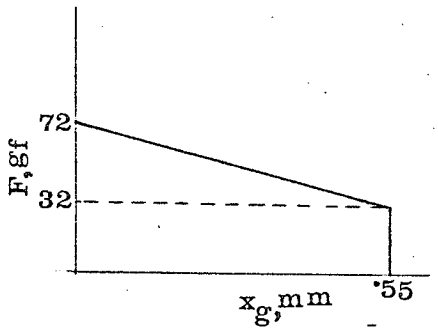

Fig. 67 Linear spring load relation.

Initial load = 32 gf = .314 N

Final load = 72 gf

Total travel x_o = .55 mm

Spring constant C = $\dfrac{(72 - 32) \times 10^{-3} \times 9.81}{.55 \times 10^{-3}} = 713.45$ N/m

The period of flux development with the armature at rest

The value of the air gap flux ϕ_g to give rise to a pull to overcome the back tension or the initial load is given by:

$$.314 \text{ N} = \frac{\phi_g^2}{2\mu_o A}$$

$$\therefore \quad \phi_g = .314 \times 2 \times 4\pi \times 10^{-7} \times (1.29 \times 10^{-4})$$

$$= 10.1750 \times 10^{-11} = 100.9 \times 10^{-7} \text{ Weber}$$

$$= \phi_{g1}$$

t_w can be calculated from formula (5.1)

$$t_w = \frac{G}{S_1} \ln \frac{1}{1 - \frac{\phi_1}{\phi_s}}$$

$$\phi_1 = \phi_{g1} \times \frac{S_L + S_o + \frac{x_o - x}{\mu_o A}}{S_L}$$

$$= 100.9 \times 10^{-7} \times \frac{993.63 \times 10^4 + 335.53 \times 10^4 + \frac{.55 \times 10^{-3}}{4\pi \times 10^{-7} \times 1.29 \times 10^{-4}}}{883.63 \times 10^4}$$

$$= 177.97 \times 10^{-7} \text{ weber}$$

$$S_1 = \frac{S_L \left(S_o + \frac{x_o - x}{\mu_o A}\right)}{S_L + S_o + \frac{x_o - x}{\mu_o A}}$$

$$= \frac{883.63 \times 10^4 \left(335.53 \times 10^4 + \frac{.55 \times 10^{-3}}{4\pi \times 10^{-7} \times 1.29 \times 10^{-4}}\right)}{883.63 \times 10^4 + 335.53 \times 10^4 + \frac{.55 \times 10^{-3}}{4\pi \times 10^{-7} \times 1.29 \times 10^{-4}}}$$

$$= \frac{883.63 \times 10^4 \left(335.53 \times 10^4 + 339.41 \times 10^4\right)}{1558.57 \times 10^4}$$

$$= 382.62 \times 10^4 \text{ At/wb}$$

$$\phi_s = \frac{192}{382.62 \times 10^4} = 501.8 \times 10^{-7} \text{ weber}$$

$$t_w = \frac{83.9 \times 10^3}{382.62 \times 10^4} \ln \frac{1}{1 - \frac{177.97 \times 10^{-7}}{501.8 \times 10^{-7}}}$$

$$= .02192 \times 2.303 \times \log \frac{1}{1 - .3546}$$

$$= 9.596 \text{ ms.}$$

Calculation of the time of operation t_1 for the first section of the travel

The time formula is given in eq. (5.11). The formula is:

$$t_1 = \sqrt{\frac{x_1}{\frac{k M_s^2}{3 mG s_1}\left(1 - e^{\frac{-s_1 t_w}{G}}\right) e^{\frac{-s_1 t_w}{G}}}}$$

Now, length of the section $x_1 = .1$ mm

$$K = \frac{1}{2 \mu_o A}\left(\frac{S_L}{S_L + S_o + \frac{x_o}{\mu_o A}}\right)^2$$

$$= \frac{1}{2 \times 4\pi \times 10^{-7} \times 1.29 \times 10^{-4}}\left(\frac{883.63 \times 10^4}{883.63 \times 10^4 + 335.53 \times 10^4 + \frac{.55 \times 10^{-3}}{4\pi \times 10^{-7} \times 1.29 \times 10^{-4}}}\right)^2$$

$$= \frac{(.5669)^2}{2 \times 4\pi \times 10^{-7} \times 1.29 \times 10^{-4}} = 9.917 \times 10^8$$

$M_s = 192$ At

$m = 7 \times 10^{-3}$ Kg

$G = 83.9 \times 10^3$ mhos

$t_w = 9.596$ ms

$S_1 = 382.62 \times 10^4$ At/wb

$$\frac{S_1 t_w}{G} = \frac{382.62 \times 10^4 \times 9.596 \times 10^{-3}}{83.9 \times 10^3} = .44$$

$$\therefore t_1 = \sqrt[3]{\frac{.1 \times 10^{-3}}{\frac{9.917 \times 10^8 \times (192)^2}{3 \times 7 \times 10^{-3} \times 83.9 \times 10^3 \times 382.62 \times 10^4} \times (1-e^{-.44})e^{-.44}}}$$

$$= 4.32 \text{ ms.}$$

Calculation for the second section of the travel

The time t_2 may be calculated from eq.(5.20) which may be repeated here:

$$x_2 = \frac{u}{n} \text{ sh } nt_2$$

$$n = \frac{c_1 - c}{m}$$

Now, the length of the section $x_2 = .55 - .1 = .45$ mm.

The velocity attained at the end of the first section is u.

In the first section $x = \chi t^3$

$$\therefore \frac{dx}{dt} = 3\chi t^2$$

$$\text{or} \quad u = 3\chi t_1^2 = 3 \times \chi \times (4.32 \times 10^{-3})^2$$

Now, $$\chi = \frac{K M_s^2}{3 mGS_1} \left(1 - e^{\frac{-s_1 t_w}{G}} \right) e^{\frac{-st_w}{G}}$$

$$= \frac{9.917 \times 10^8 \times (192)^2}{3 \times 7 \times 10^{-3} \times 83.9 \times 10^3 \times 382.62 \times 10^4} (1 - e^{-.44})e^{-.44} = 1241$$

The calculations of K and $\frac{S_1 t_w}{G}$ have already been shown.

$\therefore$ $u = 3 \times 1242 \times (4.32 \times 10^{-3})^2 = 69.53$ mm/sec.

It is difficult to find an analytical formula for c_1, but it may be attempted to find an empirical relation. c_1 may be found by measuring the pull in a model.

At the end of the first section the armature attains a velocity which is 69.53 mm/sec. and this shows that the relay armature moves quite fast. If the average acceleration is calculated it comes $\frac{69.53 \times 10^{-3}}{4.32 \times 10^{3}} = 16.09$ m/sec^2 in that section. The mass force is .1126 N or 11.48 gf. If at the end of .1 mm. distance the mass force is 11.48 gf. then it may be quite reasonable to take (11.48 x 5.5) gf = 63.14 gf at the end of .55 mm. making use of the same assumption discussed in sec. 5.3. In practice this value may be lower than the actual value.

$\therefore$ Pull = 72 + 63.14 = 135.14 gf = 1.326 N.

When the back tension is deducted from it there is obtained:

$$F - F_o = 1.326 - .314 = 1.012 \text{ N.}$$

$$\therefore \quad c_1 = \frac{1.012}{.55 \times 10^{-3}} = 1840 \text{ N/m}$$

$$\text{Hence, } n = \frac{1840 - 713.5}{7 \times 10^{-3}} = \frac{1126.5}{7 \times 10^{-3}} = 160.9285 \times 10^{3} = 401$$

Inserting the numerical values in the time formula for the second section:

$$.45 \times 10^{-3} = \frac{69.53 \times 10^{-3}}{401} \text{ sh } 401\ t_2$$

$$\text{or, sh } 401\ t_2 = \frac{401 \times .45 \times 10^{-3}}{69.53 \times 10^{-3}} = 2.5952$$

$$\therefore \quad 401\ t_2 = 1.681$$

$$t_2 = 4.19 \text{ ms.}$$

Calculation of the total time of operation t_o

Total time of operation $t_o = t_w + t_1 + t_2$

$= 9.596 + 4.32 + 4.19$

$= 18.1060$ ms.

6.8 Measurement of the time of operation

The relay shown in fig. 6.8 was made according to the design specifications given in secs. 6.2, 6.3, 6.5, 6.6 and 6.7. A constant voltage was applied across the coil to give rise to a steady-state current 25 mA. The displacement of the armature was measured by means of a photocell and storage oscilloscope. The method of displacement measurement by using a photocell is described in sec. 8.3. The trace indicating the armature position could be stored on the screen of the oscillograph for study and measurement. The x vs. t relation is shown in fig. 6.8. The total time for full operation was read from the trace on the storage oscilloscope and was found to be 15.1 ms. The calculated value of this time is 18.1 ms. which is acceptable. Table 6.2 shows the

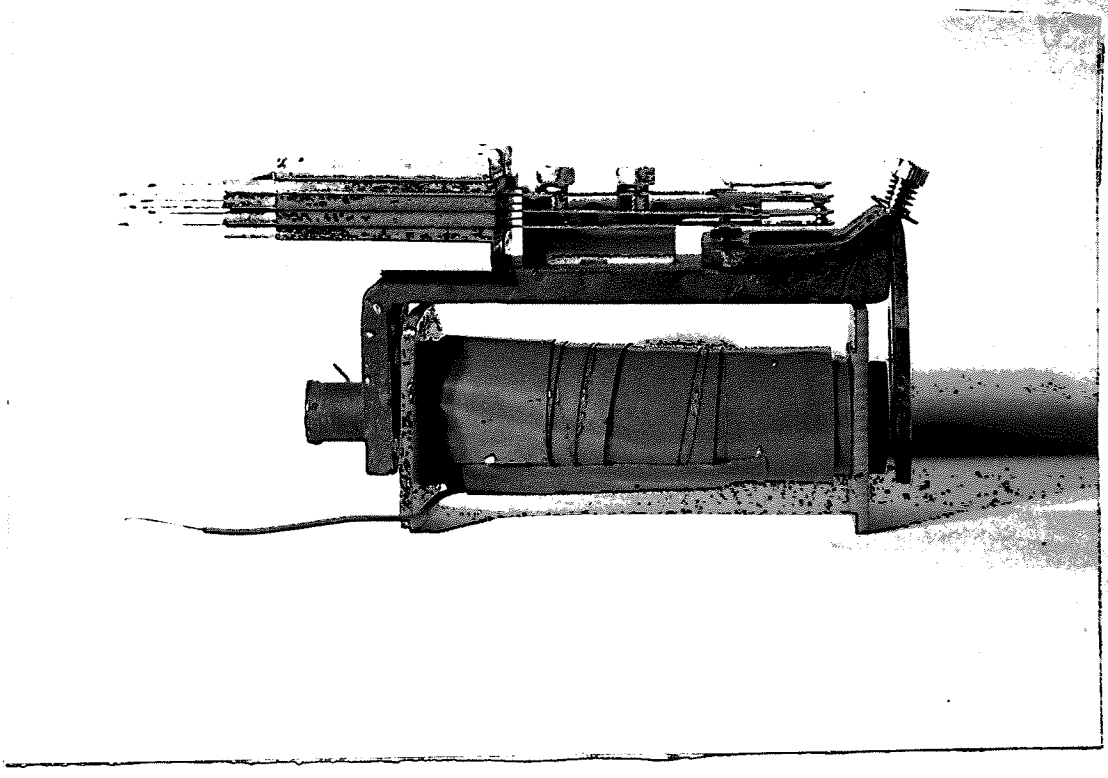

Fig. 6.8

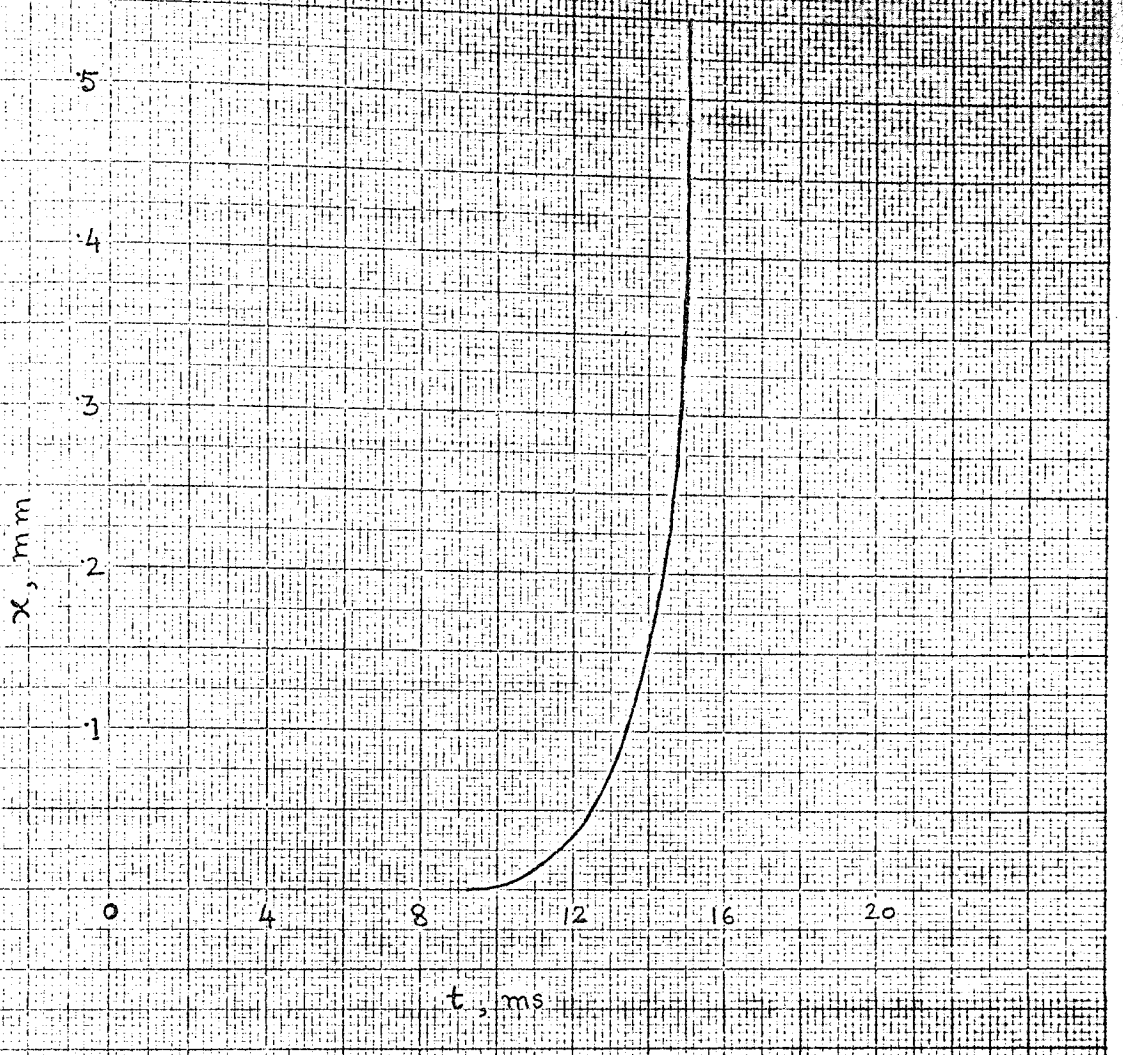

Fig. 6.9 x vs. t relation

calculated and measured times for different stages.

Table 6.2 Calculated and measured times

Measured values are taken from fig. 6.8.

Time	Calculated value ms.	Measured value ms.
t_w	9.596	9.2
t_1	4.32	4.2
t_2	4.19	1.7

6.9 Discussion.

The calculated values of t_w and t_1 agree well with their measured values. The value of t_2 may be taken to be within the acceptable range, and it is always the case that the calculated value is subject to correction by actual measurement. The calculation was intended for a design to provide the time of operation less than 20 ms and it is now clear that the calculation served the purpose giving a reasonable calculated time which is near enough to the measured value.

The reason of having the high calculated value of t_2 may be due to the inaccuracy in determining c_1; of course, it is known that the solution giving the time of operation is approximate and this may contribute a part of the discrepancy. It may be interesting to calculate t_2 from the measured value of c_1 and u.

The pull at the instant when the armature finishes its travel was measured from the value of current at that instant from the

current oscillogram. Assuming the same linear variation of pull as discussed in sec. 5.3, c_1 was calculated. The calculated pull is 2.5281 N, so the final value of the pull assumed for calculating t_2 in sec. 6.8 is about half of this value. When c_1 is calculated from the present pull value it comes to be 4025.6 N/m. The measured value of u is 83.33 mm/sec which is obtained from the relation in fig. 6.8. Taking these values of c_1 and u the time t_2 is found to be 2.94 ms. This value of t_2 is more reasonable than the previously calculated one.

Chapter 7

A RIGOROUS ANALYSIS OF THE DYNAMIC BEHAVIOUR - EXTENSION OF AHLBERG'S METHOD

7.1 Introduction

The time of operation and release of an ordinary electromagnetic relay is affected by many parameters such as, power, travel, spring load, winding design, eddy currents in the magnetic members, effective mass of the armature, magnetic circuit and frictional damping. In low speed relays some of the factors do not play a significant part but in high speed relays their effect is considerable.

In relay literature there is a want of accurate velocity and acceleration formulae. The velocity and acceleration are also affected by the parameters mentioned above. The velocity and acceleration should be critically considered, because these are of great importance when contact bounce and armature rebound are studied. It may be mentioned that mass has got a great influence on velocity and acceleration in an electromechanical system like the relay.

This chapter presents an analysis which shows how the time, velocity, acceleration and kinetic energy during operation are related to other parameters and thereby provides an insight into the performance. Ahlberg's theory is used to develop different relations considering all the four kinds of forces which influence the motion of the relay armature. How sufficiently accurate velocity and acceleration formulae can be deduced from the dynamic load relation and static pull relations combined in the same diagram, are shown. A short discussion of the

release motion is also presented. Practical calculations of dynamic characteristics from the relations developed in this chapter are given in chapter 8.

7.2 The magnetic circuit relations.

Field relations may be derived from the equivalent magnetic circuit which is discussed in detail in section 10.6 The flux and permeance relations which correspond to this circuit are derived for using them in the analysis of the dynamic behaviour. Some expressions were already derived in section 1.4 and some more expressions are derived in this section. The equivalent magnetic circuit is shown in fig 7.1.

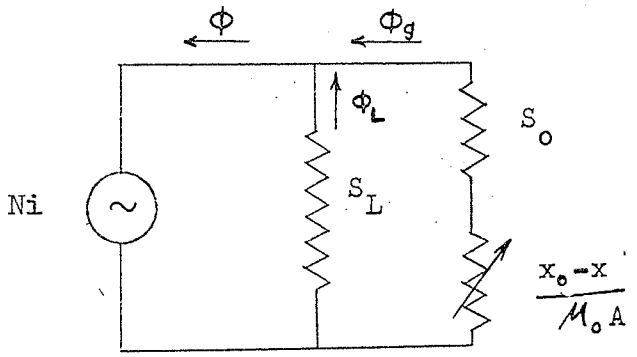

Fig.7.1 Equivalent magnetic circuit

The core flux ϕ and the air gap flux ϕ_g are given by the following expressions:

$$\phi = \frac{Ni}{S}$$

and

$$\phi_g = \frac{Ni}{S_o + \frac{x_o - x}{\mu_o A}} = M \cdot \mathcal{P}_a \qquad (7.1)$$

where $\mathcal{P}_a$ is the permeance which is given by

$$\mathcal{P}_a = \frac{1}{S_o + \frac{x_o - x}{\mu_o A}} \tag{7.2}$$

or $$\mathcal{P}_a = \frac{1}{S_o + \frac{x_g}{\mu_o A}} \tag{7.3}$$

In the right hand side of eq.(7.3), x_g is the only variable.

The ratio of ϕ and ϕ_g may be written as:

$$\frac{\phi}{\Phi_g} = \frac{\frac{Ni}{S}}{\frac{Ni}{S_o + \frac{x_o - x}{\mu_o A}}}$$

$$= \frac{S_o + \frac{x_o - x}{\mu_o A}}{S} \tag{7.4}$$

The total reluctance, S is given by:

$$S = \frac{S_L \left(S_o + \frac{x_o - x}{\mu_o A}\right)}{S_L + S_o + \frac{x_o - x}{\mu_o A}}$$

Substituting the above expression for S in (7.4) there is obtained:

$$\frac{\phi}{\phi_g} = \frac{\left(S_o + \frac{x_o - x}{\mu_o A}\right)\left(S_L + S_o + \frac{x_o - x}{\mu_o A}\right)}{S_L \left(S_o + \frac{x_o - x}{\mu_o A}\right)}$$

$$= \frac{S_L + S_o + \frac{x_o - x}{\mu_o A}}{S_L}$$

$$\text{or} \qquad \frac{\phi}{\phi_g} = 1 + \frac{S_o + \frac{x_o - x}{\mu_o A}}{S_L}$$

$$= 1 + p \cdot \frac{1}{\mathcal{P}_a} \qquad (7.5)$$

where p is the leakage permeance which is the inverse of the leakage reluctance S_L.

$$\therefore \quad p = \frac{1}{S_L} \qquad (7.6)$$

The flux, reluctance and permeance expressions corresponding to the equivalent magnetic circuit are applicable when the magnetisation is linear. In the present analysis it is assumed that the magnetisation is confined to the low density region, i.e. the permeability is constant, which is the case of linear magnetisation.

7.3 Analysis of the motion of the relay armature

The dynamic performance in operation may be critically analysed from the different relations with the help of Ahlberg's[9,10,11] theory, magnetic force formula and the equivalent magnetic circuit. Before going to the detailed discussion of the present method, Ahlberg's theory may be explained in brief.

Ahlberg's[9] theory.

This states that 'in a given magnetic system every value of pull corresponds to a unique value of flux, and every value of travel corresponds to a unique value of the permeance of the magnetic circuit!

Therefore, the pull and load characteristics in mechanical system of co-ordinates can be converted into the equivalent characteristics in magnetic system of co-ordinates, when force and travel are replaced by their magnetic equivalents, which are flux and permeance respectively.

The theory deals with the motion of a relay armature, which moves under the influence of two kinds of forces, namely, the spring load and magnetic pull, whereas, the mass and friction forces are disregarded. Showing the load as a function of permeance of the magnetic circuit, analytical design relations for the time of operation and of release, velocity and acceleration are derived. Obviously, these relations are applicable to a fictitious relay whose armature moves under the influence of only two kinds of forces, or to an actual relay in which the mass and friction forces can be disregarded. Ahlberg's theory may be applied to study the motion of an actual armature which moves under the influence of four kinds of forces.

The motion of an actual armature.

During the motion of a relay armature there are four kinds of forces which influence the motion. These four forces are the pull of the electromagnet, spring load, frictional damping force and mass force or acceleration force. The direction of forces at any instant can be easily determined if the sign of velocity and acceleration are known. Of course, the directions of the pull and load are always unchanged. During the motion,

there is a dynamic equilibrium between these four forces at every instant of time and the armature indicates the position where this momentary equilibrium exists. The armature moves forward for finding a position of static equilibrium, but it does not get it normally until it is stopped by the pole face of the electromagnet, and the static equilibrium is ultimately achieved when the armature stays in contact with the pole face.

When a current is switched on in the relay coil there is a particular value of main air-gap flux at every instant of time before and during the motion of the armature. Now, in a given magnetic system for every value of air-gap flux there is a particular value of magnetic pull. So, if the dynamic measurement of flux is taken for every position of the armature, then the values of the flux give the values of the pull at different positions. The pull F is connected to the flux by Maxwell's force formula:

$$F = \frac{\phi_g^2}{2\mu_o A}$$

where A is the pole face area of the electromagnet. This force expression is discussed in section 10.8

The pull from the dynamic flux measurement is equal to the sum of the mass force, spring retractile force and frictional damping force at every instant. Dynamic pull vs. position characteristic may be obtained from dynamic flux (ϕ_g) vs. position characteristic by using Ahlberg's theory and this may

be called dynamic load characteristic in mechanical system of co-ordinates. Dynamic air-gap flux (ϕ_g) vs. magnetomotive force characteristic which may be called the dynamic load characteristic in magnetic system of co-ordinates may be obtained from ϕ_g vs. x relation by using the same theory. Every value of the position co-ordinate x corresponds to a particular value of the permeance of the magnetic circuit and the magnetomotive force and permeance are connected by the following formula:

$$M = \frac{\phi_g}{\mathcal{P}_a}$$

$\mathcal{P}_a$ is the permeance with respect to a given length of air-gap, x_g ($= x_o - x$). $\mathcal{P}_a$ may be calculated from the equivalent magnetic circuit of the relay. The expression for $\mathcal{P}_a$ in eq.(7.2) shows that for every value of x or air-gap, x_g there is a unique value of the permeance $\mathcal{P}_a$. The direction of motion is positive when the armature moves towards the pole face of the magnet. Therefore, x = o when the armature is in open gap or 'unoperated' position. In the present analysis the total operating time consisting of the time of flux growth with the armature at rest and the time of motion, is considered in a single treatment.

Different measurements on a telephone type electromagnetic relay (type 305/2500/ABE-FG1/50, made by Magnetic Devices Ltd.) equipped with eighteen contact springs and thus having a complicated load characteristic, were made when the constant

voltage across the coil was such that the final current was 11 mA. Of course, some measured characteristics do not depend on the feeding voltage.

The methods of measurements are given in chapters 8 and 11. Oscillograms 1 and 2 in fig.7.2, show the variations of the core flux (ϕ) and position (x) of the armature with time. From these two characteristics air gap flux (ϕ_g) vs. x characteristic may be plotted. Assuming the static and dynamic field patterns are the same, a relation connecting ϕ and ϕ_g can be obtained from the equivalent magnetic circuit. The relation in (7.5) which is derived in section 7.1 is as follows:

$$\frac{\phi}{\phi_g} = 1 + \frac{p}{\mathcal{P}_a}$$

This relation may be written in the form:

$$\phi_g = \phi \frac{S_L}{S_o + S_L + \frac{x_o - x}{\mu_o A}}$$

The values of ϕ_g for plotting ϕ_g vs. x characteristic just mentioned, are calculated from the values of ϕ by using the preceding expression. The dynamic air-gap flux and core flux relations are shown in fig.7.3. From ϕ_g vs. x relation dynamic pull vs. air-gap (x_g) curve can be plotted, which is shown in fig.7.4. This curve represents the dynamic load characteristic in mechanical system of co-ordinates.

From ϕ_g vs. x relation ϕ_g vs. M relation may be derived. The latter one which may be called the dynamic load characteristic

1

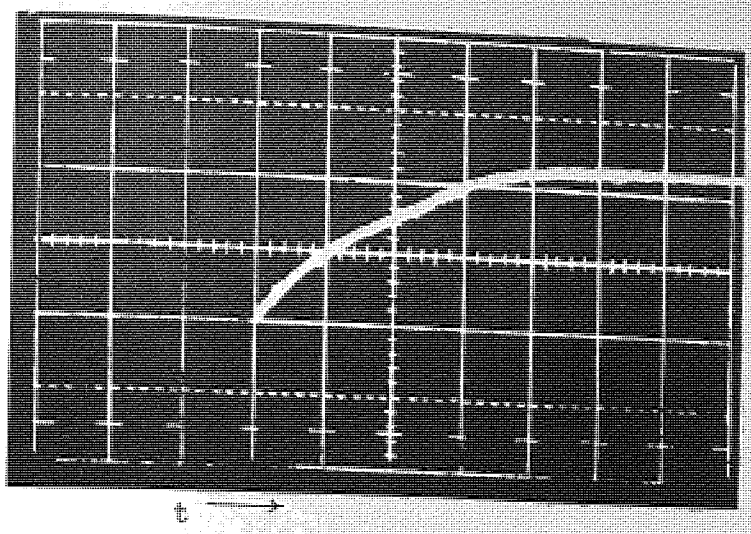

Time scale : 10 ms/scale div.

Flux scale: 80×10^{-7} Wb./div.

2

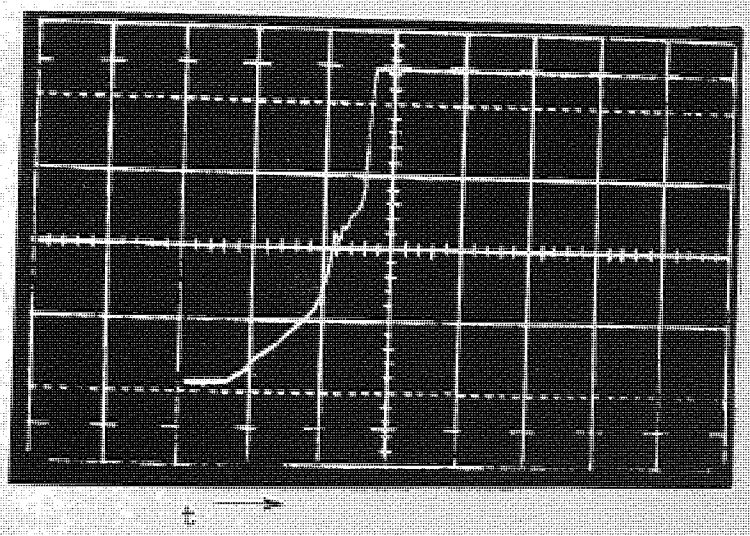

Time scale: 10 ms/div.

Position scale: .0380 mm/scale div.

Fig. 7.2 Oscillograms showing ϕ vs t and x vs t at M_a = 275 At.

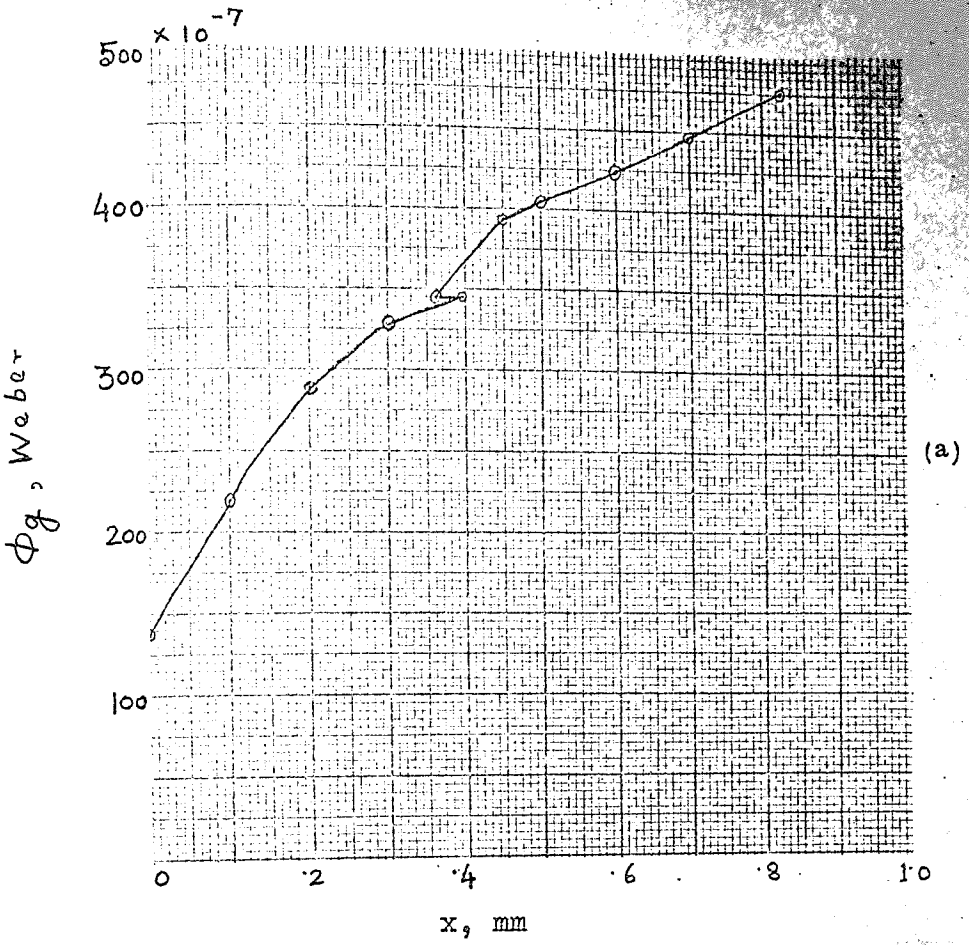
× 10⁻⁷
500
400
300
200
100
ϕ_g, Weber
0
·2
·4
·6
·8
1·0
x, mm
(a)

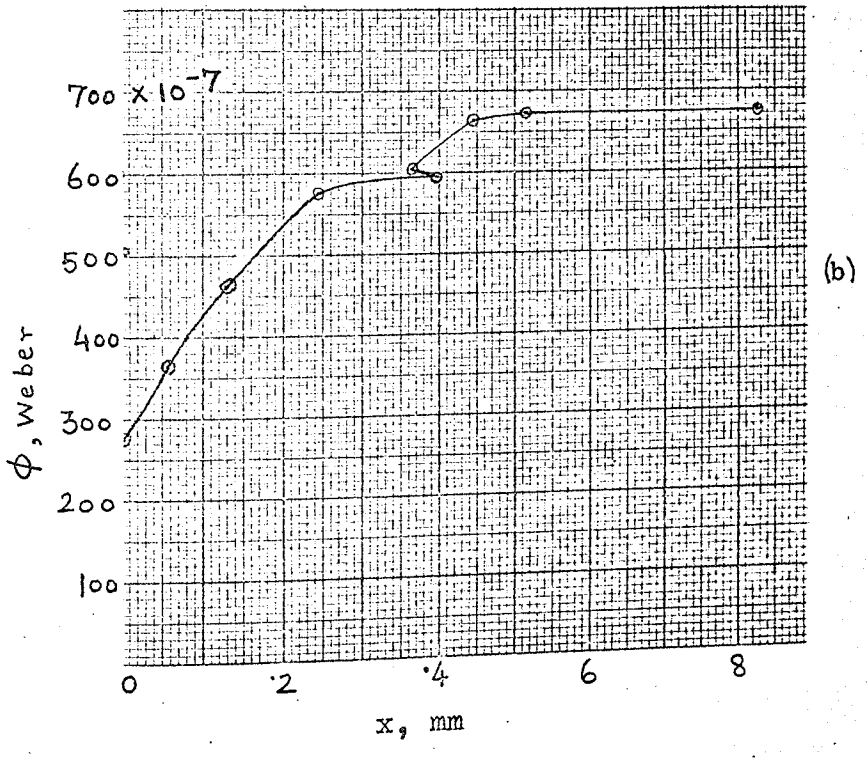
700
× 10⁻⁷
600
500
400
300
200
100
ϕ, Weber
0
·2
·4
6
8
x, mm
(b)

Fig. 7.3

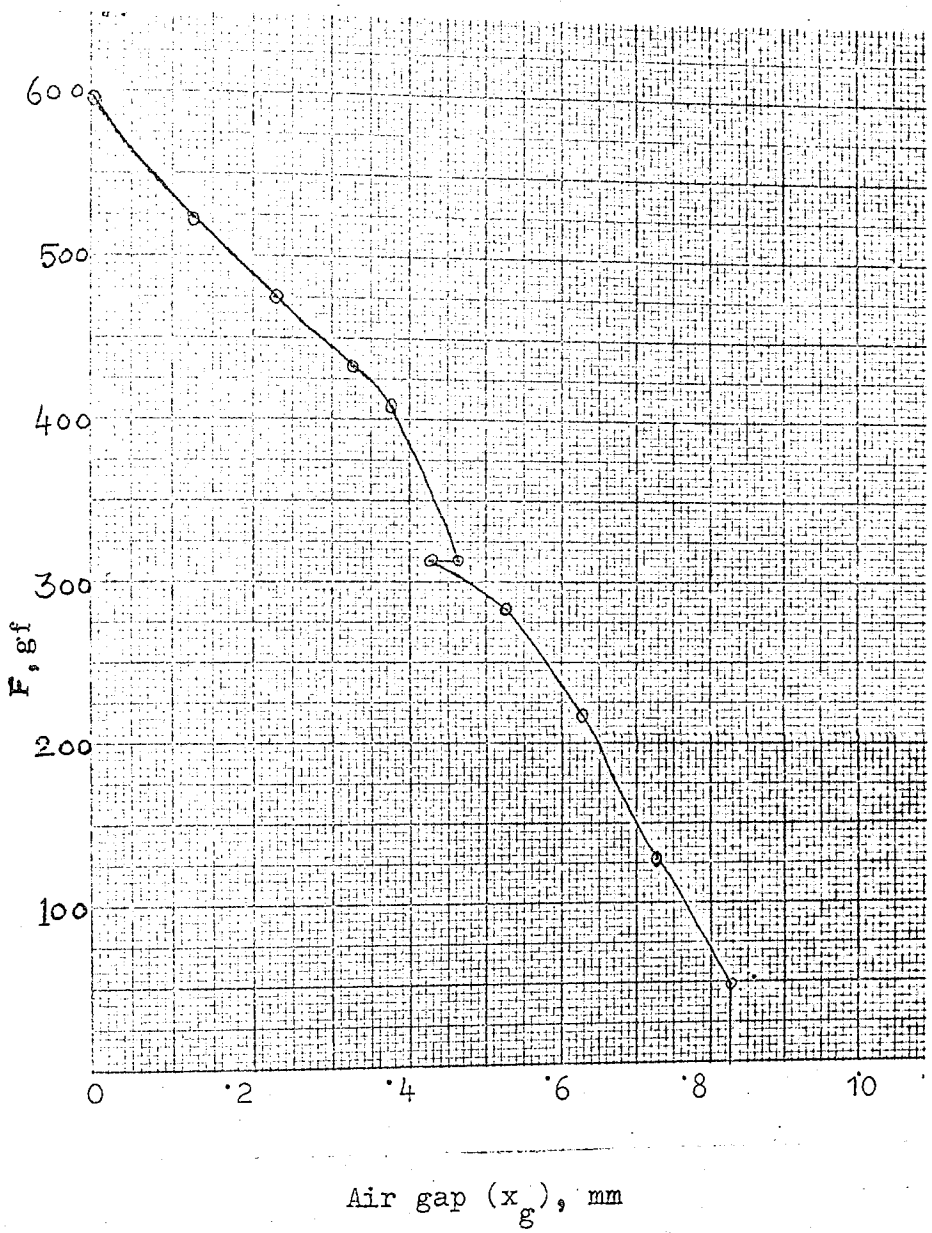

Fig. 7.4 Dynamic pull vs. air gap relation

in magnetic system of co-ordinates, is shown in fig.7.5.

Two more characteristics which are useful for the analysis may be shown. The steady state pull relation and static load relation for the same relay as obtained from the measurements are shown in figs, 7.6 and 7.7 respectively. From the characteristicsmentioned in this section the dynamic behaviour may be analysed. It may be possible to calculate the time of operation, time of release, velocity, acceleration and kinetic energy. Two approximations may be introduced. According to approximation 1, it is assumed that the permeability μ is constant. According to approximation 2, it is assumed that the line joining the adjacent load points in figs. 7.4 and 7.5 are straight. The load points in ϕ_g vs. M characteristic are indicated by the numbers 1,2,3,4 etc. in fig.7.5.

The travel of the armature may be divided into several sections following the static load points which are the points where the curve changes its slope. The load points in the dynamic load characteristics may also be fixed following the best straight portions or slightly curved portions and this method has been adopted here. The time, velocity and acceleration formulae are deduced in sections 7.5, 7.6 and 7.7 respectively. Before presenting the deductions, the eddy currents and their effects are discussed. In eq.(1.1) the term G contains G_e which is the effective conductance of the eddy-current paths. In sec.7.4, it is elucidated that the eddy-current is considered when G is taken as $(G_e + G_e)$.

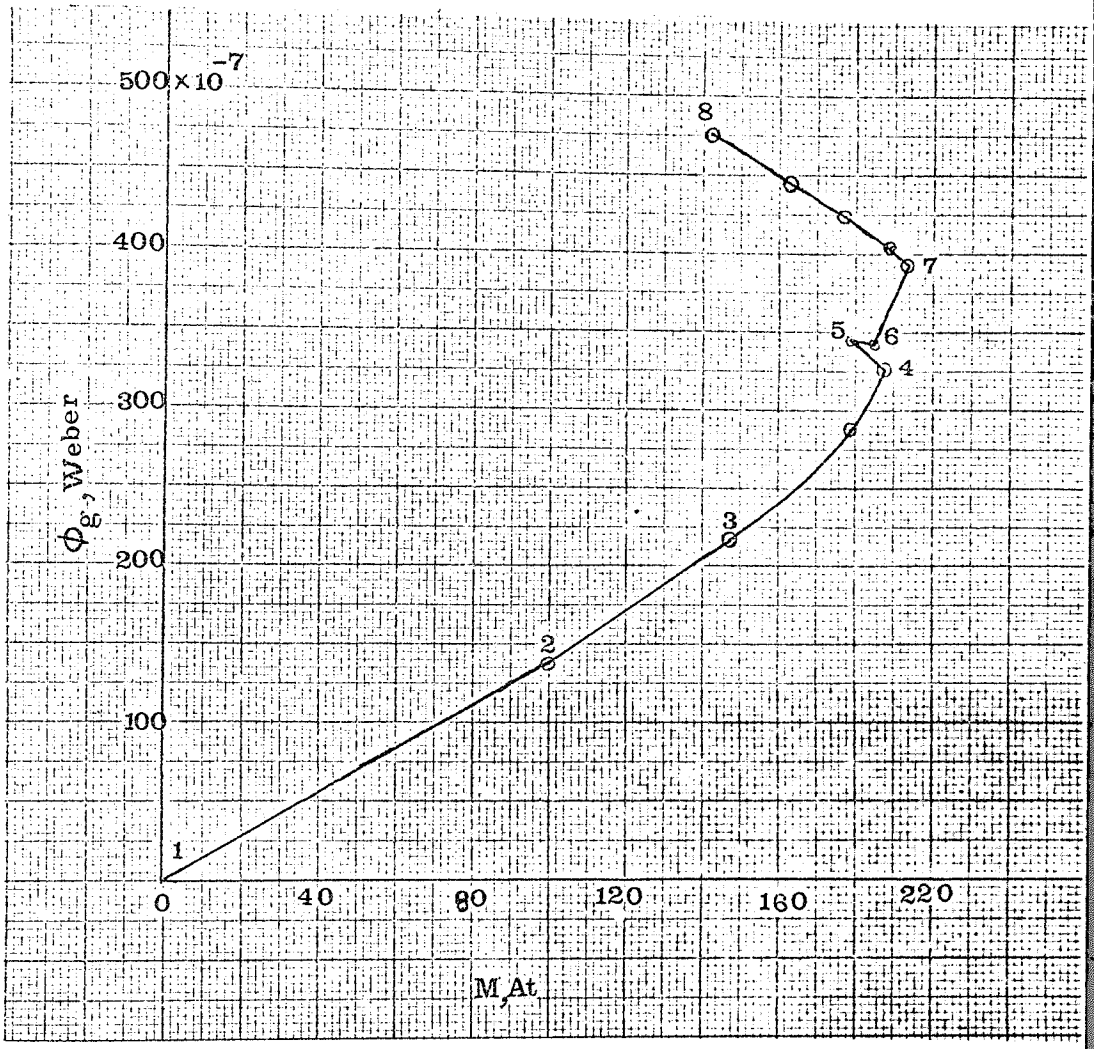

Fig. 7.5 ϕ_g vs. M relation (Dynamic load characteristic in magnetic system of co-ordinates)

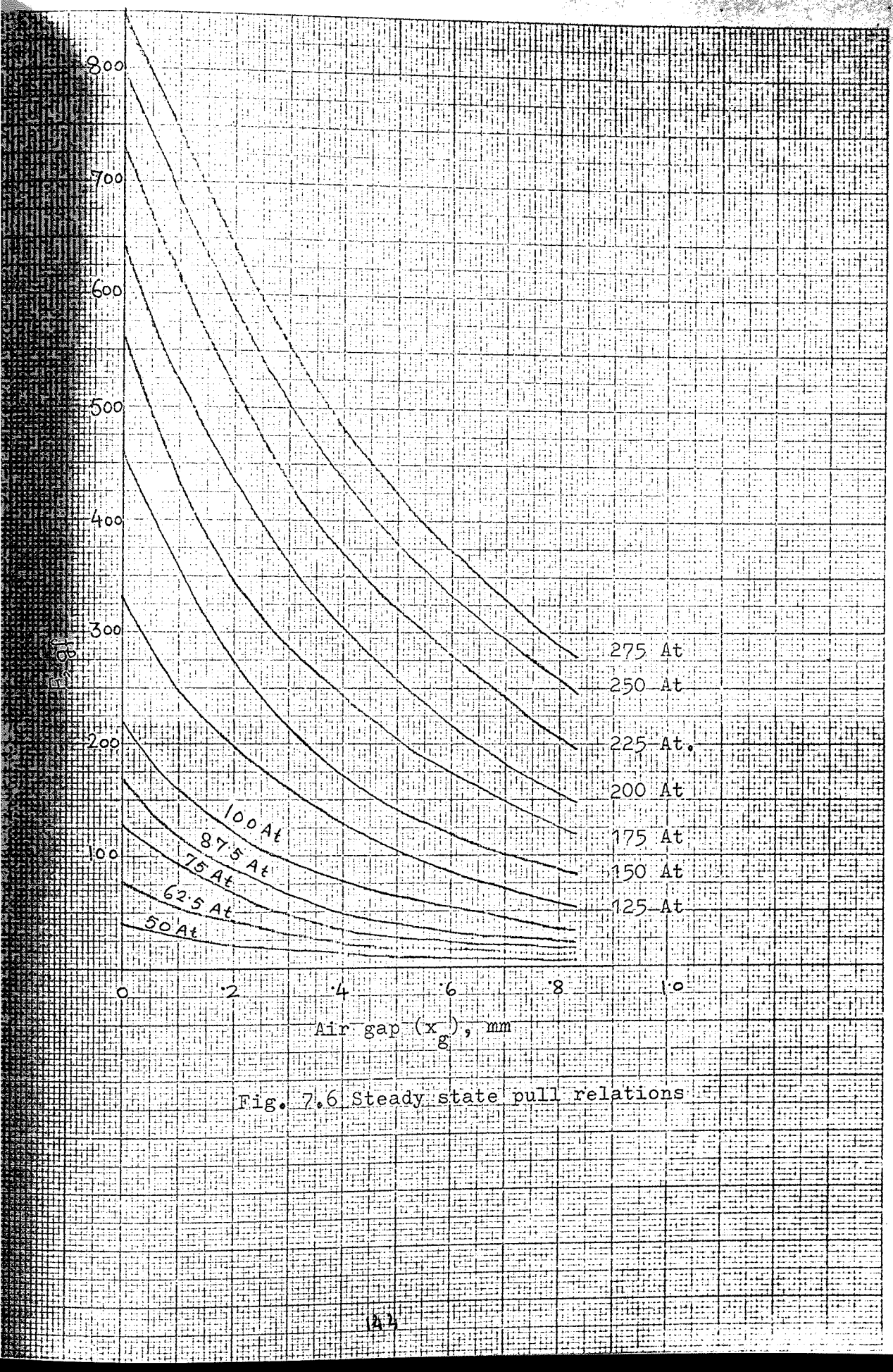

Fig. 7.6 Steady state pull relations

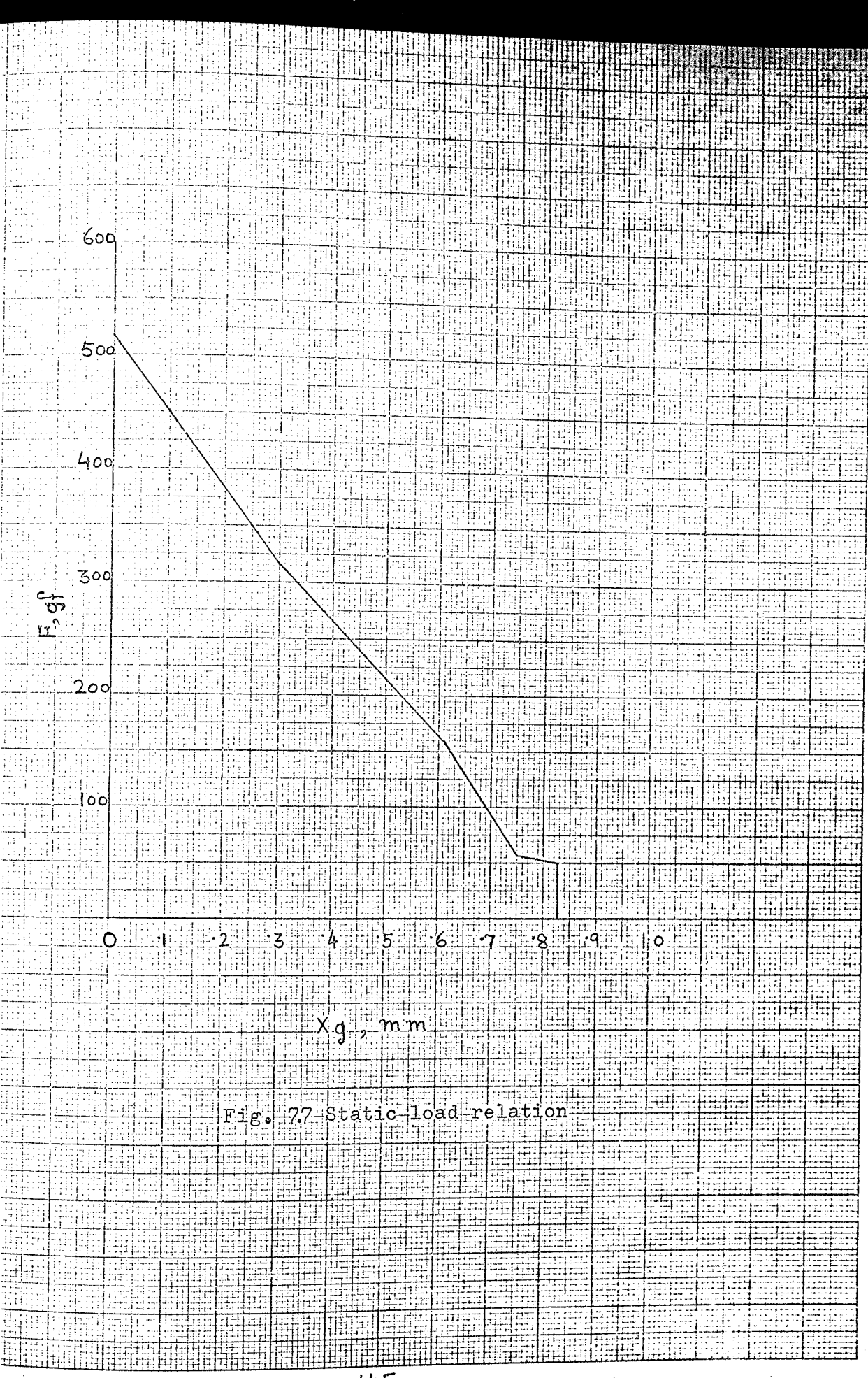

Fig. 7.7 Static load relation

7.4 Eddy-currents

These are induced in the conducting members of the magnetic structure due to the transformer induction or the time varying field and have two distinct effects. They disturb the static field pattern and produce delay in the field development. The delay can be realised simply by applying Lenz's law, according to which the eddy-currents tend to oppose the change in the field inducing it. In operation and slow release, the change of the static field pattern may be neglected and the static and dynamic field patterns may be taken to be the same. Whereas, in ordinary release, with or without a protective network, this would yield an approximate treatment.

The delaying effect of the eddy-currents will be considered here. The eddy-current pattern in the conducting members is taken to remain unchanged during the entire process of the operation and release, which includes both the cases of stationary and moving armature. Ekelöf assumes an equivalent single turn winding coupled with the main winding to replace the eddy current effect. Tomita and Ahlberg also assume the same. Ekelöf does not assume the coupling factor between the magnetising winding and the equivalent winding to be 1, but Ahlberg does so for the simplification of the mathematical analysis.

In the present analysis the eddy current equivalent winding consisting of one turn, closely coupled with the main winding, is assumed. The equivalent winding links the same flux ϕ

as the main winding does and both the windings are shown schematically in fig. 7.8.

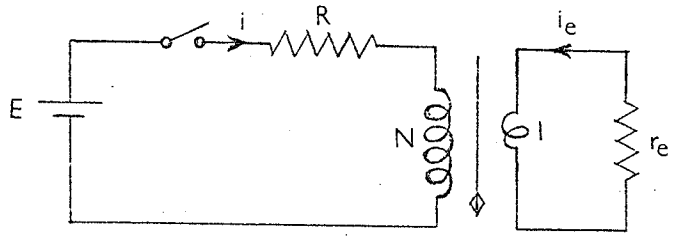

Fig. 7.9

The voltage equation for a coil of N turns linking the flux ϕ may be written as:

$$(i - I_s)\, R + N \frac{d\phi}{dt} = 0 \qquad (7.7)$$

For the main winding the equation is the same as (7.7). For eddy current winding the voltage equation becomes:

$$(i_e - o)\, r_e + 1. \frac{d\phi}{dt} = 0$$

or
$$i_e r_e + \frac{d\phi}{dt} = 0 \qquad (7.8)$$

Equation (7.7) can be written in the form:

$$M - M_s + \frac{N^2}{R} \frac{d\phi}{dt} = 0$$

or
$$G_c \frac{d\phi}{dt} = M_s - M_c \qquad (7.9)$$

Where M_c is the instantaneous magnetomotive force due to the current in the main winding,. Eq. (7.9) applies to the same winding.

Eq.(7.8) may be written in the form :

$$1.\ i_e + \frac{1}{r_e} \cdot \frac{d\phi}{dt} = 0$$

or $$M_e + G_e \frac{d\phi}{dt} = 0$$

or $$G_e \frac{d\phi}{dt} = -M_e \qquad (7.10)$$

where M_e is the instantaneous mmf produced by the eddy current equivalent winding.

Adding equations (7.9) and (7.10) there is obtained:

$$(G_e + G_e) \frac{d\phi}{dt} = M_s - (M_c + M_e) \qquad (7.11)$$

When eddy currents are ignored eq.(7.9) is applicable. In that case, eq. (7.9) may be written as:

$$G_e \frac{d\phi}{dt} = M_s - S\phi \qquad (7.12)$$

where $S\phi = M_c$. When eddy currents are taken into consideration (eq.7.11) applies and the same equation may be written in the form:-

$$(G_c + G_e) \frac{d\phi}{dt} = M_s - S\phi \qquad (7.13)$$

where $S\phi = M_c + M_e$. The static and dynamic field patterns are assumed to be the same. Comparing equations (7.12) and (7.13) it may be concluded that the eddy current effect is taken into account if G in the electrical equation (1.1) is taken as $(G_c + G_e)$.

7.5 Time of passage between two adjacent load points (A and B) during operation.

Ahlberg mentions Ekelof's time formula which is deduced from the static load characteristic neglecting mass and frictional damping forces. Similarly the time formula may be deduced from the dynamic air-gap flux vs. mmf. relation without neglecting these forces. The time formula becomes a little simplified because of using the simple flux expressions which may be deduced in terms of the constants of the equivalent magnetic circuit.

Equation (7.5) may be re-written:

$$\frac{\phi}{\phi_g} = 1 + p \cdot \frac{1}{\mathcal{P}_a}$$

Equation (1.1) gives the following relations:

$$S\phi + G \frac{d\phi}{dt} = N I_s$$

$$M + G \frac{d\phi}{dt} = N I_s = M_s$$

$$M_s - M = G \frac{d\phi}{dt}$$

$$\frac{d\phi}{dt} = \frac{1}{G} \cdot (M_s - M) \qquad (7.14)$$

Where $G = G_c + G_e$. G_c is the coil conductance and G_e is the effective conductance of the eddy current paths. Thus, the effect of eddy current has been taken into account.

From equation (7.5)

$$\phi = \phi_g \left(1 + \frac{p}{\mathcal{P}_a}\right)$$

$$= \phi_g + M p$$

$$\therefore \quad \frac{d\phi}{dt} = \frac{d}{dt}(\phi_g + Mp)$$

$$= \frac{d\phi_g}{dt} + p \cdot \frac{dM}{dt}$$

$$= \frac{d\phi_g}{dM} \cdot \frac{dM}{dt} + p \frac{dM}{dt}$$

$$\text{or} \quad \frac{d\phi}{dt} = \left(\frac{d\phi_g}{dM} + p\right) \frac{dM}{dt} \qquad (7.15)$$

From (7.14) and (7.15)

$$\frac{M_s - M}{G} = \left(p + \frac{d\phi_g}{dM}\right) \frac{dM}{dt}$$

$$\therefore \quad dt = G\left(p + \frac{d\phi_g}{dM}\right) \cdot \frac{dM}{M_s - M}$$

$$\int_A^B dt = \int_A^B G\left(p + \frac{d\phi_g}{dM}\right) \frac{dM}{M_s - M}$$

In fig.7.5 a straight line approximation of the curved portion A B (e.g. 3-4) is made and there is obtained:

$$\frac{d\phi_g}{dM} = \frac{\phi_B - \phi_A}{M_B - M_A}$$

Where ϕ_A and ϕ_B are the working air-gap fluxes and M_A and M_B are the mmf's at points A and B respectively.

$$\therefore \quad t_{A-B} = G\left(p + \frac{\phi_B - \phi_A}{M_B - M_A}\right) \ln \frac{M_s - M_A}{M_s - M_B} \qquad (7.16)$$

$$\text{or} \quad t_{A\,B} = G\left(p + \frac{\phi_B - \phi_A}{M_B - M_A}\right) 2.303 \log \frac{M_s - M_A}{M_s - M_B} \qquad (7.17)$$

Equation (7.17) gives the time formula for calculating the time of passage for a section of the travel during operation. The total time for full operation is the sum of the times needed for the individual stages.

The initial stage of the flux development with the armature at rest may be treated as a special case in which the load line in ϕ_g - M plane starts from the origin. Initially both the flux and mmf are zero; obviously, $\phi_A = 0$ and $M_A = 0$. Hence, formula (7.17) changes to:

$$t_{A\,B} = G\left(p + \frac{\phi_B}{M_B}\right) 2.303 \log \frac{M_s}{M_s - M_B}$$

$$\therefore \quad t_w = G\left(p + \frac{\phi_B}{M_B}\right) 2.303 \log \frac{M_s}{M_s - M_B} \qquad (7.18)$$

In fig.7.5 the section 1-2 gives the flux relation during this period.

Another case may be considered when $M_A = M_B = M$ for a load line in the ϕ_g - M plane. It is already shown that,

$$t_{A\,B} = \int_A^B dt = \int_A^B G\left(p + \frac{d\phi_g}{dM}\right) \frac{dM}{M_s - M}$$

$$\therefore \quad t_{A\,B} = \int_A^B G\left(p \cdot \frac{dM}{M_s - M} + \frac{d\phi_g}{M_s - M}\right)$$

In this particular case just mentioned, dM is zero

$$\therefore \quad t_{A\,B} = \int_A^B G\left(\frac{d\phi_g}{M_s - M}\right) = G\,\frac{\phi_B - \phi_A}{M_s - M} \qquad (7.19)$$

The time formula (7.17) changes to (7.19), when $M_A = M_B = M$.

7.6 Armature velocity at any position during operation

The dynamic load characteristic in fig. 7.4 and the static pull characteristics in fig.7.6 may be combined in the same diagram as shown in fig.7.9. The dynamic load curve in fig. 7.4 is represented in fig. 7.9 by fitting a number of linear segments. If it is required the number of segments may be made more to make the characteristic to represent closely the original one.

An expression for the velocity may be deduced in a similar manner as given in the papers by Ahlberg,[10,11] from the diagram in fig.7.9 Ahlberg considers an equilibrium between the static load and the magnetic pull, and the velocity formula in the papers is deduced from the diagram in which the static load and static pull characteristics are represented. Although the mathematical steps in the deduction of the velocity formula in this section are almost similar to the same in the papers just mentioned, different relations differ in detail and eventually the final formula appear in a little simplified form. As the present method uses the dynamic load characteristic, it differs basically in some respect from the method in the said papers.

The equivalent magnetic circuit is used to derive the flux and permeance relations. The ratio ϕ/ϕ_g may be given by:

$$\frac{\phi}{\phi_g} = 1 + \frac{p}{\mathcal{P}_a} \qquad (7.20)$$

which is given in sec. 7.2 as (7.5)

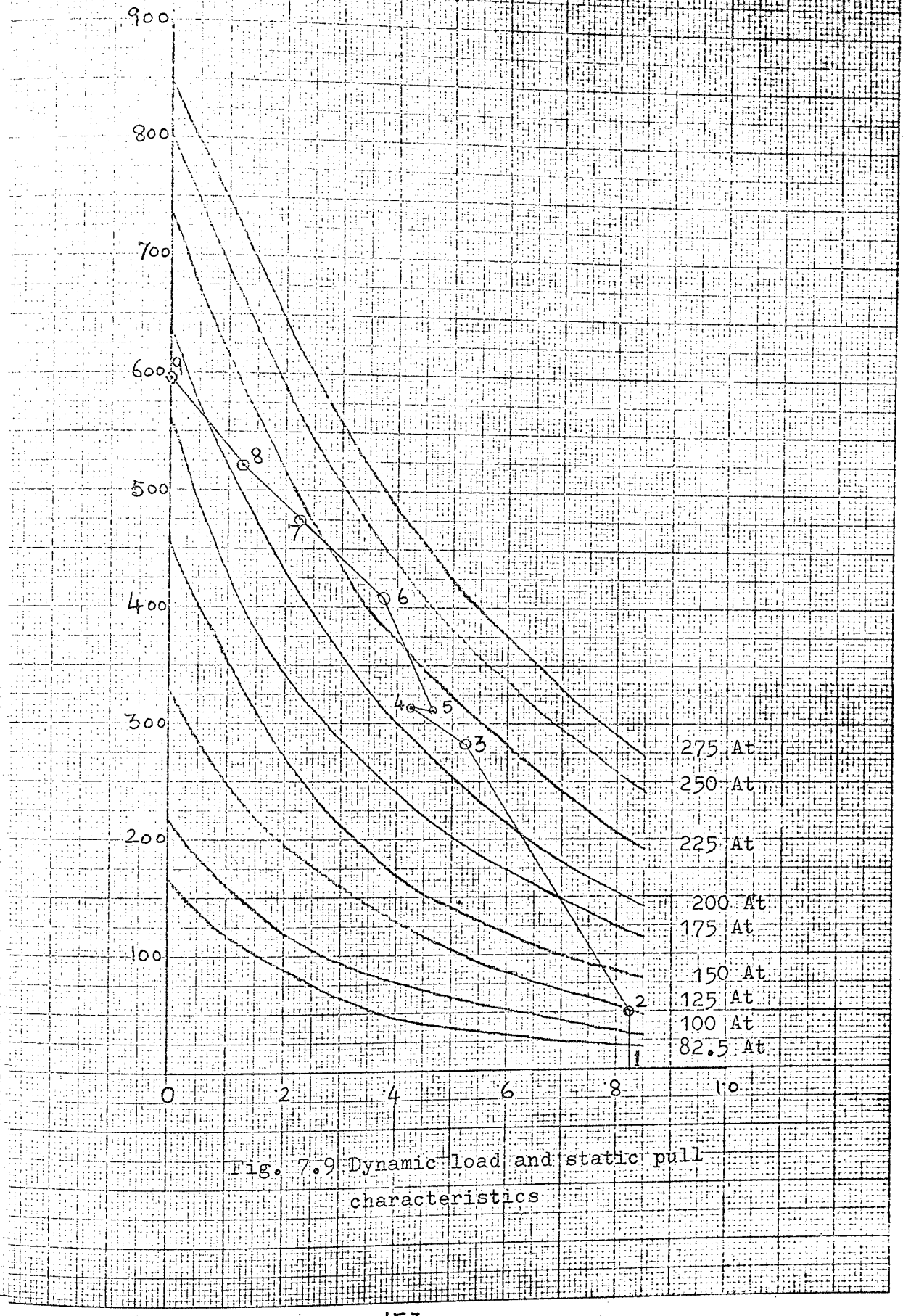

Fig. 7.9 Dynamic load and static pull characteristics

From equation (7.3)

$$\frac{1}{\mathcal{P}_a} = S_o + \frac{x_o - x}{\mu_o A} = S_o + \frac{x_g}{\mu_o A} = \beta + \delta x_g \qquad (7.21)$$

where β and δ are two constants. Here $\beta = S_o$ and $\delta = \frac{1}{\mu_o A}$.

In fig. 7.10 one segment of the dynamic load curve is shown. An instantaneous position of the armature is considered and this position is with the air gap x_g, the load F and the mmf M as indicated in the same figure. The subtangent to the pull

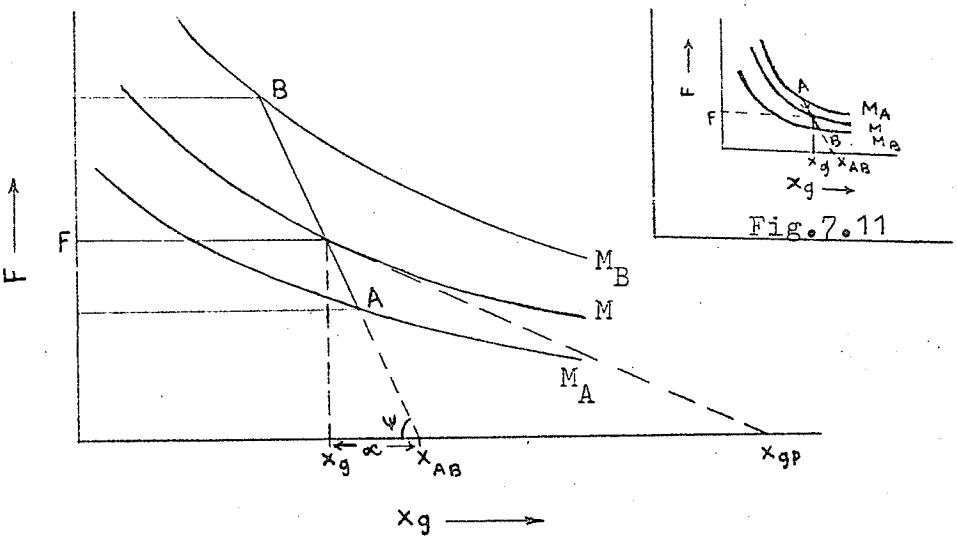

Fig. 7.10

Fig. 7.11

curve M in figure 7.9 is shown as : $s = x_g\ x_{gp}$, which may be given by:

$$s = \frac{F}{-\frac{dF}{dx_g}}$$

As $$F = \frac{\phi_g^2}{2\mu_o A} = \frac{M^2}{2\mu_o A} \cdot \frac{1}{(\beta + \delta x_g)^2} \qquad (7.22)$$

$$\therefore \quad \frac{dF}{dx_g} = - \frac{M^2}{2 \mu_o A} \cdot \frac{2 \delta}{(\beta + \delta x_g)^3}$$

Substituting this expression for $\frac{dF}{dx_g}$ in the expression for s there is obtained:

$$s = \frac{F}{- \frac{dF}{dx_g}} = \frac{\beta + \delta x_g}{2 \delta} = \frac{1}{2 \delta \wp_a}$$

$$\therefore \quad \wp_a = \frac{1}{2 \delta s} \qquad (7.22a)$$

From (7.20)

$$\phi = \phi_g \left(1 + \frac{p}{\wp_a}\right)$$

Differentiating this with respect to t there is obtained:

$$\frac{d\phi}{dt} = \left(1 + \frac{p}{\wp_a}\right) \frac{d\phi_g}{dt} - \phi_g \cdot \frac{1}{\wp_a^2} \cdot \frac{d\wp_a}{dt} \qquad (7.23)$$

In fig.7.9:

$$F = a \tan \psi$$

$$\therefore \quad \frac{\phi_g^2}{2 \mu_o A} = a \tan \psi$$

$$\text{or} \quad \phi_g^2 = 2 \mu_o A \; a \tan \psi \qquad (7.24)$$

Differentiation of eq.(7.24) gives:

$$2\phi_g \cdot \frac{d\phi_g}{dt} = 2\mu_o A \tan\psi \frac{d\alpha}{dt} = \frac{\phi_g^2}{\alpha} \cdot \frac{d\alpha}{dt}$$

$$\therefore \quad \frac{d\phi_g}{dt} = \frac{\phi_g}{2\alpha} \cdot \frac{d\alpha}{dt} \qquad (7.25)$$

Differentiating $\frac{1}{\mathcal{P}_a}$ in (7.21) there is obtained:

$$-\frac{1}{\mathcal{P}_a^2} \cdot \frac{d\mathcal{P}_a}{dt} = \delta \frac{dx_g}{dt} \qquad (7.26)$$

As $x_g = x_{AB} - \alpha$

$$\therefore \quad \frac{dx_g}{dt} = -\frac{d\alpha}{dt}$$

and $$\frac{1}{\mathcal{P}_a^2} \cdot \frac{d\mathcal{P}_a}{dt} = -\delta \cdot \frac{dx_g}{dt} = \delta \cdot \frac{d\alpha}{dt} \qquad (7.27$$

on substituting in eq.(7.23) the expressions for $\frac{d\phi_g}{dt}$ and $\frac{1}{\mathcal{P}_a^2} \cdot \frac{d\mathcal{P}_a}{dt}$ in (7.25) and (7.27) respectively, there is obtained:

$$\frac{d\phi}{dt} = \left(1 + \frac{p}{\mathcal{P}_a}\right)\left(\frac{\phi_g}{2\alpha} \cdot \frac{d\alpha}{dt}\right) - \phi_g \left(\delta \cdot \frac{d\alpha}{dt}\right)$$

$$= \left(1 + \frac{p}{\mathcal{P}_a}\right) \cdot \frac{\phi_g}{2\alpha} \cdot \frac{d\alpha}{dt} - \phi_g \cdot \delta \frac{d\alpha}{dt}$$

$$\frac{d\phi}{dt} = \left\{\left(1 + \frac{p}{\mathcal{P}_a}\right) \frac{1}{2\alpha} - \delta\right\} \phi_g \cdot \frac{d\alpha}{dt} \qquad (7.28)$$

From (7.22a) and the relation $\wp_a = \frac{\phi_g}{M}$

$$\phi_g = \frac{M}{2\,\delta\,s} \tag{7.29}$$

Substitution of the expressions for $\wp_a$ and ϕ_g in (7.22a) and (7.29) respectively, in equation (7.28) gives:

$$\frac{d\phi}{dt} = \left(\frac{1 + 2\,p\,\delta_s}{2\,\alpha} - \delta\right)\frac{M}{2\delta s} \cdot \frac{d\alpha}{dt}$$

$$= \frac{Mp}{2\,\alpha\,s}\left(\frac{1}{2\,\delta\,p} + s - \alpha\right)\frac{d\alpha}{dt} \tag{7.30}$$

It is already shown that $\frac{d\phi}{dt} = \frac{(M_s - M)}{G}$ (7.31)

which is given as (7.14)in the preceding section.

On substituting this expression for $\frac{d\phi}{dt}$ in eq.(7.30) there is obtained:

$$\frac{M_s - M}{G} = \frac{M\,p}{2\alpha s}\left(\frac{1}{2\,\delta\,p} + s - \alpha\right)\frac{d\alpha}{dt}$$

or $$\frac{d\alpha}{dt} = \frac{2}{p.G} \cdot \frac{M_s - M}{M} \cdot \frac{\alpha\,s}{\frac{1}{2\delta p} + s - \alpha} \tag{7.32}$$

Now, $x_g = x_{AB} - \alpha,$

$$\therefore \frac{dx_g}{dt} = -\frac{d\alpha}{dt}$$

The velocity at any position is given by:

$$V_o = -\frac{dx_g}{dt} = \frac{d\alpha}{dt}$$

On substituting the expression for $\frac{d\alpha}{dt}$ given by (7.32) in the preceding equation, there is obtained:

$$V_o = \frac{d\alpha}{dt} = \frac{2}{p.G} \cdot \frac{M_s - M}{M} \cdot \frac{\alpha s}{\frac{1}{2\delta p} + s - \alpha} \qquad (7.33)$$

The velocity of the armature V_o at any position during operation is, therefore, given by the formula in eq.(7.33).

In fig. 7.10 a load line A-B is shown for which the direction of motion is negative i.e., the motion is directed from A to B along the line A-B. In this case $x_{AB} - x_g = \alpha$

$$\therefore \quad \frac{d\alpha}{dt} = - \frac{d\, x_g}{dt}$$

The expression for $\frac{d\phi}{dt}$ in (7.28) remains the same.

The velocity V_o along the load line is given by

$$V_o = \frac{dx_g}{dt} = - \frac{d\alpha}{dt} \qquad (7.35)$$

$\frac{d\alpha}{dt}$ is given by eq. (7.32)

$$\therefore \quad V_o = \frac{2}{pG} \cdot \frac{M_s - M}{M} \cdot \frac{\alpha S}{\frac{1}{2\delta p} + S - \alpha} \qquad (7.34)$$

The case illustrated by the diagram in fig. 7.10 may occur in practice due to the oscillations or instability. In fact, this case is not at all desirable.

Kinetic energy of the armature during operation.

The kinetic energy is given by:

$$T = \frac{1}{2} m v_o^2$$

where m is the effective mass of the armature and v_o is the velocity.

When the velocity is positive, the formula in eq. 7.33 applies.

Hence,

$$V_o = \frac{2}{p.G} \cdot \frac{M_s - M}{M} \cdot \frac{\alpha s}{\frac{1}{2\delta p} + s - \alpha}$$

$$\therefore \quad T = \frac{1}{2} m v_o^2$$

$$= \frac{1}{2} m \left[\frac{2}{p.G} \cdot \frac{M_s - M}{M} \cdot \frac{\alpha s}{\frac{1}{2\delta p} + s - \alpha} \right]^2$$

or

$$T = \frac{2m}{p^2 G^2} \left[\frac{M_s - M}{M} \cdot \frac{\alpha s}{\frac{1}{2\delta p} + s - \alpha} \right]^2 \qquad (7.35)$$

(7.35) gives the expression for the kinetic energy of the armature at any position defined by s, α and M in fig. 7.10.

7.7 Acceleration of the armature during operation

Differentiation of the velocity expression with respect to time gives the acceleration f_o during operation, which is, therefore, given by:

$$f_o = \frac{dv_o}{dt} = \frac{d^2\alpha}{dt^2} = \frac{d}{dt}\left[\frac{2}{p.G} \cdot \frac{M_s - M}{M} \cdot \frac{\alpha s}{\frac{1}{2\delta p} + s - \alpha} \right]$$

$$= \frac{2}{pG}\left[\frac{M_s - M}{M} \cdot \frac{d}{dt}\left(\frac{\alpha s}{\frac{1}{2\delta p} + s - \alpha}\right) + \frac{\alpha s}{\frac{1}{2\delta p} + s - \alpha} \frac{d}{dt}\left(\frac{M_s - M}{M}\right)\right]$$

It may be shown that

$$f_o = \frac{2}{p^2G^2} \cdot \frac{M_s - M}{M} \cdot \frac{\alpha s}{(\frac{1}{2\delta p} + s - \alpha)^2} \left(\alpha + \frac{M_s - 2M}{M} \cdot s + 3\frac{M_s - M}{M} \cdot \frac{\alpha s}{\frac{1}{2\delta p} + s - \alpha}\right) \quad (7.36)$$

A similar expression for the acceleration is given by Ahlberg.[11]
The mass force or acceleration force is:

$$F_m = mf_o = \frac{2m}{p^2G^2} \cdot \frac{M_s - M}{M} \cdot \frac{\alpha s}{(\frac{1}{2\delta p} + s - \alpha)^2} \left(\alpha + \frac{M_s - 2M}{M} s + 3\frac{M_s - M}{M} \cdot \frac{\alpha s}{\frac{1}{2\delta p} + s - \alpha}\right) \quad (7.37)$$

7.8 Armature motion during release:

The release motion may be analysed like the motion in operation and the dynamic flux recording in release is required for that. In release, relay coil is often closed through a diode and an external resistance, as shown in fig. 7.11 or a resistance - capacitance combination, the battery being disconnected.

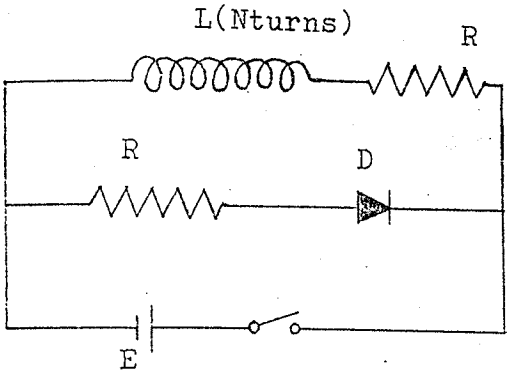

Fig. 7.12 Relay coil with diode-resistance shunt

From dynamic flux time and position-time relations, dynamic flux position relation may be made available and the motion may be analysed considering the equilibrium of four kinds of forces.

Ahlberg[9,10,11] presents an analysis of the release motion from the static load characteristic considering an equilibrium of two forces, namely pull and load.

In normal release, the eddy currents control the flux decay during the entire release process. Therefore, only the eddy current conductance Ge comes in the time formula. The motion time can be disregarded, in slow release, but not in normal release. In slow release, the coil circuit is often closed even after the battery is disconnected, and in that case both the coil current and eddy currents control the whole release process.

The decreasing magnetisation relations apply in the release

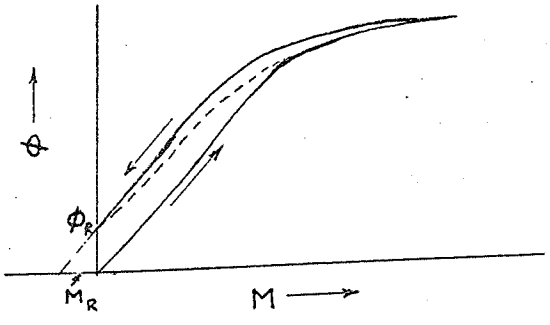

Fig. 7.13 Repeated magnetisation of $\frac{dn}{}$ electromagnet

cases, because the magnetisation decreases in all cases of release when the current is switched off. In fig. 7.12 the repeated magnetisation of an electromagnet is shown. In the closed gap position, the pull decreases to the value of the spring retractile force at this position, and this causes the release motion to start. Now this pull is determined by the decreasing magnetisation relation. For the decreasing magnetisation of an electromagnet, as in fig. 7.12, an hyperbolic approximation may be made and the following equation may be written:

$$\frac{\phi}{\phi'' - \phi} = \frac{M_R + M}{S'' \quad \phi''} \tag{7.38}$$

It may be mentioned here that the increasing and decreasing magnetisation curves of electromagnets and their magnetic members have the same hyperbolic character. Equation (7.38) may be written in an alternative form in terms of S_R and ϕ_R:

$$M = \frac{(\phi'' - \phi_R) \quad (\phi - \phi_R)}{\phi'' - \phi} \; S_R \tag{7.39}$$

where S_R is the incremental total reluctance. From (7.38) and (7.39) the ϕ vs. M relation for decreasing magnetisation in release may be found.

In slow release, the field decay conforms to the electrical equation (1.1).

In this case $NI_s = o$, the equation becomes,

$$S\phi + G\frac{d\phi}{dt} = o \tag{7.40}$$

The integral of the above equation may be written in the form:

$$t = -G \int_{\phi_2}^{\phi_o} \frac{d\phi}{M} \qquad (7.41)$$

where $M = S\phi$.

t is the time of field decay so that steady state flux ϕ_2 decreases to the value ϕ_o at which the pull becomes equal to the operated load. The pull relation conforms to the release pull characteristics and the same for operation as given in (1.4), may be applied if there is a stop pin. The pull relation in operation may be repeated here as (7.42).

$$F = \left(\frac{S_L}{S_o + S_L + \frac{x_o - x}{\mu_o A}} \right)^2 \frac{\phi^2}{2\mu_o A} \qquad (7.42)$$

when iron to iron contact is used, the gap reluctance and A for the closed gap should be separately calculated. Otherwise the same coefficient of ϕ^2 can be used in release case only ϕ should be determined from decreasing ϕ vs. Ni relation which is given in (7.38) and (7.39). The pull in release for small values of ϕ, is approximately given by:

$$F = K. \left(\frac{M_R + M}{S_R} \right)^2$$

where $$K = \left(\frac{S_L}{S_o + S_L + \frac{x_o - x}{\mu_o A}} \right)^2 \times \frac{1}{2\mu_o A}$$

In general, K is the same as in the case of operation, ϕ is determined from the decreasing magnetisation relation and t for the waiting period is determined from the relation in (7.41). Individual cases should be considered according to their merit, such as, in slow release the time of flux decay with the armature at rest, may be taken for practical purposes as the total release time neglecting the motion time which is comparatively small.

Chapter 8

MEASUREMENT OF DIFFERENT CHARACTERISTICS AND VERIFICATION OF THE RIGOROUS METHOD

8.1 Introduction

Methods of dynamic measurements of the flux ϕ and position, spring load measurement and experimental evaluation of eddy current conductance are presented. The results are calculated by using the formulae derived in chapter 7 to verify the method of analysis discussed in there. Analysis of measurements are made to get some useful conclusions.

A sample calculation of dynamic characteristics for a specific design is also presented in this chapter.

8.2 Dynamic flux measurement;

Transient magnetic flux ϕ in operation and release may be recorded after integrating $\frac{d\phi}{dt}$ by an operational amplifier used as an integrator. A search coil was evenly wound round the entire length of the core. The two ends of the search coil are connected to the input of the electronic integrator. The output from the integrator was fed into the scope. The oscillograms were photographed. The experimental arrangement is shown in fig. 8.1.

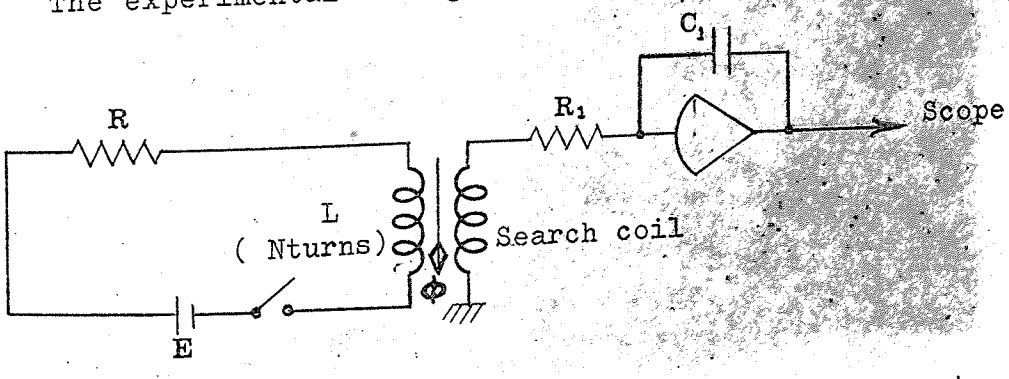

Fig.8.1 Experimental arrangement for dynamic flux measurement.

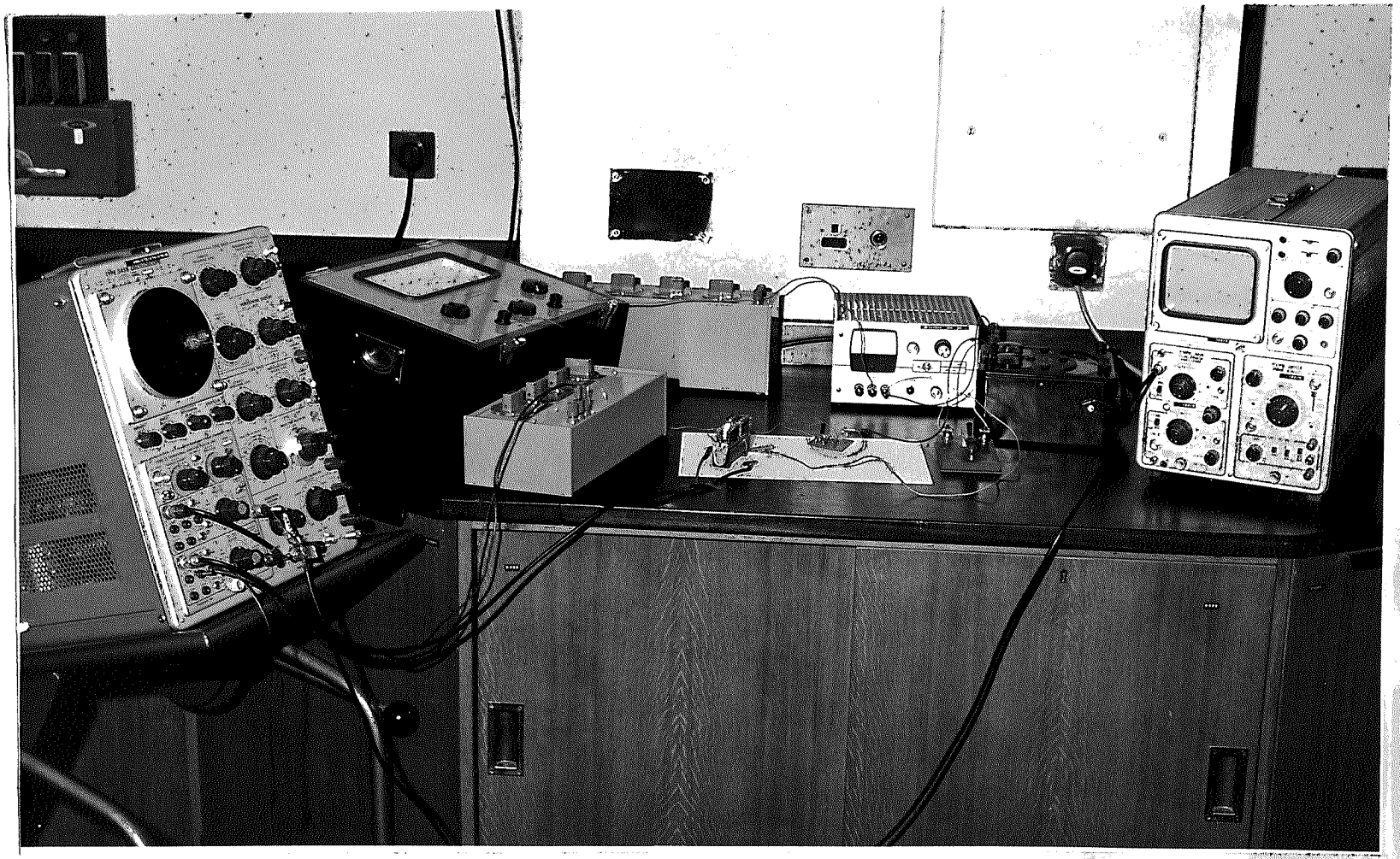

Fig.8.2 Apparatus for dynamic flux measurement

The apparatus used for the measurement is shown in fig.8.2. This included a Tektronix oscilloscope with a plug-in operational amplifier type O unit, a stabilised d.c. power supply, a precision capacitance box and a storage oscilloscope to see the transients stored on the screen before taking photographs. The time constant of the integrator was chosen 10 second and the maximum error of the recordings was less than 1% in the M_s = 275 At case and about 1% in the M_s = 225 At case in the regions of interest.

8.3 Measurement of displacement of the armature.

The displacement of the armature was measured using two different methods. In the first method an electronic digital counter/frequency meter was used to measure the time required to travel a predetermined distance. The block diagram of the experimental arrangement is shown in fig. 8.3. A metal pointer which served as a contact was fixed on a light perspex piece which was attached to the relay armature. The effective mass of the armature was kept constant. Before every measurement, the distance to be travelled was checked by the micrometer which was used in the experiment to form a make contact together with the metal pointer. The resolution in the system was .0005 inch or even less than that and a smoothe displacement vs. time curve could be plotted.

Fig. 8.4 shows the apparatus used for the measurement. This included a Marconi digital counter frequency meter, batteries for giving a constant voltage, an auxilliary relay for switching and

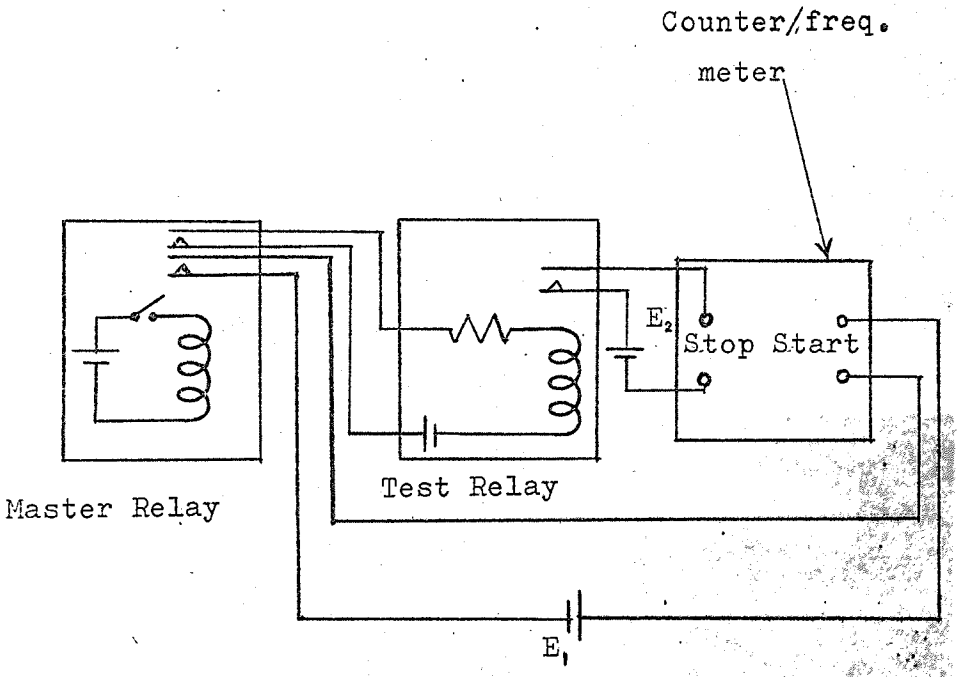

Fig. 8.3 Measurement of displacement by counter/ frequency meter.

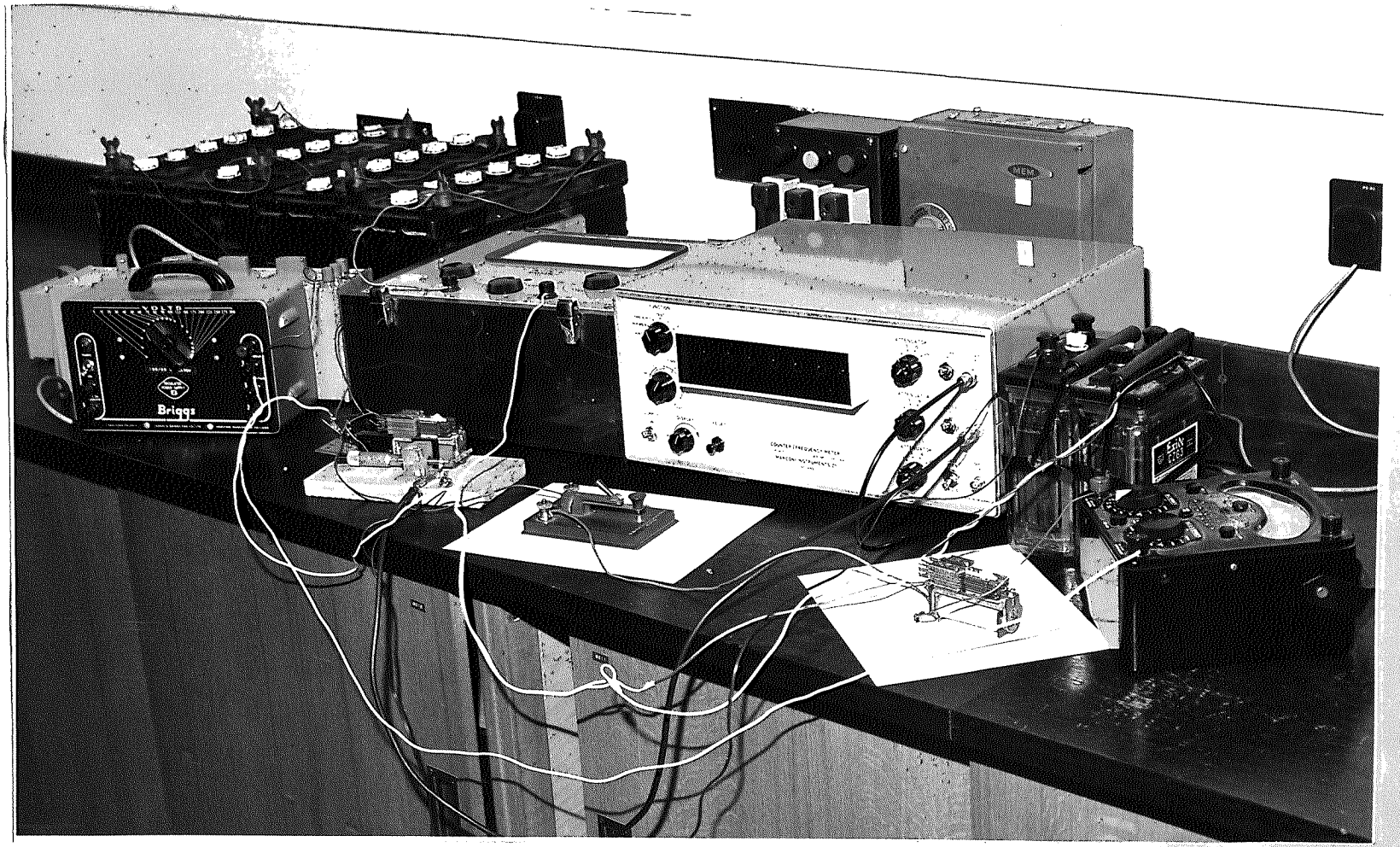

Fig.8.4 Apparatus for displacement measurement by counter/frequency meter

the test relay with the micrometer. The auxilliary relay was used to provide a trigger pulse to the counter to start counting and also to switch on a constant voltage across the test relay coil. The oscillations cannot be detected by this method, but can be detected by the method described in the following.

The other method of displacement measurement utilises the detection of an amount of light by a photocell. A silicon photovoltaic cell was used under short circuit condition and the current generated due to the incident light on the cell was fed into the virtual earth point of an operational amplifier, as in fig. 8.5. The output from the amplifier becomes a linear function of illumination. A lamp fed from a d.c. source was used to

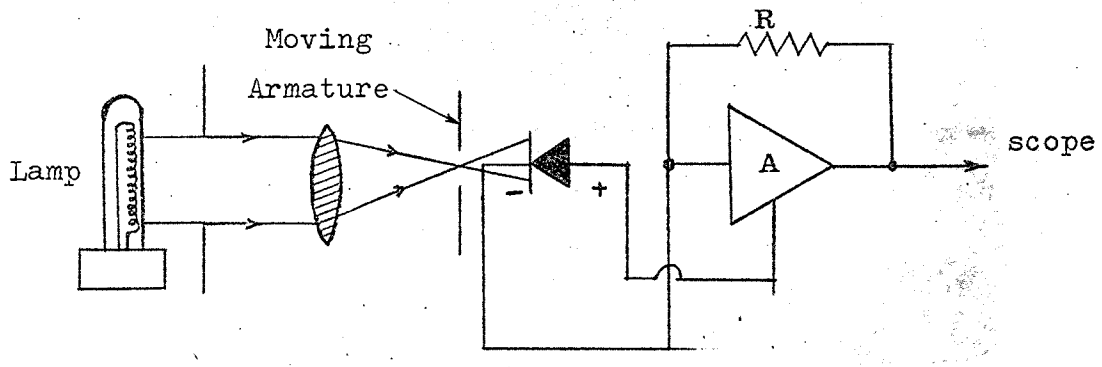

Fig. 8.5 Measurement of displacement by a photocell

illuminate the armature end of the relay through a combination of two condensing lenses such that a beam of light was allowed to pass through the opening between the armature and the pole face of the test relay. The amount of light falling on the photocell was thereby regulated by the movement of the armature. The arrangement of the system is shown in fig. 8.5. The apparatus used for the measurement by this method is shown in fig. 8.6.

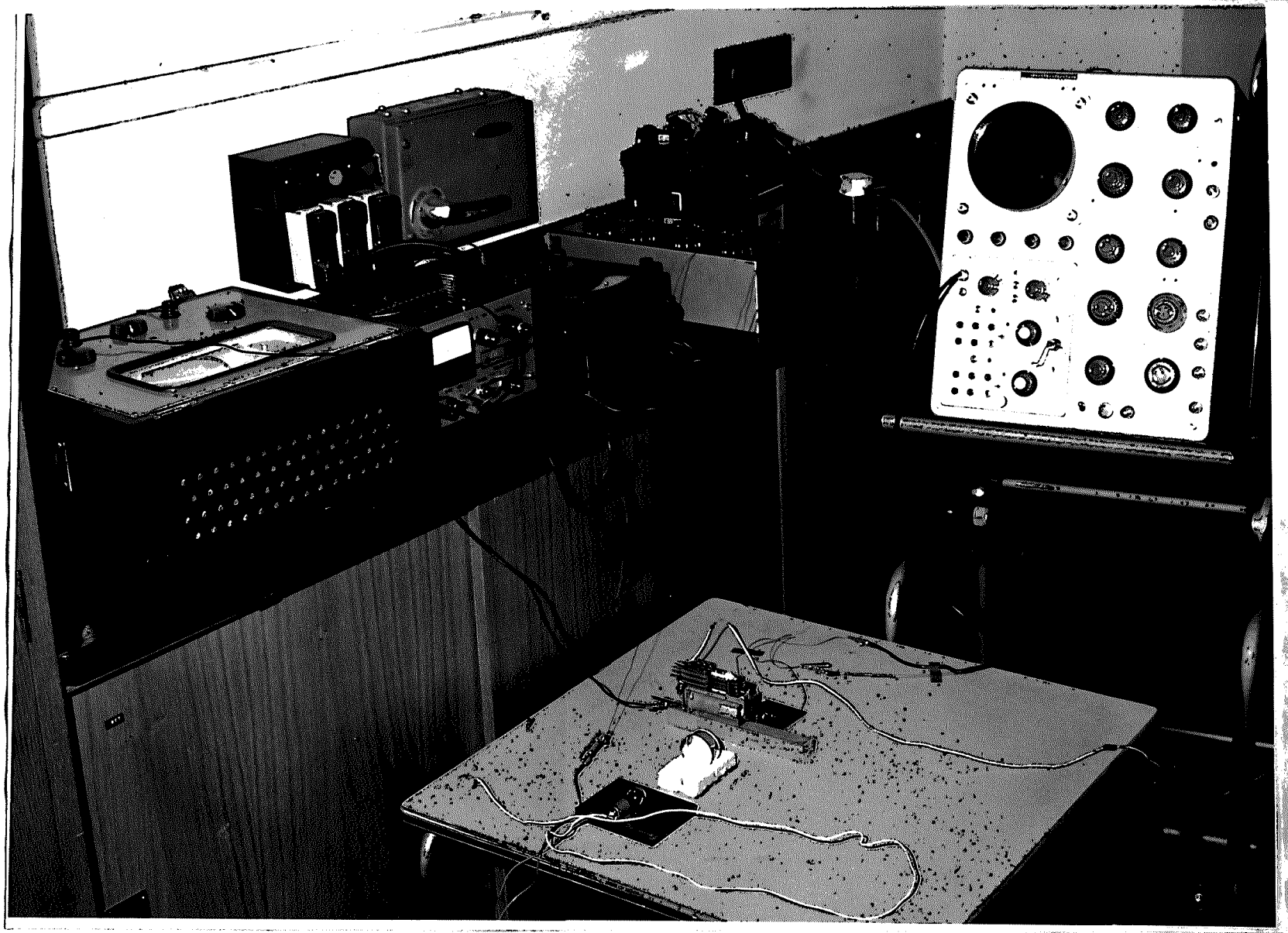

Fig.8.6 Apparatus for displacement measurement by a photocell

This included a Tektronix oscilloscope, a BPY 10 photocell, a stabilised power supply, a straight filament lamp and the combination of lenses. The picture also shows the test relay.

8.4 Measurement of spring load:

The static load with reference to the centroid of the mating area between the core and the armature was measured by putting weights on the armature to move the same against contact springs. Displacement of the armature due to putting weights was measured by a micrometer and also by feeler gauges. Static load vs. air gap relation was obtained from that measurement. The static load characteristic for the test relay equipped with 18 contact springs, which was referred to in sec. 7.3 is shown in fig. 7.7.

8.5 Experimental evaluation of eddy current conductance G_e

The time at which motion starts is given by eq. (7.18).

$$t = (G_c + G_e)\left(p + \frac{\phi_B}{M_B} \right) 2.303 \log \frac{M_s}{M_s - M_B}$$

When the back tension is constant t is directly proportional to $(G_c + G_e)$. It is already assumed that the eddy current effect is replaced by a one turn winding closely coupled with the main winding and G_e is given by $\frac{1}{r_e}$ where r_e is the resistance of the fictitious winding, which is constant.

If time t is measured for different values of G_c, then a plot of t vs. G_e should be linear, with a negative intercept on the G_c axis. This negative intercept is numerically equal to G_e. The time was measured on the test relay mentioned in section 7.3, by an electronic timer and a micrometer, the later one was used to serve as a contact as in the case of the displacement measurement described in sec. 8.3 . The coil circuit resistance was varied by putting external resistances in series with the coil. Table 8.1 shows the measured times corresponding to values of G_c. When the measurements are plotted as shown in fig.8.7 a straight line fitting the plotted points is obtained. The line is extended to get G_e. The observed value is

Table 8.1 Experimental evaluation of G_e

Test relay: Type 305/2500/ABE-FG1/50 made by Magnetic Devices Limited.

Steady state current in the coil i_s = 11 mA

Coil resistance = 2507 Ω

External series resistance Ω	$G_c \times 10^3$ mhos	t m s
0	249.30	42.63
500	207.84	37.86
1000	178.21	33.97
1500	155.97	29.50
2000	138.67	27.20
2500	124.80	24.2

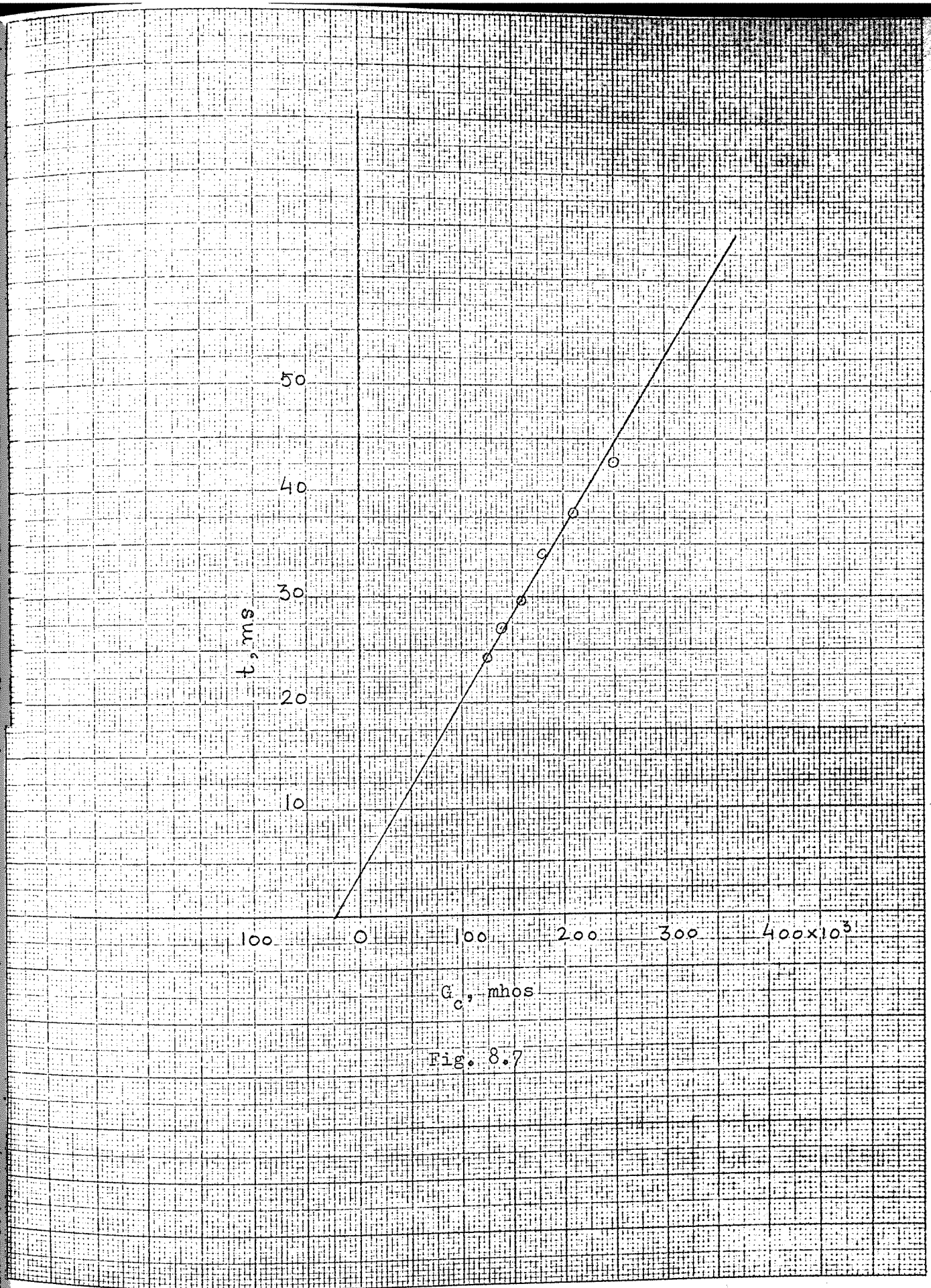

Fig. 8.7

24.6×10^3 mhos. G_e may be calculated from the formula in equation 5.22 in this case as well. The length of the core is 69 mm and ρ for the material of the core is $11.18 \times 10^{-8} \Omega$ m.

$$G_e = \frac{l}{8\pi\rho} = \frac{69 \times 10^{-3}}{8\pi \times 11.18 \times 10^{-8}} = 24.58 \times 10^3 \text{ mhos.}$$

The calculated value of G_e is in very good agreement with the measured value. For calculations in this chapter, the measured value of G_e which is 24.6×10^3 mhos is taken.

8.6 Verification of the theory presented in Chapter 7 on an electromagnetic relay. *

The test relay is the same as referred to in sections 7.3 and 8.5. The core flux (ϕ) and displacement (x) relations for steady state magnetomotive force M_s = 275 At, are shown in fig. 7.2. From these oscillograms, ϕ corresponding to the armature position x may be found and corresponding air gap flux ϕ_g may be calculated from the equivalent magnetic circuit. Table 8.2 shows ϕ, ϕ_g and x.

Table 8.2 Flux corresponding to the armature position

Relay: Type 305/2500/ABE - FG1/50

M_s = 275 At, $S_o = 299 \times 10^4$ At/wb, $S_L = 715 \times 10^4$ At/wb

$\mu_o A = .1935 \times 10^{-9}$ H.m

* This section verifies the previously presented relay armature motion analysis (Section 7.3, p.134); the time equation (equ.7.17,p.150); the velocity equation (equ.7.33,p.158); and the acceleration equation (equ.7.36,p.160).

x m m	ϕ x 10^{-7} Weber	$\frac{S_L}{S_o + S_L + \frac{x_o - x}{\mu_o A}}$	ϕ_g x 10^{-7} Weber
0	277	0.4960	137.40
.1	426	0.5144	219.13
.2	539	0.5343	287.99
.3	590	0.5558	327.92
.3992	596	0.5789	345.02
.365	604	0.5707	344.70
.45	665	0.5914	393.28
.5	670	0.6044	404.95
.6	672	0.6320	424.70
.7	673	0.6622	445.66
.827	674	0.7051	475.24

From x the permeance $\mathcal{P}_a$ given by equation (7.2) may be calculated. The instantaneous magnetomotive force M for a particular value of ϕ_g may be calculated from equation (7.1). Table 8.3 shows ϕ_g and M corresponding to different armature positions.

Table 8.3 Air gap flux and magnetomotive force

x m m	x 10^{-7} Weber	$\frac{1}{\mathcal{P}_a} = S_o + \frac{x_o - x}{\mu_o A}$ x 10^4 At/Wb	$M = \phi_g / \mathcal{P}_a$ At
0	137.4	726.39	99.81
.1	219.13	674.71	147.85
.2	287.99	623.03	179.43

.3	327.92	571.35	187.36
.3992	345.02	520.08	179.44
.365	344.70	537.75	185.36
.45	393.28	493.83	194.21
.5	404.95	467.99	189.51
.6	424.70	416.31	176.81
.7	445.66	364.63	162.50
.827	475.24	299	142.1

The values of ϕ_g and M in this table may be plotted to obtain the ϕ_g - M characteristic which is the dynamic load characteristic in magnetic system of co-ordinates shown in fig. 7.5 From this characteristic the time of operation for the full operation or a section of the travel can be calculated, which is given in the following.

Calculation of the time of operation at M_s = 275 At

Some essential data

Final coil current = 11 mA.

Final magnetomotive force M_s = 275 At

External resistance connected in series with the coil = 0 Ω

Eddy current conductance $G_e = 24.6 \times 10^3$ mhos

Coil conductance $G_c = 249.300 \times 10^3$ mhos.

$G = G_c + G_e = 249.30 \times 10^3 + 24.6 \times 10^3 = 273.90 \times 10^3$ mhos

Leakage permeance = $\frac{1}{S_L}$ = p = 1.3986×10^{-7} Wb/At.

In fig. 7.5 the points indicated by 1, 2, 3 etc. are the load points which indicate loads at corresponding armature positions.

Table 8.4 Data for the load points

Load points	ϕ_g x 10^{-7} Weber	M At
1	0	0
2	137.40	99.81
3	219.13	147.85
4	327.92	187.36
5	345.02	179.44
6	344.70	185.36
7	393.28	194.21
8	475.24	142.1

Line 1 - 2

The time formula is given in eq. (7.18)

$$t_{1-2} = t_w = G\left(p + \frac{\phi_B}{M_B}\right) 2.303 \log \frac{M_s}{M_s - M_B}$$

$$= 273.90 \times 10^3 \left(1.3986 \times 10^{-7} + \frac{137.40 \times 10^{-7}}{99.81}\right) \times 2.303 \times \log \frac{275}{275 - 99.81}$$

$$= 273.90 \times 10^3 \left(1.3986 \times 10^{-7} + 1.3766 \times 10^{-7}\right) \times 2.303 \times \log \frac{275}{175.19}$$

$$= 34.29 \text{ ms.}$$

Line 2 - 3

The time formula is given in eq. (7.17) which applies to the rest of the lines as well. The time formula is:

$$t_{AB} = G\left(p + \frac{\phi_B - \phi_A}{M_B - M_A}\right) \; 2.303 \log \frac{M_s - M_A}{M_s - M_B}$$

t_{2-3} is therefore given by:

$$t_{2-3} = 273.90 \times 10^3 \times \left(1.3986 \times 10^{-7} + \frac{219.13 \times 10^{-7} - 137.40 \; 10^{-7}}{147.85 - 99.81}\right) \times$$

$$2.303 \times \log \frac{275 - 99.81}{275 - 147.85}$$

$$= 273.90 \times 10^3 \times (1.3986 \times 10^{-7} + 1.7012 \times 10^{-7}) \times 2.303 \times \log 1.3778$$

$$= 273.90 \times 10^3 \times 3.0998 \times 10^{-7} \times 2.303 \times .1392 = 27.22 \text{ ms.}$$

Line 3 - 4

$$t_{3-4} = 273.90 \times 10^3 \times \left(1.3986 \times 10^{-7} + \frac{327.92 \times 10^{-7} - 219.13 \times 10^{-7}}{187.36 - 147.85}\right) \times$$

$$2.303 \times \log \frac{275 - 147.85}{275 - 187.36}$$

$$= 273.90 \times 10^3 \times (1.3986 \times 10^{-7} + 2.7534 \times 10^{-7}) \times 2.303 \times \log 1.4508$$

$$= 273.90 \times 10^3 \times 4.1520 \times 10^{-7} \times 2.303 \times .1617 = 42.35 \text{ ms.}$$

Line 4 - 5

$$t_{4-5} = 273.90 \times 10^{3} \times \left(1.3986 \times 10^{-7} + \frac{345.02 \times 10^{-7} - 327.92 \times 10^{-7}}{179.44 - 187.36}\right)$$

$$\times 2.303 \times \log \frac{275 - 187.36}{275 - 179.44}$$

$$= 273.90 \times 10^{3} \times \left[1.3986 \times 10^{-7} + (-2.1590) \times 10^{-7}\right] \times 2.303 \times$$

$$\log .9171$$

$$= 273.90 \times 10^{3} \times (-.7604) \times 10^{-7} \times 2.303 \times (-.0376)$$

$$= 1.8 \text{ ms.}$$

Line 5 - 6

$$t_{5-6} = 273.90 \times 10^{3} \times \left(1.3986 \times 10^{-7} + \frac{344.70 \times 10^{-7} - 345.02 \times 10^{-7}}{185.36 - 179.44}\right)$$

$$\times 2.303 \times \log \frac{275 - 179.44}{275 - 185.36}$$

$$= 273.90 \times 10^{3} \times \left[1.3986 \times 10^{-7} + (-.0540) \times 10^{-7}\right] \times 2.303 \log 1.066$$

$$= 273.90 \times 10^{3} \times 1.3446 \times 10^{-7} \times 2.303 \times .0277 = 2.35 \text{ ms.}$$

Line 6 - 7

$$t_{6-7} = 273.90 \times 10^{3} \times \left(1.3986 \times 10^{-7} + \frac{393.28 \times 10^{-7} - 344.70 \times 10^{-7}}{194.21 - 185.36}\right) \times$$

$$2.303 \log \frac{275 - 185.36}{275 - 194.21}$$

$$= 273.90 \times 10^{3} \times \left(1.3986 \times 10^{-7} + 5.4892 \times 10^{-7}\right) 2.303 \log 1.1095$$

$$= 273.90 \times 10^{3} \times 6.8878 \times 10^{-7} \times 2.303 \times .0453 = 19.68 \text{ ms.}$$

Line 7 - 8

$$t_{7-8} = 273.90 \times 10^{3} \times \left(1.3986 \times 10^{-7} + \frac{475.24 \times 10^{-7} - 393.28 \times 10^{-7}}{142.1 - 194.21}\right)$$

$$2.303 \log \frac{275 - 194.21}{275 - 142.1}$$

$$= 273.90 \times 10^{3} \left[1.3986 \times 10^{-7} + (-1.5728)\right] \times 2.303 \times \log .6078$$

$$= 273.90 \times 10^{3} \times (-.1742) \times 10^{-7} \times 2.303 \times (-.2162)$$

$$= 2.38 \text{ m.s.}$$

The total time for full operation = $t_{1-2} + t_{2-3} + t_{3-4} + t_{4-5} + t_{5-6} + t_{6-7} + t_{7-8}$ = 34.29 + 27.22 + 42.35 + 1.8 + 2.35 + 19.68 + 2.38 = 130.07 ms.

The observed time for full operation is 131 ms.

The time calculated from the measured ϕ v x relations as shown above, agrees very well with the observed time.

The times of operation for different sections have been calculated from fig. 7.5.

Table 8.5 shows the calculated times for different armature positions.

Table 8.5 Calculated times of passage at M_s = 275 At

At x = 0, $t_w = t_{1-2}$ = 34.29 ms

x m m	Calculated time m s
.1	61.51
.3	103.86
.45	127.69
.827	130.07

The values of x and calculated times in table 8.5 are plotted as shown in fig. 8.8. From this figure, the time required to close the normally open contacts is found to be 127.9 ms. at which the useful relay operation is complete.

Calculation of velocities at M_s = 275 At

The velocity of the armature at any position may be calculated from the diagram in which the dynamic load and static pull characteristics are combined, as discussed in section 7.6. The dynamic load characteristic for which M_s is 275 At, is given in fig. 7.9 in which the pull characteristics for different mmf's are also given. Table 8.6 shows the pull at different air gaps and these values of the pull are plotted against the corresponding values of the air gap to give the dynamic pull characteristic as shown in figs. 7.4 and 7.9. Of course, in fig. 7.9 the pull curve is represented by fitting a number of linear segments in the curve in fig. 7.4, as mentioned in section. 7.6

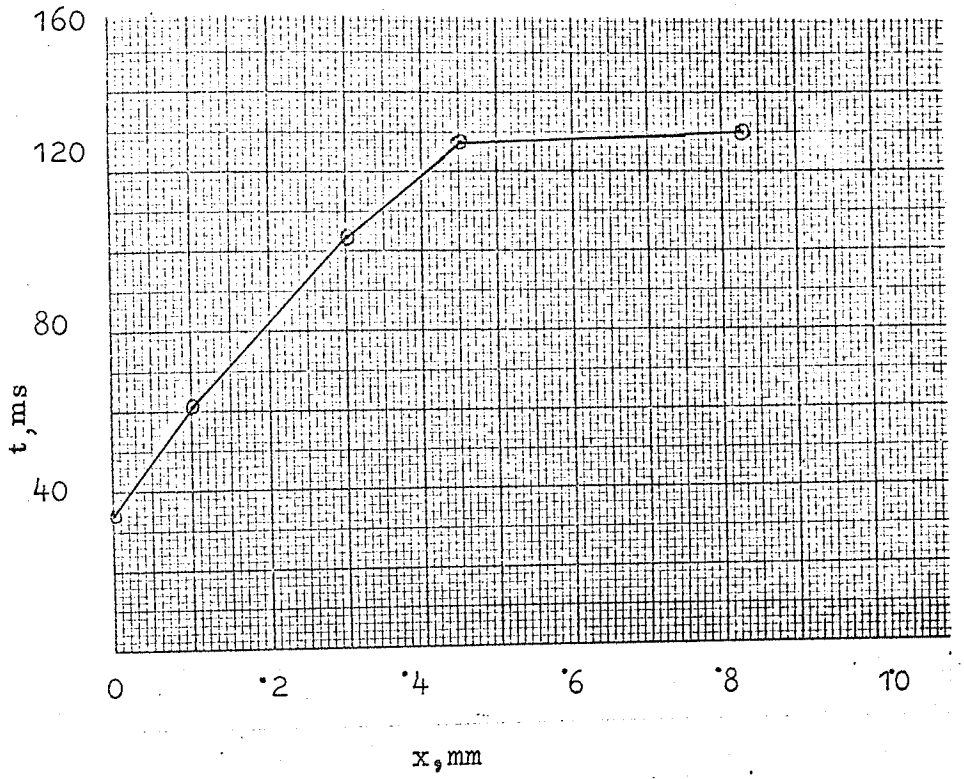

Fig. 8.8 Calculated times of passage

Table 8.6 Pull and air gap

M_s = 275 At

x_g = air gap,

The value of x_g is put at zero when the armature is operated; of course, there still remains a residual air gap.

x m m	x_g m m	ϕ_g x 10^{-7} Wb	$F = \frac{\phi_g^2}{2\mu_o A}$ Newton	F g f
0	.827	137,40	.4878	49.725
.1	.727	219.13	1.241	126.51
.2	.627	287.99	2.14	218.15
.3	.527	327.92	2.78	283.39
.399	.428	345.02	3.08	313.98
.365	.462	344.70	3.07	312.96
.45	.377	393.28	4.0	407.76
.5	.327	404.95	4.24	432.23
.6	.227	424.70	4.66	475.04
.7	.127	445.66	5.13	522.95
.827	0	475.24	5.84	595.33

The velocity formula which is given in equation (7.33) is:

$$V_o = \frac{2}{pG} \cdot \frac{M_s - M}{M} \cdot \frac{\alpha \; s}{\frac{1}{2\delta p} + s - \alpha}$$

For calculating the velocity α, s and M for the load points are needed.

These may be found in fig. 7.9. Table 8.6 shows the data for the load points. These load points are not the same as in the ϕ_g - M plane shown in fig. 7.5. 1 is a load point where normally open contacts operate.

Table 8.7 M, α and s for the load points.

Load points	On load line	M At	α m m	s m m
3	2 - 3	214.42	.365	.665
4	4 - 5	209.04	4.89	.59
6	6 - 7	235	.912	.68
7	6 - 7	221	1.067	.762
9	8 - 9	186.3	1.01	.47
1	6 - 7	229.46	.99	.6

The numerical values of α, s and M for different load points may be inserted in the velocity formula to obtain the velocities at different positions of the armature. For line 1 - 2 the velocity is of course zero.

In the velocity formula given above, p, G and M_s are already known.

$$\delta = \frac{1}{\mu_o A} = 5.1679 \times 10^9, \text{ as } \mu_o A = .1935 \times 10^{-9} \text{ H.m.}$$

$$\frac{1}{2\delta p} = \frac{1}{2 \times 5.1679 \times 10^9 \times 1.3986 \times 10^{-7}} = 6.92 \times 10^{-4} \text{ m}$$

$$\frac{2}{p.G} = \frac{2}{1.3986 \times 10^{-7} \times 273.90 \times 10^{3}} = 52.21$$

velocity at point 3 on line 2 - 3

$$V_o = 52.21 \times \frac{275 - 214.42}{214.42} \times \frac{.365 \times 10^{-3} \times .665 \times 10^{-3}}{6.92 \times 10^{-4} + .665 \times 10^{-3} - .365 \times 10^{-3}}$$

$$= 52.21 \times \frac{60.58}{214.42} \times \frac{.365 \times 10^{-3} \times .665 \times 10^{-3}}{.9920 \times 10^{-3}}$$

$$= 3.61 \times 10^{-3} \text{ m/sec.}$$

Velocity at point 4 on line 4 - 5.

The velocity formula was given in eq.(7.34) for a load line like this one.

$$V_o = - 52.21 \times \frac{275 - 209.04}{209.04} \times \frac{4.89 \times 10^{-3} \times .59 \times 10^{-3}}{6.92 \times 10^{-4} + .59 \times 10^{-3} - 4.89 \times 10^{-3}}$$

$$= - 52.21 \times \frac{65.96}{209.04} \times \frac{4.89 \times 10^{-3} \times .59 \times 10^{-3}}{- 3.6080 \times 10^{-3}}$$

$$= 13.17 \times 10^{-3} \text{ m/sec.}$$

The direction of motion is of course negative as may be seen in fig. 7.9.

Velocity at point 6 on line 6 - 7

$$V_o = 52.21 \times \frac{275 - 235}{235} \times \frac{.912 \times 10^{-3} \times .68 \times 10^{-3}}{6.92 \times 10^{-4} + .68 \times 10^{-3} - .912 \times 10^{-3}}$$

$$= 52.21 \times \frac{40}{235} \times \frac{.912 \times 10^{-3} \times .68 \times 10^{-3}}{.4600 \times 10^{-3}} = 11.98 \times 10^{-3} \text{ m/sec.}$$

Velocity at point 7 on line 6 - 7

$$V_o = 52.21 \times \frac{275 - 221}{221} \times \frac{1.067 \times 10^{-3} \times .762 \times 10^{-3}}{6.92 \times 10^{-4} + .762 \times 10^{-3} - 1.067 \times 10^{-3}}$$

$$= 52.21 \times \frac{54}{221} \times \frac{1.067 \times 10^{-3} \times .762 \times 10^{-3}}{.387 \times 10^{-3}}$$

$$= 26.79 \times 10^{-3} \text{ m/sec.}$$

Velocity at point 9 on line 8 - 9

$$V_o = 52.21 \times \frac{275 - 186.3}{186.3} \times \frac{1.01 \times 10^{-3} \times .47 \times 10^{-3}}{6.92 \times 10^{-3} + .47 \times 10^{-3} - 1.01 \times 10^{-3}}$$

$$= 52.21 \times \frac{88.7}{186.3} \times \frac{1.01 \times 10^{-3} \times .47 \times 10^{-3}}{.1520 \times 10^{-3}}$$

$$= 77.62 \times 10^{-3} \text{ m/sec.}$$

Velocity at point 1 given in table 8.6 on line 6 - 7

$$V_o = 52.21 \times \frac{275 - 229.46}{229.46} \times \frac{.99 \times 10^{-3} \times .6 \times 10^{-3}}{6.92 \times 10^{-4} + .6 \times 10^{-3} - .99 \times 10^{-3}}$$

$$= 52.21 \times \frac{45.54}{229.46} \times \frac{.99 \times 10^{-3} \times .6 \times 10^{-3}}{.3020 \times 10^{-3}}$$

$$= 20.39 \times 10^{-3} \text{ m/sec.}$$

The lever arm ratio between the load and pull is .8163. So the velocity with which the normally open contacts close is:

$$V_o = 20.39 \times 10^{-3} \times .8163 = 16.64 \times 10^{-3} \text{ m/sec.}$$

The measured velocities at different positions of the armature from the slope of the position oscillogram in fig. 7.2 may be compared with the calculated velocities. Table 8.8 shows these velocities.

Table 8.8 Calculated and measured velocities at M_s = 275 At

x m m	Calculated Velocity mm/sec	Measured Velocity mm/sec
.451	11.98	9.6
.6	26.79	42.3
.827	77.62	60

Calculation of extra kinetic energy released in the relay structure due to the impact of the armature.

The velocity attained at the end of the motion is 77.62×10^{-3} m/sec. which is the velocity at load point 9.

The effective mass of the armature for the test relay is 9.31 gms.

$$\therefore \quad \text{K.E.} = T = \tfrac{1}{2} m v_o^2 = \tfrac{1}{2} \times 9.31 \times 10^{-3} \times (77.62 \times 10^{-3})^2$$

$$= \tfrac{1}{2} \times 9.31 \times 10^{-3} \times 6.0249 \times 10^{-3}$$

$$= 28.05 \times 10^{-6} \text{ J.}$$

Calculation of accelerations at M_s = 275 At

The acceleration is calculated for three load points. The formula is:

$$f_o = \frac{2}{G^2 p^2} \frac{M_s - M}{M} \frac{\alpha s}{\left(\frac{1}{2\delta p} + s - \alpha\right)^2} \left(\alpha + \frac{M_s - 2M}{M} \cdot s + 3 \frac{M_s - M}{M} \frac{\alpha s}{\frac{1}{2\delta p} + s - \alpha}\right)$$

$$\frac{1}{2\delta p} = 6.92 \times 10^{-4} \text{ m}$$

$$\frac{2}{G^2_p{}^2} = \left(\frac{2}{Gp}\right)^2 \times \tfrac{1}{2} = (52.21)^2 \times \tfrac{1}{2} = 13.629 \times 10^2$$

The load points are shown in fig. 7.9.

Acceleration at point 6 on line 6 - 7.

$$f_o = 13.629 \times 10^2 \times \frac{275 - 235}{235} \times \frac{.912 \times 10^{-3} \times .68 \times 10^{-3}}{(6.92 \times 10^{-4} + .68 \times 10^{-3} - .912 \times 10^{-3})^2}$$

$$\times \left(.912 \times 10^{-3} + \frac{275 - 2 \times 235}{235} \times .68 \times 10^{-3} + 3\,\frac{275 - 235}{235}\right.$$

$$\left. \times \frac{.912 \times 10^{-3} \times .68 \times 10^{-3}}{6.92 \times 10^{-4} + .68 \times 10^{-3} - .912 \times 10^{-3}}\right)$$

$$= 13.629 \times 10^2 \times \frac{40}{235} \times \frac{.912 \times 10^{-3} \times .68 \times 10^{-3}}{(.4600 \times 10^{-3})^2} \times (.912 \times 10^{-3} - .564 \times 10^{-3}$$

$$+ .6882 \times 10^{-3})$$

$$= .704 \text{ m/sec.}^2$$

Acceleration at point 7 on line 6 - 7

$$f_o = 13.629 \times 10^2 \times \frac{275 - 221}{221} \times \frac{1.067 \times 10^{-3} \times .762 \times 10^{-3}}{(6.92 \times 10^{-4} + .762 \times 10^{-3} - 1.067 \times 10^{-3})}$$

$$\times \left(1.067 \times 10^{-3} + \frac{275 - 2 \times 221}{221} \times .762 \times 10^{-3} + 3\,\frac{275 - 221}{221}\right.$$

$$\left. \times \frac{1.067 \times 10^{-3} + .762 \times 10^{-3}}{6.92 \times 10^{-4} + .762 \times 10^{-3} - 1.067 \times 10^{-3}}\right)$$

$$= 13.629 \times 10^2 \times \frac{54}{221} \times \frac{1.067 \times 10^{-3} \times .762 \times 10^{-3}}{(.387 \times 10^{-3})^2} \times (1.067 \times 10^{-3}$$

$$- .5756 \times 10^{-3} + 1.5396 \times 10^{-3})$$

$$= 3.672 \text{ m/sec.}^2$$

Acceleration at point 8 on line 7 - 8

$$f_o = 13.629 \times 10^2 \times \frac{275 - 186.3}{186.3} \times \frac{1.01 \times 10^{-3} \times .47 \times 10^{-3}}{(6.92 \times 10^{-4} + .47 \times 10^{-3} - 1.01 \times 10^{-3})}^2$$

$$\times \left(1.01 \times 10^{-3} + \frac{275 - 2 \times 186.3}{186.3} \times .47 \times 10^{-3} + 3 \frac{275 - 186.3}{186.3}\right.$$

$$\left. \times \frac{1.01 \times 10^{-3} \times .47 \times 10^{-3}}{6.92 \times 10^{-4} + .47 \times 10^{-3} - 1.01 \times 10^{-3}} \right)$$

$$= 13.629 \times 10^2 \times \frac{88.7}{186.3} \times \frac{1.01 \times 10^{-3} \times .47 \times 10^{-3}}{(.1520 \times 10^{-3})^2} \times (1.01 \times 10^{-3}$$

$$- .2462 \times 10^{-3} + 4.4605 \times 10^{-3})$$

$$= 69.65 \text{ m/sec.}^2$$

Calculation of mass forces at M_s = 275 At

Let F_m in the acceleration force of the armature which has effective mass mgm.

$$\therefore F_m = m f_o.$$

At point 6

$$F_m = 9.31 \times 10^{-3} \times .704 = 6.5542 \times 10^{-3} \text{ N}$$

$$= .6681 \text{ gf.}$$

At point 7

$$F_m = 9.31 \times 10^{-3} \times 3.672 = 34.1863 \times 10^{-3}$$

$$= 3.48 \text{ gf.}$$

At point 8

$$F_m = 9.31 \times 10^{-3} \times 69.65$$

$$= .6484 \text{ N}$$

$$= 66.1 \text{ gf.}$$

Conclusions

The calculations for M_s = 275 At have been shown. The calculated and measured times for full operation have already been compared and it may be seen that they agree very well. The velocities found by calculation are also acceptable. Better results may be obtained by fitting the pull curve with more number of linear segments. If α is the same as determined by the tangent at the point concerned, then the calculated velocity may be expected to be agreeing very well with the measured one. Calculations show that the mass force is quite high at the end of the motion. Therefore, for a speed relay which is suppled with enough power, this force may be quite high and may have a considerable influence on the motion. The calculations are useful for development studies and the values of velocity, acceleration and kinetic energy may be useful in the study of bouncing and rebound oscillations. If the armature continuously strikes the pole face of the electromagnet with a high velocity, the residual air gap may change causing the change of reluctance of the magnetic circuit. The calculation of the final velocity will, therefore, be helpful to give considerations to control the final velocity to eliminate this undesirable change of the air gap.

8.7 A similar verification as in sec.8.6 when the applied voltage is different.

The test relay is the same as referred to in secs. 7.3, 8.5 and 8.6. An investigation on this relay when M_s is 275 At was presented in sec. 8.6. A similar investigation is presented in this section when M_s is 225 At.

The oscillograms in fig. 8.9 give the core flux (ϕ) and displacement (x) relations when the steady state magnetomotive force M_s is 225 At. From these oscillograms, ϕ corresponding to the armature position x may be found and corresponding air gap flux ϕ_g may be calculated from the equivalent magnetic circuit. Table 8.9 shows ϕ, x, ϕ_g and M. The calculation of M corresponding to ϕ_g and x is similar as in sec. 8.6. The magnetic circuit constants are the same as given in the same section.

Table 8.9 Flux, armature position and magnetomotive force at M_s = 225 At

x m m	ϕ x 10^{-7} Weber	$\frac{S_L}{S_o + S_L + \frac{x_o - x}{\mu_o A}}$	ϕ_g x 10^{-7} Weber	$\frac{1}{a} = S_o + \frac{x_o - x}{\mu_o A}$ x 10^4 At/Wb	M A t
0	277.82	0.496	137.8	726.39	100.1
0.077	498	0.5101	254	686.50	174.4
0.097	512	0.5139	263.1	676.26	178
0.1	528	0.5144	271.6	674.71	183.3
0.2	563	0.5343	300.8	623.03	187.4

0.315	570.95	0.5592	319.3	563.59	180
0.3	574.18	0.5558	319.1	571.35	182.3
0.35	585	0.5672	331.8	545.51	181
0.45	626	0.5914	370.2	493.83	182.8
0.5	635	0.6044	383.8	467.99	179.6
0.6	642	0.6320	405.7	416.31	168.9
0.7	643	0.6622	425.8	364.63	155.3
0.827	644	0.7051	454.1	299	135.8

The values of ϕ and ϕ_g from this table are plotted against x as shown in figs. 8.10 and 8.11 respectively. ϕ_g is plotted against M to give the dynamic load characteristic in magnetic system of co-ordinates as shown in fig. 8.12. From this characteristic the time of operation can be calculated.

Calculation of the time of operation at M_s = 225 At

Some essential data:

Final coil current i_s = 9 mA

Final magnetomotive force M_s = 225 At

External resistance connected in series with the coil = 0 Ω

G and p are the same as given in sec. 8.6.

1

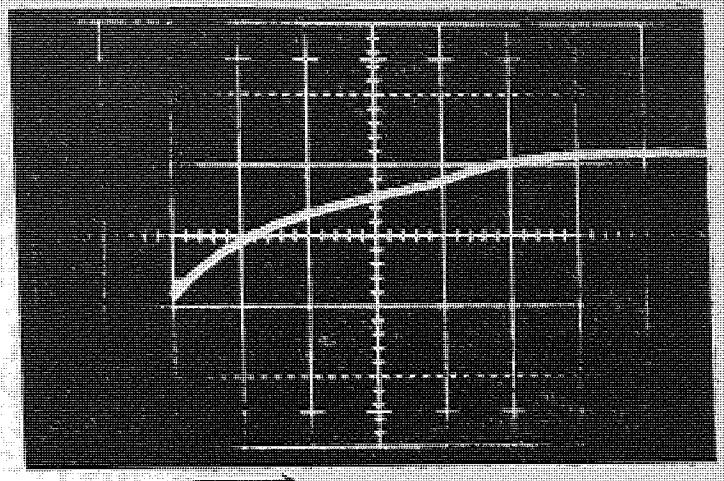

Time scale: 10 ms/scale div.

Flux scale: 80×10^{-7} Wb/scale div.

2

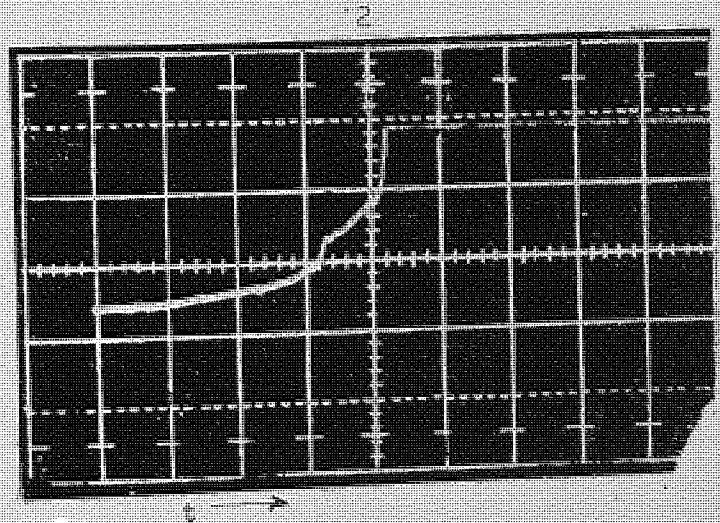

Time scale: 10ms/ scale div.

Position scale: .0755mm/scale div.

Fig. 8.9 Oscillograms showing Φ vs.t and x vs.t at M_s=225At.

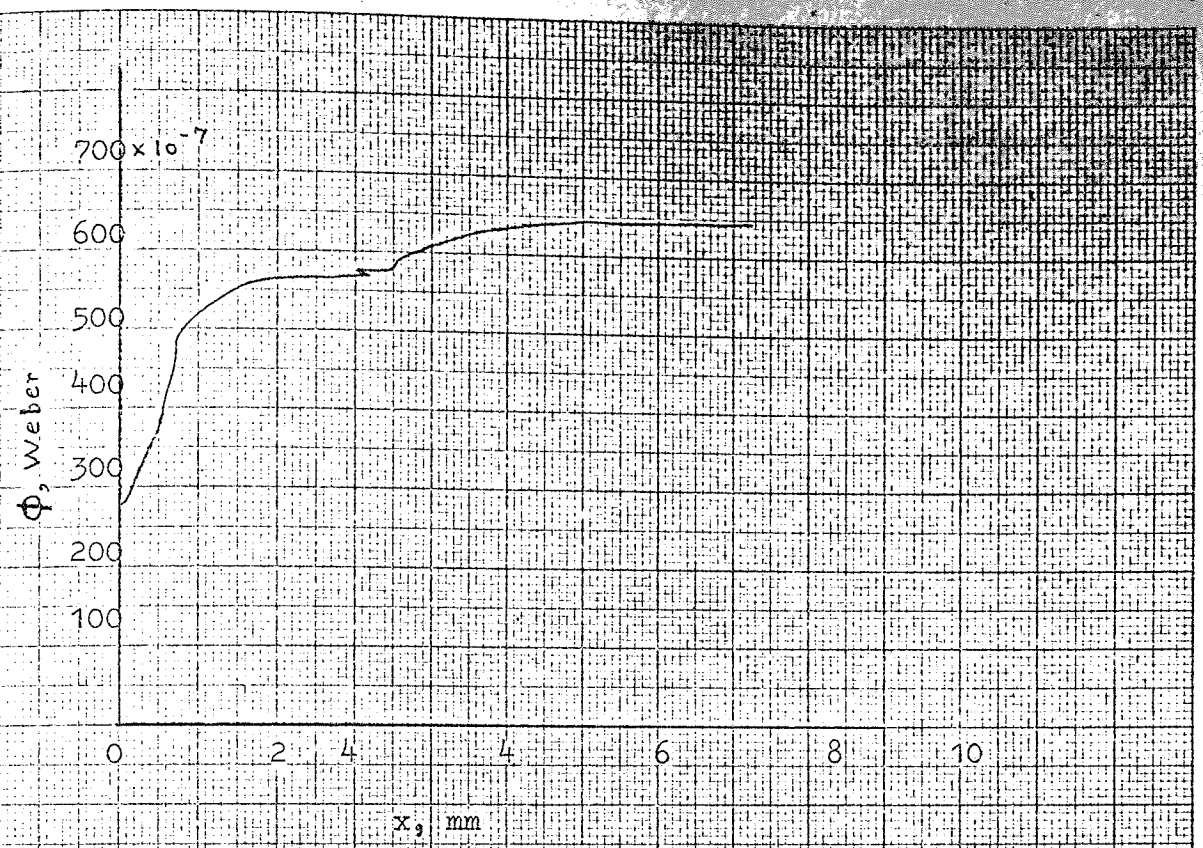

Fig. 8.10 Φ-x curve

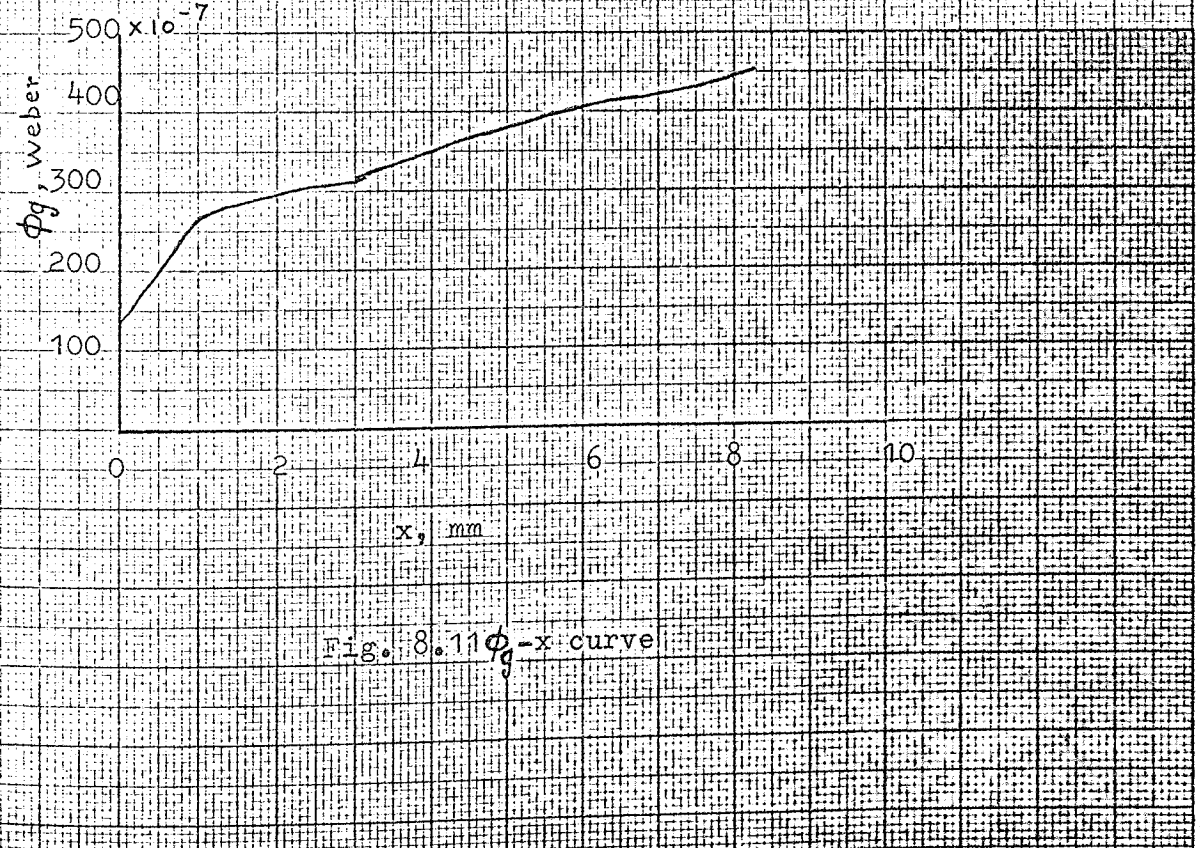

Fig. 8.11 Φ_g-x curve

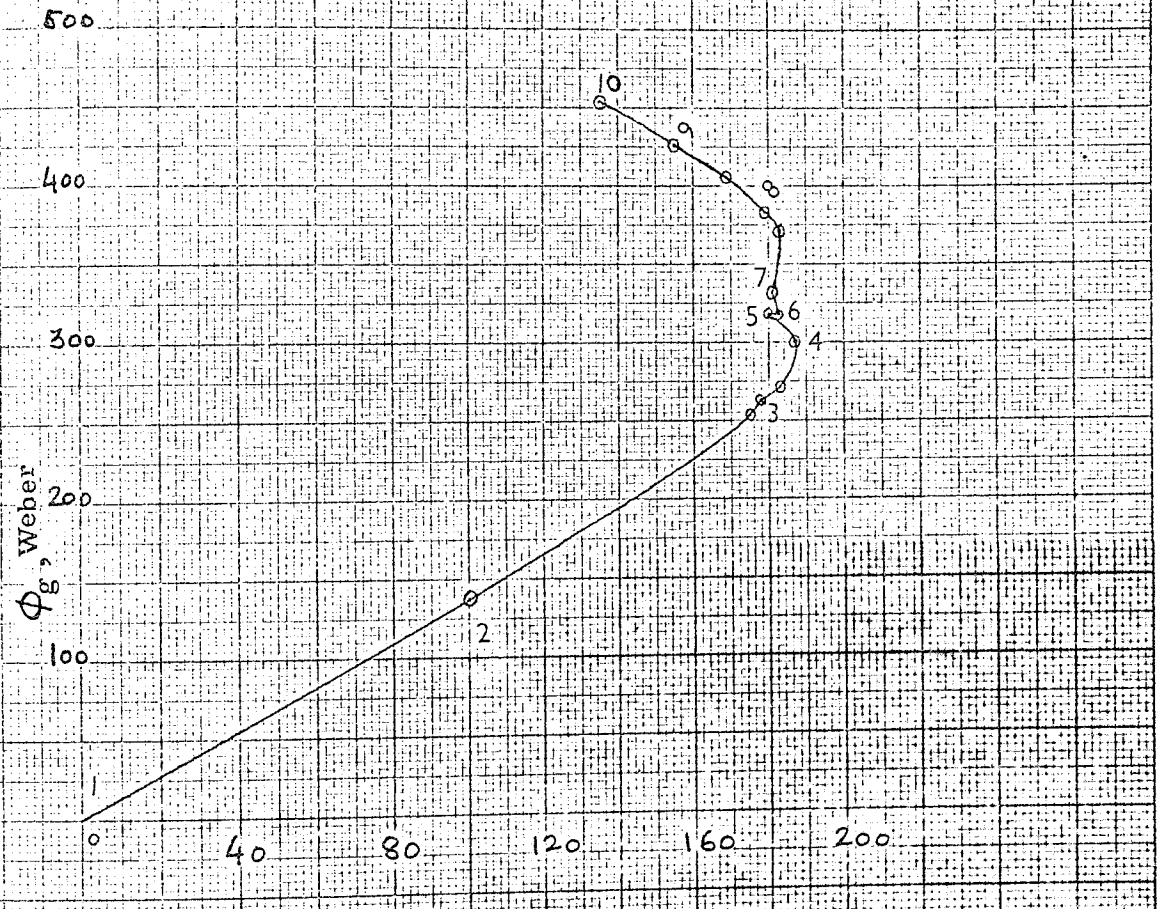

Fig. 8.12 Φ_g - M (Dynamic load characteristic in magnetic system of co-ordinates)

Table 8.10 shows the data for the load points in the curve in fig.8.12.

Table 8.10 Data for the load points

Load point	ϕ_g x 10^{-7} Weber	M At
1	0	0
2	137.8	100.1
3	263.1	178
4	300.8	187.4
5	319.3	180
6	319.1	182.3
7	331.8	181
8	383.8	179.6
9	425.8	155.3
10	454.1	135.8

Line 1 - 2

The time formula is:

$$t_{AB} = t_w = G\left(p + \frac{\phi_B}{M_B}\right) 2.303 \log \frac{M_s}{M_s - M_B}$$

$G = 273.90 \times 10^3$ mhos

$p = 1.3986 \times 10^{-7}$ Wb/At

$$t_{1-2} = 273.90 \times 10^3 \left(1.3986 \times 10^{-7} + \frac{137.8 \times 10^{-7}}{100.1}\right) 2.303 \log \frac{225}{225 - 100.1}$$

$= 44.73$ ms.

Line 5 - 6

$$t_{5-6} = 273.90 \times 10^{3}\left(1.3986 \times 10^{-7} + \frac{319.1 \times 10^{-7} - 319.3 \times 10^{-7}}{182.3 - 180}\right)$$

$$2.303 \log \frac{225 - 180}{225 - 182.3}$$

$$= 1.76 \text{ ms}$$

Line 6 - 7

$$t_{6-7} = 273.90 \times 10^{3}\left(1.3986 \times 10^{-7} + \frac{331.8 \times 10^{-7} - 319.1 \times 10^{-7}}{181 - 182.3}\right)$$

$$2.303 \log \frac{225 - 182.3}{225 - 181}$$

$$= 6.86 \text{ ms.}$$

Line 7 - 8

$$t_{7-8} = 273.90 \times 10^{3}\left(1.3986 \times 10^{-7} + \frac{383.8 \times 10^{-7} - 331.8 \times 10^{-7}}{179.6 - 181}\right)$$

$$2.303 \log \frac{225 - 181}{225 - 179.6}$$

$$= 30.89$$

Line 8 - 9

$$t_{8-9} = 273.90 \times 10^{3}\left(1.3986 \times 10^{-7} + \frac{425.8 \times 10^{-7} - 383.8 \times 10^{-7}}{155.3 - 179.6}\right)$$

$$2.303 \log \frac{225 - 179.6}{225 - 155.3}$$

$$= 3.87 \text{ ms.}$$

Line 9 - 10

$$t_{9-10} = 273.90 \times 10^{3}\left(1.3986 \times 10^{-7} + \frac{454.1 \times 10^{-7} - 425.8 \times 10^{-7}}{135.8 - 155.3}\right) 2.303 \log \frac{225 - 155.3}{225 - 135.8}$$

$$= .36 \text{ ms}$$

The time for full operation = $t_{1-2} + t_{2-3} + t_{3-4} + t_{4-5} + t_{5-6} + t_{6-7} + t_{7-8} + t_{8-9} + t_{9-10}$ = 44.73 + 80.5 + 33.06 + 5.42 + 1.76 + 6.86 + 30.89 + 3.87 + .36 = 207.45 ms.

The observed time for full operation can be read from x vs.t oscillogram and this is 214 ms. The time calculated from the measured ϕ vs. x relation as shown above, agrees well with the observed time.

Calculation of velocities at M_s = 225 At

Velocities can be calculated in a similar manner as shown in sec. 8.6. The magnetic pull may be calculated from ϕ_g and the values of ϕ_g and x from the curve in fig 8.11 are given in table 8.11. The calculated values of pull F and air gap x_g from ϕ_g and x respectively are also given in this table.

Table 8.11 Pull and air gap

x m m	x m m	ϕ_g x 10^{-7} Weber	$F = \frac{\phi_g^2}{2\mu_o A}$ Newton	F gf
0	.827	137.8	.4907	50
.077	.75	254	1.67	170
.1	.727	271.6	1.91	194.3
.2	.627	300.8	2.34	238.3
.315	.512	319.3	2.634	268.5
.3	.527	319.1	2.631	268.2
.35	.477	331.8	2.84	290
.45	.377	370.2	3.54	361
.5	.327	383.8	3.81	388
.6	.227	405.7	4.25	433.5
.7	.127	425.8	4.68	477.6
.827	0	454.1	5.33	543

The dynamic pull curve is obtained by plotting the values of the pull given in this table and this is shown in fig. 8.13. This pull curve is represented in fig. 8.14 by fitting a number of linear segments. The steady-state pull characteristics are also combined in the same diagram. Velocities at different positions of the armature may be calculated from this diagram.

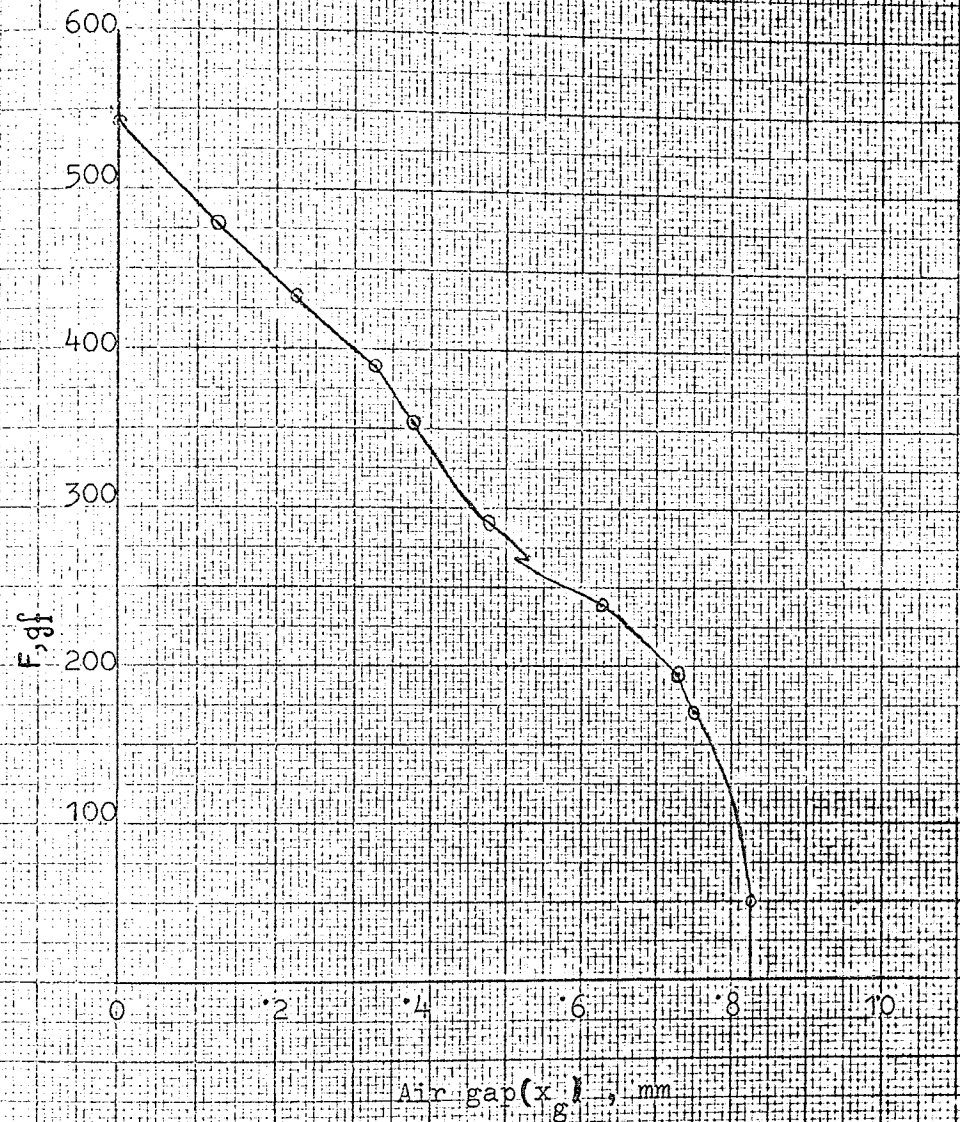

Fig. 8.13 Dynamic pull curve

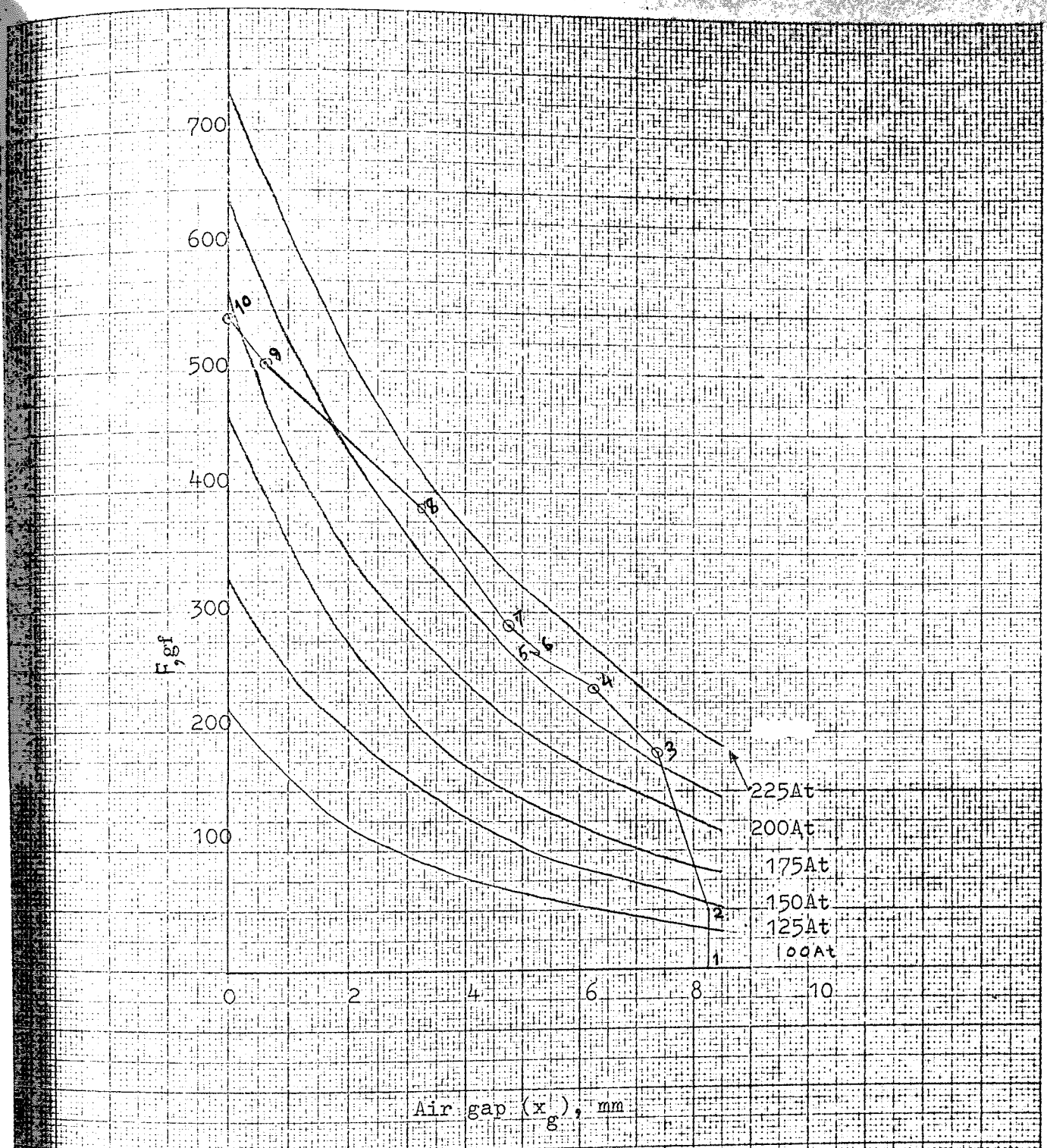

Fig. 8.14 Dynamic load and static pull characteristics

The velocity formula is :

$$V_o = \frac{2}{pG} \cdot \frac{M_s - M}{M} \cdot \frac{a\ s}{\frac{1}{2\delta p} + s - a}$$

$\frac{2}{pG}$ and $\frac{1}{2\delta p}$ have already been calculated in sec. 8.6

Table 8.12 M, a and s for the load points from fig. 8.14

Load points	On load line	M At	a m m	s m m
3	2 - 3	206	.13	.63
6	5 - 6	208.1	13.41	.543
7	7 - 8	208.3	.448	.493
8	7 - 8	214	.598	.523
10	9 - 10	170.75	.94	.363
1	6 - 7	215.5	.865	.61
1'	4 - 5	212	.953	.63

For line 1 - 2 in fig. 8.14 velocity is zero.

Velocity at point 3 on line 2 - 3.

$$V_o = 52.21 \times \frac{225 - 206}{206} \times \frac{.13 \times 10^{-3} \times .63 \times 10^{-3}}{(6.92 \times 10^{-4} + .63 \times 10^{-3} - .13 \times 10^{-3})}$$

$$= 52.21 \times \frac{19}{206} \times \frac{.13 \times 10^{-3} \times .63 \times 10^{-3}}{1.192 \times 10^{-3}} = .331 \times 10^{-3} \text{ m/sec.}$$

Velocity at point 6 on line 5 - 6

The velocity formula for this load line was given in eq. (7.34)

$$V_o = -52.21 \times \frac{225 - 208.1}{208.1} \times \frac{13.41 \times 10^{-3} \times .543 \times 10^{-3}}{6.92 \times 10^{-4} + .543 \times 10^{-3} - 13.41 \times 10^{-3}}$$

$$= 52.21 \times \frac{16.9}{208.1} \times \frac{13.41 \times 10^{-3} \times .543 \times 10^{-3}}{6.92 \times 10^{-4} + .543 \times 10^{-3} - 13.41 \times 10^{-3}}$$

$$= 52.21 \times \frac{16.9}{208.1} \times \frac{13.41 \times 10^{-3} \times .543 \times 10^{-3}}{- 12.175 \times 10^{-3}}$$

$$= 2.54 \times 10^{-3} \text{ m/sec.}$$

Velocity at point 7 on line 7 - 8

$$V_o = 52.21 \times \frac{225 - 208.3}{208.3} \times \frac{.448 \times 10^{-3} \times .493 \times 10^{-3}}{(6.92 \times 10^{-4} + .493 \times 10^{-3} - .448 \times 10^{-3})}$$

$$= 52.21 \times \frac{16.7}{208.3} \times \frac{.448 \times 10^{-3} \times .493 \times 10^{-3}}{.737 \times 10^{-3}}$$

$$= 1.25 \times 10^{-3} \text{ m/sec.}$$

Velocity at point 8 on line 7 - 8

$$V_o = 52.21 \times \frac{225 - 214}{214} \times \frac{.523 \times 10^{-3} \times .598 \times 10^{-3}}{(6.92 \times 10^{-4} + .523 \times 10^{-3} - .598 \times 10^{-3})}$$

$$= 52.21 \times \frac{11}{214} \times \frac{.523 \times 10^{-3} \times .598 \times 10^{-3}}{.617 \times 10^{-3}}$$

$$= 1.36 \times 10^{-3} \text{ m/sec.}$$

Velocity at point 10 on line 9 - 10

$$V_o = 52.21 \times \frac{225 - 170.75}{170.75} \times \frac{.94 \times 10^{-3} \times .363 \times 10^{-3}}{(6.92 \times 10^{-4} + .363 \times 10^{-3} - .94 \times 10^{-3}}$$

$$= 52.21 \times \frac{54.25}{170.75} \times \frac{.94 \times 10^{-3} \times .363 \times 10^{-3}}{.1150} = 49.20 \times 10^{-3} \text{ m/sec.}$$

At load point 1 where the length of the air gap x_g = .3 mm, the normally open contacts close.

Velocity at point 1 on line 6 - 7

$$V_o = 52.21 \times \frac{225 - 215.5}{215.5} \times \frac{.865 \times 10^{-3} \times .61 \times 10^{-3}}{(6.92 \times 10^{-4} + .61 \times 10^{-3} - .865 \times 10^{-3})}$$

$$= 52.21 \times \frac{9.5}{215.5} \times \frac{.865 \times 10^{-3} \times .61 \times 10^{-3}}{.437 \times 10^{-3}}$$

$$= 2.78 \times 10^{-3} \text{ m/sec.}$$

At load point 1' where the length of the air gap x_g = .61 mm, the normally closed contacts break.

Velocity at point 1' on line 4 - 5

$$V_o = 52.21 \times \frac{225 - 212}{212} \times \frac{.953 \times 10^{-3} \times .63 \times 10^{-3}}{(6.92 \times 10^{-4} + .63 \times 10^{-3} - .953 \times 10^{-3})}$$

$$= 52.21 \times \frac{13}{212} \times \frac{.953 \times 10^{-3} \times .63 \times 10^{-3}}{.369 \times 10^{-3}}$$

$$= 5.21 \times 10^{-3} \text{ m/sec.}$$

The velocity with which the normally open contacts close is:

$$V_o = 2.78 \times 10^{-3} \times .8163 = 2.269 \times 10^{-3} \text{ m/sec.}$$

where .8163 is the lever arm ratio between the load and pull.

The velocity with which the break contacts separate is:

$$V_o = 5.21 \times 10^{-3} \times .8163 = 4.253 \times 10^{-3} \text{ m/sec.}$$

The measured velocities at different positions of the armature from the slope of the position oscillogram in fig. 8.9 may be compared with the calculated velocities. Table 8.13 shows these velocities.

Table 8.13 Calculated and measured velocities.

x m m	Calculated velocity mm/sec	Measured velocity mm/sec.
.351	1.25	1.61
.503	1.36	3
.527	2.78	4

Calculation of extra kinetic energy released in the relay structure due to the impact of the armature.

The velocity attained at the end of the motion is 49.20×10^{-3} m/sec.

$$\therefore \text{ K.E.} = T = \tfrac{1}{2} m v_o^2 = \tfrac{1}{2} \times 9.31 \times 10^{-3} \times (49.20 \times 10^{-3})^2$$

$$= 11.27 \times 10^{-6} \text{ J}$$

Calculation of acceleration at M_s = 225 At

The acceleration formula which should be used has been mentioned in sec. 8.6. The values of $\frac{1}{2\delta p}$ and $\frac{2}{G^2 p^2}$ are the same as used in sec. 8.6.

The load points are shown in fig. 8.14 from which the positions of the armature can be easily determined.

Acceleration at point 7 on line 7 - 8

$$f_o = 13.629 \times 10^2 \times \frac{225 - 208.3}{208.3} \times \frac{.44 \times 10^{-3} \times .493 \times 10^{-3}}{(6.92 \times 10^{-4} + .493 \times 10^{-3} - .448 \times 10^{-3})^2}$$

$$\times \left(.448 \times 10^{-3} + \frac{225 - 2 \times 208.3}{208.3} \times .493 \times 10^{-3}\right.$$

$$\left. + 3 \frac{225 - 208.3}{208.3} \times \frac{.448 \times 10^{-3} \times .493 \times 10^{-3}}{(6.92 \times 10^{-4} + .493 \times 10^{-3} - .448 \times 10^{-3})}\right)$$

$$= 2.95 \times 10^{-3} \text{ m/sec.}^2$$

Acceleration at point 8 on line 7 - 8

$$f_o = 13.629 \times 10^2 \times \frac{225 - 214}{214} \times \frac{.523 \times 10^{-3} \times .598 \times 10^{-3}}{(6.92 \times 10^{-4} + .598 \times 10^{-3} - .523 \times 10^{-3})^2}$$

$$\times \left(.598 \times 10^{-3} + \frac{225 - 2 \times 214}{214} \times .523 \times 10^{-3}\right.$$

$$\left. + 3 \frac{225-214}{214} \times \frac{.523 \times 10^{-3} \times .598 \times 10^{-3}}{6.92 \times 10^{-4} + .598 \times 10^{-3} - .523 \times 10^{-3}}\right)$$

$$= 10.32 \times 10^{-3} \text{ m/sec.}^2$$

Acceleration at point 10 on line 9 - 10

$$f_o = 13.629 \times 10^2 \times \frac{225 - 170.75}{170.75} \times \frac{.94 \times 10^{-3} \times .363 \times 10^{-3}}{(6.92 \times 10^{-4} + .363 \times 10^{-3} - .94 \times 10^{-3})^2}$$

$$\times \left(.94 \times 10^{-3} + \frac{225 - 2 \times 170.75}{170.75} \times .363 + 3\,\frac{225 - 170.75}{170.75}\right.$$

$$\left. \times \frac{.94 \times 10^{-3} \times .363 \times 10^{-3}}{6.92 \times 10^{-4} + .363 \times 10^{-3} - .94 \times 10^{-3}}\right)$$

$$= 39.35 \text{ m/sec.}^2$$

Calculation of mass forces at M_s = 225 At

At point 7

$$F_m = 9.31 \times 10^{-3} \times 2.95 \times 10^{-3} = 27.4645 \times 10^{-6} \text{ N}$$

$$= .0028 \text{ gf}$$

At point 8

$$F_m = 9.31 \times 10^{-3} \times 10.32 \times 10^{-3} = 96.0792 \times 10^{-6} \text{ N}$$

$$= .0098 \text{ gf}$$

At point 10

$$F_m = 9.31 \times 10^{-3} \times 39.35 = .3663 \text{ N}$$

$$= 37.34 \text{ gf.}$$

Conclusions

The calculations for M_s = 225 At have been shown for a comparison and also for another verification of the rigorous method. The three measured values of velocities shown in table 8.13 agree quite well with their calculated values. The values of accelerations and mass forces are comparatively smaller than those for 275 At case. The mass force at the end of the motion is quite considerable. The acceleration at point 7 in fig. 8.14 is positive and this suggests that the velocity should increase, which is confirmed by the higher calculated velocity at point 8.

The negative velocities physically existing as shown in the x vs. t characteristics for both the cases are found in the calculations. The calculated values of the time, velocity and acceleration shown in secs. 8.6 and 8.7 are for an existing relay on which measurements could be made to get the dynamic load characteristic. It is not possible at present to find an analytical expression for the dynamic load characteristic which depends on many parameters. As the acceleration changes with the feeding voltage, so the characteristic does. The dynamic load characteristic is not like the static one which remains the same as specified even when the feeding voltage changes. Estimation of the dynamic characteristics by using the time, velocity and acceleration formulae requires a dynamic load characteristic to be assumed for a specified voltage. The procedure for the estimation is discussed in sec. 8.8.

Step by Step Procedure for Estimating Time, Velocity, and Acceleration (When Applied Voltage Specified):
Ref: Section 8.8

1) Derive a reference spring load characteristic by Ahlberg's method.

2) Add a dynamic load characteristic, of arbitrary positive slope (with respect to the reference characteristic) to account for mass force.

3) Calculate the operation time (t_o) for this dynamic load characteristic.

4) The acceleration is calculated from a separate diagram that combines this dynamic load characteristic with the (separately derived) static pull characteristics.

5) The required spring load characteristic is calculated from this dynamic load characteristic (2) and the mass force determined by the acceleration calculation (4).

8.8 Estimation for design

The calculation of time, velocity and acceleration is presented in secs. 8.6 and 8.7; a similar calculation may be adopted to estimate these for design purposes. The procedure is to find first a reference spring load characteristic for a specific design by using Ahlberg's method or the rational design theory. Then it is required to assume a dynamic load characteristic for a specified applied voltage E. The slope of the dynamic load characteristic is arbitrary but should be slightly greater than the static load characteristic. The two characteristics change their slope at the same position of the armature as shown in fig. 8.15 where oab is the proposed dynamic load characteristic and ocd is the reference spring load characteristic. From the

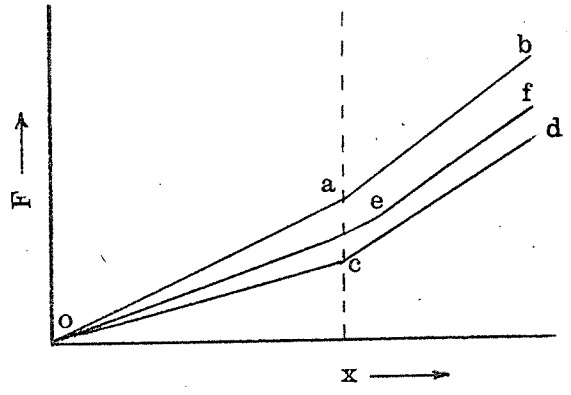

FIG. 8.15

assumed dynamic load characteristic, for a specified value of E, the required static load characteristic can be determined accurately after estimating mass force and frictional damping forces which are made available from the estimated acceleration and velocity. It is already

shown how velocity and acceleration can be calculated from the dynamic load characteristic and static pull characteristics. Knowing the mass and frictional damping forces, the spring load may be determined for every position of the armature from the following relation:

$$F - m\ddot{x} - \tau\dot{x} = c\,x$$

Where F is the pull from the dynamic load characteristic, cx is the spring load, m is the effective mass of the armature and τ is frictional damping coefficient. For specifying the spring load cx is taken for convenience, but it does not signify that c is a constant. It is well known that c is variable for a non-linear spring load.

Suppose the calculated spring load relation is oef, then this represents the static load characteristic of the relay for which oab is the dynamic load characteristic for a specified contant voltage E. Now for the development of the relay the calculated static load curve should be divided into a few sections by fitting straight lines representing closely the original curve for obtaining a practical spring configuration. In the following section a design calculation by making use of this procedure is presented.

8.9 A sample design calculation

The magnetic structure of the test relay on which the check of the rigorous method of the dynamical analysis was done, was chosen for the design. Results of the measurement of the equivalent magnetic

circuit constants are given in sec. 11.4. The remaining air gap when the armature is operated is different from the same in the original structure and the total travel x_o is also different. These alterations would change the closed gap reluctance S_o whereas the leakage reluctance S_L remains the same. G is the same as for the test relay.

The equivalent magnetic circuit constants for the present structure.

$$S_o = 299 - \frac{.04 \times 10^{-3}}{.1935 \times 10^{-9}} = 299 - 20.67$$

$$= 278.33 \times 10^4 \approx 278 \times 10^4 \text{ At/wb}$$

$$S_L = 715 \times 10^4 \text{ At/wb}$$

$$\mu_o A = .1935 \times 10^{-9} \text{ H.m}$$

Determination of the reference spring load characteristic by Ahlberg's method (ref.10,11)

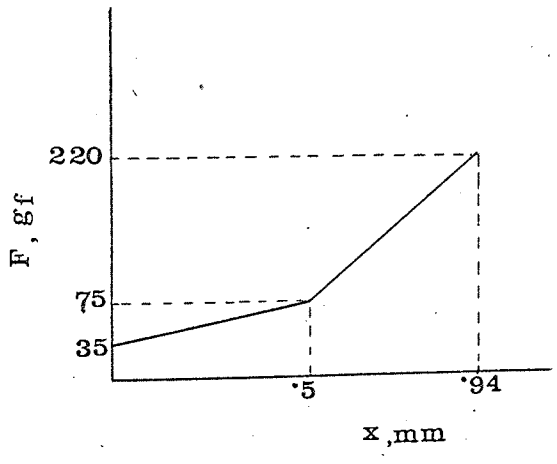

Fig. 8.16 Spring load characteristic

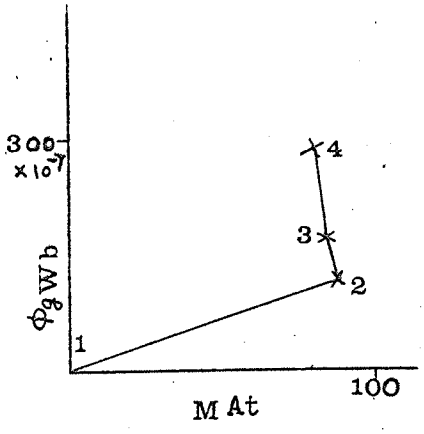

Fig.8.17

Residual air gap = .26 mm

Total travel x_o = .94 mm

The static load characteristic in fig. 8.16 is converted into its equivalent ϕ_g vs. M characteristic as shown in fig. 8.17 The load points are 1, 2, 3 and 4 as shown on the ϕ_g - M plane. The calculations needed to get the magnetic equivalents are given in the following :

At x = 0

$$\mathcal{P}_a = \frac{1}{S_o + \frac{x_o - x}{\mu_o A}} = \frac{1}{278 \times 10^4 + \frac{.94 \times 10^{-3}}{.1935 \times 10^{-9}}} = 1.300 \times 10^{-7} \text{ Wb/At}$$

$$\phi_g = \sqrt{F \times 2 \mu_o A} = \sqrt{35 \times 10^{-3} \times 9.81 \times 2 \times .1935 \times 10^{-9}}$$

$$= 115.2 \times 10^{-7} \text{ Weber}$$

$$M = \frac{\phi_g}{a} = \frac{115.2 \times 10^{-7}}{1.30 \times 10^{-7}} = 88.62 \text{ At}$$

At x = .5 mm

$$\mathcal{P}_a = \frac{1}{278 \times 10^4 + \frac{(.94 - .5) \times 10^{-3}}{.1935 \times 10^{-9}}} = 1.970 \times 10^{-7} \text{ Wb/At}$$

$$\phi_g = \sqrt{75 \times 10^{-3} \times 9.81 \times 2 \times .1935 \times 10^{-9}} = 168.2 \times 10^{-7} \text{ Weber}$$

$$M = \frac{168.2 \times 10^{-7}}{1.970 \times 10^{-7}} = 85.38 \text{ At}$$

At x = .94

$$\mathcal{P}_a = \frac{1}{S_o}$$

$$\therefore \mathcal{P}_a = \frac{1}{278 \times 10^4} = 3.596 \times 10^{-7} \text{ Wb/At}$$

$$\phi_g = \sqrt{220 \times 10^{-7} \times 9.81 \times 2 \times .1935 \times 10^{-9}} = 289 \times 10^{-7} \text{ Weber}$$

$$M = \frac{289 \times 10^{-7}}{3.596 \times 10^{-7}} = 80.37 \text{ At}$$

The values of ϕ_g are plotted against corresponding values of M as shown in fig. 8.17.

Calculation of the time of operation from the characteristic in fig. 8.17 is given below:-

Line 1 - 2

The time formula is:

$$t_{AB} = t_w = G\left(p + \frac{\phi_B}{M_B}\right) 2.303 \log \frac{M_s}{M_s - M_B}$$

$M_s = 300$ At $\quad i_s = 12$ mA

$$t_{1-2} = 273.90 \times 10^3 \left(1.3986 \times 10^{-7} + \frac{115.2 \times 10^{-7}}{88.62}\right) 2.303 \log \frac{300}{300 - 88.62} = 25.87 \text{ ms.}$$

Line 2 - 3

The time formula is:

$$t_{AB} = G\left(p + \frac{\phi_B - \phi_A}{M_B - M_A}\right) 2.303 \log \frac{M_s - M_A}{M_s - M_B}$$

$$t_{2-3} = 273.90 \times 10^3 \left(1.3086 \times 10^{-7} \frac{168.2 \times 10^{-7} - 115.2 \times 10^{-7}}{85.38 - 88.62}\right) 2.303 \log \frac{300 - 88.62}{300 - 85.38}$$

$= 6.23$ ms.

Line 3 - 4

$$t_{3-4} = 273.90 \times 10^{3} \left(1.3986 \times 10^{-7} + \frac{289 \times 10^{-7} - 168.2 \times 10^{-7}}{80.37 - 85.38}\right)$$

$$2{,}303 \log \frac{300 - 85.38}{300 - 80.37}$$

$$= 15.37 \text{ ms.}$$

The total time of operation = $t_{1-2} + t_{2-3} + t_{3-4}$

$$= 25.87 + 6.23 + 15.37$$

$$= 47.47 \text{ ms.}$$

Calculation of the time of operation from the dynamic load characteristic.

Fig. 8.18 shows the reference spring load and assumed dynamic load characteristics. The time of operation is calculated in the following from the dynamic load characteristic which is the upper curve in the figure.

At x = 0

$$\mathcal{P}_a = 1.300 \times 10^{-7} \text{ Wb/At}$$

$$\phi_g = 115.2 \times 10^{-7} \text{ Weber}$$

$$M = 88.62 \text{ At}$$

These have been calculated before while calculating the time of operation from the reference spring load characteristic.

At x = .5 mm

$$\mathcal{P}_a = 1.970 \times 10^{-7} \text{ Wb/At}$$

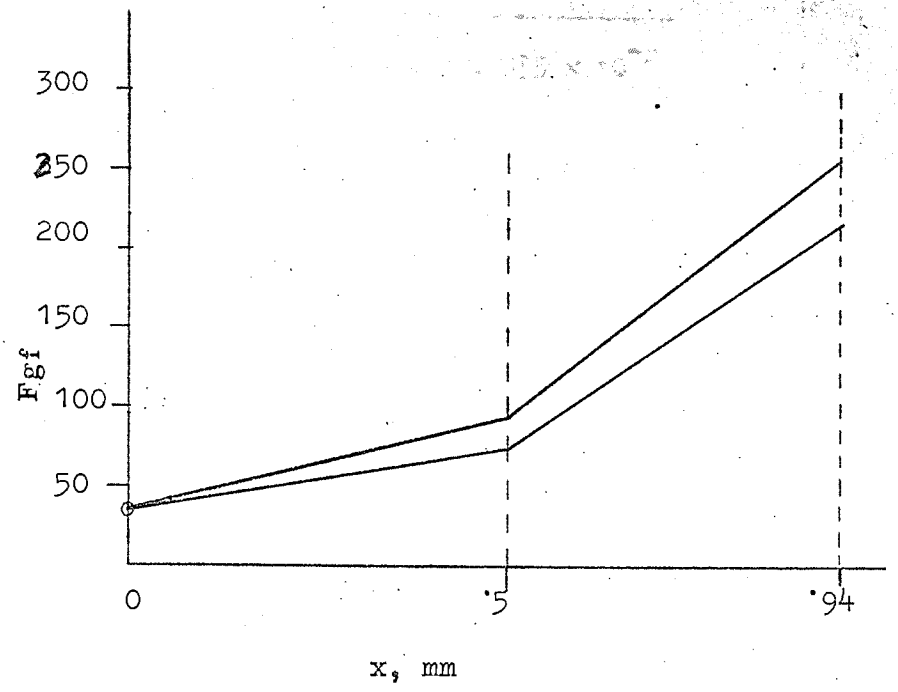

Fig.8.18 Reference spring load and assumed dynamic load characteristics.

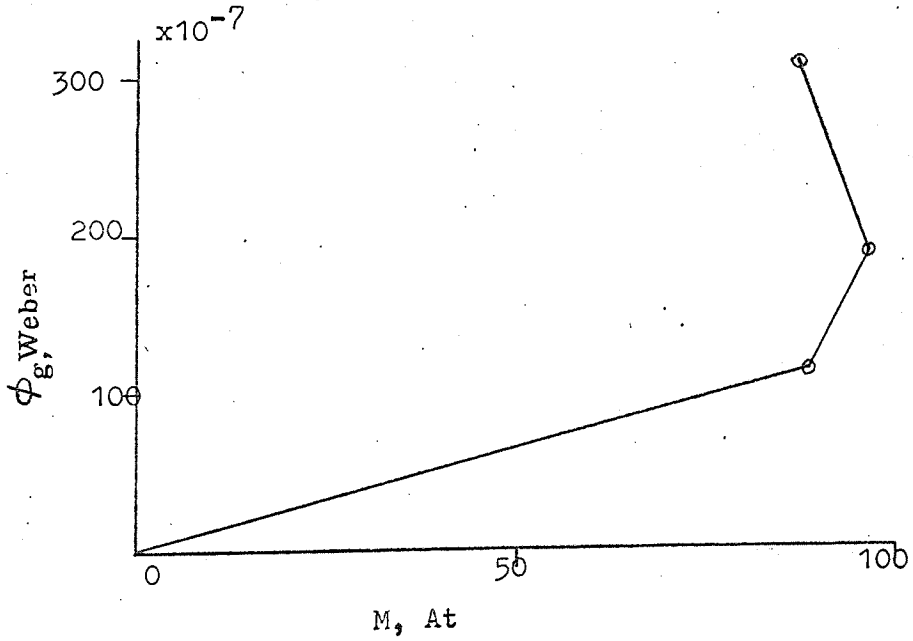

Fig.8.19 Dynamic load characteristic in magnetic system of co-ordinates

$$\phi_g = \sqrt{95 \times 10^{-3} \times 9.81 \times 2 \times .1935 \times 10^{-9}}$$

$$= 190 \times 10^{-7} \text{ Weber}$$

$$M = \frac{190 \times 10^{-7}}{1.970 \times 10^{-7}} = 96.4 \text{ At}$$

At x = .94 mm

$$\mathcal{P}_a = 3.596 \times 10^{-7} \text{ wb/At}$$

$$\phi_g = \sqrt{260 \times 10^{-3} \times 9.81 \times 2 \times .1935 \times 10^{-9}}$$

$$= 314 \times 10^{-7} \text{ Weber}$$

$$M = \frac{314 \times 10^{-7}}{3.596 \times 10^{-7}} = 87.32 \text{ At}$$

The values of ϕ_g for different positions of the armature are plotted against corresponding values of M as shown in fig. 8.19.

Line 1 - 2

t_{1-2} has already been calculated before.

$t_{1-2} = t_w = 25.87$ ms.

Line 2 - 3

The time formula is:

$$t_{AB} = G\left(p + \frac{\phi_B - \phi_A}{M_B - M_A}\right) \; 2.303 \log \frac{M_s - M_A}{M_s - M_B}$$

$$t_{2-3} = 273.90 \times 10^3 \left(1.3986 \times 10^{-7} + \frac{190 \times 10^{-7} - 115.2 \times 10^{-7}}{96.4 - 88.62}\right)$$

$$2.303 \log \frac{300 - 88.62}{300 - 96.4}$$

$= 11.25$ ms.

Line 3 - 4

$$t_{3-4} = 273.90 \times 10^{3} \times \left(1.3986 \times 10^{-7} + \frac{314 \times 10^{-7} - 190 \times 10^{-7}}{87.32 - 96.4}\right)$$

$$2.303 \log \frac{300 - 96.4}{300 - 87.32}$$

$= 14.67$ ms

∴ The total time for full operation

$= t_{1-2} + t_{2-3} + t_{3-4}$

$= 25.87 + 11.25 + 14.67$

$= 51.79$ ms.

The calculated times are plotted against x as shown in fig. 8.20.

Calculation of the proposed spring load characteristic for the design.

Friction forces are neglected in this case. The spring load can be determined by subtracting the mass force from the pull available from the dynamic load characteristic in fig. 8.18 The dynamic load characteristic and the steady state pull characteristics are combined in the same diagram as shown in fig. 8.21. As the magnetic structure is the same as in the case of the test relay in secs. 8.6 and 8.7 except the residual air gap and total travel (x_o), the pull curves measured on the test relay may be used in this case. These pull curves are given in fig 11.6 from which the pull curves limited to the range of

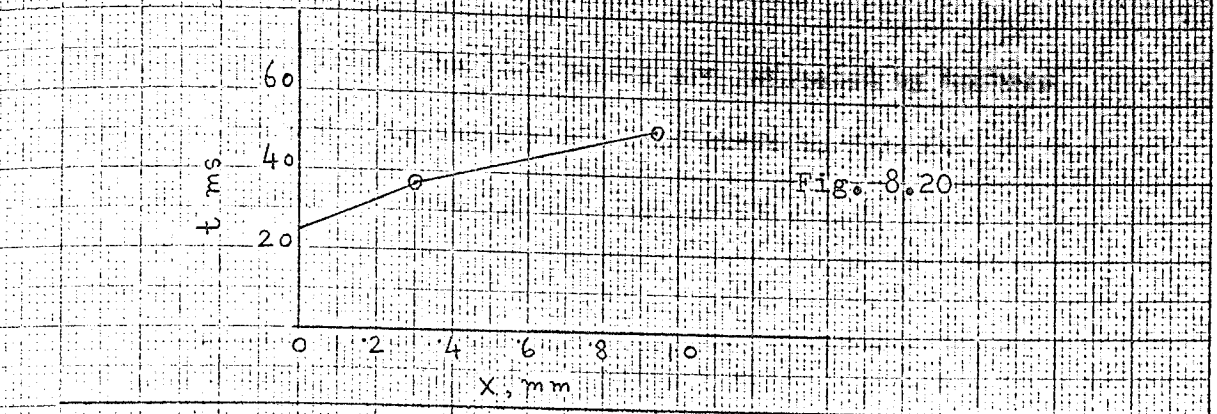

Fig. 8.20

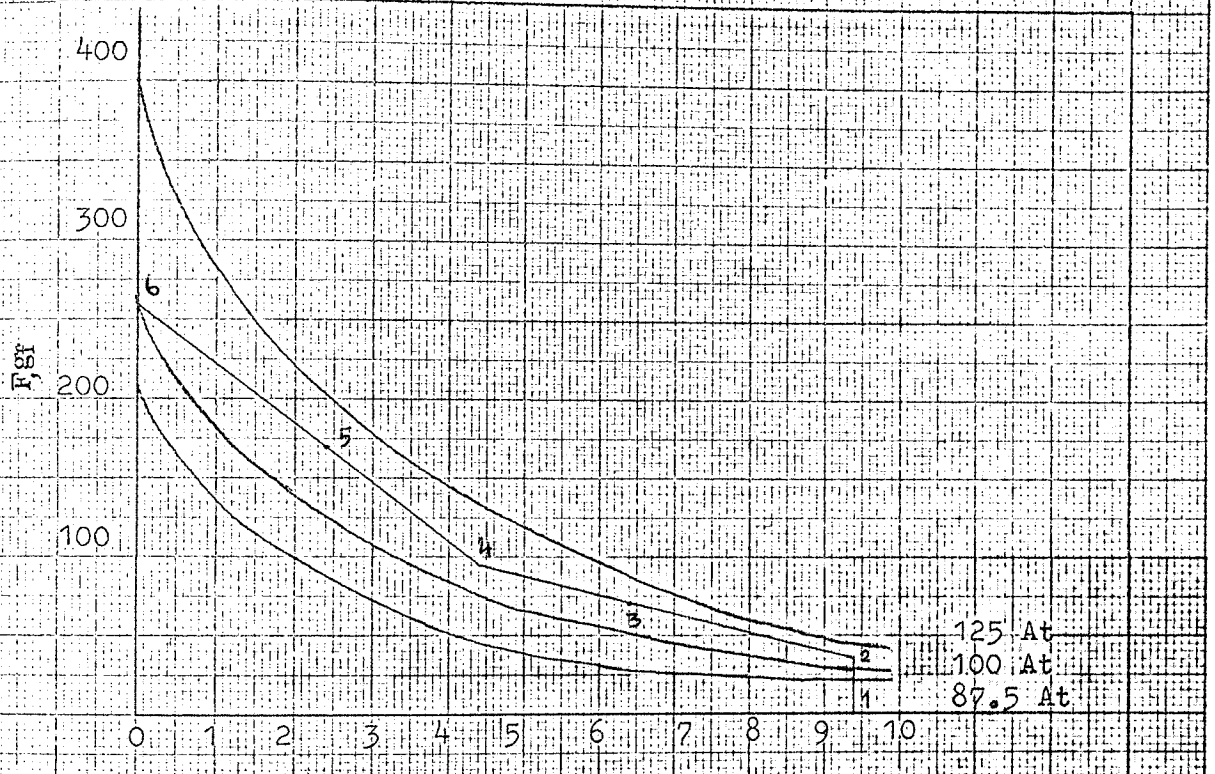

Fig. 8.21 Dynamic load and static pull characteristics

interest are taken. The load points are indicated by numbers 1, 2, 3, 4, 5 and 6 on the dynamic load curve in fig. 8. Table 8. shows the data for the load points.

TABLE 8.

Load Point	$\frac{M}{A\ t}$	α	s
3	114	.56	.4
4	108.8	.76	.51
5	115	.455	.51
6	100	.695	.15

Acceleration at point 3 on line 2 - 4

$$f_o = 13.629 \times 10^2 \times \frac{300 - 114}{114} \times \frac{.56 \times 10^{-3} \times .4 \times 10^{-3}}{(6.92 \times 10^{-4} + .4 \times 10^{-3} - .56 \times 10^{-3})^2}$$

$$\times \left(.56 \times 10^{-3} + \frac{300 - 2 \times 114}{114} \times .4 \times 10^{-3} \times 3 \times \frac{300 - 114}{114} \times \frac{.56 \times 10^{-3} \times .4 \times 10^{-3}}{6.92 \times 10^{-4} + .4 \times 10^{-3} - .56 \times 10^{-3}}\right)$$

$$= 13.629 \times 10^2 \times \frac{300 - 114}{114} \times \frac{.56 \times 10^{-3} \times .4 \times 10^{-3}}{(.5320 \times 10^{-3})^2}$$

$$(.56 \times 10^{-3} + .2526 \times 10^{-3} + 2.0610 \times 10^{-3})$$

$$= 5.05 \text{ m/sec}^2$$

Acceleration at point 4 on line 2 - 4

$$f_o = 13.629 \times 10^2 \times \frac{300 - 108.8}{108.8} \times \frac{.76 \times 10^{-3} \times .51 \times 10^{-3}}{(6.92 \times 10^{-4} + .51 \times 10^{-3} - .76 \times 10^{-3})^2}$$

$$\times \left(6.92 \times 10^{-3} + \frac{300 - 2 \times 108.8}{108.8} \times .51 \times 10^{-3} + 3 \times \frac{300-108.8}{108.8}\right.$$

$$\left. \times \frac{.76 \times 10^{-3} \times .51 \times 10^{-3}}{6.92 \times 10^{-4} + .51 \times 10^{-3} - .76 \times 10^{-3}}\right)$$

$$= 13.629 \times 10^2 \times \frac{300 - 108.8}{108.8} \times \frac{.76 \times 10^{-3} \times .51 \times 10^{-3}}{(.4420 \times 10^{-3})^2}$$

$$\times (.76 \times 10^{-3} + .3862 \times 10^{-3} + 4.6077 \times 10^{-3})$$

$$= 27.3 \text{ m/sec}^2$$

Acceleration at point 5 on line 4 - 6

$$f_o = 13.629 \times 10^2 \times \frac{300 - 115}{115} \times \frac{.455 \times 10^{-3} \times .51 \times 10^{-3}}{(6.92 \times 10^{-4} + .51 \times 10^{-3} - .455 \times 10^{-3})^2}$$

$$\times \left(.455 \times 10^{-3} + \frac{300 - 2 \times 115}{115} \times .51 \times 10^{-3} + 3 \times \frac{300 - 115}{115}\right.$$

$$\left. \times \frac{.455 \times 10^{-3} \times .51 \times 10^{-3}}{6.92 \times 10^{-4} + .51 \times 10^{-3} - .455 \times 10^{-3}}\right)$$

$$= 13.629 \times 10^2 \times \frac{185}{115} \times \frac{.455 \times 10^{-3} \times .51 \times 10^{-3}}{(.7470 \times 10^{-3})^2} \times (.455 \times 10^{-3}$$

$$+ .3103 \times 10^{-3} + 1.4986 \times 10^{-3})$$

$$= 2.1 \text{ m/sec}^2$$

Acceleration at point 6 on line 4 - 6

$$f_o = 13.629 \times 10^2 \times \frac{300 - 100}{100} \times \frac{.695 \times 10^{-3} \times .15 \times 10^{-3}}{(6.92 \times 10^{-4} + .15 \times 10^{-3} - .695 \times 10^{-3})^2}$$

$$\times \left(.695 \times 10^{-3} + \frac{300 - 2 \times 100}{100} \times .15 \times 10^{-3} + 3 \times \frac{300 - 100}{100}\right.$$

$$\left. \times \frac{.695 \times 10^{-3} \times .15 \times 10^{-3}}{6.92 \times 10^{-4} + .15 \times 10^{-3} - .695 \times 10^{-3}}\right)$$

$$= 13.629 \times 10^2 \times \frac{300 - 100}{100} \times \frac{.695 \times 10^{-3} \times .15 \times 10^{-3}}{(.1470 \times 10^{-3})^2}$$

$$\times (.695 \times 10^{-3} + .19 \times 10^{-3} + 4.2551 \times 10^{-3})$$

$$= 67.06 \text{ m/sec}^2$$

Mass forces.

At point 3

$$F_m = m \times f_o = 8.1 \times 10^{-3} \times 5.05 \text{ N} = 4.17 \text{ gf}$$

At point 4

$$F_m = 8.1 \times 10^{-3} \times 27.3 \text{ N} = 22.54 \text{ gf}$$

At point 5

$$F_m = 8.1 \times 10^{-3} \times 2.1 \text{ N} = 1.73 \text{ gf}$$

At point 6

$$F_m = 8.1 \times 10^{-3} \times 67.06 \text{ N} = 55.4 \text{ gf}$$

Spring retractile forces

Spring load at point 2 in fig. 8.21

$F = 35$ gf

Spring load at point 3,

F = Pull-mass force

$= 72 - 4.17 = 67.83$ gf

Spring load at point 4

$F = 95 - 22.54 = 72.46$

Spring load at point 5

$F = 169 - 1.73 = 167.27$ gf

Spring load at point 6

$F = 260 - 55.4 = 204.6$ gf

The spring loads at different points are plotted to give the proposed spring load characteristic as shown in fig. 8.22. The values at point 3 and 5 are ignored while plotting the curve, because the calculated acceleration at these points are comparatively smaller than the other two values.

Calculation of velocities

The velocities may be calculating using the formula (7.33). M, α and s are given in table 8.14.

Fig. 8.21 is referred

Velocity at point 4 on line 2 - 4

$V_o = 80.5 \times 10^{-3}$ m/sec.

Velocity at point 5 on line 4 - 6

$V_o = 26.1 \times 10^{-3}$ m/sec.

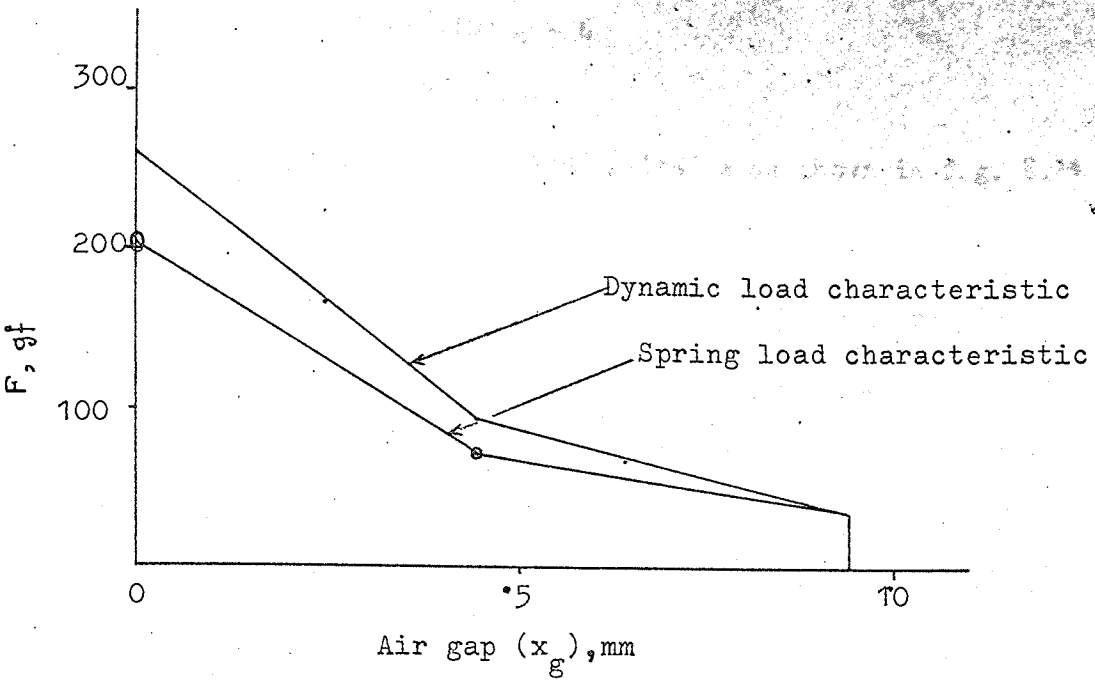

8.22
Fig. Assumed dynamic load and proposed spring load characteristics

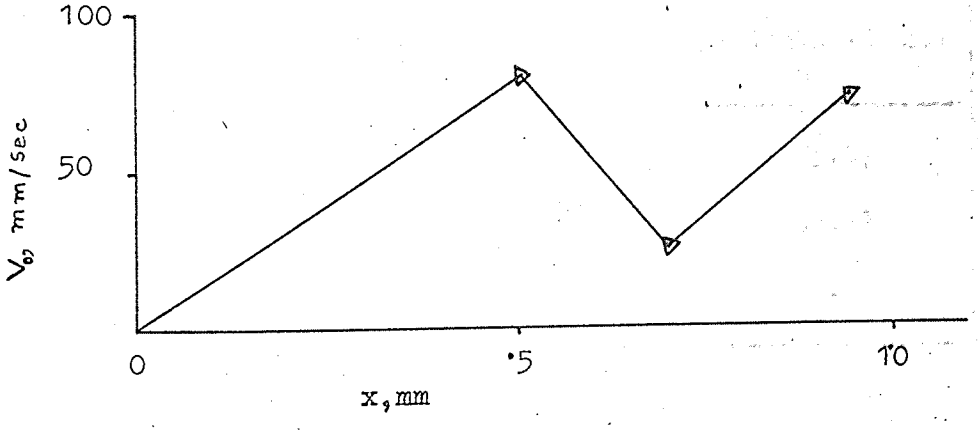

Fig.8.23 Calculated velocity vs. position

Velocity at point 6 on line 4 - 6

$$V_o = 74.1 \times 10^{-3} \text{ m/sec.}$$

The calculated velocities are plotted against x as shown in fig. 8.23

Design Development

The contact springs were mounted on the relay structure and the load was adjusted to give the proposed spring load characteristic shown in fig. 8.22. Oscillograms 1 and 2 in fig. 8.24 show the x vs. t characteristic and the V vs. t characteristic respectively. The negative velocities indicated in the upper curve are confirmed in the lower curve as well. Table 8.15 shows the measured and calculated times and Table 8.16 shows the measured and calculated velocities. The measured velocities are obtained from the x vs. t oscillogram in fig. 8.24.

Table 8 Measured and calculated times

Quantity	Measured time m s	Calculated time m s
t_{1-2}	19	25.87
t_{1-3}	36	37.12
t_{1-4}	52.8	51.79

1

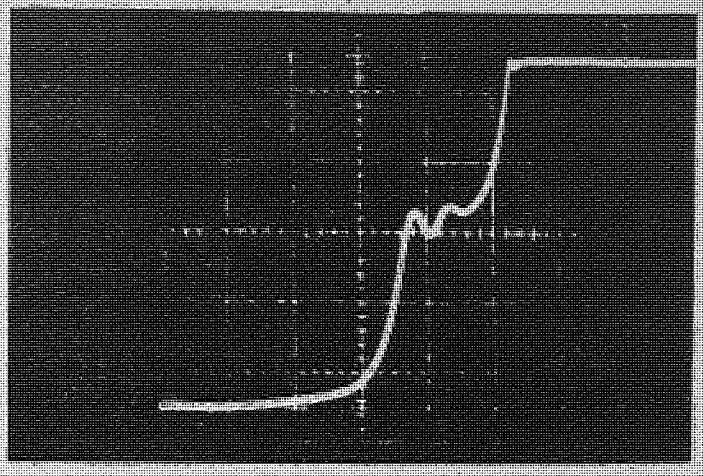

x

t

Time scale : 2 ms/scale div.

Position scale: .0373 mm/scale div.

2

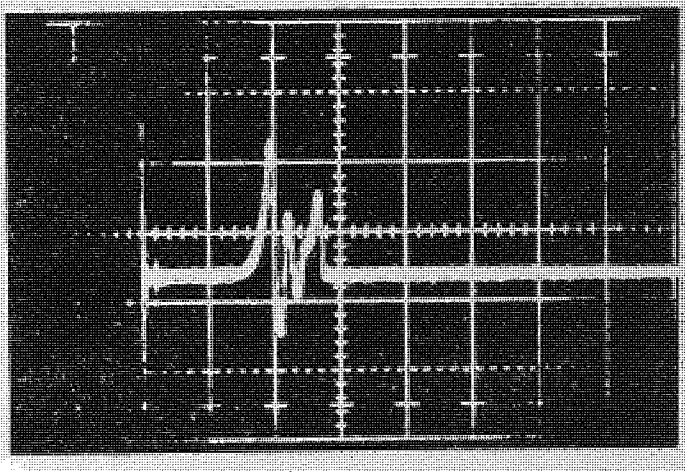

V_o

t

Fig. 8.24

Table 8. Measured and calculated velocities

Load point	x m m	Measured Velocity mm / sec	Calculated Velicity mm / sec
4	.5	100	80.5
5	.7	40	26.1
6	.94	82.5	74.1

The agreement between the calculated and measured times are good. The calculated velocities agree quite well with the measured ones. These are lower than the measured values.

It may be concluded that the design calculations using the theory presented in chapter 7 has been shown to be satisfactory. The theory is, therefore, applicable not only to the development studies based on measurements, but also to the estimation of the dynamic characteristics for design purposes.

8.10 Discussions

The calculation of the time of operation, velocity and acceleration from the measured ϕ vs. x relation has been shown in secs. 8.6 and 8.7. These results are very useful in development studies. A design calculation is also shown in sec. 8.9. The estimated time of operation agrees well with the measured time. The velocity and acceleration calculated from the dynamic load characteristic and steady state pull characteristics are acceptable. Care should be taken in determining the pull characteristics and in dividing the dynamic load characteristic by the linear segments.

The method of determining velocities and accelerations seems justified. There is a great disagreement between the calculated and measured values of velocities and accelerations in Ahlberg's method. This disagreement may be due to the disregarding of the mass force. As the velocity depends upon α which in turn depends on the slope of the load curve whose dynamic characteristic is different from the static one. Therefore, use of the static load characteristic instead of the dynamic one which takes into account the mass force, is most probably the cause of the disagreement. The present method, however, shows a way of determining velocities and accelerations, which is acceptable and will be of great significance in the control of velocity to minimise bouncing and rebound oscillations. The measurements and calculations show that α, M and s change for the same position of the armature for different steady state magnetomotive forces. Therefore, control of velocity for minimising bouncing and rebound oscillations should be studied in conjunction with the values of α, M and s for different positions. The time has been calculated from the ϕ_g vs. M characteristic and it may be interesting to see how this characteristic changes with more feeding voltage. ϕ_g and M for every position of the armature for different steady state mmfs would be of interest. When contact bounce, armature rebound and stability of the motion are investigated a critical analysis of the dynamic performance by this present method would be of great help. All the three features are connected with the velocity which in turn is related to acceleration. If velocity

is reduced then the time of operation would increase. The analysis would guide in which way the change should be made to reduce the velocity at a particular position without affecting the time significantly. The analysis of the acceleration formula and calculation of acceleration at a position would be of interest. For considering retardation condition the analysis would be essential. This condition is discussed in sec. 9.7. Dynamic measurement of the flux and position after adding more mass, changing the spring load and friction, and changing the other parameters will be of great interest in further research.

From the results presented in this chapter and the above discussions, it may be concluded that the theory of the rigorous method of analysis presented in chapter 7 has been proved to be satisfactory.

There are some interesting features to be observed in the theory. If the time of operation is calculated from the dynamic load characteristic in magnetic system of co-ordinates, then the time for all sections of the travel comes positive. This is the case even when the direction of motion is negative due to oscillations. Whereas Ahlberg gets negative time for some sections of the travel while calculating the time from the static load characteristic in magnetic system of co-ordinates. Time cannot be negative, and this proves the discrepancy of Ahlberg's method. No negative time has been observed in the calculations.

Another interesting feature is that $\frac{1}{2\delta p} + s - \alpha$ is always positive when the direction of motion is positive which proves that the motion is under the control of the electromagnet, and the armature regulates its own speed. The pull is generated such as to balance the other three forces. It may be mentioned here that Ahlberg gets negative velocity for some sections. He suggests some measures to reduce the actual velocity which is great in those sections. The measures may reduce the velocity,but it seems there is no need of taking such measures only because of the reason that the calculated velocity comes negative. In fact there is a self stabilisation in a relay, the slope of the dynamic load curve is adjusted by the relay itself in such a way that the calculated velocity will always come positive, when the direction of motion is positive. Of course, the negative velocity occurs physically and it is difficult to take this into account quantitatively in the design calculation. If the armature enters into a new section with a greater velocity there may be an oscillatory motion. Precautions from this kind of trouble may be taken from the design calculations. The actual behaviour should be studied in models after making necessary measurements and the analysis of the measurements as made in this chapter would give clear pictures in which way the necessary measures or change should be made to get the required performance.

Chapter 9

MISCELLANEOUS DYNAMIC PROBLEMS.

REED RELAYS

9.1 Introduction

Following the rigorous analysis and the experimental verification, some dynamic phenomena and the problems associated with them are discussed in this chapter.

Reed relays are becoming increasingly useful in many fields and may be made to act as very high speed electromagnetic relays. This chapter presents a brief discussion on these relays and application of Ahlberg's theory on them is also considered.

9.2 Stability of the armature motion

The motion may be called stable if the armature moves forward towards the pole face of the magnet during operation and away from the face during release. It is normally desired that the armature should continuously move forward to actuate the contacts during operation.

The stability condition in operation may, therefore, be defined thus, the motion is stable if there exists a positive velocity. Negative velocities are caused by shock, oscillations due to discontinuous change of load and hesitation chattering due to insufficient pull. Some considerations may be given on the stability, yet this should be observed in practice. The x vs. t curves in figs. 7.2 and 8.9 show negative velocities which are caused by the armature oscillations. It may be observed that oscillations are more prominent

in the case for which M_s is greater.

The calculations in secs. 8.6 and 8.7 also give negative velocities for those sections in which the oscillations occur. This kind of oscillations may be avoided by reducing the speed with which the armature enters into the sections, and the condition of retardation should be considered for which the acceleration formula in equation 7.36 would be of help.

If $' \frac{1}{2\delta p} + s - \alpha '$ in the denominator of the velocity formula (7.33) is negative, then the velocity is also negative. In the practical investigations and in the analogue computation this expression was always found positive for a forward motion. It seems when α tends to increase the motion is accelerated and the slope of the dynamic load curve changes to reduce α. Therefore, it is difficult to establish a mathematical criterion for the stability condition from the velocity formula.

During development studies an effort should be given to avoid the negative velocities which physically exist.

9.3 Influence of mass on the armature motion

When the relay is supplied with high power the acceleration becomes great, so does the mass force. The motion is then significantly controlled by mass. It is discussed in sec. 4.6 of Peek and Wagar[3] that in a mass controlled relay, the time of motion varies as the cube root of the mass. When the input power is low it is evident that the time of motion is controlled by the load; the time

then varies directly as the load. In a high speed relay where the spring load is light, the mass force may be quite high and mass has a great influence on the time of operation. In a low speed relay, mass does not influence the time appreciably, but the influence on the velocity and acceleration is great irrespective of high and low speeds.

The kinetic energy varies directly as the mass. Because of this energy of the armature, oscillations occur and a heavy mass may produce oscillations of higher amplitude.

9.4 Contact bounce

This is quite well known among relay users and causes various troubles. Normally rapid and transient reclosures of open contacts and reopenings of closed contacts are called contact bounce, which is caused mainly by armature rebound and contact spring vibration. There is another type of contact bounce or chatter which is popularly known as hesitation chatter. The term 'chatter' is better applicable in this particular case and may be regarded as a general term for both 'bounce' and 'chatter'. The hesitation chatter is caused due to the slow development during operation and decay during release, of the magnetic pull.

Spring vibration chatter develops due to the impact of the closing contact and the shock of the impact of the armature on the core or backstop.

Armature oscillations are induced due to the impact of the

armature on the core or backstop and sudden change of load when the armature enters into contact with the springs from the rest position. Both the causes give rise to armature rebound first, which in turn gives rise to oscillations causing contact bounce.

Effect of contact bounce.

When an inductive circuit is switched on through a relay contact, the inductive kick is generated due to bouncing of the contact. Contact bounce causes electric discharge across the contacts enhancing the rate of erosion and reducing contact life. It also disturbs the function of the switching system which may contain complicated electronic circuits.

9.5 Armature impact and rebound

The armature moves under the influence of four kinds of forces and acquires a velocity at the end of the motion in operation and release. It hits the face of the magnet at the end of the 'operate motion' and backstop at the end of the release motion. The impact produces a vibration in the relay structure and a reversal of motion or rebound in both the cases; this rebound is prominent in the later one. The amount of movement in the backward direction depends upon the velocity with which the armature hits. Armature rebound causes malfunction of the contacts as mentioned earlier. The magnitude of the reverse velocity depends on the co-efficient of restitution as well.

Effect of armature impact:

Armature impact causes contact chatter which has already been

mentioned. Besides this, the impact produces shock through the whole relay structure which becomes ultimately weak. Continuous impact with a high velocity might change the residual air gap making wear on the pole face or changing the thickness of the non-magnetic stop. Other major wear problems are present, which are associated with the armature hinge point and the insulating supports on which the contact springs are propped. Wear in the first case causes the change of reluctance of the magnetic circuit and the same in the second case, changes the contact spacing. These are harmful and undesirable.

9.6 Elimination or reduction of contact bounce and of armature rebound.

As it has already been discussed in sections 9.4 and 9.5 that contact bounce and armature rebound are harmful to the switching systems, it is therefore necessary to eliminate or at least reduce them. Different mechanical parts in a relay are liable to vibration which may be eliminated or reduced by giving some mechanical considerations. The contact spring vibration may be avoided by giving sufficient contact force which is all the time greater than the force variation in vibration. Similarly armature rebound may be completely avoided by supplying sufficiont back tension and travel. Now all these methods would affect the 'operate time', power requirements and relay load and may not be advantageous in many applications. There are other mechanical considerations to be given to minimise contact

chatter and armature rebound. The small mechanical impedance of the springs will decrease the force variations and small armature mass will reduce the rebound. Dissipation of kinetic energy is also a means in general of reducing contact bounce and armature rebound. This dissipation can be affected by two methods, one of which is the damping of the motion and the other one is the diversion of the kinetic energy to the ineffective modes of motion. Of course, the achievement of adequate damping for this purpose in a relay is difficult and more attentions may therefore be given to the other method.

Apart from the mechanical consideration, it remains to be seen, what other considerations may be given to reduce these two serious defects in a relay. Coming to the case of contact bounce, it may be concluded that the high velocity of the moving contact and of the armature is the primary factor. Regarding armature rebound, surplus kinetic energy is the main factor to be considered, and this kinetic energy is proportional to the square of the velocity and to the first power of the mass. Therefore, armature rebound may be controlled more by controlling velocity rather than reducing mass.

From the preceding discussion, it appears that the control of velocity is of great significance in reducing contact bounce and armature rebound.

The velocity depends on the electrical and mechanical parameters which are related to it in the velocity formula. The formula would

be of help to give electrical and mechanical considerations for reducing speed. Before going to the considerations on the control of velocity it may be desirable to present a short discussion on the elimination of armature oscillations due to the discontinuous changes of spring load. These oscillations also give rise to contact bounce as mentioned in sec. 9.4.

It has been seen that in modern relays the armature oscillations do not get damped easily because of less frictional damping in the system. An easy method of avoiding this kind of oscillations is to keep the armature in contact with the contact springs at rest.

9.7 Control of velocity

The velocity formula for the operation is given in eq. 7.33 which may be rewritten in the following as eq.(9.1).

$$V_o = \frac{2}{Gp} \frac{M_s - M}{M} \frac{\alpha s}{\frac{1}{2\delta p} + s - \alpha} \qquad (9.1)$$

From the formula it is easily realised that the velocity decreases when G is increased. G can be increased by reducing the coil circuit resistance. Increase of G affects the speed during the entire motion and the total time of operation increases.

When the last contact operates, the switching action is completed. An additional load may be included in the rest of the travel and this load should start at a zero value. α may be expected to decrease due to the additional load and the final velocity will decrease if s does not change significantly.

The velocity with which one contact strikes another depends on lever arm ratio between the load and pull. By changing this ratio both the contact velocity and the final velocity of the armature may be reduced. The latter velocity decreases because of less travel which may be affected by the increase of the lever arm ratio.

The final velocity of the armature and the speed during the entire motion may be changed by changing the leakage reluctance of the magnetic circuit. The velocity formula may be written in the form:

$$V_o = \frac{2}{G} \cdot \frac{M_s - M}{M} \cdot \frac{a\,s}{\frac{1}{2\delta} + sp - ap} \qquad (9.2)$$

If for a section of the travel $s > a$ then the velocity diminishes when the leakage permeance p increases or the leakage reluctance decreases.

If $s < a$ then the velocity increases for the same condition.

In equation (9.2) δ is $\frac{1}{\mu_o A}$, where A is the pole face area. Increase of the pole face area diminishes the speed during operation.

It will be of great significance to consider the retardation condition from the acceleration formula in the control of velocity. The acceleration expression may be rewritten here as eq.(9.3).

$$f_o = \frac{2}{G^2 p^2} \frac{M_s - M}{M} \frac{a\,s}{(\frac{1}{2\delta p} + s - a)^2} \left(a + \frac{M_s - 2M}{M} \cdot s \right.$$

$$\left. + 3 \frac{M_s - M}{M} \frac{a\,s}{\frac{1}{2\delta p} + s - a} \right) \qquad (9.3)$$

As already mentioned for any load point on the dynamic load curve $\frac{1}{2\delta p} + s - a$ is always positive for a stable motion. Therefore the condition for retardation which is apparent from the acceleration formula is given by:

$$a + \frac{M_s - 2M}{M} s + 3\frac{M_s - M}{M} \frac{a s}{\frac{1}{2\delta p} + s - a} < 0$$

Therefore, $\frac{M_s - 2M}{M} s$ should be a negative quantity to retard the motion.

The eddy current has an influence on the velocity. As G in (9.1) is $G_c + G_e$, increase of G_e or the eddy current conductance diminishes the speed of the armature.

9.8 Reed relays

These are electromagnetic relays which are different from the conventional ones and have no distinct core, armature and contact carrying springs. But all the functions of the core, armature and contact spring of a conventional relay are served by the two reeds. A reed relay consisting of a coil and two reeds may , therefore, be treated like an ordinary electromagnetic relay considering all its special features. Among reed relays there are both neutral and permanent magnet biased relays. Ellwood originated the reed switch in the Bell Telephone Laboratories and carried out its early development. The magnetic circuit of a reed relay with an air return path may be treated like a leaky electrical transmission line. The mathematical treatment for this is given by Peek.[44] A simpler case

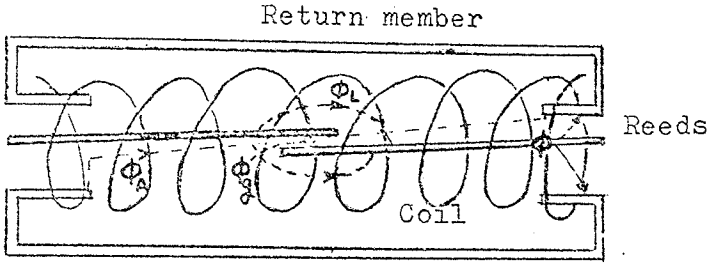

(a)

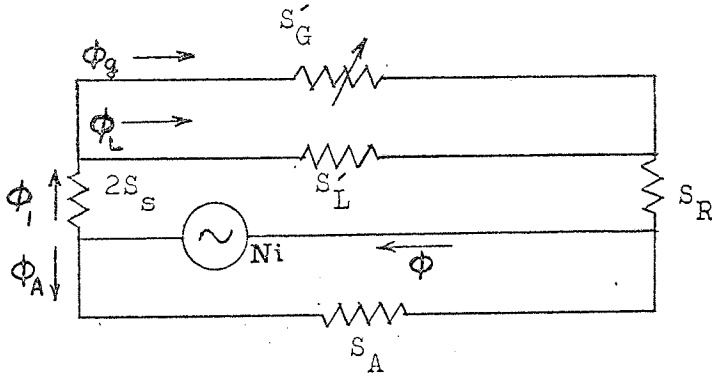

(b)

Fig. 9.1

with a magnetic return path which is tightly coupled may be considered, and the field relations may be represented by a magnetic circuit with lumped parameters. This kind of representation is also possible in the relay with an air return path.

Fig. 9.1 shows the structural schematic of a reed relay with a return member at the top. The magnetic circuit for this is as shown below in the same figure. S_R is the reed reluctance and $2\,S_s$ is the sleeve gap reluctance. The gap reluctance for the working air gap is S_G' whereas, S_L' is the leakage reluctance for the flux ϕ_L. The coil magnetomotive force develops an air flux ϕ_A which is shown in the magnetic circuit in the branch containing the reluctance S_A.

Analysis of the dynamic performance

The magnetic circuit in fig. 9.1 may be replaced by the one in fig. 9.2a. The condition of equivalence is similar as in the

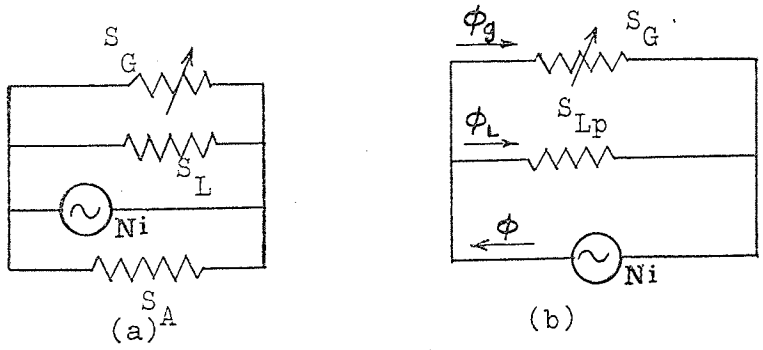

Fig. 9.2

case of the design and equivalent magnetic circuits discussed in sec.10.5 The equivalence will hold if the reed reluctance S_R remains

constant. But the reeds get easily saturated and S_R varies. Knowing fully well about the approximate nature, S_R may be taken a constant quantity assuming a linear magnetisation. The circuit in fig. 9.2(a) may be replaced by the one in fig. 9.2(b). S_{LP} is equal to the parallel combination of S_A and S_L. Estimation of the circuit constants in fig. 9.1 is discussed in the paper by Peek.[44] Pull relations are also discussed in the same paper.

The magnetic circuit in fig. 9.2(b) is similar to the equivalent magnetic circuit in sec. 10.5 , which has two parallel branches. It is easy to establish a relation between ϕ and ϕ_g from the present magnetic circuit of a reed relay. When this relation is established Ahlberg's Theory[5] or the method of analysis presented in secs. 7.3, 7.4 and 7.5 may be applied in a similar way as in the case of an ordinary relay. When Ahlberg's Theory is applied only load and pull is considered and the stiffness of the reeds gives the load characteristic from which the time of operation, velocity and acceleration may be calculated. In calculating the velocity and acceleration the pull characteristics are needed.

In development studies, models can be made for study and measurement, based on the initial estimation. Pull and load measurements, and the measurements needed to analyse the dynamic performance as described in sec. 7.3 may be made. Analysis of the measurements by using Ahlberg's Theory would serve as a guide in further work in the reed relay development.

Chapter 10

THE MAGNETIC CIRCUIT

10.1 Introduction

The relations between the stored energy of the magnetic field and the magnetising current and the position of the armature are used in determining both the static and dynamic characteristics of electromagnetic relays. These relations may be expressed in terms of the magnetic circuit, which is discussed in the present chapter. It is shown that the low density magnetisation relations may be treated in terms of an equivalent magnetic circuit with lumped parameters, which is known as the "equivalent" circuit used in the study of the dynamic behaviour presented in the previous chapters. The determination of the constants of the equivalent circuit is given in chapter 11 along with the results of magnetisation and pull measurements.

10.2 The static field pattern

A current in a relay coil gives rise to a magnetic field, the distribution of which is quite complicated in and around the relay. In addition to the main flux which passes from the core to the main air gap, armature, another small air gap, a yoke, the heel piece and back to the core, there are leakage fluxes in the air between different parts of the relay. The main flux path is identified by the nearly closed iron path of the electro-magnet. Because of the large difference between the values of the absolute permeability for iron and air, the leakage flux in

the air always leaves the iron in a nearly perpendicular direction.

It helps to determine the field pattern from the nearly closed iron path as indicated above. Leakage fluxes in different parts may partly be identified by putting iron filings or placing a small compass needle. Hall probe can detect the leakage flux in the air between core and yoke, indicating the magnitude of the flux as well. It was observed by means of a hall probe that the leakage flux varies along the length of the core and at one point it is zero. From this point the direction of the flux changes.

The flux paths in a relay are shown in figure 10.1. The working air gap flux in between the armature and the pole face gives rise to a magnetic pull causing movement of the armature. Now it may appear surprising that this flux does not depend very much on leakage condition. It is similar to a parallel combination of resistances connected across a battery with small internal resistance in which the change of resistance in one branch affects the current in the other branch negligibly. In static condition the magnetic pull is of great interest. For determining static properties such as the static pull relations, ampere turn sensitivity and work capacity the pull is needed to be known.

The main flux in the core varies in magnitude due to distributed leakage flux. It should be mentioned here that the increase of leakage flux slightly diminishes the main air gap

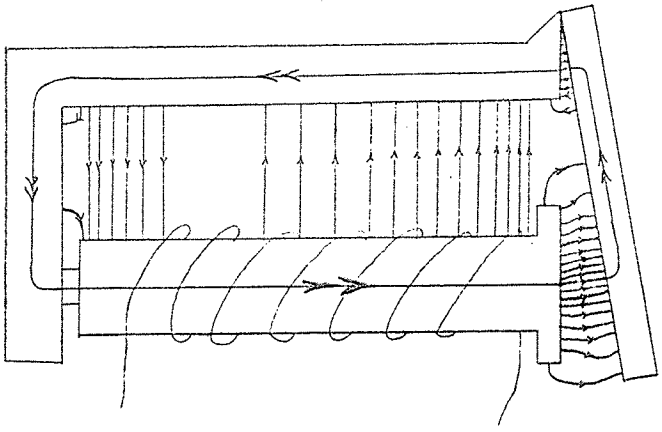

Fig. 10.1 Flux paths in a relay

flux but the maximum core flux at a particular point in the core increases considerably. The increase of core flux does not affect the static performance very much if saturation in the core does not occur, but has a great influence on the dynamic performance. If the electrical and mechanical conditions are non-stationary, the core flux gives rise to a back e.m.f. which has influence on the magnetising current. The back e.m.f. is caused by the change of the core flux due to the variation of magnetising current with time and due to the motion of the armature. The induced e.m.f. during dynamic operation controls the current in the relay coil and, therefore, has a great influence on the motion of the armature. As part of the induced e.m.f. is also caused by the variation of the leakage flux during dynamic condition, obviously the leakage has also a great influence on the motion. These influences were analysed in the previous chapters on the analysis of dynamic performance, assuming the static and dynamic field patterns to be the same.

10.3 The concept of a magnetic circuit

The three relations which should be satisfied simultaneously in a magnetic field, may be expressed mathematically as:

$$\mathcal{B} = \mu \mathcal{H} = \mu_o \mu_r \mathcal{H} \qquad (10.1)$$

$$\int_S \mathcal{B}.ds = 0 \qquad (10.2)$$

$$\oint \mathcal{H}.dl = i \qquad (10.3)$$

Where $\mathcal{H}$ and $\mathcal{B}$ are the field - intensity and flux density

vectors, and ds denotes an infinitesimal surface. The equations (10.1),(10.2) and (10.3) are all in rationalised MKS units. The field relations are usually expressed in equivalent differential form for analytical purposes and may be written in the form

$$\nabla \times \mathcal{H} = j \qquad (10.4)$$

$$\nabla . \mathcal{B} = o \qquad (10.5)$$

where j is the current density vector. Equations(10.4) and (10.5) apply at all points in the field.

It is difficult to deal with the three dimensional field problem which can be reduced with good approximation for analysis to a one dimensional problem of the magnetic circuit, whose concept simplifies the matter tremendously. This magnetic circuit may be employed to solve the field problem of the electromagnetic relay and is useful in the study of the static and dynamic behaviour.

The magnetic circuit is similar to the electrical circuit and ohm's law and kirchlof's law of the later are applicable to the former as well. The analogies between electric and magnetic circuits are quite well known. A magnetic circuit with lumped parameters is similar to an electrical network and offers the advantages of simplicity and generality in analysis.

10.4 The magnetic circuit of electromagnetic relays

A detail analysis of the magnetic circuit of electromagnetic relays is given in a paper by Ekelöf.[12] He treats the magnetic circuit like a transmission line with distributed constants. The transmission line analogy may be explained briefly.

A steady-state condition is assumed, which means the magnetising current is steady in the coil and the armature is at rest. The core and yoke together form a uniform "magnetic transmission line", carrying the main flux $\phi(x)$ as shown in fig. 10.2. The yoke serves as a return member in the trans-

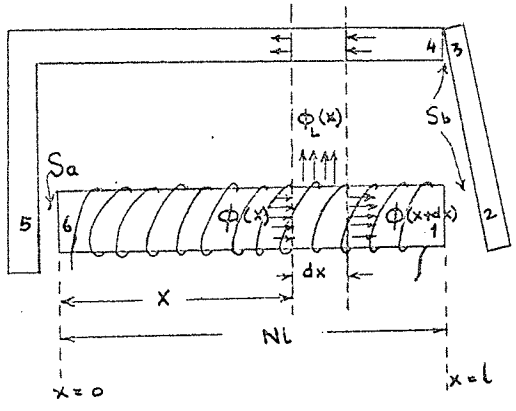

Fig. 10.2 The magnetic circuit of a relay

mission system. The leakage flux $\phi_L(x)$ from the core to the yoke passes perpendicularly between the two members and is assumed to be existing all along the length of the core. This leakage flux is like the leakage current in an electrical transmission line. An infinetesimal length dx of the "magnetic transmission line" with the distribution of core flux and leakage flux in it is shown in fig. 10.2.

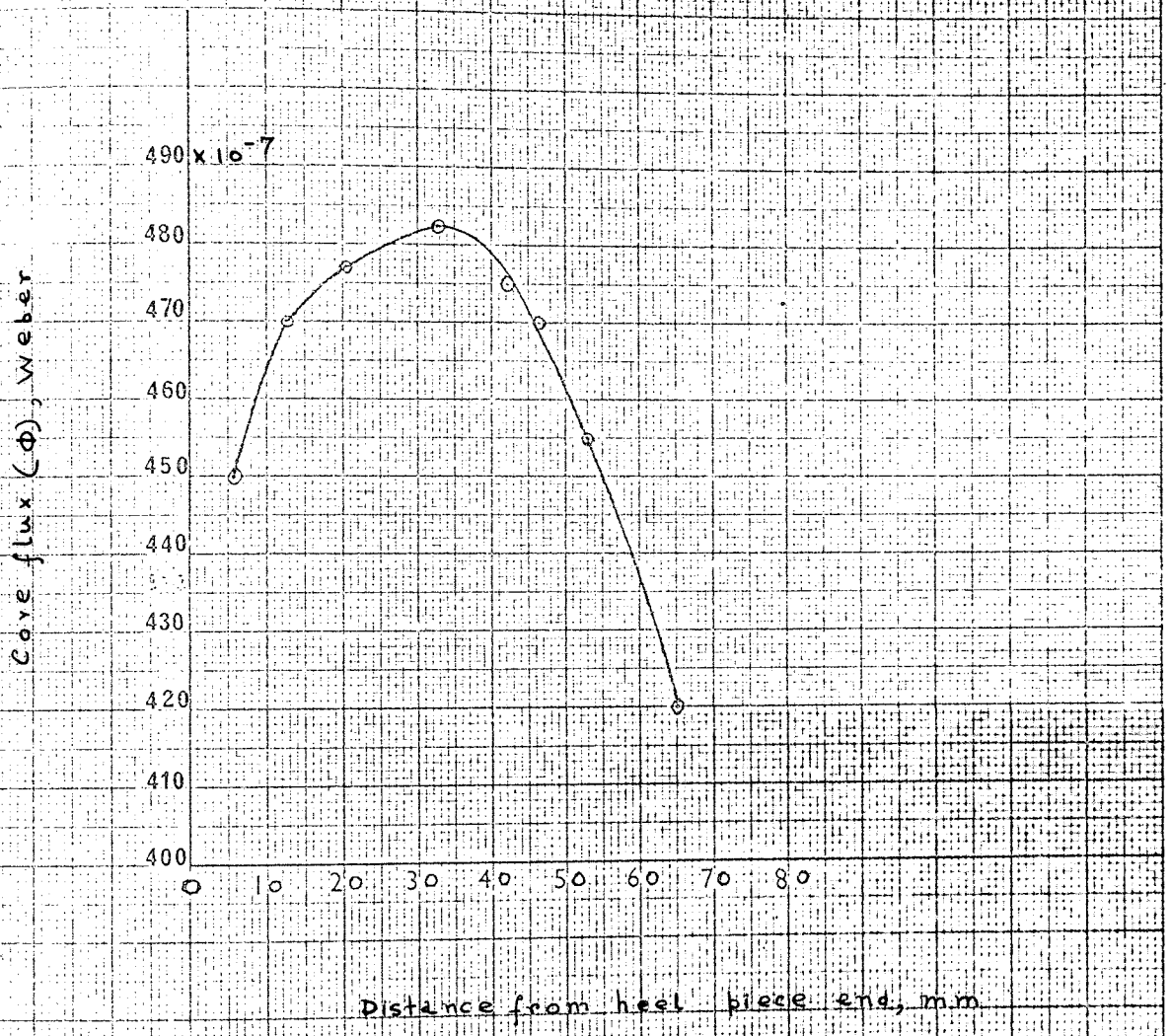
490 x 10⁻⁷
480
470
460
450
440
430
420
410
400
Core flux (Φ), Weber
0
10
20
30
40
50
60
70
80
Distance from heel piece end, m.m.

Fig 10.3

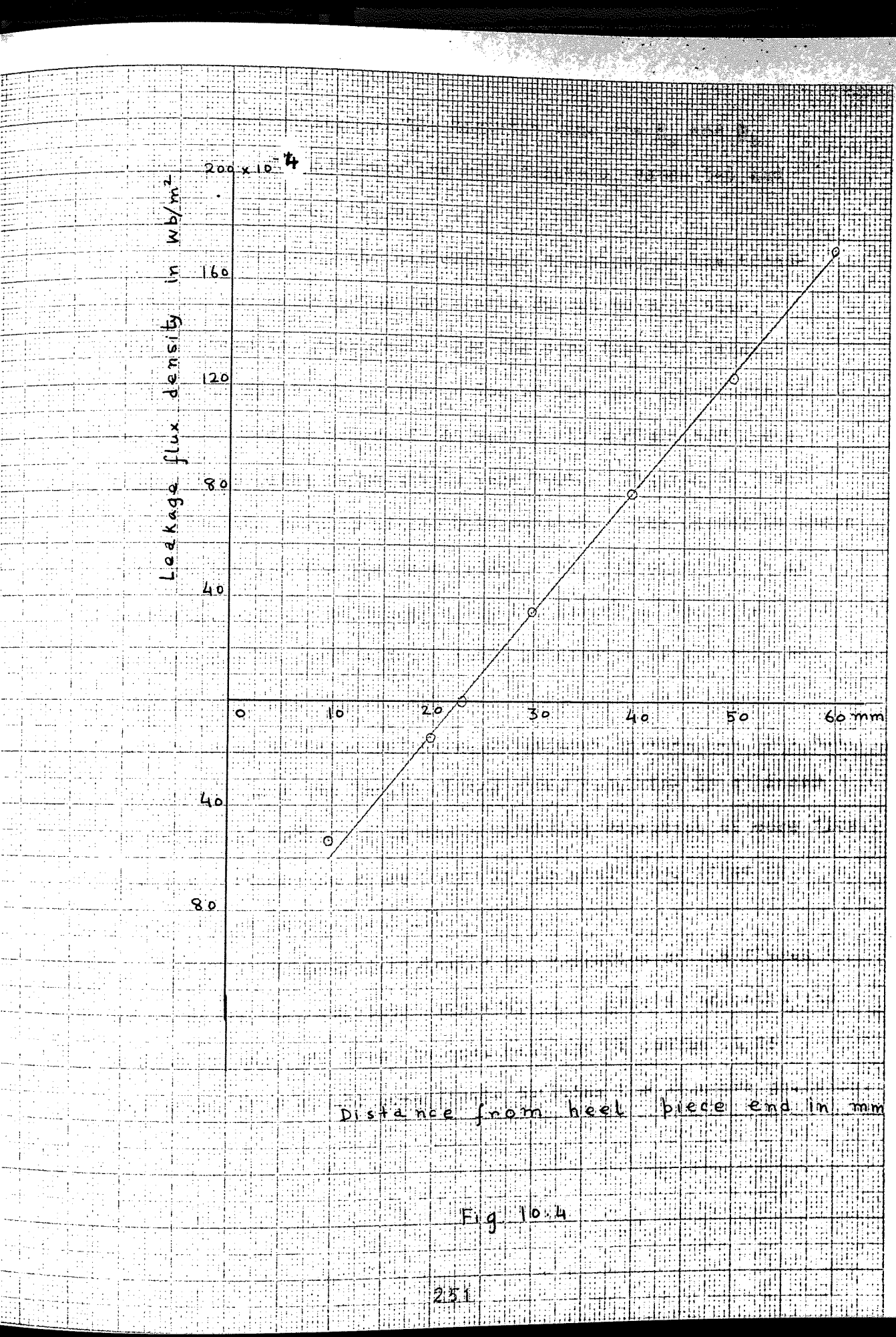
Leakage flux density in Wb/m²
200 x 10⁻⁴
160
120
80
40
0
10
20
30
40
50
60 mm
40
80
Distance from heel piece end in mm

Fig 10.4

The terminations of the magnetic line are $\mathcal{S}_a$ and $\mathcal{S}_b$ representing respectively the reluctances of paths 5-6 and 1-2-3-4 in the same figure.

After deriving the differential equations to the transmission line considering the length dx and solving them, Ekelöf gives the expressions for the core flux and leakage flux at an arbitrary cross-section of the core (equations 16 and 17). Measurements of ϕ and ϕ_L by a fluxmeter and a hall effect probe respectively were made. Figures 10.3 and 10.4 show the results of the measurements. The curves in these figures are not for the same relay. The variation of ϕ is parabolic and ϕ_L is linear along the length of the core. If the leakage is small and the total reluctance of the core and yoke is also not significant, then there would be a linear variation of magnetic potential difference between the core and the yoke, along the length of the core, resulting in a linear variation of leakage flux and a parabolic variation of core flux. These variations in x are shown in the analytical forms by Ekelof (equations 27 and 28).

Fig. 10.5 shows graphically the variation of the fluxes as given by the analytical expressions. Here x indicates the length of the core from the heel end, and of course it is different from x, the co-ordinate defining the armature position.

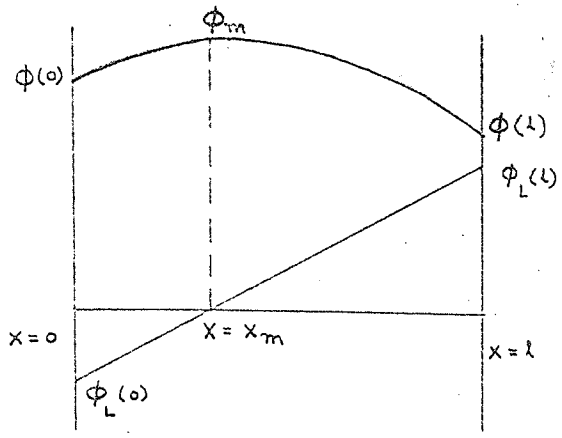

Fig.10.5 Variation of the core and leakage fluxes

In figure 10.5 the core flux is maximum at $x = x_m$ and varies parabolically with x, whereas the leakage flux vanishes at $x = x_m$ and varies linearly with x from a negative minimum value $\phi_L(o)$ to a positive maximum value $\phi_L(1)$.

Analytical expressions for the magnetic circuit can be developed in terms of the transmission line analogy as shown by Ekelöf. When approximate solutions to the transmission line equations is obtained instead of a rigorous one, a useful picture of the flux distribution is found, which is shown in fig. 10.5. The distribution of flux suggests the use of magnetic circuits with lumped parameters and the schematic representation of the magnetic circuit with lumped parameters giving finally the "equivalent" and "design" circuits are described in the following section.

10.5 The equivalent and design magnetic circuits.

The analysis of the magnetic circuit by transmission line analogy, suggests a point in the core where the flux is maximum and the leakage flux is zero. If all the mmf is thought to be concentrated at the point, then the transmission line with distributed constants may be replaced by the magnetic circuit of fig. (10.6a) which gives an equivalent expression for (ϕ_{av}) the average core flux as may be derived after assuming negligible core reluctance in the "magnetic transmission line". An expression for ϕ_{av} after making the assumption is shown in section 9.2 of Peek and Wager (eq. 9.9). S_b represents the reluctance of the combination of the main gap, heel gap and armature, whereas, S_a represents the reluctance of the heel end of the magnet. S_{La} and S_{Lb} in combination account for the leakage between the core and yoke. When the core reluctance ($S_c = S_{c2}$) is added to the circuit in fig.10.6a, another circuit results, which is shown in fig.10.6b. In this later circuit a yoke reluctance term (S_y) which is included in the core reluctance term in the transmission line analysis is also added. It may be seen that this circuit is approximately identical to that of fig. 10.7, which is

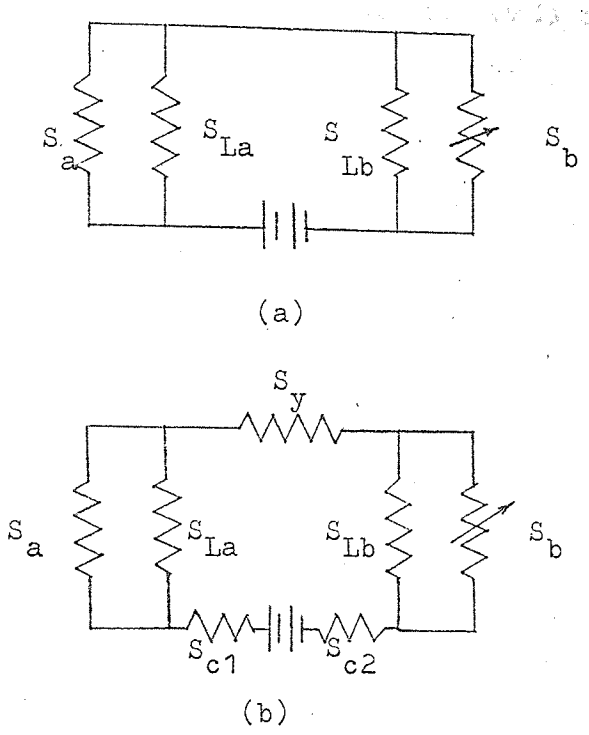

Fig. 10.6 Magnetic circuits with lumped parameters

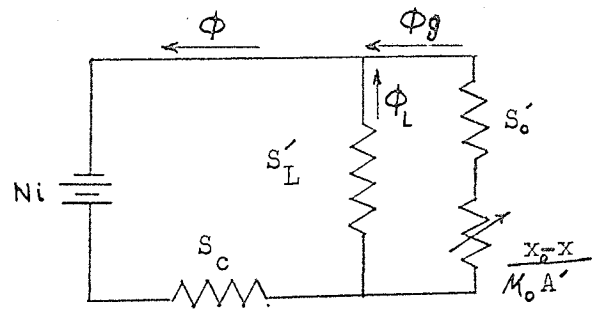

Fig. 10.7 Design Magnetic circuit

a series parallel circuit. This circuit is called the design magnetic circuit which is usually assumed in estimating the circuits constants from the design dimensions. S_c is the core reluctance, S_o' is the closed gap reluctance for the working air-gap flux ϕ_g, which takes into account the fixed portions of S_a and S_b such as the reluctance of the return path, joint, and residual air-gaps. S_g' represents the variable part of S_b caused by the motion of the armature. S_L' is the leakage reluctance which is fixed and takes into account the combined effect of the leakage due to S_{La} and S_{Lb}, and fringing across the air gaps. ϕ is the total flux linked by the coil and ϕ_L is the leakage flux.

Fig. 10.6 shows the magnet structure in the simple hinged armature relay. S_o' is given by :

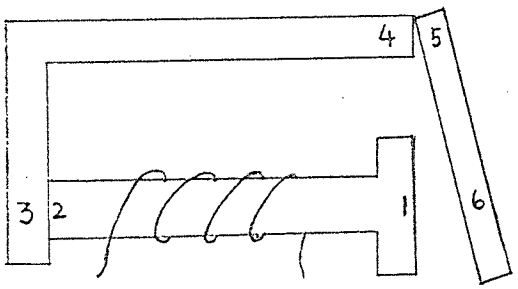

Fig.10.8 Magnet structure in a relay.

$$S_o' = S'_{2-3} + S'_{3-4} + S'_{5-6} + S'_{go} + S'_h$$

where S'_{2-3}, S'_{3-4} and S'_{5-6} are the reluctances of the component parts of the magnet structure as indicated by the numbers, and S'_{go} and S'_h are the reluctances of the main air gap and heel air gap

respectively when the armature is operated. There is a nonmagnetic separator in between the armature and the pole face, and a residual air gap remains when the armature is in 'closed gap' position. S'_{go} and S'_h are given by:

$$S'_{go} = \frac{x_{go}}{\mu_o A'}$$

and $$S'_h = \frac{x_h}{\mu_o a_h}$$

where x_{go} and x_h are the gap separations and A' and a_h are the mating areas of the two surfaces at the main gap and heel gap respectively. A' is obviously the pole face area of the electromagnet.

The magnetic circuit in fig. 10.7 is generally employed to describe the magnetisation relations in the simple electromagnets in the low density and high density regions provided the core is the only member where saturation occurs in the high density case. In the low density region for which the magnetisation is linear, the field relations may be derived by using an equivalent magnetic circuit which is shown in fig. 10.9 The flux expressions will then contain the constants of this circuit. The equivalent magnetic circuit is algebraically equivalent to the "design" circuit and the constants of the two circuits may be related to each other to fulfil this condition. After estimating the constants of the design magnetic

circuit from the dimensions of the magnet., the equivalent magnetic circuit constants can be evaluated from the "design" values. The advantage of using this circuit is that the flux

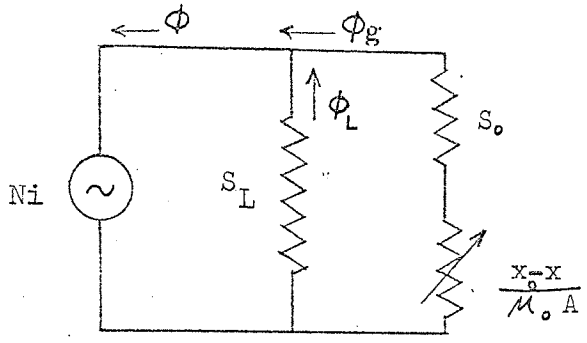

Fig. 10.9 Equivalent magnetic circuit.

expressions may be derived in simpler terms and thus makes it easy to describe the various performances of electromagnetic relays. A full description of the equivalent magnetic circuit is given in a paper by Peek.[64] A similar description is also given in section 3.2 of Peek and Wagar.

As already mentioned, both the "design" and "equivalent" circuits represent the field relations satisfactorily when the magnitisation is linear. Now these two circuits are equivalent if they give the same flux vs. mmf relation for all values of x, the co-ordinate defining the armature position. Therefore, to make the two circuits equivalent the reluctances of these should be such that the expressions for the total reluctance S are identical for all values of x.

The total reluctance S of the equivalent magnetic circuit is given by:

$$S = \frac{S_L \left(S_o + \frac{x_o - x}{\mu_o A}\right)}{S_L + S_o + \frac{x_o - x}{\mu_o A}} \qquad (10.6)$$

$$\text{or} \quad S = S_L - \frac{\mu_o A S_L^2}{\mu_o A (S_L + S_o) + x} \qquad (10.6a)$$

The total reluctance S of the design magnetic circuit is given by:

$$S = S_c + \frac{S_L' \left(S_o' + \frac{x_o - x}{\mu_o A'}\right)}{S_L' + S_o' + \frac{x_o - x}{\mu_o A'}} \qquad (10.7)$$

$$\text{or,} \quad S = S_c + S_L' - \frac{\mu_o A' (S_L')^2}{\mu_o A' (S_L' + S_o') + x} \qquad (10.7a)$$

Now the equivalent and design magnetic circuits have the same ϕ vs. Ni relation if both the expressions (10.6a) and (10.7a) are identical, and this is so when the following conditions are satisfied:

$$\begin{aligned} S_L &= S_c + S_L' \\ \mu_o A S_L^2 &= \mu_o A' (S_L')^2 \\ \mu_o A (S_L + S_o) &= \mu_o A' (S_L' + S_o') \end{aligned} \qquad (10.8)$$

From relations (10.8) the following equations may be established:

$$S_L = S_c + S_L'$$

$$\mu_o A = \mu_o \frac{A'}{\sigma 2} \qquad (10.9)$$

$$S_o = \sigma^2 . S_o' + \sigma . S_c$$

$$\sigma = 1 + S_c / S_L'$$

Now using equations (10.9) the constants of the equivalent circuit may be evaluated from the "design" circuit.

The constant of the "equivalent" circuit may be determined from the magnetisation and pull measurements. These constants for a telephone type electromagnetic relay were determined by the flux measurements using a flux-meter and the details of this measurement is given in section 11.3

The equivalent magnetic circuit may be used in the analysis of dynamic performance assuming the static and dynamic field patterns to be the same. The total reluctance S for the circuit is given by eq. 10.6 and the total flux ϕ linked by the coil may be obtained by dividing the magnetomotive force M (= Ni) by S. Thus,

$$\phi = \frac{M}{S} = \frac{Ni}{S} \qquad (10.10)$$

$$\text{or} \quad \phi = \frac{Ni}{\dfrac{S_L \left(S_o + \dfrac{x_o - x}{\mu_o A} \right)}{S_L + S_o + \dfrac{x_o - x}{\mu_o A}}} \qquad (10.11)$$

The working air-gap flux ϕ_g may be expressed in terms of the same circuit as follows:

$$M = Ni = \phi_g \left(S_o + \frac{x_o - x}{\mu_o A}\right) = \phi_L S_L \qquad (10.12)$$

where ϕ_L is the total leakage flux. From equations (10.12)

$$\phi_g = \frac{Ni}{S_o + \frac{x_o - x}{\mu_o A}} \qquad (10.13)$$

$$\phi_L = \frac{Ni}{S_L} \qquad (10.14)$$

ϕ is, of course, $\phi_g + \phi_L$. ϕ and ϕ_g are given by the equation:

$$\phi_g \left(S_o + \frac{x_o - x}{\mu_o A}\right) = \phi \left(\frac{S_L \left(S_o + \frac{x_o - x}{\mu_o A}\right)}{S_L + S_o + \frac{x_o - x}{\mu_o A}}\right)$$

$$\therefore \quad \phi_g = \phi \cdot \frac{S_L}{S_L + S_o + \frac{x_o - x}{\mu_o A}} \qquad (10.15)$$

10.6 The case of armature saturation

Saturation normally occurs in the core and the design magnetic circuit is sufficient for the schematic representation. This magnetic circuit can take into account the variable core reluctance, which is given by:

$$S_c' = S_c \frac{\phi'' - \phi'}{\phi'' - \phi} \qquad (10.16)$$

Where S_c is the constant reluctance in the low density region, (10.17)
S_c' is the reluctance when $\phi > \phi'$, and ϕ'' is the saturation flux. ϕ' is the upper limit of linear magnetisation and corresponds to the maximum absolute permeability μ which is used in describing the low density field relations. The expression in eq.(10.16) is derived by making the hyperbolic approximation to the magnetisation curve, which permits the use of the well known Froehlich-Kennely equation. When the core reluctance is constant in the low density region the design magnetic circuit may be replaced by the "equivalent" circuit to give the same ϕ vs. M relation and the conditions of equivalence are given in equations (10.9).

If saturation occurs first in the armature, the magnetic circuit in fig. 10.10 is required for the schematic representation.

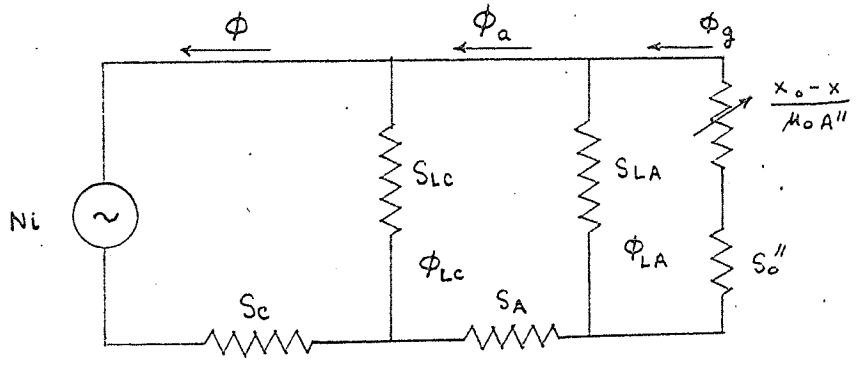

Fig. 10.10 Design magnetic circuit - armature saturation

The core reluctance S_c may be taken constant even when saturation starts in the core itself provided the term S_A is dominant. Now S_A varies with ϕ_a and may be given by:

$$S_A = S_A'' \frac{\phi_a''}{\phi_a'' - \phi_a} = S_A' \frac{\phi_a'' - \phi_a'}{\phi_a'' - \phi_a} \qquad (10.17)$$

for $\phi_a > \phi_a'$, while $S_A = S_A'$ for $\phi < \phi_a'$.

Here S_A' is the minimum value of the armature reluctance and ϕ_a' is the flux corresponding to the upper limit of linear magnetisation.

If the magnetic circuit in fig. 10.10 is taken for the representation of the field relation in the low density region, terms are constants except for the gap reluctance, which varies linearly with x. Therefore the equivalent magnetic circuit and the design magnetic circuit in fig. 10.10 may be shown equivalent for the linear magnetisation. In case of armature saturation the magnetic circuit in fig. 10.10 will apply. It is already mentioned that the design magnetic circuit in fig. 10.7 applies in case of core saturation. In low density region, however, the two magnetic circuits just mentioned may be shown to be equivalent to the equivalent magnetic circuit and this immediately suggests that "equivalent" circuit is applicable in all cases.

The dynamic performance was explained assuming the linear magnetisation. The static and dynamic performances must be explained by using the magnetic circuit in fig. 10.10 for armature saturation case and the circuit in fig. 10.7 for core saturation case; and in each case, the corresponding armature and core reluctances are to be evaluated by using the hyperbolic approximation to the magnetisation curves of the material.

10.7 Energy in the magnetic field

When a magnetic field is established in a region, energy is delivered to the same from the source. This energy remains as a stored one and comes back to the original system when the field is removed. This process is completely reversible in vacuum. But for a region which contains a magnetic material that exhibits hysteresis phenomena the energy cannot be fully recovered. This is the same for even a relay with a locked armature.

Expressions for the field energy U per unit volume of a medium can be derived easily. The well known expressions may be writted as:

$$U = \frac{B^2}{2\mu} = \frac{B\,H}{2} \qquad (10.18)$$

where B is the flux density and H is the field intensity. The most significant fact is that the mechanical work is available from the field energy which exists in an air gap. This is very true in case of an electromagnetic relay which utilises this mechanical output to do work against the contact springs for switching purposes.

When a steady current flows in the coil of a relay a field is established in the working air-gap and the magnetic pull developed acts on the armature and pole face, both of which in effect attract each other. In the static condition the magnitude of this force depends on various parameters and this is shown in the following section. In the dynamic condition the same pull relation may be

used assuming the static and dynamic field patterns to be the same, but the variation of the pull with time is very complicated and is a subject matter of relay dynamics, which was discussed in detail in the previous chapters.

The stored energy in the magnetic field and its variation with coil current and armature position determine primarily the static and dynamic performances. The establishment of some more relations will make it clear how stored energy is influenced by different paramters. Referring to the magnetisation curves in fig. 10.11 an alternative expression for U may be written as

$$U = \int_0^{\phi} Ni \cdot d\phi. \qquad (10.19)$$

Where N is the number of turns of the coil, i is the current in it and ϕ is the total flux linked by it. The two curves are for two air gaps x_{g1} and x_{g2} respectively. For the linear magnetisation the total reluctance S is a function of x only and may be given by:

$$S = \frac{Ni}{\phi}$$

Now, integration of (10.19) gives:

$$U = \frac{(Ni)^2}{2\,S}$$

Putting $S\phi$ for Ni in the preceding expression the other expressions for U may be derived, which are given by:

$$U = \frac{S\,\phi^2}{2} \qquad (10.20)$$

From (10.20) $$U = \frac{Ni\,\phi}{2} \qquad (10.21)$$

The two mangentisation curves in fig. 10.11 are plotted from actual measurements on a relay for two air gaps.

Measured values of the flux corresponding to the different values of ampere turns are given in Table 10.1.

TABLE 10.1 Measured fluxes for two fixed air gaps.

xg mm	.177		.632	
	Ni At	ϕ x10^{-7} Weber	Ni At	ϕ 10^{-7} x Weber
	22.25	84.1	22.0	56.82
	42.5	218.18	41.25	131.81
	62.75	339.39	60.0	207.57
	82.5	446.96	82.5	300.0
	121.75	613.63	111.5	416.66
	133.5	651.50	150.5	537.87
	150	704.5	230.0	742.42
	194.5	787.8	300.0	850.0
	227.5	848.4	352.5	909.0
	275.5	901.50	400.0	946.0
	340.0	954.50	435.0	969.6
	365.0	969.60	501	1000.0
	425.0	997.0		
	507.5	1030.30		

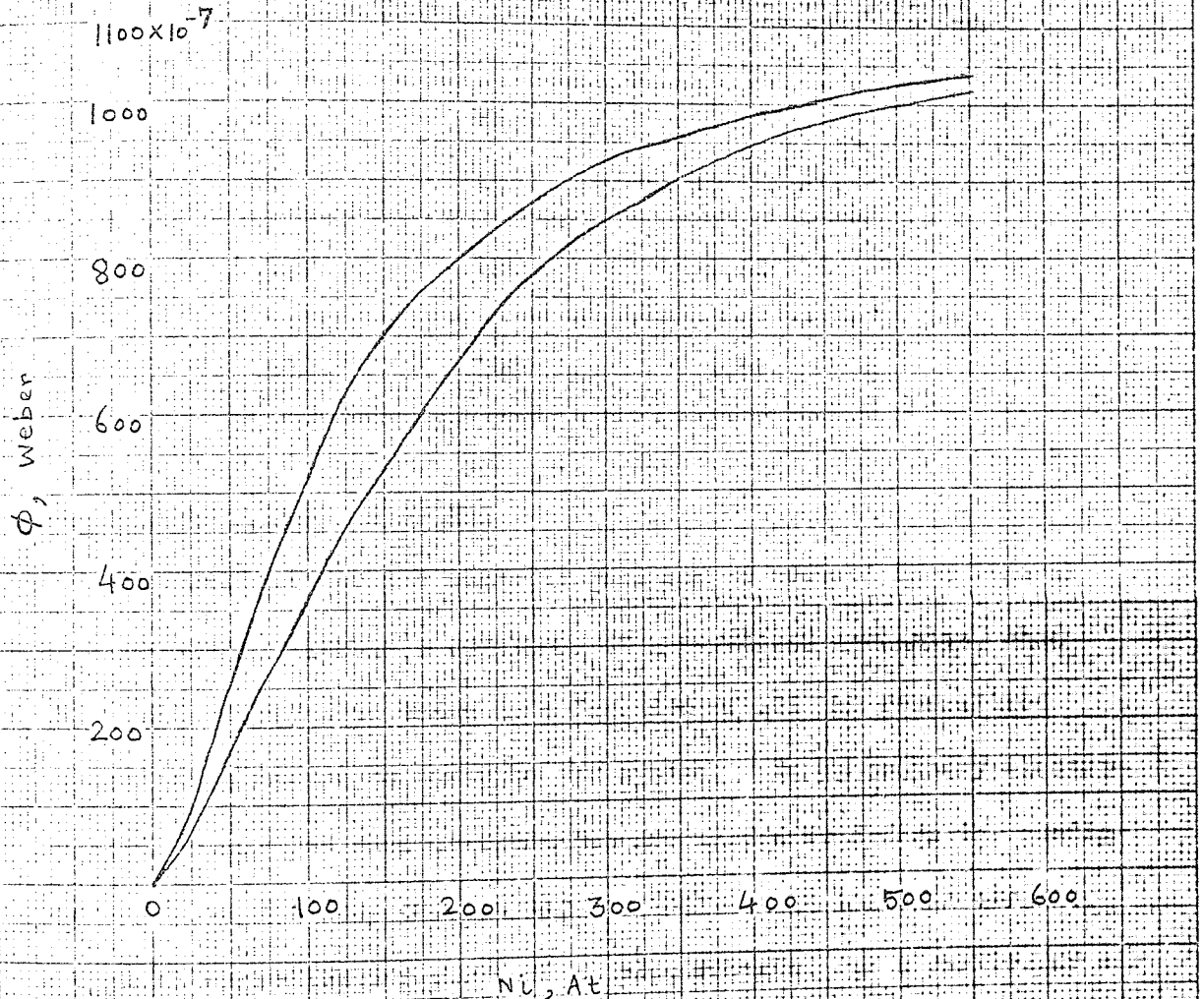
1100×10⁻⁷
1000
800
600
400
200
φ, Weber
0
100
200
300
400
500
600
Ni, At

Fig 10.11

Calculated values of the field energy in the low density region for two points, one on each curve in fig. 10.11 are given in table 10.2 for interest.

TABLE 10.2 Field energy (U) for two different air gaps (x_g)

x_g mm	Ni At	U $\times 10^{-3}$ Joule
.177	100	2.60
.622	100	1.84

10.8 Magnetic pull relations

Expressions for the magnetic pull may be derived in a general form by using Lagrange's equations of generalised mechanics, when the field energy U is taken as a function of all the generalised co-ordinates needed to describe the system. In an ordinary electromagnetic relay two such co-ordinates are needed to define the configuration when the eddy current term is included in the coil circuit. A typical magnetisation curve of an electromagnet for a particular air gap x_g is shown in fig. 10.12. It is shown in sec. 10.2 of Peek and Wagar that the Lagrangian function W may be represented graphically in the figure by the area between the magnetisation curve and the

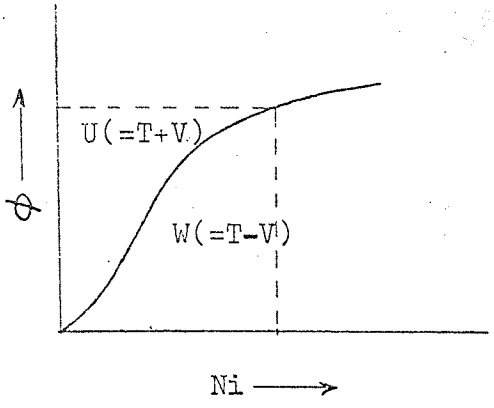

Fig. 10.12 Energy functions in magnetisation

axis of Ni.

A force expression may be derived from the mechanical equation given by Lagrange's equation which is:

$$\frac{d}{dt}\left(\frac{\delta W}{\delta \dot{q}}\right) - \frac{\delta W}{\delta q} = Q \qquad (10.22)$$

Where q and $\dot{q}$ are the generalised position and velicity respectively, and Q is the external applied force. The mechanical equation may be obtained by putting the armature position x for q and $\dot{x}$ for $\dot{q}$ in the preceding equation. This is given by:

$$\frac{d}{dt}\left(\frac{\partial W}{\partial \dot{x}}\right) - \frac{\partial W}{\partial x} = Q$$

where W is a function of i and x. Assuming W to be independent of x, this equation becomes:

$$F = -\frac{\partial W}{\partial x}\ (i, x)$$

where F is the external force which is to be applied to keep x constant or in other words the magnetic pull developed is -F.

for x constant.

Equation (10.26)becomes:

$$\frac{\partial U}{\partial x}\ (\phi,\ x) = -\frac{\partial W}{\partial x}\ (i,\ x)$$

It has already been shown that $F = \frac{\partial W}{\partial x}\ (i,\ x)$

So,

$$F = -\frac{\partial U}{\partial x}\ (\phi,\ x) \qquad (10.27)$$

Expressions (10.23) and (10.27) are the general pull expressions of an electromagnet.

When the magnetisation is linear the equivalent magnetic circuit may be used to obtain the field relation, and the field energy U may be given by the following equation as discussed in the preceding section.

$$U = \frac{Ni\,\phi}{2}$$

From equation (10.27) F is

$$F = -\frac{\partial U}{\partial x}\ (\phi \text{ constant})$$

or $$F = -\frac{\partial}{\partial x}\left(\frac{Ni\,\phi}{2}\right) = -\frac{\partial}{\partial x}\left[\tfrac{1}{2}\,Ni\,(\phi_L + \phi_g)\right]$$

$$= -\tfrac{1}{2}\frac{\partial}{\partial x}\left[(Ni\,\phi_L + Ni\,\phi_g)\right]$$

$$= -\tfrac{1}{2}\left[\frac{\delta}{\delta x}\ (Ni\,\phi_L) + \frac{\partial}{\partial x}\ (Ni\,\phi_g)\right]$$

$$= -\tfrac{1}{2}\left[\frac{\delta}{\partial x}\ (\phi_L^{\,2}\,S_L) + \frac{\partial}{\partial x}\ (\phi_g^{\,2})\ \left(S_o + \frac{x_o - x}{\mu_o\,A}\right)\right]$$

As ϕ is constant, $\frac{\partial}{\partial x}\ (\phi_L^{\,2}.\ S_L) = 0.$

So the pull F is given by:

$$F = \frac{\partial W}{\partial x} \quad (i, x) \tag{10.23}$$

Now T and V are the total kinetic and potential energies of the system. The Lagrangian function is T - V and the Hamiltonian function is T + V. The relation connecting the two functions may be given by:

$$T + V = \sum_j \dot{q}_j \; p_j - (T - V) \tag{10.24}$$

where $\dot{q}_j$ and p_j are the generalised velocity and momentum respectively, and the summation extends over all the co-ordinates. For the curve in fig. 10.3, the air gap is constant i.e., x is constant; $\sum_j \dot{q}_j \; p_j$ is, therefore, $Ni\,\phi$. The total energy U, or T + V, is given by:

$$U = Ni\,\phi - W \tag{10.25}$$

U is, therefore, represented graphically in figure 10.12 by the area between the magnetisation curve and the axis of ϕ.

The field energy U can be taken as a function, any pair of the three variables ϕ, Ni and x. Taking U and W as functions of ϕ and x, and Ni and x respectively, and differentiating (10.25) with respect to x, there is obtained:

$$\frac{\partial U}{x} + \left[\frac{\partial U}{\partial \phi} - Ni\right] \frac{d\phi}{dx} = \left[\phi - \frac{\partial W}{\partial Ni}\right] \frac{d(Ni)}{dx} - \frac{\partial W}{\partial x} \tag{10.26}$$

Both the bracketed terms are zero, because, U and W are given by

$$U = \int Ni \; d\phi$$

and $$W = \int \phi \; . \; d\,(Ni)$$

$$\therefore \quad F = -\frac{1}{2}\frac{\partial}{\partial x}\left[(\phi_g^2)\quad\left(S_o + \frac{x_o - x}{\mu_o A}\right)\right]$$

$$= -\frac{\phi_g^2}{2}\quad\frac{\partial}{\partial x}\quad\left(S_o + \frac{x_o - x}{\mu_o A}\right) = -\frac{\phi_g^2}{2} \times \left(-\frac{1}{\mu_o A}\right)$$

$$\text{or} \quad F = \frac{\phi_g^2}{2\mu_o A} \qquad (10.28)$$

The relation in (10.28) can at once be recognised as the Maxwell's law for the pull between two parallel plane surfaces of area A when ϕ_g is the flux in the gap between them. From the equivalent magnetic circuit ϕ_g is :

$$\phi_g = \left(\frac{S_L}{S_L + S_o + \frac{x_o - x}{\mu_o A}}\right) \times \phi$$

$$\therefore \quad F = \left(\frac{S_L}{S_L + S_o + \frac{x_o - x}{\mu_o A}}\right)^2 \times \frac{\phi^2}{2\mu_o A} \qquad (10.29)$$

When the design magnetic circuit of fig. 10.7 is used to represent the field relations, then expression for the pull may be derived in terms of this circuit from equation (10.27). For ϕ constant, the only term in U that varies with x is that corresponding to the gap. The energy associated with an air gap of reluctance $\frac{x_o - x}{\mu_o A'}$ is $\frac{\phi_g \Delta M}{2}$, because the potential difference ΔM is $\phi_g \cdot \frac{x_o - x}{\mu_o A'}$. So the energy is given by:

$$U_1 = \phi_g^2 \cdot \frac{x_o - x}{2\mu_o A'}$$

Now, $$F = -\frac{\partial U_1}{\partial x} \quad (\phi \text{ constant})$$

or $$F = -\frac{\partial}{\partial x}\left(\phi_g^2 \frac{x_o - x}{\mu_o A'}\right)$$

or $$F = \frac{\phi_g^2}{2 \mu_o A'} \qquad (10.30)$$

This kind of derivation is also applicable in the case of the equivalent magnetic circuit. Equation (10.30) may be written in the form:

$$F = \left(\frac{S_L'}{S_L' + S_o' + \frac{x_o - x}{\mu_o A'}}\right)^2 \cdot \frac{\phi^2}{2 \mu_o A'} \qquad (10.31)$$

At $\phi = \phi'$ when the two magnetic circuits are equivalent, the pull must be the same. It may be shown by using the transformations given in equation (10.9) that the two pull expressions (10.29) and (10.31) are identical. Hence these two expressions give the identical values of the pull for all values of the flux ϕ. Expressions (10.29) is therefore a general expression for the magnetic pull at both low and high density regions provided the core is the member in which saturation first takes place. In the dynamical analysis this pull expression is used assuming the static and dynamic field patterns to be the same.

Chapter 11

DETERMINATION OF MAGNETIC CIRCUIT CONSTANTS FROM MAGNETISATION MEASUREMENTS

PULL MEASUREMENTS.

11.1 Introduction

The constants of the equivalent magnetic circuit may be determined from the magnetisation measurements and can be compared with the estimated values from the dimensions of the magnet. The measurements and their analysis to determine the constants are presented in this chapter. Pull measurements made for different steady state ampere turns to show the variation of the pull with the length of the air gap, are also given.

11.2 Measurement of the B-H characteristic of the magnetic material

A toroid sample of swedish iron was taken. Swedish iron according to specification DTD 5092 or 5102 is a soft magnetic material and a good choice for relays. When the sample was properly annealed a magnetising winding was provided and the sample was made ready for test. A known steady current was allowed to flow in the coil. Reversing the current the change of flux was measured by means of a search coil and a 'Norma' light spot flux-meter. In flux measurements the flux meter determines the time integral of the induced voltage $d(N\phi)/dt$ giving the quantity $N\phi$, from which ϕ can be calculated. Of course, in reversing, the reading should be divided by 2.

The B-H curve for the material is shown in fig. 11.1. From this curve B-μ_r relation may be derived by using the following equation:

$$B = \mu_o \mu_r H.$$

Table 11.1 shows the calculated values of μ_r corresponding to the values of B. The μ_r vs. B curve is shown in fig. 11.2.

Table 11.1 Relative permeability corresponding to flux density

(a)		(b)	
B wb/m^2	μ_r	B wb/m^2	μ_r
.05	1194	.7	5000
.1	1809	.74	5100
.2	2745	.8	5050
.3	3512	.9	4777
.4	4218	1.0	4423
.5	4523	1.2	3153
.6	4777	1.4	1467

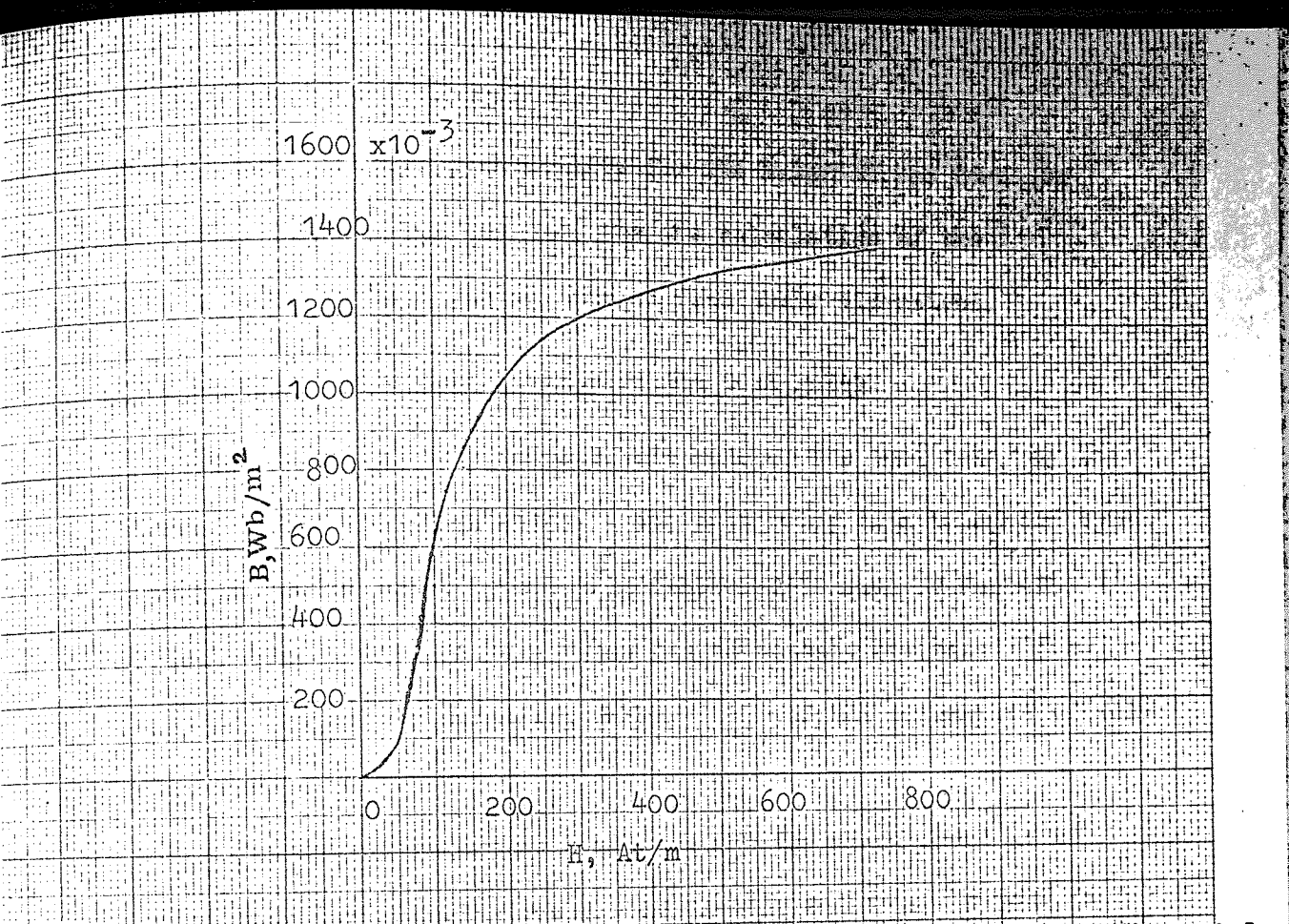

Fig. 11.1 B-H curve for the magnetic material

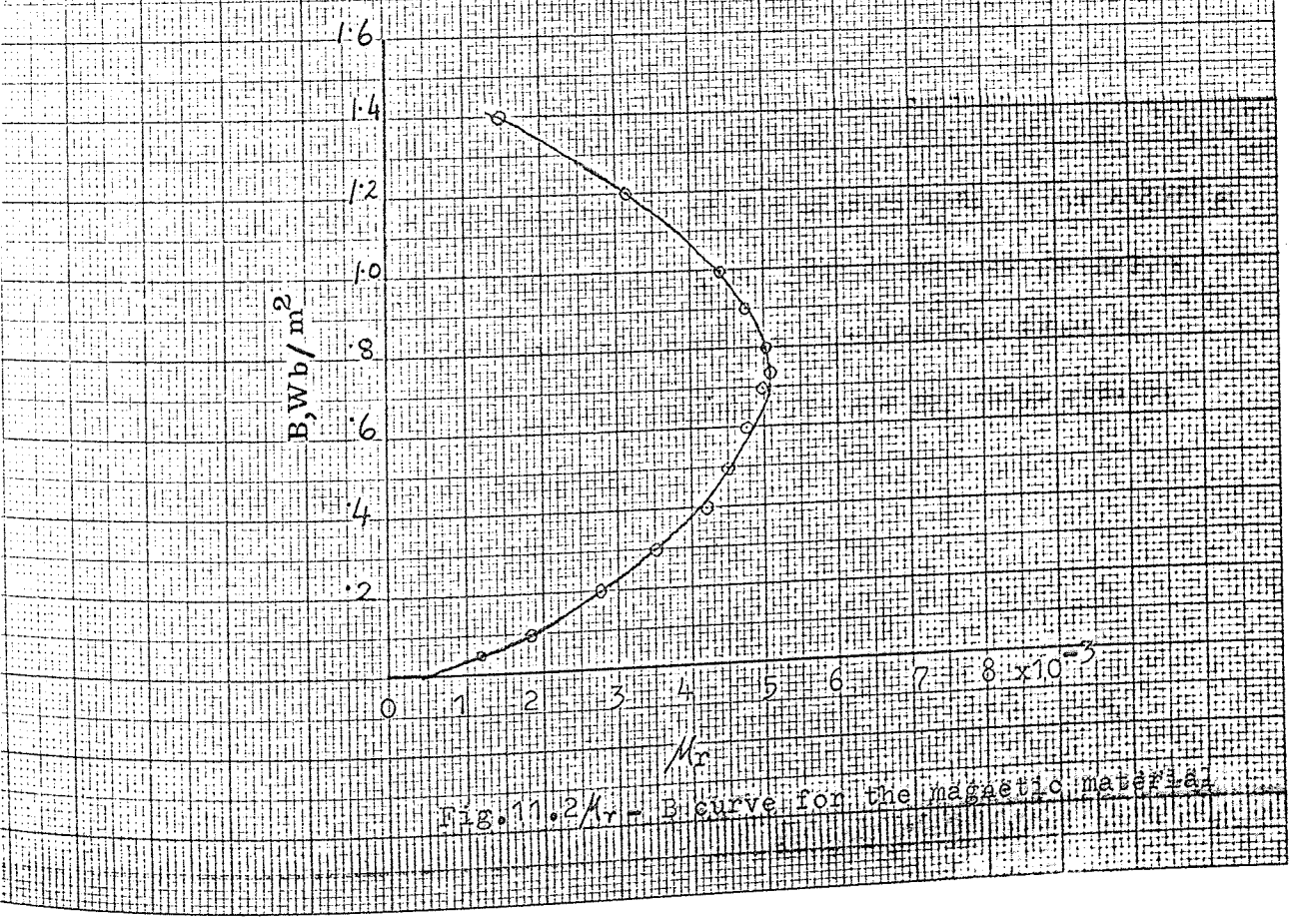

Fig. 11.2 μ_r - B curve for the magnetic material

The maximum relative permeability for the material was found to be 5100. This value was used for the calculation of the reluctances of the magnetic members from their dimensions.

11.3 Magnetisation measurements on the test relay.

Magnetisation measurements were made on the test relay by the 'Norma' light spot flux meter. The test relay is a telephone type electromagnetic relay type 305/2500/ABE-FG1/50 made by Magnetic Device's Ltd. The complete relay has 18 contact springs. For analogue computer simulation, some of the parameters of this relay were used.

A convenient reference condition for the measurement is to demagnetise the magnet structure completely and this was done in this present case. The average flux linking each turn of the coil was measured by a flux meter and a search coil, which was evenly wound over the core along the whole length.

Table 11.2 shows the results of the measurements. Non-magnetic spacers were used to vary the air gap. For a constant air gap, ϕ was measured for different values of the magnetomotive force Ni. Here the length of the air gap includes the air gap which remains when the armature is operated.

Table 11.2 Results of magnetisation measurements

Air gap $x_g' = x_g + .3$ mm

(a) Air gap = .177 mm

Ni At	ϕ x 10^{-7} Weber	S x 10^4 At/wb
22.25	84.1	264.5
42.5	218.18	194.7
62.75	339.39	184.8
82.5	446.96	184.5
121.75	613.63	198.4
133.5	651.50	204.9
150	704.5	212.9
194.5	787.8	246.8
227.5	848.4	268.0
275.5	901.50	305.6
340.0	954.50	356.2
365.0	969.60	376.4
507.5	1030.30	492.5

(b) Air gap = .380 mm

Ni At	ϕ x 10^{-7} Weber	S x 10^4 At/wb
22.0	69.7	
43.0	172.72	351
65.0	281.81	325
87.25	378.78	326.1
107.75	469.69	321.6
130	549.24	329.1
162.5	655.30	345.7
185	712.12	360.9
257.5	848.48	432.7
320	912.87	500
375	954.5	559.7
500	984.8	492.5

(c) Air gap = .419 mm

Ni At	ϕ x 10^{-7} Weber	S x 10^{4} At/wb
21.5	64.39	333.9
41.25	153.03	269.5
60.0	242.42	247.5
77.75	321.21	242
102.5	421.21	243.3
135.	545.45	247.5
170	651.51	260.9
230	787.87	291.9
352.5	931.81	378.2
435	977.27	445.1
500	1000	500

(d) Air gap = .622 mm

Ni At	ϕ x 10^{-7} Weber	S x 10^{4} At/wb
22	56.82	387.1
41.25	131.81	312.9
60	207.57	289
82.5	300	275
111.5	416.66	267.6
150.5	537.87	279.8
230	742.42	309.7
352.5	909	387.7
435	969.6	448.6
501	1000	501

(e) Air gap = .787 mm

Ni At	ϕ x 10^{-7} Weber	S x 10^{4} At/wb
21.5	51.5	417.4
41.25	116.70	353.4
73.5	231.80	317
102.5	328.8	311.7
122.5	392.4	312.1
170	537.9	316
230.	689.4	333.6
327.5	856.1	382.5
425	939.39	452.4
504.5	977.27	516.2

(f) Air gap = .863 mm

Ni At	ϕ x 10^{-7} Weber	S x 10^{4} At/wb
21.25	50.76	418.6
60	178.78	335.6
82.5	257.57	320.3
110.75	348.48	317.8
150	469.69	319.3
194	590.90	328.3
227.5	670.45	339.3
322.5	840.90	383.5
427.5	939.39	455
500	977.27	511.6

(g) Air gap = 1.016

Ni At	ϕ x 10^{-7} Weber	S x 10^{4} At/wb
21	48.48	433.1
40.5	109.1	371.2
72.75	215.15	338.1
95	284.84	333.5
110	334.84	328.5
148	446.96	331.1
192.5	568.18	338.8
237.5	704.54	337
335	848.40	394.8
425	931.81	456.1

(h) Air gap = 1.193 mm

Ni At	ϕ x 10^{-7} Weber	S x 10^{4} At/wb
21	44.70	469.7
40.5	98.86	409.6
60	154.54	388.2
32.5	221.21	372.9
112.75	309.09	364.7
153	416.66	367.2
203.75	549.24	370.9
296.25	746.21	397
352.5	833.33	423
425	909.09	467.5
500	954.54	523.8

When the results of the magnetisation measurements shown in table 11.2 are plotted to show the variation of the total reluctance S with Ni for a fixed air gap, 8 reluctance curves are obtained as shown in fig. 11.3. The magnetisation measurement may be plotted to show the ϕ vs. Ni relation as well, which was shown in fig. 10.11 for the same relay for two fixed air gaps taking the results from table 11.2 and 11.2 respectively.

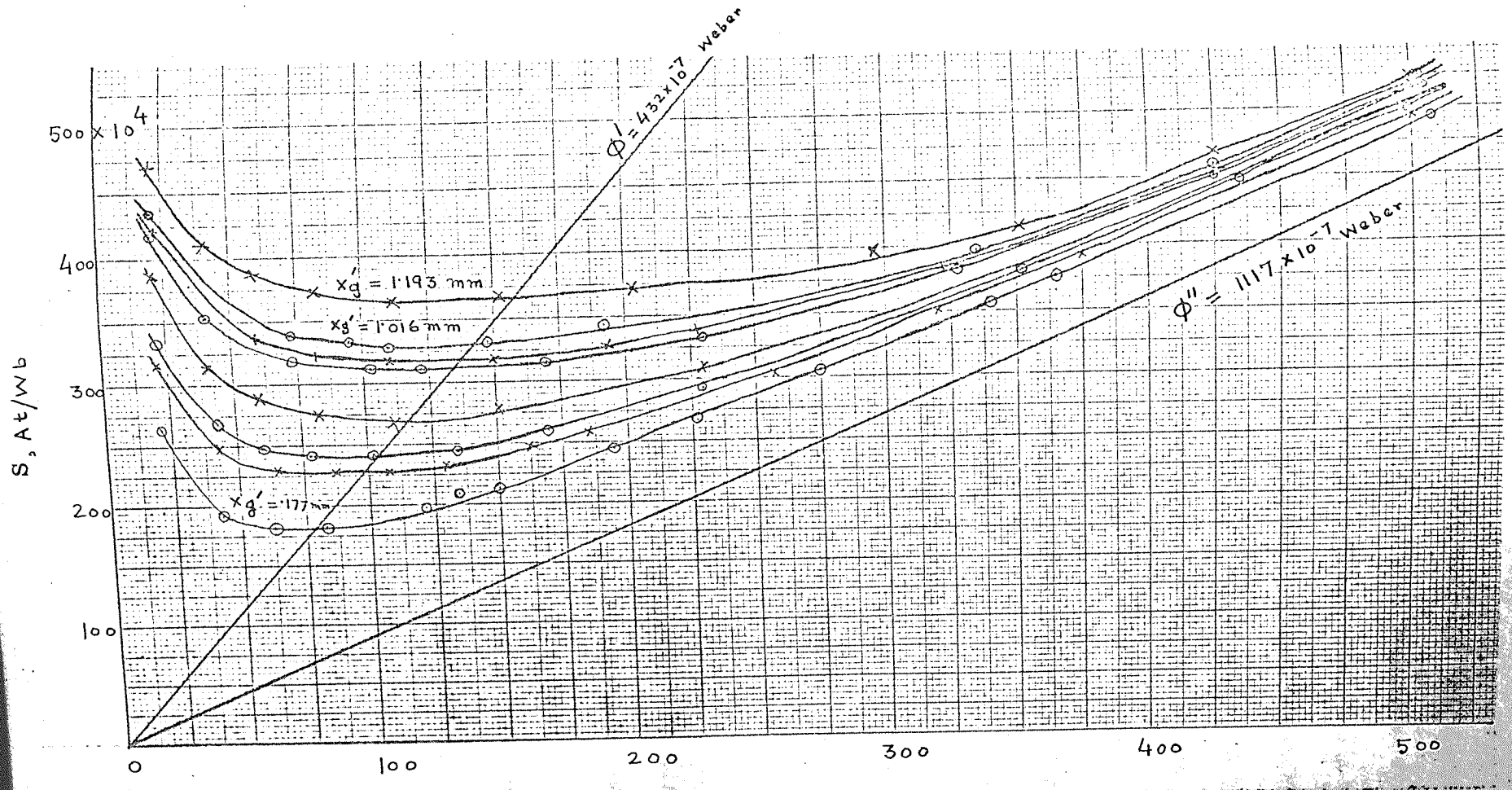

Fig.11-3 Measured reluctance curves

Each reluctance curve has a comparatively flat characteristic near the point indicating the minimum reluctance which corresponds to the maximum permeability at $\phi = \phi'$. All the minimum reluctance points on the curves lie on a common flux line indicated by ϕ' which is the flux corresponding to the upper limit of linear magnetisation or to the end of low density region. ϕ'' is the saturation flux.

11.4 Evaluation of the equivalent magnetic circuit constants from magnetisation measurements.

From the observed magnetisation relations the minimum reluctance $S'(x_g)$ corresponding to the maximum permeability may be easily obtained. In normal use a relay magnet is undergone, a repeated magnetisation which is shown in fig. 11.5 From this figure it is apparent that the increasing and decreasing magnetisation points are both linear up to the knees. Therefore, a constant reluctance $(= \frac{Ni}{\phi})$ may be taken in increasing magnetisation up to the knee which corresponds to ϕ'. This suggests that for engineering purposes, $S'(x_g)$ may be taken to be the total reluctance throughout the low density region in operation.

The equivalent magnetic circuit applies in low density region and $S'(x_g)$ may be taken as the total reluctance of the circuit. Therefore,

$$\frac{1}{S'(x_g)} = \frac{1}{S_L} + \frac{1}{S_o + \frac{x_o - x}{\mu_o A}}$$

$$\frac{1}{S'(x_g)} = \frac{1}{S_L} + \frac{\mu_o A}{\mu_o A S_o + (x_o - x)} \qquad (11.1)$$

or $$\frac{1}{S'(x_g)} = \frac{1}{S_L} + \frac{\mu_o A}{\mu_o A S_o + x_g} \qquad (11.2)$$

If x_{gc} is a value of an air gap, the length of which indicates a central reference position of the armature defined by x_g here, then $\mathcal{P}_{(x_{gc})}$ is the reciprocal of $S'(x_g)$ for $x_g = x_{gc}$. The expression for $\mathcal{P}_{(x_{gc})} - \mathcal{P}_{(x_g)}$ obtained from (11.2) may be given by:

$$\frac{x_g - x_{gc}}{\mathcal{P}_{(x_{gc})} - \mathcal{P}_{(x_g)}} = \mu_o A \left(S_o + \frac{x_{gc}}{\mu_o A}\right)^2 + \left(S_o + \frac{x_{gc}}{\mu_o A}\right)(x_g - x_{gc}) \qquad (11.3)$$

The ratio given by (11.3) varies linearly with x_g when the reluctance values are given by expression (10.6).

Table 11.3 shows x_g and $\mathcal{P}_{(x_g)}$. $S'(x_g)$ is obtained from the curves in fig. 11.3 to give $\mathcal{P}_{(x_g)}$.

Table 11.3 Air gap (x_g) and total permeance ($\mathcal{P}_{(x_g)}$)

$\phi' = 432 \times 10^{-7}$ Weber $\quad x_g' = x_g + .3$ mm

x_g' mm	x_g m m	$S'(x_g)$ x 10^4 At/wb	$\mathcal{P}_{(x_g)}$ x 10^{-7} wb/At
.177	- .1230	180	5.56
.380	+ .080	225.2	4.44
.419	+ .119	240	4.17
.622	+ .322	268	3.73

Table- 11.3(contd.)

x_g' m m	x_g m m	$S'(x_g)$ x 10^4 At/wb	$\mathcal{P}(x_g)$ x 10^{-7} wb/At
.787	+ .487	312	3.21
.863	+ .563	317.5	3.15
1.016	+ .716	330	3.03
1.193	+ .893	364	2.75

Fig. 11.4 shows the x_g vs. $\mathcal{P}(x_g)$ curve plotted from table 11.3. The values of $\mathcal{P}(x_g)$ for different values of $x_g - x_{gc}$ may be obtained from this curve. Table 11.4 shows $\frac{x_g - x_{gc}}{\mathcal{P}(x_{gc}) - \mathcal{P}(x_g)}$ for different values of $x_g - x_{gc}$, which are plotted as shown in fig 11.4, referred to the upper and right-hand scales.

Table 11.4

$$\mathcal{P}(x_{gc}) = 3.4 \times 10^{-7} \text{ wb/At}$$

$x_g - x_{gc}$ m m	$\mathcal{P}(x_g)$ x 10^{-7} wb/At	$\frac{x_g - x_{gc}}{\mathcal{P}(x_{gc}) - \mathcal{P}(x_g)}$ x 10^3
- .1	3.64	4.17
- .2	3.92	3.85
- .3	4.33	3.23
- .4	4.87	2.72
- .5	5.55	2.33
+ .1	3.21	5.26

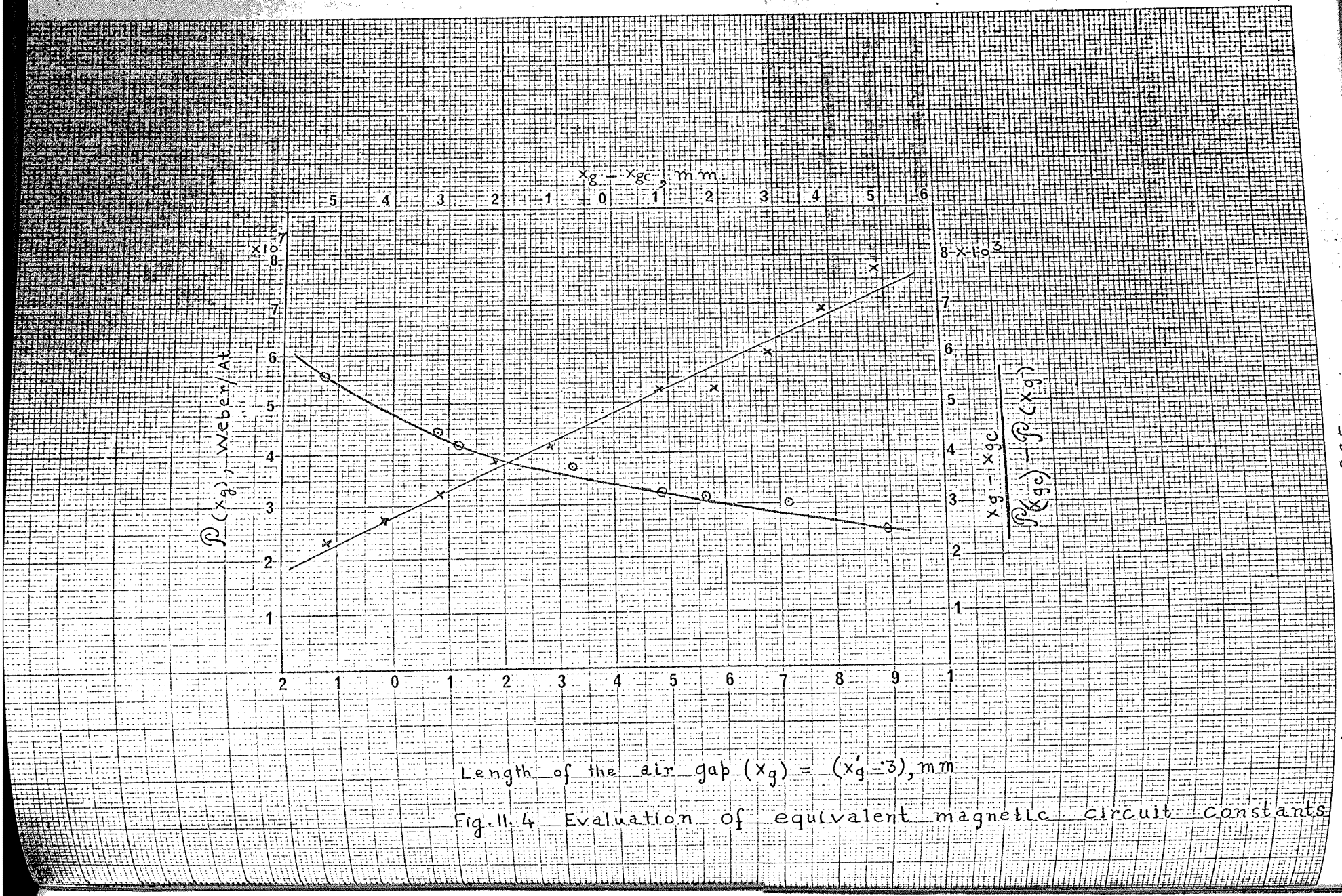

Fig. II. 4 Evaluation of equivalent magnetic circuit constants

Table- 11.4(contd.)

$x_g - x_{gc}$ m m	$\mathcal{P}_{(x_g)}$ x 10^{-7} wb/At	$\frac{x_g - x_{gc}}{\mathcal{P}_{(x_{gc})} - \mathcal{P}_{(x_g)}}$ x 10^3
+ .2	3.10	5.26
+ .3	3.0	6.0
+ .4	2.94	6.9
+ .5	2.9	7.7

As already indicated this linear plot conforms to equation 11.3, and the slope and intercept from this plot give the values of the following:

$$\text{Slope} = S_o + \frac{x_{gc}}{\mu_o A}$$

$$\text{Intercept} = \mu_o A \left(S_o + \frac{x_{gc}}{\mu_o A}\right)^2$$

Therefore, S_o and $\mu_o A$ may be evaluated from the slope and intercept of the line, and S_L may be determined from equation (11.2) by putting the values of x_{gc} and $\mathcal{P}_{(x_{gc})}$ which correspond to a central reference position, for x_g and $\frac{1}{S'(x_g)}$ respectively.

From fig. 11.4 the slope and intercept are:

$$\text{Slope} = 4.98 \times 10^6$$

$$\text{Intercept} = 4.8 \times 10^3$$

$$\mu_o A = \frac{4.8 \times 10^3}{(4.98 \times 10^6)^2} = .1935 \times 10^{-9} \text{ H.m}$$

$$S_o + \frac{x_{gc}}{\mu_o A} = 4.98 \times 10^6$$

$$\therefore \quad S_o = 4.98 \times 10^6 - \frac{.385 \times 10^{-3}}{.1935 \times 10^{-7}} = 299 \times 10^4 \text{ At/wb}$$

$$\mathcal{P}(x_{gc}) = \frac{1}{S_L} + \frac{\mu_o A}{\mu_o A\, S_o + x_{gc}}$$

$$\text{or} \quad 3.6 \times 10^{-7} = \frac{1}{S_L} + \frac{.1935 \times 10^{-9}}{.1935 \times 10^{-9} \times 299 \times 10^4 + .3 \times 10^{-3}}$$

$$\therefore \quad S_L = 715 \times 10^4 \text{ At/wb}$$

Here $\mathcal{P}(x_{gc})$ and x_{gc} correspond to $x_g = .3$ mm.

The constants of the equivalent magnetic circuit of the test relay as determined from the magnetisation measurements are given again in the following:

$$S_o = 299 \times 10^4 \text{ At/Wb}$$

$$S_L = 715 \times 10^4 \text{ At/Wb}$$

$$\mu_o A = .1935 \times 10^{-9} \text{ H.m}$$

11.5 Estimation of the magnetic circuit constants

For comparison with the values determined from the magnetisation measurements the equivalent magnetic circuit constants may be estimated from the dimensions of the magnetic structure. The method of estimation is the same as described in sec.6.3 for another similar structure. Table 11.5 shows the estimated values and the results obtained from the magnetisation measurements.

Table 11.5 Comparison of the observed and estimated equivalent magnetic circuit constants

Quantity	Estimated Value	Measured Value
S_o	290×10^4 At/wb	299×10^4 At/wb
S_L	708×10^4 At/wb	715×10^4 At/wb
$\mu_o A$	$.2140 \times 10^{-9}$ H.m	$.1935 \times 10^{-9}$ H.m

11.6 Repeated magnetisation of the electromagnet

The electromagnet in a relay undergoes repeated magnetisation in operation and release. Therefore, the repeated magnetisation of an electromagnet is of great importance. Fig. 11.5 shows such a magnetisation for a fixed air gap. ϕ_R is the residual flux and M_R contributes to the effective magnetomotive force $(Ni + M_R)$ in decreasing magnetisation and subsequent remagnetisation.

11.7 Pull measurements on the test relay

The various experimental procedures that are usually employed to determine the steady state magnetic pull, are all equivalent to using a spring balance to apply a force opposing the pull. A spring balance in combination with a manually operated device to raise the balance slowly against the pull acting on the armature which was attached to the hook of the balance, was, therefore, used to measure that steady state magnetic pull. A nonmagnetic shim was inserted in the gap between the armature and the pole face to maintain a fixed air gap and of course, a constant magnetising current was

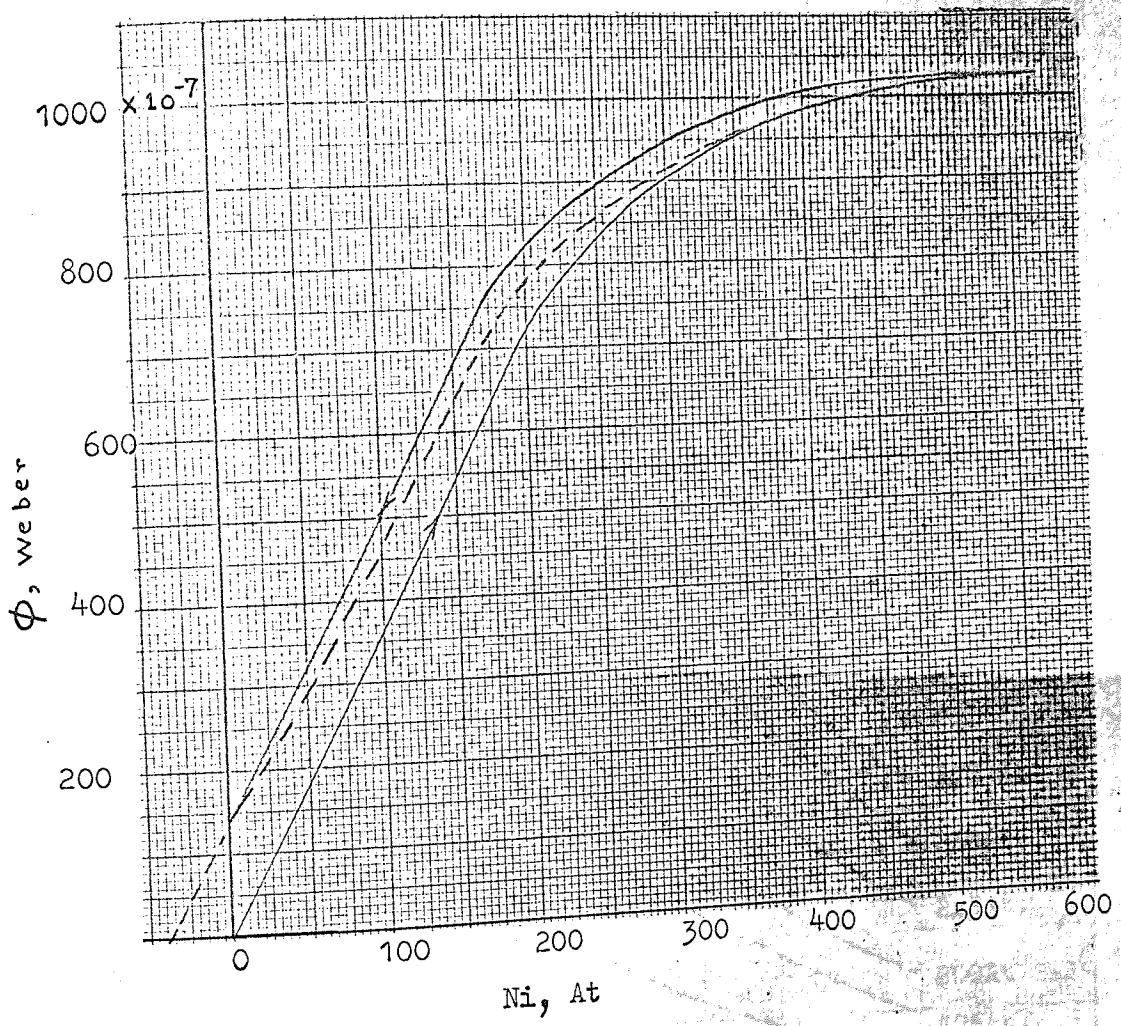

Fig. 11.5 Repeated magnetisation of the electromagnet

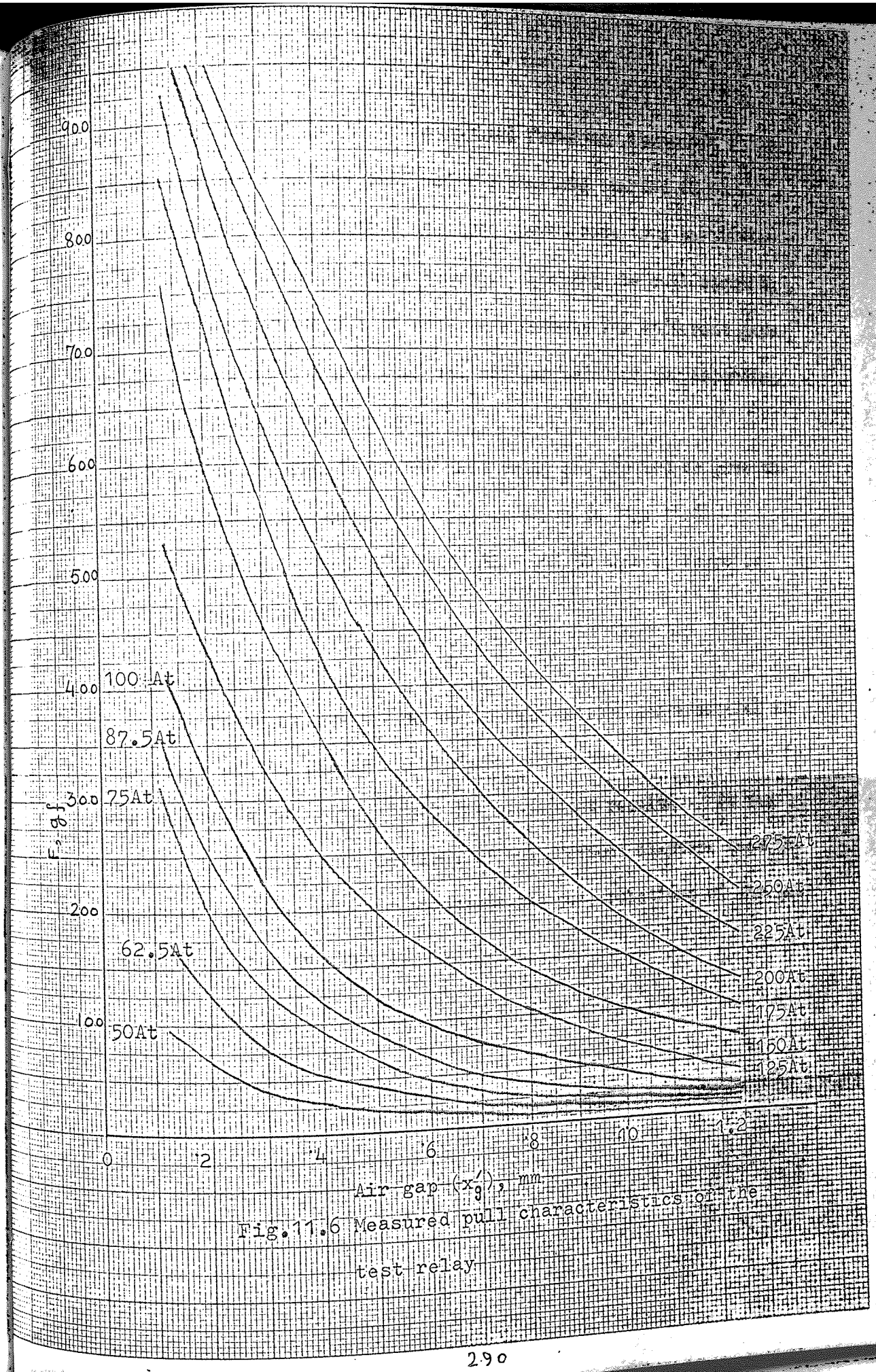

Fig.11.6 Measured pull characteristics of the test relay

maintained in the coil. The applied force was increased until it became equal to the pull and the armature started to move. The steady-state pull thus measured corresponds to a particular air gap and particular ampere-turn. Keeping the coil current fixed successive series of such measurements for different gaps would give steady state pull vs. air gap relation corresponding to a particular ampere-turn.

Pull measurements of the test relay are plotted to give the steady state pull characteristics as shown in fig. 11.6

Test relay : Type 305/2500/ABE - FG1/50 made by Magnetic Devices Limited.

11.8 Discussion

The measurements presented in this chapter are essential in the study of the static and dynamic performances. Inaccuracy in the measurements would affect the subsequent results. It was mentioned in different sections of the previous chapters that the measured magnetic circuit constants and pull relations of the test relay were used on various occasions.

Chapter 12

CONCLUSIONS

The time of operation of the electromagnetic relay may be estimated by using the two theories namely, the rational theory presented in chapter 5 and the theory for the rigorous analysis given in chapter 7. In the preliminary design calculations the time for a specific switching application may be determined after finding a suitable magnetic structure. The calculation of the magnetic circuit constants from the design dimensions of the magnet was discussed in chapter 6. The steady state pull characteristics can be computed from the estimated constants. After finding the static characteristics a suitable spring and coil configuration may be found by using the above mentioned theories. It may be mentioned here that the calculated time would be more accurate when the rigorous analysis is used. The calculation of the dynamic characteristics would be of great importance and the measures against bouncing, rebound oscillations and other undesirable phenomena may be taken when the calculated results are known. Higher velocities give rise to more bouncing and more oscillations. It was discussed in chapter 9 that the control of velocity is of great importance regarding minimisation of bouncing and rebound oscillations. The analysis would give directions in which way the change should be made to reduce the velocity.

After preliminary design estimates, models may be built for study and measurement. Actual measurements in models and analysis

of measurements by using the theories would determine the optimum conditions for a proposed design considering the required time of operation, the stability of the armature motion, the minimisation of bouncing and the other requirements. Of course, the considerations of relay economics must be given.

The computer programme may be used to compute the time of operation for design purposes when a suitable analogue computer with some logic facilities are available. Use of unit scaling makes it suitable for any computer irrespective of its base voltage. The velocity, acceleration and kinetic energy can be computed for different cases and the change of those due to the change of the other parameters can be easily observed. The optimum conditions may be determined to give lower velocity at the time of operation of the normally open contacts and at the instant the armature hits the magnet face. Thus, both the bouncing and rebound oscillations would be reduced.

The computer technique is one of the three methods described in the thesis for the analysis of the dynamic performance of electromagnetic switching relays. The other two methods mentioned previously are the rational design theory and the rigorous method. The three methods have their individual merits. The computer technique would be useful for analysis, synthesis and prediction of the relay behaviour and would be of importance in designing relays for various speeds of operation, and in performance analysis of an existing relay.

The theory for the rational design deals with the solution to the two dynamic equations, and mass comes explicitly in the time and flux formulae and other parameters also do so. Therefore, designers would get a guidance from the various analytical relations derived, in which way the parameters should be changed to get a required performance. The design shown is for a moderately fast relay. The agreement between the calculated and measured times is acceptable. Better agreement may be expected for slow speed relays. The theory may provide a comparative study with the method of rigorous analysis which does not give simple explicit expressions containing mass. Although, the latter method is a comparatively rigorous one considering the scope it gives for the dynamical analysis the second method was needed to be developed for getting a simple approach.

The rigorous analysis which uses Ahlberg's theory, considers the extension of the theory to study the motion of the armature which moves under the influence of four kinds of forces. Qualitative as well as quantitative considerations may be given in the control of time, velocity and acceleration. The experiments and a sample design established the method and proved its suitability. The theory for the analysis may be applied in other similar electromagnetic devices. A practical study of minimisation of bouncing by controlling velocity by changing different parameters may be suggested.

The theory mentioned in the preceding paragraph and the computer

technique may be applicable in the performance analysis of reed relays and polarised relays, and a theoretical and practical study may be suggested. It was discussed in chapter 9 how Ahlberg's theory could be applied in reed relays. A study may be suggested for the application of the rational design theory in electromagnetic contactors and power electromagnets.

The velocity and acceleration formulae deduced from the diagram combining the dynamic load characteristic and the steady state pull characteristics have been proved to be acceptable. The designer would get a guidance from the analysis of the formulae to consider different factors to reduce the velocity and acceleration when it is desired.

APPENDIX 1

SYMBOLS FOR THE COMPUTING COMPONENTS

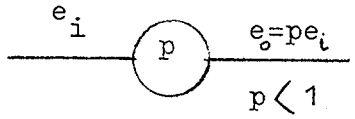

Potentiometer

Operational amplifier

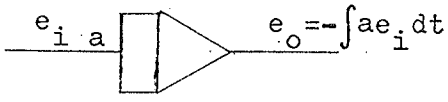

Integrator

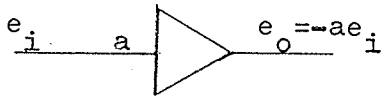

Inverter

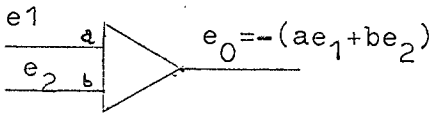

Summer

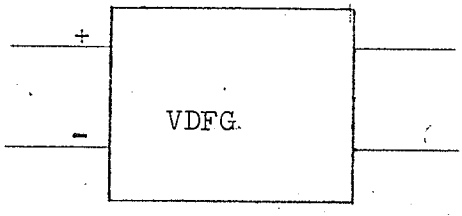

Function generator

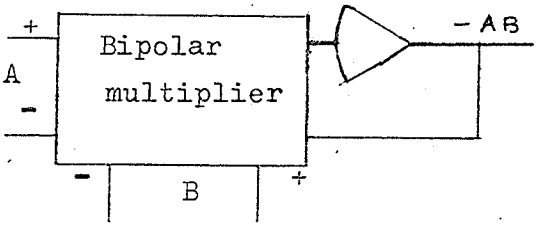

Bipolar multiplier

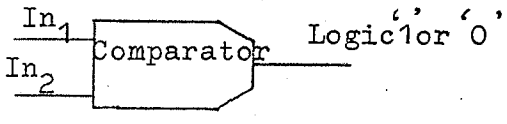

Comparator

APPENDIX 2

$$x = (4M_2 - M_1)\frac{a}{4\gamma^2} + (M_1 - 2M_2)\frac{a}{2\gamma} + \frac{a(M_2 - M_1)}{2}t^2 - (4M_2 - M_1 e^{-\gamma t})$$

$$\frac{a}{4\gamma^2} e^{-\gamma t}$$

The expression for x in the above equation may be simplified in the following manner:

$$x = (4M_2 - M_1)\frac{a}{4\gamma^2} + (M_1 - 2M_2)\frac{a}{2\gamma} + \frac{a(M_2 - M_1)}{2}t^2 - (4M_2 - M_1 e^{-\gamma t})$$

$$\frac{a}{4\gamma^2} e^{-\gamma t}$$

$$= (4M_2 - M_1)\frac{a}{4\gamma^2} + (M_1 - 2M_2)\frac{a}{2\gamma} + \frac{a(M_2 - M_1)}{2}t^2 - \left[4M_2 - M_1\right.$$

$$\left.(1 - \gamma t + \frac{\gamma^2 t^2}{2!} - \frac{\gamma^3 t^3}{3!} + \ldots)\right]\frac{a}{4\gamma^2}(1 - \gamma t + \frac{\gamma^2 t^2}{2!} - \frac{\gamma^3 t^3}{3!} + \ldots)$$

$$= (4M_2 - M_1)\frac{a}{4\gamma^2} + (M_1 - 2M_2)\frac{a}{2\gamma} + \frac{a(M_2 - M_1)}{2}t^2 - \left[4M_2 - M_1 + \right.$$

$$M_1\gamma t - M_1\frac{\gamma^2 t^2}{2!} + M_1\frac{\gamma^3 t^3}{3!} - 4M_2\gamma t + M_1\gamma t - M_1\gamma^2 t^2 + M_1\frac{\gamma^3 t^3}{2!} +$$

$$\left.\frac{4M_2\gamma^2 t^2}{2!} - \frac{M_1\gamma^2 t^2}{2!} + \frac{M_1\gamma^3 t^3}{2!} - \frac{4M_2\gamma^3 t^3}{3!} + \frac{M_1\gamma^3 t^3}{3!}\right],$$

neglecting the terms with higher powers of t.

$$\text{or, } x = (4M_2 - M_1)\frac{\alpha}{4\gamma^2} + (M_1 - 2M_2)\frac{\alpha t}{2\gamma} + \frac{\alpha(M_2 - M_1)}{2}t^2 - \left[(4M_2 - M_1)\frac{\alpha}{4\gamma^2} + \right.$$

$$(M_1 - 2M_2)\frac{\alpha t}{2\gamma} + (M_2 - M_1)\frac{\alpha t^2}{2} - \frac{M_1 \alpha t}{4\gamma} + \frac{3}{8}M_1 \alpha t^2 +$$

$$\frac{M_1 \alpha t}{4\gamma} - \frac{M_1 \alpha t^2}{4} - \frac{M_1 \alpha t^2}{8} + \left(\frac{M_1 \gamma^3 t^3}{3!} + \frac{M_1 \gamma^3 t^3}{2!} + \frac{M_1 \gamma^3 t^3}{2!}\right.$$

$$\left.\left. - \frac{4M_2 \gamma^3 t^3}{3!} + \frac{M_1 \gamma^3 t^3}{3!}\right)\frac{\alpha}{4\gamma^2}\right]$$

$$= (4M_2 - M_1)\frac{\alpha}{4\gamma^2} + (M_1 - 2M_2)\frac{\alpha t}{2\gamma} + \frac{\alpha(M_2 - M_1)}{2}t^2 -$$

$$(4M_2 - M_1)\frac{\alpha}{4\gamma^2} - (M_1 - 2M_2)\frac{\alpha t}{2\gamma} - (M_2 - M_1)\frac{\alpha t^2}{2}$$

$$+ \left(\frac{M_1 \gamma^3 t^3}{3!} + \frac{M_1 \gamma^3 t^3}{2!} + \frac{M_1 \gamma^3 t^3}{2!} - \frac{4M_2 \gamma^3 t^3}{3!} + \frac{M_1 \gamma^3 t^3}{3!}\right)$$

$$\frac{\alpha}{4\gamma^2}$$

$$= \left[M_1 \gamma^3 t^3 \left(\frac{1}{6} + \frac{1}{2} + \frac{1}{2} + \frac{1}{6}\right) - 4M_2 \frac{\gamma^3 t^3}{3!}\right]\frac{\alpha}{4\gamma^2}$$

$$= \left(\frac{4}{6}M_2 \gamma^3 t^3 - \frac{4}{3}M_1 \gamma^3 t^3\right)\frac{\alpha}{4\gamma^2}$$

$$\therefore x = \left(\frac{M_2}{6} - \frac{M_1}{3}\right)\gamma \alpha t^3$$

$$= \chi t^3 \qquad \text{where, } \chi = \frac{\gamma\alpha}{3}\left(\frac{M_2}{2} - M_1\right)$$

REFERENCES

1. Thompson, S.P. 'The Electromagnet' (E. & F.N. Spon, London, 1892), 452 pp.
2. Hunt, F.V. : 'Electroacoustics' (Harvard University Press,1954), 260 pp.
3. Peek Jr, R.L. & Wagar, H.N. : 'Switching Relay Design (D.Van Nostrand Company, Inc.,1955), 478 pp.
4. Johnson, C.L. : 'Analogue Computer Techniques' (McGraw-Hill, 1956), 264 pp.
5. Mackay, Donald M. & Fisher, Michael E. :'Analogue computing at Ultra-high speed' (Chapman & Hall, 1965), 395 pp.
6. Jackson, A.S. : 'Analogue Computation' (McGraw-Hill,1960), 652 pp.
7. Korn, Granino. A : 'Fast Analog-Hybrid Computation with Digital Control : The Astrac II System', Proc. of the 4th International Analogue Computation Meeting, Sept.1964, Brighton, pp.13 - 17.
8. McLachlan, N.W. : 'Ordinary Non-linear Differential Equations' (Oxford,1950), 201 pp.
9. Ahlberg, C. : 'On the Dynamic Behaviour of Electromagnetic Relays. A Theoretical and Practical Study', Ericsson Tech. 21(1965). No.1, pp. 3 - 110.
10. Ahlberg, C. : 'On the Dynamic Characteristics of the Electromagnetic Relay', Ericsson Review 42 (1965), No.4, pp. 121 - 132.
11. Ahlberg, C. : 'A Theory for the Dynamic Behaviour of an Electromagnetic Relay', Proceedings of the 15th Annual National Relay Conference, Oklahoma State University,1967, pp.20-1 - 20-21.

12. Ekelöf, S. : 'The Magnetic Circuit of Telephone Relays - A Study of Telephone Relays (1)', Ericsson Tech.9 (1953), No.1, pp. 51 - 82.

13. Ekelöf, S. : 'Theory of Electromagnetically Delayed Telephone Relays. A Study of Telephone Relays (2)', Ericsson Tech. 9 (1953). No.2, pp. 141 - 224.

14. Ekelöf, S. : 'The Development and Decay of the Magnetic Flux in a Non-Delayed Telephone Relay. A Study of Telephone Relays (3)', Ericsson Tech. 13 (1957). No.2, pp. 259 - 308.

15. Ekelöf, S. : 'A Theory of the Eddy Current Equivalent Winding and its Application to the Closing of Non-Delayed Telephone Relays. A Study of Telephone Relays (4)', Ericsson Tech.17 (1961). No.1, pp. 103 - 137.

16. Roters, H.C. : 'Electromagnetic Devices' (John Wiley & Sons, Inc., 1963), 561 pp.

17. Chougnet, P. : 'Relais électromagnétiques. Performances, Consitution, mesures' (Eyrolles, Paris, 1961), 260 pp.

18. Peek Jr, R.L.: 'Estimation and Control of the Operate Time of Relays. Part 1 - Theory', Bell Syst. Tech. J. 33(1954):1, pp 109 - 143.

19. Logan, M.A. : 'Estimation and control of the operate time of relays. Par II - Design of optimum windings', Bell Syst. tech. J. 33(1954) : 1, pp. 144 - 186.

20. Bähler, W.Th. : 'Die Theorie des Telephonrelais', Elektrotech Z. 49(1928) : 49, 50, pp. 1780, 1810.

21. Bähler, W.Th. : 'Die Theorie des Telephonrelais', Delft 1926, 221 pp.

22. Logan, M.A. : 'Dynamic Measurements on Electromagnetic Devices', Bell Syst. tech. J. 32(1953) : 6, pp. 1413 - 1467.

23. Norton, E.L. : 'Dynamic Measurements on Electromagnetic Devices', Trans. A.I.E.E. 64 (1945) : 2, pp. 151 - 156

24. Kennelly, A.E.: 'Magnetic Reluctance', Trans. A.I.E.E. 8(1891) : October, pp 485 - 543.

25. 9th Relay Conference Papers, Oklahoma State University, U.S.A., April 1961, 99 pp.

26. 10th Relay Conference Papers, Oklahoma State University, U.S.A., April 1962, 121 pp.

27. 11th Relay Conference Papers, Oklahoma State University, U.S.A., April 1963, 195 pp.

28. 12th Relay Conference Papers, Oklahoma State University, U.S.A., April 1964, 26-1 pp.

29. 13th Relay Conference Papers, Oklahoma State University, U.S.A., April 1965, 35-9 pp.

30. 14th Relay Conference Papers, Oklahoma State University, U.S.A., April 1966, 24-18 pp.

31. NARM Relay Testing Procedures, Issue A, U.S.A., 85 pp.

32. Okada, Knbokoya, Shinohara. : 'Dynamical Analysis of Non-polarized Relay', collec. of Memor. Treat. from Electro-Tech. Lab. Nippon Telegraph and Telephone Pub.Corpn., 1948, pp 331 - 342.

33. Masuzawa, K. & Tomita, Y. : 'Motional Equations of Vibrating Parts of Electromagnetic Relays', Journal of the Inst. of Elect. Comm. Engrs, Japan 41(1958) : 3, pp 244 - 249

34. Shinohara, T. : 'Dynamic Performance of Switching Relays in Operation and Release', Journal of the Inst. of Elect. Comm. Engrs, Japan 41 (1958) : 3, pp. 249 - 259.

35. Tomita, Y. : 'Effects of the Force Factor and the Eddy Current on the Operate and Release time of the Ordinary Relay', Review of the Elect. Comm. Lab. Japan 9(1961) : 1/2, pp 72 - 84.

36. Jasse, E. : 'Die Electromagnete' (Berlin 1930), 198 pp.

37. Perugini, M.M. : 'The electromagnetic relay is probably the least understood, least standardised and the most abused of all components used in electronic equipment" - Leon D. Carr, 8th Annual NARM Relay Symposium, May 1960', Electronic Equipment Engineering, June, 1963, pp. 45 - 53.

38. Ekelof, S., Bengtson, L. Kihlberg, G. & Leithammel, P. : 'Integrating Amplifier for oscillographic recording of magnetic flux', Chalmers Tekniska Hogskolas Handlinger (1951) : 121, pp. 2 - 23

39. Walker, R.C. : 'Relays for Electronic and Industrial Control' (Chapman & Hall Ltd. 1953), 303 pp.

40. Dummer, G.W.A. & Hyde, N.E. : 'Connectors Relays and Switches' (Pitman 1966), pp. 138 - 189.

41. Palmer. : 'Relays in Automatic Telephony' (Pitman)

42. Miller, D.D. : 'Design Characteristics of Electromagnets for Telephone Relays', Bell Syst. tech. J. 3(1924) pp.204-219.

43. Hougaard, O.M. & Perreault, G.E. : 'Development of Reed Switches and Relays', Bell Syst. tech. J. 34(1955) pp. 309 - 332.

44. Peek, R.L. : 'Magnetization and Pull Characteristics of Mating Magnetic Reeds', Bell Syst. tech. J. 40(1961) pp. 523 - 546.

45. M.I.T.Staff.: 'Magnetic circuits and transformers', (John Wiley & Sons, Inc. 1955), pp. 1-253.

46. Karo,D. : 'Electrical Measurements-Part I (Macdonald,London,1961)

47. Karo,D. : 'Electrical Measurements-Part II' (Macdonald,London,1969)

48. Welsby, V.G. : 'Inductance Coils' (Macdonald:London 1960)

49. Golding,E.W. & Widdis,F.C. : 'Electrical Measurements and Measuring Instruments' (Pitman, 1963)

50. Kibble,T.W.B. : 'Classical Mechanics', (McGraw-Hill,1966) 296 pp.

51. Brailsford,F. : 'Magnetic Materials', (Methnen & Co.Ltd.,London, 1960) 188 pp.

52. Hammond,P. : 'Electromagnetism for Engineers' (Pergamon Press, 1965) 209 pp.

53. Plousey, Robert & Collin, R.E. : 'Principles and Applications of Electromagnetic Fields' (McGraw-Hil, 1961) 553 pp.

54. Bruinsma, A.H. : 'Circuits Using Direct Current Relays' (Iliffe Books Ltd, 1965).

55. Gourishanker,V. : 'Electromechanical Energy Conversion' (International Textbook Company, 1965).

56. Hi-G Relay Engineering Mannual - Part I, (Hi-G Inc. U.S.A. 1967), pp. 1 - 15.

57. Glass, J.G. : 'Hinged armature relays', The English Electric Journal 19(1964). No.1, pp. 2 - 11.

58. Ekelöf,S. : 'On the calculation of relay windings', Ericsson Tech.(1933). No.2, pp. 15 - 22

59. Lakatos, E. : 'Problem solving with the analogue computer', Bell Laboratories Record, March 1951, pp. 109 - 114.

60. Jeans,J.H. : 'The Mathematical Theory of Electricity and Magnetism', (University Press, Cambridge, 1908) 536 pp.

61. Kraus,J : 'Electromagnetics' (McGraw-Hill, 1953), 604 pp.

62. Keller,A.C. : 'Design of Relays', Bell Syst. tech. J.33(1954) No.1, pp. 1 - 2

63. Wagar, H.N. : 'Relay Measuring Equipment' Bell Syst.tech. J. 33(1954) No.1, pp. 3 - 22

64. Peek Jr, R.L. & Wagar, H.N. : 'Magnetic Design of Relays', Bell Syst.tech. J. 33(1954) : 1, pp. 23 - 78

65. Peek Jr, R.L.:'Principles of slow release Relay Design', Bell Syst. tech. J. 33 (1954) : 1, pp. 187 - 217.

66. Peek Jr, R.L. :'Analysis of Measured Magnetisation and Pull Characteristics', Bell Syst. tech. J. 33 (1954) : 1, pp.79 - 108.